TECHNISCHE UNIVERSITÄT MÜNCHEN

WACKER Lehrstuhl für Makromolekulare Chemie

Expansion and Modulation of Mesenchymal Stem Cells on Biomaterials in Bioreactors

Julia Hupfeld

Vollständiger Abdruck der von der Fakultät für Chemie
der Technischen Universität München zur Erlangung des akademischen Grades eines

Doktors der Naturwissenschaften

genehmigten Dissertation.

Vorsitzender: Univ.-Prof. Dr. Johannes Buchner

Prüfer der Dissertation:

1. Univ.-Prof. Dr. Dr. h.c. Bernhard Rieger
2. apl. Prof. Dr. Ralf Huss (Ludwig-Maximilians-Universität München)

Die Dissertation wurde am 6.2.2013 bei der Technischen Universität München eingereicht und durch die Fakultät für Chemie am 16.4.2013 angenommen.

This work was performed from April 2010 to February 2013 at Roche Diagnostics GmbH, Penzberg in collaboration with Prof. Dr. Dr. h.c. Bernhard Rieger, Wacker Lehrstuhl für Molekulare Chemie, Technische Universität München.

Eidesstattliche Erklärung

Ich erkläre an Eides statt, dass ich die bei der promotionsführenden Einrichtung
Fakultät für Chemie
der TUM zur Promotionsprüfung vorgelegte Arbeit mit dem Titel:
Expansion and Modulation of Mesenchymal Stem Cells on Biomaterials in Bioreactors
in
Wacker Lehrstuhl für Makromolekulare Chemie
(Fakultät, Institut, Lehrstuhl, Klinik, Krankenhaus, Abteilung)
unter der Anleitung und Betreuung durch:
Univ.-Prof. Dr. Dr. h.c. Bernhard Rieger
ohne sonstige Hilfe erstellt und bei der Abfassung nur die gemäß § 6 Abs. 6 und 7 Satz 2 angegebenen Hilfsmittel benutzt habe.

(x) Ich habe keine Organisation eingeschaltet, die gegen Entgelt Betreuerinnen und Betreuer für die Anfertigung von Dissertationen sucht, oder die mir obliegenden Pflichten hinsichtlich der Prüfungsleistungen für mich ganz oder teilweise erledigt.
(x) Ich habe die Dissertation in dieser oder ähnlicher Form in keinem anderen Prüfungsverfahren als Prüfungsleistung vorgelegt.
( ) Die vollständige Dissertation wurde in .....
veröffentlicht. Die promotionsführende Einrichtung .....
hat der Vorveröffentlichung zugestimmt.
(x) Ich habe den angestrebten Doktorgrad noch nicht erworben und bin nicht in einem früheren Promotionsverfahren für den angestrebten Doktorgrad endgültig gescheitert.
( ) Ich habe bereits am .....
bei der Fakultät für .....
der Hochschule .....
unter Vorlage einer Dissertation mit dem Thema .....
.....
die Zulassung zur Promotion beantragt mit dem Ergebnis:
.....
Die öffentlich zugängliche Promotionsordnung der TUM ist mir bekannt, insbesondere habe ich die Bedeutung von § 28 (Nichtigkeit der Promotion) und § 29 (Entzug des Doktorgrades) zur Kenntnis genommen. Ich bin mir der Konsequenzen einer falschen Eidesstattlichen Erklärung bewusst.

Mit der Aufnahme meiner personenbezogenen Daten in die Alumni-Datei bei der TUM bin ich
(x) einverstanden, ( ) nicht einverstanden.

München, den 5.2.2013

Unterschrift

Acknowledgements

This work has only been possible through the support of many people.

First of all, sincere thanks go to my Doktorvater Prof. Dr. Bernhard Rieger for his support and advice and for introducing me to the world of thermoresponsive polymers.

I am deeply grateful to Prof. Dr. Ralf Huss for the opportunity to work on this exciting project, for his support and advice throughout the project and for life-saving medical advice.

A heartily thank you to Dr. Heike Wegmeyer and Dr. Markus Neubauer for their scientific advice and support throughout the last three years. I very much appreciated your fast proof-reading and that you always had your doors open for all kinds of questions.

Warm thanks to Dr. Ning Zhang for providing me with polymer and polymer-coated surfaces and his patience in answering the many chemical questions I have had.

I thank Katia Rodewald for fascinating SEM pictures, Dr. Jürgen Funk and Christelle Zundel for histological analysis of chondrogenesis pellets, and Dr. Thomas Friess and Esther Abraham for support regarding the Bio-Plex Assays.

Many thanks go to Dr. Nicola Beaucamp and her team for giving me a new “home” after the TCI break up and for giving us the opportunity to perform the large-scale experiments, for which Dr. Max Lechner and his team kindly provided their facilities. Very special thanks to Dr. Ingo Gorr, Christian Schwald, Manuel Mayer and Alois Filgertshofer - you “rocked” that project! Thanks to Heike Homfeldt and Ulrich Steegmans for the nice welcome to their lab.

Heartily thanks to the former TCI group: to Dr. Monika Bähner for giving me the great chance to work on this project; to Dr. Ann-Marie Broeske, Dr. Saskia Knothe, Jennifer Kuhlen, Dr. Karin Küntzer, Dr. Mathias Leddin, Christoffer v. Schwerin, Dr. Annina Nisselbeck, Kornelius Wiechmann for experimental and scientific advice, unforgettable work and non-work related discussions; to Marion Conrad for keeping our lab organized and for introduction to the “oberbairische” world; to Laura Diener, Ailine Pauschert, Laura Strobl for experimental help; to Ricarda Hope-Söhngen and Christina Haffner for administrative assistance.

I would like to thank Dr. Jens Bolle for helpful work and non-work related conversations.

I deeply appreciate the support of my “American parents” Cathy and Chris.

Many, many thanks go to Bastian for supporting me in his very own way.

Finally, I am deeply grateful to my parents for their never-ending support, encouragement and motivation which keep me going.

I thank Roche Diagnostics GmbH for financial support.

Abbreviations

AF	Alexa Fluor®
AM	amniotic membrane
API	active pharmaceutical ingredient
ATP	adenosine-5'-triphosphate
BM	bone marrow
C	Celsius
CFSE	5(6)-carboxy-fluorescein-diacetat-N-succinimidylester
CFU-F	colony forming unit-fibroblasts
d	day
DNA	deoxyribonucleic acid
DPBS	Dulbecco's Phosphate-Buffered Saline
ECM	extracellular matrix
EGDM	ethylene glycol dimethacrylate
ESC	embryonic stem cell
F	flask
FCS	fetal calf serum
FDA	Food and Drug Administration
FGF	fibroblast growth factor
FGF	fibroblast growth factor
FITC	fluorescein isothiocyanate
FSC	forward scatter
GMP	Good Manufacturing Practice
h	hour
HGF	hepatocyte growth factor
HLA II	human leukocyte antigen
IL	interleukin
IL1-ra	interleukin 1 receptor antagonist
INF-γ	interferon γ
IPA	Ingenuity Pathway Analysis
iPS cell	induced pluripotent stem cell
ISCT	International Society for Cell Therapy
LCST	lower critical solution temperature

MC	microcarrier
MCP-1	monocyte chemotactic protein-1
M-CSF	macrophage colony-stimulating factor
MEM	Minimum Essential Medium
min	minute
MSC	mesenchymal stem cell
NGF	nerve growth factor
NK	natural killer
PBMC	peripheral blood mononuclear cell
PBS	phosphate buffered saline
pCO_2	partial pressure of carbon dioxide
PCR	polymer chain reaction
PDAVP	poly(dialkyl vinylphosphonate)
PDEVP	poly(diethyl vinylphosphonate)
PDMVP	poly(dimethyl vinylphosphonate)
PE	phycoerythrin
PEG	polyethylene glycol
PEGDM	poly(ethylene glycol dimethacrylate)
PEI	Paul Ehrlich Institute
PHA-L	phytohemagglutinin-L
PNIPAAM	poly(N-isopropylacrylamide)
pO_2	partial pressure of oxygen
POx	poly(2-oxazoline)
POx	poly(2-oxazoline)
qRT-PCR	quantitative real-time PCR
RDG	arginine, aspartic acid, glycine
RIN	RNA integrity number
RNA	ribonucleic acid
RT	room temperature
s	second
SC	stem cell
SDF-1	stromal cell-derived factor-1
SEM	scanning electron microscopy
SI-GTP	surface-initiated group transfer polymerization

SSC	side scatter
T	temperature
TCA	tricarboxylic acid
TNF-α	tumorn necrosis factor α
UC	umbilical cord
VEGF	vascular endothelial growth factor

Table of Contents

1 Introduction

Hematopoietic stem cell transplantation represents the first stem cell therapy developed and is clinical routine today. Many hurdles and objections had to be overcome after Nobel Prize winner E. Donnall Thomas and colleagues performed the first bone marrow transplantations in the late 1950s. Today, however, hematopoietic stem cell transplantation saves the lives of thousands of patients suffering from leukemia or other diseases of the hematopoietic system (Appelbaum, 2012). More recently, mesenchymal stem cells (MSCs, also called mesenchymal stromal cells) have emerged as a promising therapeutic modality. Clinical application of MSCs requires administration of large amounts of cells, which is opposed by the limited number of MSCs that can be isolated from tissue (Santos et al., 2013). Therefore, extensive cell expansion is a crucial step regarding the development of a biopharmaceutical "off-the shelf" cell therapy product. "Off-the-shelf" shall hereby illustrate that, similar to traditional pharmaceuticals, this cellular product is generated in a large-scale manufacturing process, stored, shipped, and ready to use for *ad hoc* administration to patients. Special considerations have to be given to the manufacturing process itself. According to the paradigm that "the process is the product" the process determines properties and quality of the active pharmaceutical ingredient (API) and thereby safety and efficacy of the final therapeutic product (Zuniga and Calvo, 2009, Polastro, 2001). For market approval of cellular products, tight control of the complex manufacturing process, according to Good Manufacturing Practice (GMP) and requirements of regulatory agencies such as the Paul-Ehrlich-Institut (PEI, Germany) or Food and Drug Administration (FDA, USA) is mandatory (Knothe and Neubauer, 2013, Sensebe et al., 2011).

The following sections first provide an introduction into the concept of MSCs, their biology and therapeutic application, and the influence of culture conditions on MSCs. Then, the manufacturing process and suitable bioreactor formats are addressed. In the last section, an innovative technology for optimized MSC expansion will be introduced.

1.1 Mesenchymal Stem Cells

Stem cells (SCs) are unspecialized cells which are characterized by their long-term self-renewal capacity and multilineage differentiation potential. According to their differentiation potential, SCs are classified as totipotent, pluripotent or multipotent:

- Totipotent SCs have the ability to differentiate into all cells of an organism, including extraembryonic tissues. In mammals, the zygote and early embryonic blastomeres up to at least the 4-cell stage embryo are totipotent (Van de Velde et al., 2008, Mitalipov and Wolf, 2009).
- Pluripotent SCs have the capacity to differentiate into cells of all three germ layers (endoderm, mesoderm or ectoderm) (Mitalipov and Wolf, 2009).
- Multipotent SCs have the ability to differentiate into multiple cell types of the same germ layer they are derived from but not into cells from all three germ layers (Kolios and Moodley, 2013)

Human stem cells can be classified into three main groups: embryonic stem cells (ESCs), induced pluripotent stem (iPS) cells and adult stem cells. ESCs are pluripotent cells isolated from the inner cell mass of the blastocyst (Thomson et al., 1998). Recent groundbreaking work of the group of Yamanak and Thomson led to the development of iPS cells (Takahashi et al., 2007, Yu et al., 2007). iPS cells are adult somatic cells which, through introduction of specific genes, become pluripotent. Regarding SC therapy, the high tumorigenic risks of ESCs and iPS cells, as well as the ethical concerns associated with ESCs, clearly limit their clinical use, making adult stem cells more attractive candidates for clinical therapy (Blum and Benvenisty, 2008, Prockop et al., 2010a, Salem and Thiemermann, 2010). Adult stem cells can be isolated from a variety of differentiated, adult tissues containing so-called “stem cell niches” for these multipotent cells (Ohlstein et al., 2004).

MSCs are multipotent, adult stem cells. They have originally been described by Friedenstein and colleagues as hematopoiesis-supporting stromal cells of the bone marrow with osteogenic differentiation potential (Friedenstein et al., 1968). Friedenstein also showed a high proliferative capacity of so-called colony forming unit-fibroblasts (CFU-Fs) (Friedenstein et al., 1974). These CFU-Fs were proposed to be called “stromal stem cells” by Owen (Owen, 1988), and a few years later, Caplan popularized the term “mesenchymal stem cells” (Caplan, 1991). However, researchers started to avoid the term “stem cell” due to lack of *in vivo* demonstration of self-renewal and the International Society for Cellular Therapy (ISCT) suggested the term “mesenchymal stromal cells” for the unfractionated fibroblast-like, plastic adherent cell population (Horwitz et al., 2005).

MSCs can be isolated from virtually all postnatal tissues of the body (da Silva Meirelles et al., 2006). Bone morrow (BM) is the earliest and best described MSC source but cells have been isolated from other tissues such as adipose tissue (Zuk et al., 2001), skeletal muscle (Sinanan

et al., 2004), amniotic membrane (AM) (Marongiu et al., 2010, Ilancheran et al., 2009), umbilical cord (UC) blood (Erices et al., 2000), or UC matrix (Wharton's Jelly) (Seshareddy et al., 2008). MSCs from multiple organs were shown to have a perivascular origin (Crisan et al., 2008), suggesting the perivascular niche as one possible *in vivo* location of MSCs (da Silva Meirelles et al., 2008). In this work, MSCs isolated from human whole umbilical cord (UC) or amnion membrane (AM) were employed. The amniotic membrane is the inner layer of the placenta, facing the fetus (Knorr and Denk, 2002).

Once isolated, MSCs are a heterogeneous population of plastic-adherent cells with fibroblast-like, spindle-shaped morphology. So far, no specific and unique MSC marker has been identified and various tissue sources, diverse isolation protocols and cultivation conditions hinder the comparison of studies from different laboratories (Wagner and Ho, 2007). Regarding this problem, the ISCT has proposed three minimal criteria to define MSCs (Dominici et al., 2006). First, they must be plastic-adherent. Second, MSCs must express CD73, CD90 and CD105 but lack expression of the hematopoietic markers CD11b or CD14, CD19 or CD79a, CD34, CD45, and HLA II. Finally, they must have the capacity for osteogenic, chondrogenic, and adipogenic differentiation.

The tri-lineage differentiation potential is well-described in the literature (Pittenger et al., 1999, Prockop, 1997). Additionally, differentiation into other cells of the mesodermal origin such as cardiomyocytes has been shown (Makino et al., 1999). Differentiation across germ layers, i.e. transdifferentiation, has also been shown, including differentiation into hepatocyte (Christ and Dollinger, 2010) or neuronal cells (Woodbury et al., 2000, Kopen et al., 1999) but remains highly controversial (Uccelli et al., 2008, Bieback et al., 2012).

1.2 MSC Therapy

1.2.1 Clinical Application of MSCs

MSCs have been employed in many pre-clinical and clinical studies as reviewed extensively in the literature in both autologous (donor is recipient) and allogeneic (donor is different from receipient) settings (Salem and Thiemermann, 2010, Satija et al., 2009, Mimeault et al., 2007, Caplan, 2009). The most prominent application of MSCs is probably in graft-versus-host disease (GvHD) (Le Blanc et al., 2007, Le Blanc et al., 2008). Other MSC-based clinical and pre-clinical studies include, for example, the treatment of osteogenesis imperfecta, myocardial infarction, stroke, multiple sclerosis, Crohn's Disease, diabetes mellitus, liver fibrosis,

pulmonary fibrosis or critical limb ischemia (http://www.clinicaltrials.gov). Generally speaking, many indications for MSC treatment rely on the immunomodulatory and regenerative effects of MSCs which make them attractive candidates for treatment of autoimmune, degenerative or chronic diseases. More recently, studies also focus on improving MSC therapy by increasing their therapeutic potency or increasing their homing to the designated tissue sites (Wagner et al., 2009). Potential means to modify MSCs include genetic modifications or priming through culture conditions and/or biochemical factors (Satija et al., 2009, Wagner et al., 2009).

Numerous characteristics of MSCs make them attractive candidates for therapy:

a) They are expandable *ex vivo* in cell culture which is a prerequisite to obtain sufficient cell numbers for human application due to the low frequency of MSCs in tissues.
b) They are immune privileged, making allogenic therapy and development of an "off-the-shelf" cellular product for a wide range of patients possible (Le Blanc et al., 2003, Griffin et al., 2010).
c) They are rather easy to isolate from various tissues in the body (da Silva Meirelles et al., 2006) without the ethical concerns associated with ESC isolation.
d) Cultured MSCs possess a low risk of malignant transformation, whereas the risk of tumor formation is high for ESCs or iPS cells (Prockop et al., 2010b).
e) They have been reported to home to injured tissue (Karp and Leng Teo, 2009).
f) They secrete paracrine and endocrine factors through which they mediate their therapeutic function (Karp and Leng Teo, 2009, Yagi et al., 2010).
g) They are multipotent and are able to differentiate into mature tissue cells upon induction, an important property for tissue replacement and engineering applications (Gao and Caplan, 2003).

Cell therapies require large amounts of cells: a dose in the order of 10^6 MSCs/kg body weight is commonly applied in clinical trials (Ringden et al., 2006, Sato et al., 2010, Subbanna, 2007). Administration of multiple doses over the course of treatment further increases the required amount of cells. This demand is opposed by the limited number of cells obtained by isolation from tissue. For example, only 0.001% to 0.01% of mononuclear BM cells are MSCs (Pittenger et al., 1999). MSC frequency in UC and AM was found to be somewhat higher: 0.2% to 1.8% (UC) or 0.03% to 33.3% (AM) of isolated cells were MSCs as determined by CFU-F assays and an average of 2×10^7 to 3.5×10^7 cells per isolation have been obtained (unpublished data). Therefore cell expansion is an essential part in manufacturing

sufficient doses of a pharmaceutical MSC product (see Table 1). With regard to patient treatment, an allogeneic, “off-the-shelf” cell product may be advantageous over autologous products as it provides means to treat large numbers of patients and is ready to use in case of urgent medical treatment. Depending on the disease progression, obtaining high quality starting material for autologous therapy may also be difficult in diseased patients (Knothe and Neubauer, 2013). On the other hand, allogeneic treatment is associated with the risk of severe immune response (Li and Zhong, 2009). Even though still discussed controversially, this risk can be addressed by the immune privileged properties of MSCs (Le Blanc et al., 2003, Griffin et al., 2010).

1.2.2 Mode of Action

Originally, MSCs were assumed to exert their therapeutic benefit through homing to the respective tissue site and differentiation into mature tissue cells after systemic administration, but more recently a general consensus has evolved that MSCs mainly act through secretion of paracrine and endocrine factors (Figure 1) (Horwitz and Dominici, 2008, da Silva Meirelles et al., 2009). Through these factors, MSCs modulate therapeutically relevant biological functions; they are able to modulate the immune response, inhibit apoptosis and fibrosis, support angiogenesis, hematopoiesis, proliferation, and differentiation of other progenitor cells or attract other cells by secretion of chemoattractant molecules (da Silva Meirelles et al., 2009).

Immune modulation is probably the most extensively studied property of MSCs. Different cell types of the immune response have been shown to be inhibited or regulated by MSCs *in vivo* and *in vitro* (Marigo and Dazzi, 2011). While the anti-proliferative effect on T lymphocytes is probably the best described immunomodulatory property of MSCs, they also inhibit proliferation and activation of natural killer (NK) cells (Spaggiari et al., 2008), inhibit maturation of naive dendritic cells (DC) (Jung et al., 2007, Ramasamy et al., 2007), and modulate cytokine secretion of macrophages to an anti-inflammatory response (Nemeth et al., 2009). Depending on the environment, MSCs have also been reported to suppress B cell proliferation and to inhibit their antibody secretion (Marigo and Dazzi, 2011). Immunomodulatory function of MSCs has been shown to be induced by an inflammatory environment which can be mimicked *in vitro* by proinflammotry cytokines such as TNF-α or IFN-γ (Ren et al., 2008, Krampera et al., 2003).

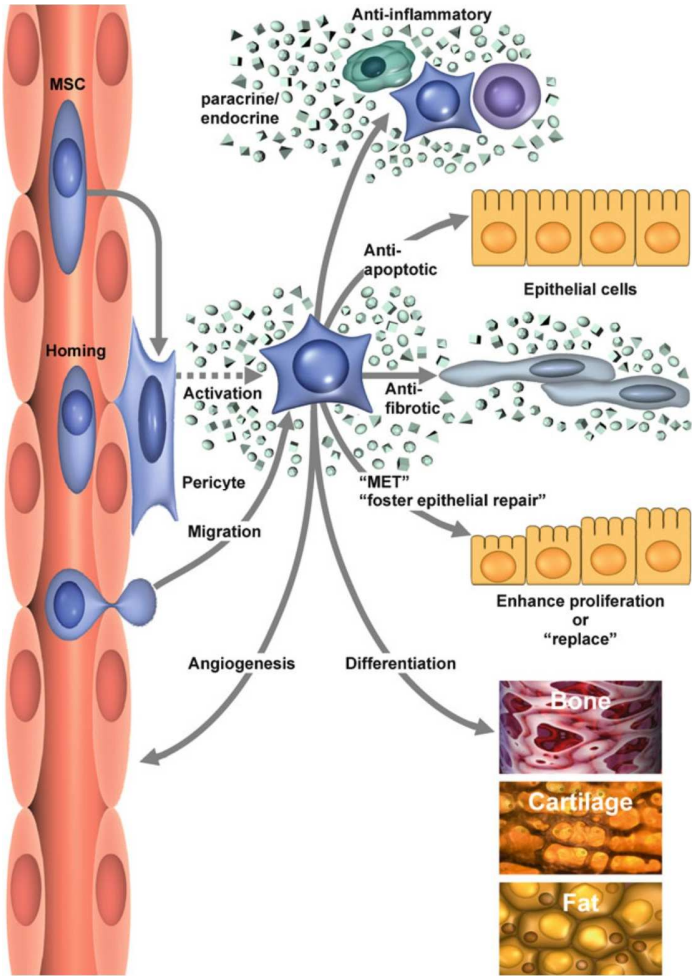

Figure 1: MSC mode of action. After intravenous injection, MSCs have been proposed to exert their therapeutic function through homing to the injured tissue, extravasation from blood vessels and secretion of paracrine and endocrine factors through which they may modulate the immune response, apoptosis, fibrosis, and angiogenesis. Differentation or re-differentation processes have also been suggested as potential mode of actions. Figure adopted from Neubauer et al., 2012.

Additionally, MSCs have been described to migrate or "home" to the site of injury after administration (Karp and Leng Teo, 2009). MSCs migration has been shown to take place, for example, along chemotactic gradients and signaling along the stromal cell-derived factor 1 (SDF-1) - C-X-C chemokine receptor type 4 (CXCR4) axis and c-met - hepatocyte growth factor (HGF) axis have been most extensively studied (Ratajczak et al., 2006, Neuss et al., 2004). However, the therapeutic relevance of MSC homing is discussed controversially as only a small fraction of MSCs "home" after administration and cell-free supernatants may also have therapeutic effects (Horwitz and Dominici, 2008, Bi et al., 2007) .

1.3 MSC Culture

1.3.1 Influence of Culture Conditions

Isolated MSCs are a heterogeneous cell population *per se*, and further heterogeneity arises due to high-donor to-donor variability, different donor age and tissue (Ilancheran et al., 2009, Lv et al., 2012, Phinney et al., 1999, Siddappa et al., 2007, Prockop and Oh, 2012, Hauser et al., 2010, Kern et al., 2006, Stenderup et al., 2003). Moreover, different culture conditions are also know to influence MSC growth and function and the variety of different culture protocols employed in the MSC field further hamper comparison of results from different laboratories (Wagner and Ho, 2007). Generally, MSCs are expanded in standard cell culture media such as alpha-MEM or DMEM using 10% - 20% fetal calf serum (FCS). Addition of FCS leads to an undefined medium with high batch-to-batch variance. Moreover, using an animal-derived supplement bears the risk of transmitting infectious diseases, microbiological contamination, or xenogenic proteins. Xenogenic proteins can induce severe immune reactions in patients (Jung et al., 2012a). Therefore, MSC expansion in chemically defined, serum-free media is studied extensively (Chase et al., 2010, Fekete et al., 2012, Lindroos et al., 2009). Likewise, pooled human serum or platelet lysate is being investigated (Doucet et al., 2005, Kocaoemer et al., 2007, Stute et al., 2004).

Cultivation of MSCs has been reported to alter cell characteristics including loss of multipotency or down-regulation of cell surface markers (Harichandan and Buhring, 2011, Siddappa et al., 2007). Upon extended cultivation, MSCs become senescent (Bruder et al., 1997, Banfi et al., 2000, Wagner et al., 2008). In accordance with the Hayflick limit (Hayflick and Moorhead, 1961), this occurs after about 30 to 40 population doublings. Senescence has additionally been reported to be increased by high glucose levels (Stolzing et al., 2006).

Furthermore, general culture parameters such as growth factors, glucose and glutamine concentrations, medium, and plating density have been shown to influence MSC proliferation (Sotiropoulou et al., 2006). As one example, low density plating has been shown to influence MSC morphology and to select for rapidly dividing, “recycling stem cells” (RS-1) with high multilineage differentiation potential (Colter et al., 2000, Sekiya et al., 2002).

Culture surface parameters such as surface topography, architecture hydrophobicity, stiffness, roughness, or charge can also regulate cell adhesion, morphology, and function (Chang and Wang, 2011, Kim et al., 2010). Regarding MSCs, studies have for example reported on an influence of substrate stiffness on MSC: An increased potential for osteogenic differentation on stiff matrix and adipogenic differentiation on soft matrix was found, mediated through cell

shape-dependent regulation of RhoA activity (Engler et al., 2006, Park et al., 2010, McBeath et al., 2004). With regard to substrate influences, ECM interactions have also been shown to influence MSC fate through mechanisms of mechanotransduction (Figure 2) (Guilak et al., 2009). Moreover, MSC properties and differentiation potential were found to be influenced by mechanical stimuli, in particular shear stress. Most often described is a shear stress-related induction of MSCs towards osteogenic differentiation (Sharp et al., 2009, Arnsdorf et al., 2009, Kreke et al., 2008, Li et al., 2004, Glossop and Cartmell, 2009)..

Last but not least, general cell culture parameters such as osmolality, pH value, and nutrient supply have to be considered. Nutrient supply and cell metabolism is discussed below. Maintenance of a suitable and constant osmolality is important regarding osmotic pressure and membrane potential (Sanchez and Lopez-Zapata, 2010). Mammalian cell culture is commonly performed using 270 – 320 mOsmol/kg (Waymouth, 1970). Incorrect pH values can impair cell growth and lead to cell damage and therefore pH levels should be monitored carefully. Usually mammalian cell cultures are performed at pH 7.2 to 7.4. (GE Healthcare, 2005).

In summary, culture conditions can modulate MSC function and fate in a variety of ways (see also Figure 2). According to the biopharmaceutical paradigm that “the process is the product,” this provides means to adjust MSC characteristics according to their therapeutic application but also makes the detailed characterization of the final cell product an essential requirement for its therapeutic use.

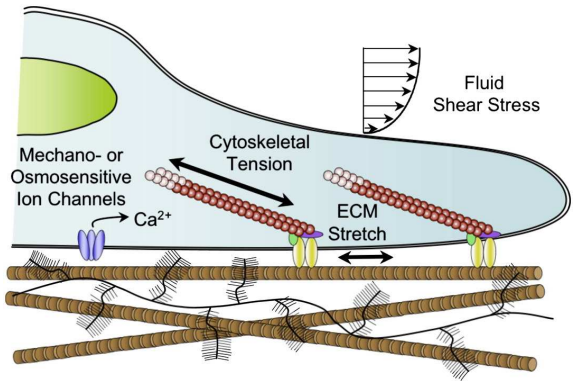

Figure 2: Modulation of cell fate. Different mechanical forces have been described to influence cell fate, including osmotic and shear stresses or stress arising due to altered biochemical interactions with the extracellular matrix (ECM). Mechanotransduction has been shown to be mediated through integrin-mediated cytoskeletal modulation and cell shape alterations, which ultimately lead to altered cell growth and functions. As another mechanism of meachanotransduction, involvement of Ca^{2+} ion channels has been suggested. Figure adopted from Guilak et al., 2009.

1.3.2 Metabolism

Monitoring of cell metabolism is essential to optimize cell culture conditions and bioreactor performance. Cell growth and viability can be improved by monitoring and controlling the concentration of (toxic) metabolites and maintaining concentrations of energy sources at appropriate levels (Cruz et al., 1999). Mammalian cells mainly use glucose and glutamine as energy sources (Glacken, 1988). Glucose can be catabolized by oxidative phosphorylation, yielding about 30 to 38 mol ATP/mol glucose, or by anaerobic glycolysis, yielding 2 mol ATP and 1 mol lactate per mol glucose. Glutamine can be catabolized through various pathways, yielding different amounts of ATP. In principle, glutamine catabolism is initialized by deamination of glutamine to glutamate, followed by conversion to α-ketoglutarate, yielding a total of 1 to 2 mol NH_3 per mol glutamine (Schneider et al., 1996). α-ketoglutarate can then enter the tricarboxylic acid (TCA) cycle and is metabolized to pyruvate which in turn can be metabolized to lactate. Alternatively, pyruvate can be fully oxidized to CO_2 via the TCA cycle or partially oxidized to aspartate or alanine (Schneider et al., 1996, Glacken, 1988). Depending on the pathway taken, catabolism of glutamine can be energy efficient, yielding 24 to 27 mol ATP and 2 mol NH_3 by complete oxidization of glutamine or energy inefficient yielding only 6 to 9 mol ATP, 1 mol NH_3, and 1 mol lactate or alanine/aspartate (Schneider et al., 1996). In addition to its metabolism, glutamine can decompose spontaneously in culture medium, leading to ammonia increase (Tritsch and Moore, 1962). Hence, more stable dipeptides such as GlutMAX™ (L-alanyl-L-glutamine) are frequently used in cell culture.

As noted above, catabolism of glucose and glutamine does not only produce energy but is also accompanied by production of metabolites such as lactate and ammonia which are known for their cellular toxicity and inhibition of cell growth (Glacken, 1988). Lactate leads to accumulation of hydrogen ions, i.e. the culture pH decreases (Jordi Joan and Francesc, 2005). Therefore, pH levels should be controlled carefully, especially at high cell densities where lactate production is high (GE Healthcare, 2005). The toxic effects of ammonia and ammonium have been attributed to their different transport mechanisms across cell membranes - ammonia readily diffuses across cell membranes while ammonium is actively transported - leading to disturbance of transmembrane ion gradients and intracellular pH levels (Schneider et al., 1996, Martinelle et al., 1996).

1.4 Bioreactors and MSC Bioprocessing

1.4.1 Bioprocessing of MSCs

As discussed above (1.2), MSC therapy requires large amount of cells, making the expansion process a necessary requirement for development of a cell therapeutic product. Special considerations have to be given to the manufacturing process, as the process itself may determine characteristics of the final product (Polastro, 2001, Zuniga and Calvo, 2009). This is already a critical issue regarding production of traditional biologics and may become even more challenging regarding manufacturing of an allogeneic "off-the-shelf" cellular product due to the high biological complexity of the cells (Knothe and Neubauer, 2013). Hence, to obtain a high quality cell-based medicinal product, special considerations have to be given to the MSC manufacturing process to ensure maintenance of MSC characteristics and therapeutic relevant functions. An ideal expansion process should be scalable, adaptable to GMP compliance, and provide means for cost-efficient, controllable, and reproducible production of a high quality cell product.

Table 1: Cell expansion is a crucial requirement for manufacturing a cell therapy product. Depending on the cell source, 10^5 cells can be assumed to be isolated from a tissue. A single clinical dose commonly consists of approximately 10^6 cells/kg. Based on these assumptions, 10 population doublings yield 1 clinical dose. As long-term expansion leads to senescence and potentially genetic instability, it can be assumed that up to 20 population doublings can be performed, yielding 1,100 clinical doses (Knothe and Neubauer, 2013, Lepperdinger et al., 2008, Bobis et al., 2006).

Assumed number of isolated cells: 10^5		
Population doublings	**MSC yield**	**Doses (≈10^6cells)**
3	8.0×10^5	0
10	1.0×10^8	1
15	3.3×10^9	33
20	1.1×10^{11}	1100

For expansion, anchorage-dependent cells such as MSCs require a surface to attach and grow on. Traditionally, adherent cells are cultivated under static conditions in 2D monolayers on tissue culture dishes or flasks. Using this expansion method, the production of large cell quantities is challenging as it involves handling of numerous flasks, making it labor-intensive and prone to variability and contamination. State of the art technologies for large-scale cultivation of anchorage-dependent cells include roller bottles and multilayer flask systems (Mather, 1998). However, these technologies still have limitations concerning available sur-

face area, handling as well as control and regulation of the system and usually do not provide means for a fully closed, automated process.

Stirred bioreactors, which are routinely used in the pharmaceutical industry for GMP-compliant production of cell culture-derived biopharmaceuticals, provide means to overcome afore mentioned limitations (Warnock and Al-Rubeai, 2006). These bioreactors can be equipped with online monitoring sensors for process control and automated regulation of parameters such as temperature, pH value, pO_2, pCO_2, osmolality and nutrients/metabolites. Scale-up of these bioreactors can be achieved easily by increasing vessel size; working volumes of up to 15,000 l are in operations today (Kelley, 2007). Sufficient aeration, a critical parameter especially in large-scale and high density cultures, can be ensured by direct sparging of air or oxygen (Lüllau and Fenge, 2005). Additionally, in contrast to a static process, cultures are agitated by impellers, which provide homogenous culture suspensions. Furthermore, optimal nutrient supply can be implemented through different feeding regimes such as batch, fed-batch or perfusion.

Usually, stirred bioreactors are used for cultivation of suspension cells, but after the introduction of microcarrier-based cell expansion by van Wenzel (van Wezel, 1967), anchorage-dependent cells have also successfully been cultivated in stirred bioreactors. Microcarriers are small microspheres on which adhesion-dependent cells can be cultivated in 2D monolayers or, by employing macroporous microcarriers, in 3D culture. Due to their advantageous surface area to volume ratio, microcarriers provide much larger culture surface areas in smaller volumes compared to standard flask expansion (see Table 2). Therefore, combining microcarriers with routinely used stirred bioreactor systems offers an excellent method for a scalable, controlled, regulated and closed expansion process. Industrial applications of microcarrier-based cell culture primarily involve production of vaccines and recombinant proteins (GE Healthcare, 2005, Tharmalingam et al., 2011). Other biomedical applications are in tissue engineering (Hong et al., 2008) or development of artificial organs such as the liver (Xu et al., 2003). Various microcarriers are commercially available (see Table 3). They differ mainly in size, porosity, material composition, and surface coating. In addition to microcarriers listed in Table 3, diethylaminoethyl (DEAE) cellulose and other commercially available resins (e.g. DE52 from Whatman or Toyopearl from Tosho Bioscience) have been used for microcarrier-based cell cultivation even though they are primarily marketed for chromatography applications (Chen et al., 2011). Non-commercial microcarrier formats such as liquid microcarriers have also been applied for research use (Keese and Giaever, 1983).

Table 2: Advantageous surface-to-volume ratio of microcarriers. To obtain the same surface area only 1.4 g microcarriers are needed and culture medium usage can be reduced to 10% of the medium volume required for standard expansion in cell stacks.

	Cell stacks (e.g. Cell Factory, Nunc)	Microcarrier (e.g. Cytodex 1, GE Healthcare)
Culture surface [cm²]	6320	6320
Amount	10 stacks	1.4 g
Medium [ml]	2000	~200

Table 3: Commonly used commercially available microcarriers. Abbreviation: n.d. no data

Name	Manufacturer	Porosity	Core materials	Surface coating	Surface charge	Density (g/mL)	Diameter (µm)
Cytodex 1	GE Healthcare	microporous	cross-linked dextran	diethylaminoethyl	+	1.03	147 - 248
Cytodex 3	GE Healthcare	microporous	cross-linked dextran	collagen type 1	none	1.04	141 - 211
Cytopore 1& 2	GE Healthcare	macroporous	cross-linked cellulose	diethylaminoethyl	+	1.03	200 - 280
Cytoline 1	GE Healthcare	macroporous	polyethylene with silica	none	-	1.32	lentil shape; 0.5–1.1 mm
2D Microhex	Nunc	microporous	hydrophilized polystyrene	none	n.d.	1.05	hexagonal; length: 125, thickness: 25
Hillex	Solohill Engineering	microporous	modified polystyrene	trimethylammonium	+	1.12	90-212
Hillex II	Solohill Engineering	microporous	modified polystyrene	trimethylammonium	+	1.11	160-180
Glass	Solohill Engineering	microporous	crosslinked polystyrene	high silica glass	none	1.02	125-212
Plastic	Solohill Engineering	microporous	crosslinked polystyrene	none	none	1.02	125-212
Plastic Plus	Solohill Engineering	microporous	crosslinked polystyrene	none	+	1.02	125-212
Pronectin F	Solohill Engineering	microporous	cross-linked polystyrene	recombinant fibronectin	yes	1.02	125-212
FACT III	Solohill Engineering		Cross-linked polysyrene	Type 1 porcine collagen	+	1.02	125 - 212
CarboSeed S 400, 800, S/S	Cinvention	microporous	carbon	covalently bound Ca^{2+}, Mg^{2+}, S^{6-}	yes	1.02-1.07	400 / 800
CultiSpher-S	Percell Biolytica	microporous	cross -linked gelatin	none	n.d.	n.d.	n.d.
CultiSpher-G	Percell Biolytica	microporous	cross-linked gelatin	none	n.d.	1.04	130-380
Rapid Cell	MP Biomedicals	microporous	Glas	n.d.	-	1.03	150 - 210

Even though microcarrier-based expansion in stirred bioreactors has many advantages, some considerations have to be made for process development. The importance of the culture environment on cell characteristics has been discussed above. Switching from static flasks to microcarrier-based expansion changes the cell environment. For example, depending on the microcarriers' material and shape, cells are exposed to an altered substrate composition with spherical architecture. Furthermore, by switching from static to stirring conditions shear forces are generated which can lead to cell damage and influence cell characteristics. Additional cell damage can also result from cell-microcarrier collisions (Cherry and Papoutsakis, 1988). Furthermore, direct gas sparging, which is required for adequate oxygenation in large-volume, high-density cultures may cause cell damage (Papoutsakis, 1991, Spier and Griffiths, 1983). Sparging is also known to cause foam formation which can entrap microcarriers in the foam layer, thus eliminating them from the culture medium (Bauer et al., 2000).

Besides stirred bioreactors, alternative formats such as hollow-fiber bioreactors, packed and fluidized bed bioreactors, rotating wall vessels, or single use wave-mixed bag bioreactor have been employed for large-scale expansion of anchorage-dependent cells. Hollow fiber bioreactors such as the Quantum® Cell Expansion System (Terumo BCT, www.terumobct.com) provide high cell densities in a closed, automated expansion environment. However, scale-up is cost-intensive and also limited by diffusional gradients and drawing cell samples during the expansion process is not possible (Warnock and Al-Rubeai, 2006). In packed bed (also known as fixed bed) bioreactors, cells are cultured within a fixed matrix of high density macroporous microcarriers such as porous glass or ceramic beads or polyester disks (Meuwly et al., 2007). Fluidized bed bioreactors also employ a matrix to culture cells but here, the matrix is "fluidized" by a vertical upward flow of medium (Waugh, 1999). To minimize shear stress, rotating wall vessels have been developed (Goodwin et al., 1993). However, this bioreactor format is limited regarding scale-up (Rodrigues et al., 2011).

In addition to glass or stainless steel bioreactors, disposable plastic bioreactors have become more and more popular with many different formats available on the market (Shukla and Gottschalk, 2012, Eibl et al., 2010). Commonly employed wave-mixed bag bioreactor consists of single-use plastic bags placed on rocking devices. These bioreactors apply wave motions to hold cultures in suspension. Coupling this system with the microcarrier technology also allows expansion of anchorage-dependent cells. While such a single-use system provides

many advantages regarding sterility, (cross-)contamination and handling, drawbacks, such as the potential interaction of leachables and extractables from plastic with the cultivated cells or increased running costs due to single-use and limitations regarding scalability exist (Eibl et al., 2010).

An alternative approach to surface-dependent cultivation is the adoption of adherent cells to culture in suspension. A popular example are CHO cells which can be adopted to grow in suspension (Hamilton and Ham, 1977). Regarding MSCs, successful cultivation in 3D aggregates or spheroids has been shown (Serra et al., 2009, Subramanian et al., 2011, Bartosh et al., 2010, Frith et al., 2010a). Some authors suggest an increase of MSC therapeutic potential through this cultivation method (Frith et al., 2010a, Bartosh et al., 2010), but clearly, this altered cultivation method changes cell characteristics as shown by modified proliferation, stem cell marker expression, cell shape and differentiation potential (Serra et al., 2009, Frith et al., 2010b). A substantial problem of cultivation in 3D aggregates is the impaired mass transfer of oxygen, nutrients and metabolites (Glicklis et al., 2004). As cells within aggregates are exposed to very different culture environment compared to cells from the outer layer, this cultivation method may not be applicable for the generation of a standardized, preferably homogenous cell product.

1.4.2 Microcarrier-based Expansion of MSCs in Bioreactors

Even though microcarriers provide a promising technology for large-scale expansion of adherent cells, MSCs are still commonly expanded in less complex systems such as roller bottles or multilayer cell stacks (Jung et al., 2012b). Only recently, investigation of microcarrier-based MSC expansion has begun. Studies which have reported on successful cultivation are summarized in Table 3. Most of these studies employed BM-derived MSCs and Cytodex or CultiSpher microcarriers in stirred bioreactors with a focus on process development and optimization. Very limited data regarding effects of the stirred bioreactor process on MSC characteristics and function are available since most studies only show maintenance of MSC phenotype and tri-lineage differentiation potential(Frauenschuh et al., 2007, Eibes et al., 2010, Chen et al., 2006). However, more recently Sart et al. and Trseng et al. reported on an influence of microcarrier-expansion on MSC differentiation potential. Using gelatin or collagen-

coated microcarriers, they observed alterations of the MSC cytoskeleton and an increase of osteogenic and/or adipogenic differentiation capacity (Sart et al., 2012, Tseng et al., 2012).

Despite the often emphasized potential of microcarrier technology for use in large-scale expansion, the maximal culture volume employed in MSC studies is still rather low with only two studies using culture volumes of 1 l or above (Elseberg et al., 2012, Sart et al., 2009) of which only the study of Elseberg et al. performed bioreactor MSC cultures under controlled and regulated conditions.

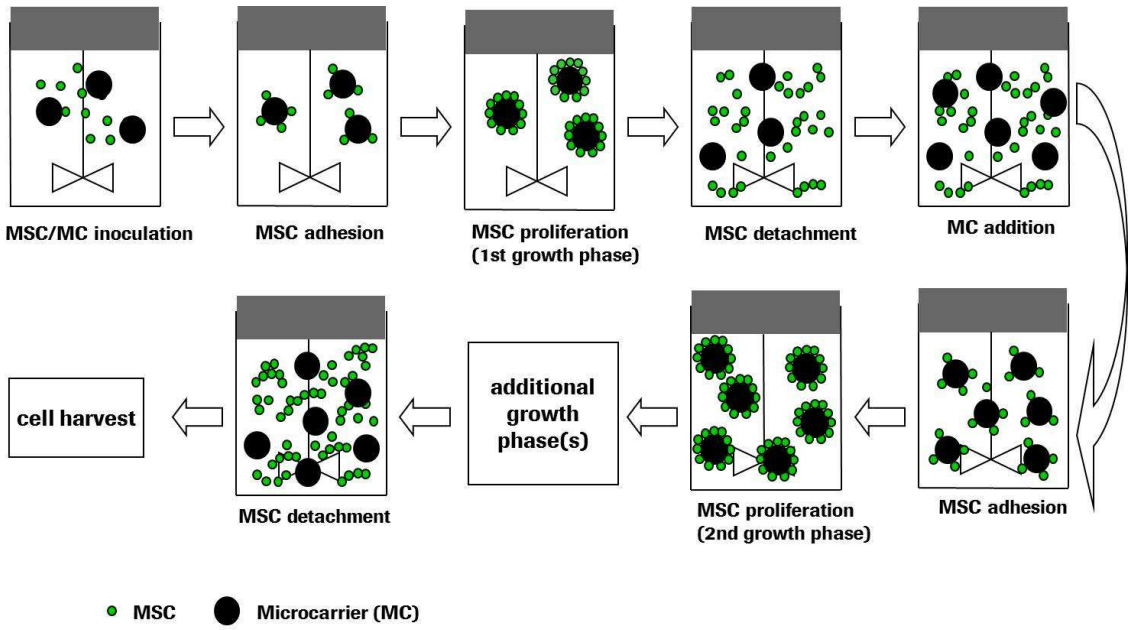

Figure 3: Outline of a potential microcarrier-based expansion process. A stirred bioreactor is inoculated with MSCs and microcarriers. After a first adhesion and proliferation phase, confluent MSCs are detached enzymatically from microcarriers. Surface can be increased by microcarrier addition. Further growth phases can follow until the cells are finally harvested.

Table 4: Studies using microc arrier-based MSC expansion. Abbreviations: g goat; h human; m mouse; r rat; rb rabbit; p porcine; n.d. no data; reg regulated conditions

Author	Year	Cells	Micocarrier	Bioreactor	Max. volume
Boa-san et al.	2009	BM MSC, h	Cytodex 3	n.d.	n.d.
Boo et al.	2011	BM MSC, rb	Cytodex 1	spinner flask	25 ml
dos Santos et al.	2011	(BM)MSC, h	CultiSpher-S	spinner flasks	50 ml
Eibes et al.	2010	BM MSC, h	CultiSpher-S	spinner flask	n.d.
Elsberg et al.	2012	MSC-TERT cell line, h	glass surface	stirred bioreactor, reg	1.68 l
Ferrari et al.	2012	BM MSC, p	Cytodex 1	spinner flask	200 ml
Frauenschuh et al.	2007	BM MSC, p	Cytodex 1, 2 & 3	spinner flask	40 ml
Hewitt et al.	2010	placenta MSC, h	Cytodex 3	spinner flask	250 ml
Kedong et al.	2010	co-culture UCB-HSCs & MSCs, h	glass coated polystyrene	spinner flask rotating wall vessel	100 ml 40 ml
Park et al.	2010	BM MAPC, r	Cytodex 1	spinner flask	100 ml
Rivkin et al.	2007	BM MSC, m	fibrin microbeads	rotating polypropylene tube	n.d.
Sart et al.	2010	ear MSC, r	CultiSpher-S, Cytodex 3	spinner flask	100 ml
Sart et al.	2009	ear & BM MSC, r	CultiSpher-S	spinner flask	1 l
Sart et al.	2012	ear MSC, r	(gelatin-coated) CultiSpher-S, Cytodex 3, Cytopore 2, Chitosan	spinner flask	100 ml
Schop et al.	2010	BM MSC, h	Cytodex 1&3, ProNectionF, Plastic Plus, Collagen, Plastic, Glass, HillexII,FACTIII,	spinner flask	50 ml
Schop et al.	2008	BM MSC, g	Cytodex 1	spinner flask	50 ml
Serra et al.	2008	pancreatic SC, cell line, r	Cytodex 1 & 3	stirred bioreactor, reg	250 ml
Sun et al.	2010	BM MSC, h	CultiSpher-G	spinner flask	200 ml
Timmins et al.	2012	placenta MSC, h	CultiSpher-S	CultiBag	500 ml
Tseng et al.	2012	BM MSC, h	collagen-coated and non-coated Solohill polystyrene microcarrier	petri dishes	n.d.
Weber et al.	2007	MSC-TERT cell line, h	Biosilon, Cytodex 1&3, P102-L, Rapidcell	spinner flask	250 ml
Weber et al.	2010	MSC-TERT cell line, h	non-porous glass spheres	fixed-bed bioreactor	300 ml
Yang et al.	2007	BM MSC, r	CultiSpherS, Cytodex1, Cytopore 2	spinner flask	n.d.
Yang et al.	2010	BM MSC, h	PNIPAAM-coated Cytodex 3	spinner flask	30 ml
Yu et al.	2009	placenta MSC, h	Cytodex 3	stirred bioreactor	n.d.
Yuan et al.	2012	BM MSC, h	CultiSpher-S	spinner flask	125 ml
Zangi et al.	2006	BM MSC, r	fibrin microbeads	rotating polypropylene tubes	10 ml

1.5 Stimuli-responsive Polymers

As noted above, the expansion process is crucial for quality and properties of the manufactured biopharmaceutical product. This section discusses thermoresponsive polymers and their potential to improve expansion culture of adherent cells such as MSCs. Transferring the thermoresponsive polymer technology to microcarrier-based MSC expansion would provide a promising approach for combining the advantages of both technologies in an innovative expansion process (see Figure 4). To my knowledge, only one study has so far investigated MSC expansion on thermoresponsive microcarriers (Yang et al., 2010b).

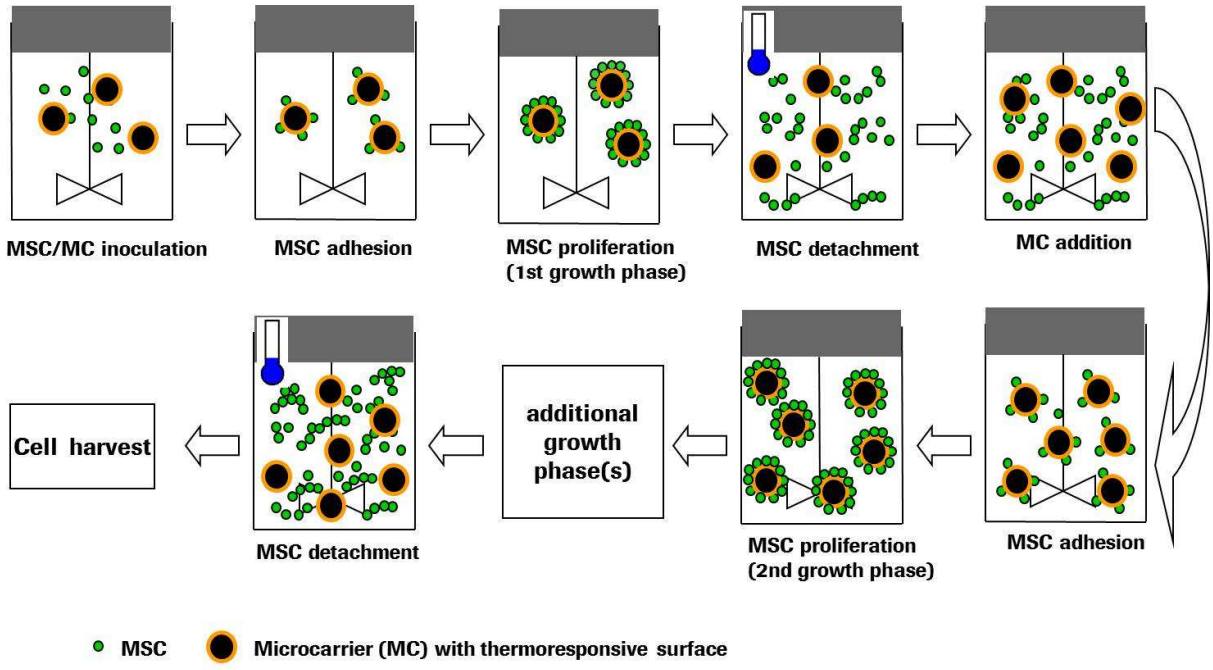

Figure 4: Advanced expansion process on thermoresponsive microcarriers. In contrast to the basic expansion process in Figure 3, the harsh enzymatic detachment can be avoided by temperature induced MSC detachment leading to a new, innovative expansion process.

1.5.1 Introduction

Polymers that can alter their physicochemical properties in response to external stimuli are of great interest in many disciplines, ranging from engineering (Barker et al., 2000) to textile industry (Crespy and Rossi, 2007) to medicine (Ward and Georgiou, 2011). In particular, such stimuli-responsive or “smart” polymers are being developed for biomedical applications such as drug delivery (Bajpai et al., 2008), tissue engineering (Yamato et al., 2001), chromatography (Maharjan et al., 2008), gene delivery (Twaites et al., 2005) or cell culture (Takezawa et al., 1990).

Various stimuli, such as temperature, mechanical stress, pH value, or light, can influence the properties of "smart" polymers (Gil and Hudson, 2004). Since temperature is a parameter which can be controlled easily both *in* and *ex vivo,* temperature-responsive polymers provide the biggest group of stimuli-responsive polymers (Gil and Hudson, 2004). Depending on the temperature, the polymers can undergo reversible conformational changes: at temperatures above their lower critical solution temperature (LCST), the polymers are present in a hydrophobic, globule conformation and precipitate from solution. By lowering the temperature below the LCST, the polymers switch to a hydrophilic, coil conformation and become soluble (see Figure 5). This coil-to-globule transition is fully reversible and driven by interactions of polymer chains and solvent (e.g. water) molecules (Smith and Bedrov, 2003). At temperatures below the LCST, hydrogen bonds between water and polymer molecules lead to hydration and dissolving of the polymer. Upon increasing the temperature above the LCST, the polymer-water interactions are diminished whereas hydrophobic intra- and intermolecular polymer interactions become entropically favorable. Macroscopically, this leads to precipitation of the polymers, which also allows for LCST determination of polymers in bulk solution by cloud point measurements (Boutris et al., 1997).

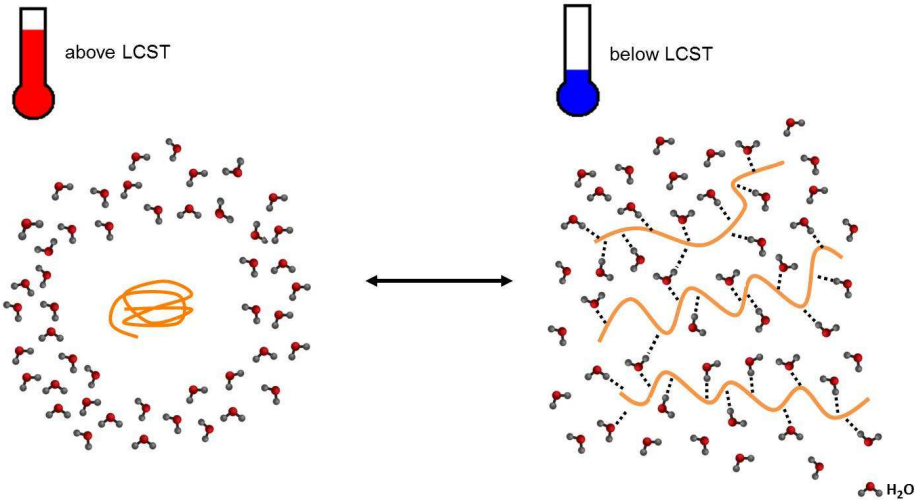

Figure 5: LCST-dependent, reversible solubility and conformational changes of thermoresponsive polymers. Left: globule, aggregated polymer; right: hydrated polymer in coil conformation. LCST lower critical solution temperature.

From a thermodynamic perspective, the LCST phenomenon is associated with a negative mixing entropy ΔS and a negative (i.e. exotherm) mixing enthalpy ΔH for solutions of thermoresponsive polymers (Smith and Bedrov, 2003). According to

$$\Delta G = \Delta H - T\Delta S \qquad \textbf{Equation 1}$$

ΔG (Gibbs free energy) is negative at low temperatures (below the LCST). With increasing temperature T, ΔG increases and eventually, at temperatures above the LCST, ΔG becomes positive which results in phase separation of polymer and solvent and polymer precipitation.

The thermoresponsive polymer studied most extensively is poly(N-isopropylacrylamid) (PNIPAAM). PNIPAAM has a LCST around 32 °C, i.e. in a physiologically relevant range, which makes it especially interesting for biomedical applications. Besides to PNIPAAM, polyethylene glycol (PEG) is often employed for biomedical applications (Ward and Georgiou, 2011). Other polymers from classes such as poly(dialkyl vinylphosphonate)s (PDAVP) and poly(2-oxazoline)s (POx) also show thermoresponsive behavior (Zhang et al., 2012b) (Diehl and Schlaad, 2009). The molecular structures of the mentioned polymers are depicted in Figure 6.

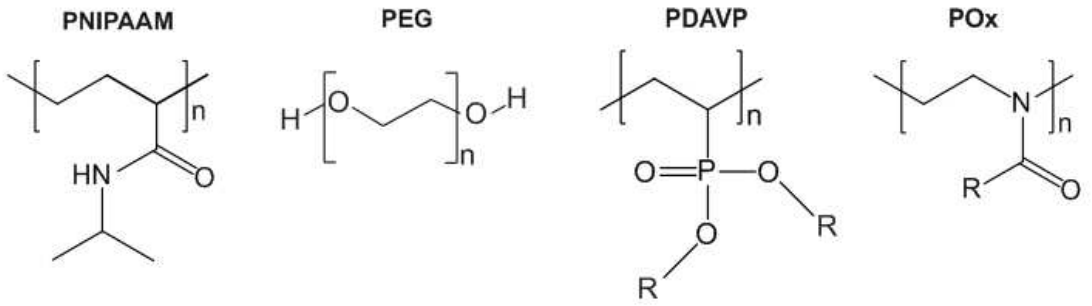

Figure 6: Thermoresponsive Polymers. PNIPAAM poly(N-isopropylacrylamid); PEG polyethylene glycol; PDAVP poly(dialkyl vinylphosphonate); P(Ox) poly(2-oxazoline).

1.5.2 Thermoresponsive Polymers for Cell Culture

Adherent cells such as MSCs are commonly detached from surfaces by proteolytic enzymatic treatment, use of chemical dissociation buffers containing chelating agents or mechanical scraping (Heng et al., 2009, Batista et al., 2010). However, such treatment can destroy cell membranes, surface molecules and ECM, leading to reduced cell viability or impaired cell function (Canavan et al., 2005a, Canavan et al., 2005b, Batista et al., 2010). Thermoresponsive surfaces allow temperature-controlled cell detachment, thereby providing an attractive technology to avoid harsh enzymatic treatment (see Figure 7). In particular, this technology may have a major advantage for clinical applications of MSCs which requires harvest of high-quality and functional cells as the cells themselves are the therapeutic product. By coating or grafting to surfaces, the switchable property of thermoresponsive polymers can be transferred to the surfaces, resulting in temperature-dependent changes of the surface hydrophobicity. Depending on the cell type, there is an optimum range of hydrophobicity for cell attachment and standard tissue culture treated polystyrene surfaces display contact angles of 48° to 56° (Dewez et al., 1998, Curtis et al., 1983, Saltzman, 2000). Therefore, cell attachment and detachment can be controlled by temperature regulation; at temperatures above the LCST, where the surface is hydrophobic, cells readily adhere to the surface. By temperature reduction below the LCST, the polymeric surface becomes hydrophilic and cells detach from the surface.

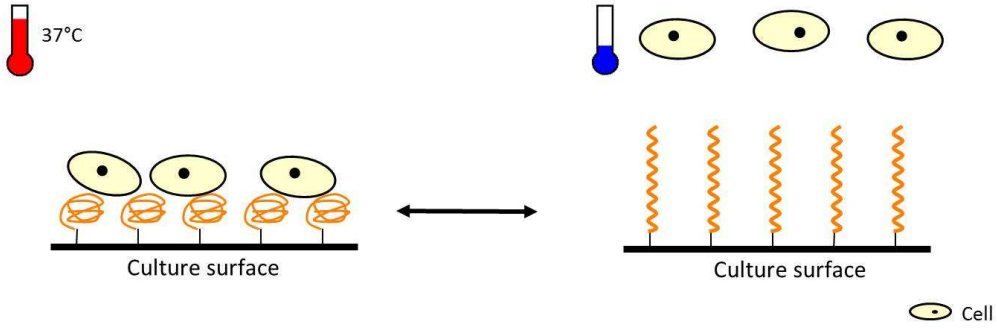

Figure 7: Temperature-induced cell detachment from thermoresponsive surfaces.

Having an LCST of 32 °C, PNIPAAM is a well suited thermoresponsive polymer for cell culture purposes. Most cells are cultured at 37 °C, i.e. above the LCST of PNIPAAM, where PNIPAAM-coated surfaces are more hydrophobic and cells can attach. By lowering the temperature below 32 °C, cells can be detached as it has been shown for many different cells such as hepatocytes (Yamada et al., 1990), smooth muscle cells (Chen et al., 2008), endothelial cells (Kushida et al., 1999) or BM MSCs (Yang et al., 2012).

The mechanism of cell attachment and detachment has been recently evaluated by theoretical analysis of Halperin and Kroger (Halperin and Kroger, 2012). According to their model, at temperatures above the LCST, ECM proteins derived from serum or produced by the cells themselves favor binding to the hydrophobic surface and cell attachment is mediated through integrin binding to ECM proteins (focal adhesions, see Figure 8). In focal adhesions, distances between the ECM-coated surface and cell membrane were found to be about 25 nm (Iwanaga et al., 2001). Upon temperature decrease below the LCST, hydration leads to swelling of the polymer layer, thereby pushing away cells from the surface. While focal adhesions are maintained, this results in constraints of the polymer brush layer by the cell membrane. This in turn generates an upward force f_{cell} (Figure 9b). f_{cell} leads to tension and eventually dissociation of integrin-ECM binding, thus releasing cells from the surface (Figure 9b and c). Additionally, f_{cell} can also lead to cell detachment with ECM proteins bound to the cells. Evidence for both, detachment with ECM bound to cells or surface, has also been observed experimentally (Canavan et al., 2005b). In addition to this passive detachment of cells, active cellular processes have been found to be involved, including cellular metabolism, signal transduction, and cytoskeletal remodeling (Okano et al., 1995, Yamato et al., 1999).

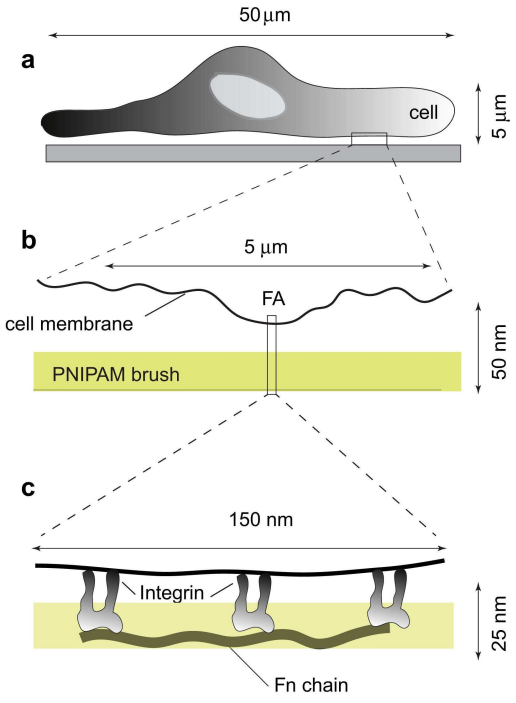

Figure 8: Schematic illustration of cell attachment to thermoresponsive surfaces. Different magnification of cell attachment to thermoresponsive surfaces at 37 °C according to the model of Halperin and Kroger (a). Cells adhere to surface via focal adhesions (FA, b), i.e. through integrin-mediated binding to surface adsorbed ECM proteins (c). Fn fibronectin (ECM protein). Figure adopted from Halperin and Kroger, 2012.

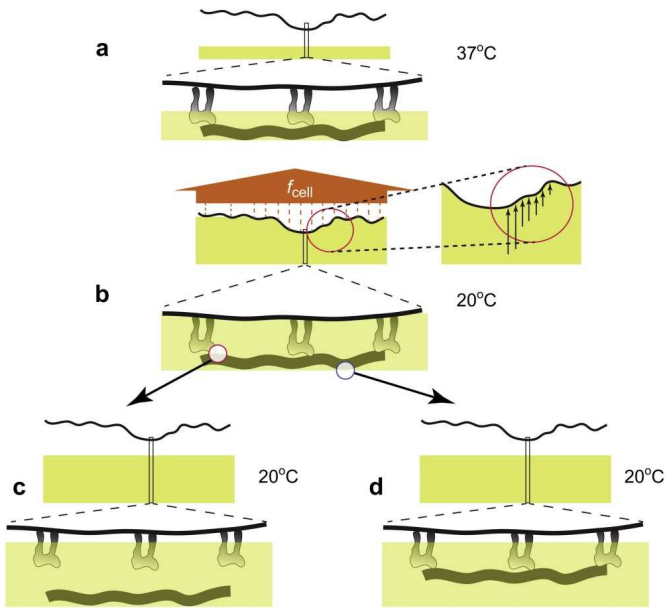

Figure 9: Schematic illustration of cell detachment from thermoresponsive surface. At 37 °C, cells adhere to collapsed polymer brush (a). Upon cooling, the polymer layer swells, generating the upward force f_{cell} which pushes against the cell wall of adhering cells (b). Eventually, f_{cell} leads to dissociation of integrin-ECM binding (c) or complete detachment of the ECM (ECM bound to cells, d). Adopted from Halperin and Kroger, 2012.

Starting in 1990, Okano and colleagues have established a thermoresponsive surface based on PNIPAAM (Yamada et al., 1990). Their research led to development of the commercially available UpCell^{TM} surface (Nunc, ThermoScientific). This PNIPPAM-based surface has been successfully used for cultivation of many cell types. While single cell harvest from this surface is highly dependent on cell density, a focus of application is cell sheet production for tissue engineering. For this, temperature-induced detachment is well suited as intracellular contacts are preserved. Some of the produced cell sheets have already entered clinical settings in ophthalmology or reconstructive plastic surgery (Nishida et al., 2004, Yamato et al., 2007).

PNIPAAM-coated surfaces are widely produced using radiation-induced grafting methods. Additionally, surface initiated living radical polymerization methods have been developed more recently as reviewed by Nagase et al. (Nagase et al., 2009).

PNIPAAM-coated cell surfaces remain the only commercially available thermoresponsive surface up to date, but other thermoresponsive polymers and co-polymers have been investigated as cell culture surface coatings (Gil and Hudson, 2004). As reviewed by Gil and Hudson, some of the research focuses on controlling the LCST by introduction of co-monomers or introduction of bioconjugates, in particular RDG peptides, for controlled cell attachment (Gil and Hudson, 2004). Besides coated-surfaces, thermoresponsive polymers are also employed for hydrogel-based cell cultures (Li et al., 2012, Zhang et al., 2013).

2 Objective of This Work

Expansion of mesenchymal stem cells (MSCs) is an essential prerequisite for the development of an “off-the-shelf” cell product and its application in clinical therapy since the number of MSCs isolated from tissue is extremely small compared to the large number of cells administered to patients. Moreover, as the manufacturing process determines properties and quality of the biopharmaceutical product, tight process control and monitoring is essential. State of the art cell culture technologies, however, have several drawbacks which make them unfavorable for large-scale expansion of a clinical cell product. Microcarrier-based cultivation in stirred bioreactors provides excellent means for a GMP-compliant expansion process of adhesion-dependent cells. Therefore, a scalable microcarrier-based expansion process for MSCs is to be developed in this work. It is well-known that cultivation conditions may alter cell fate and function (Wagner and Ho, 2007). Yet a detailed evaluation of the influence of microcarrier-based expansion on MSC characteristics and functions, as compared to standard cultivation methods, is still missing in the field. Thus, a central aim of this thesis is the comparative analysis of MSCs from two different sources and three donors expanded on microcarriers or in standard cell culture flasks. In particular, this study shall go beyond evaluation of minimal MSC criteria as defined by the International Society for Cellular Therapy (ISCT) (Dominici et al., 2006) and include analysis of extended phenotype, immunomodulatory function, morphology, secretion of growth factors and cytokines, and gene expression patterns.

Furthermore, a crucial point regarding cultivation of adhesion-dependent cells is the need for cell dissociation from the culture surface for harvest or passaging. As traditional enzymatic or mechanical detachment methods can be cell damaging, alternative methods are highly desired in an MSC manufacturing process to ensure product quality and properties. Therefore, an aim of this work is the evaluation of temperature-induced MSC detachment from thermoresponsive surfaces. In addition to commercially available PNIPAAM-coated surfaces, newly developed thermoresponsive surfaces shall be assessed regarding MSCs attachment, proliferation and detachment.

3 Results

3.1 Process Development and Optimization

Clinical administration of MSCs requires large quantities of cells. However, this demand is opposed by the limited number of cells that can be obtained by isolation from tissue. Therefore, a crucial step in developing an allogeneic, “off-the-shelf” therapeutic MSC product is the establishment of a GMP-compliant MSC expansion process. Bioreactors provide optimal means for a controllable, reproducible, scalable and cost-efficient expansion process and, by combination with microcarriers, they allow for cultivation of adherent cells such as MSCs.

3.1.1 Evaluation of Different Microcarriers for MSC Expansion

An essential first step in developing a microcarrier-based expansion process is the selection of a suitable microcarrier type. For the work presented here, microcarriers should not only be non-toxic and stable in cell culture over long periods of time but also be made of animal-free materials as this reduces the risk of transmission of infectious pathogens or xenogenic proteins. Xenogenic proteins can induce severe immune reactions in patients. Furthermore, only microporous, but not macroporous, microcarriers were considered. While macroporous microcarriers provide protection of shear stress for cells growing inside porous, they also bear the risk of 3D cell growth which may lead to undesired cell differentiation (Datta et al., 2006, Holtorf et al., 2005). Additionally, nutrient supply may be hampered for cells growing inside porous and cell harvest is also more difficult than from microporous microcarriers (GE Healthcare, 2005). From the various commercially available microcarriers, six different microcarriers were pre-selected (s. Table 5). These microcarriers were evaluated for their suitability to support UC and AM MSC attachment and proliferation. Evaluation consisted of microscopic monitoring of cell proliferation, cell number determination, metabolite measurements, and determination of viable and metabolically active cells.

Table 5: Overview of different microcarriers evaluated in this work.

	Core material	Surface coating	Charge	Density [g/ml]	Size [µm]
Cytodex 1 (GE Healthcare)	cross-linked dextran	positively charged N,N-diethylaminoethyl groups	+	1.03	147 - 248
2D Microhex (Nunc)	polystyrene	Nunclon Δ surface	n.d.	1.05	sides 125, thickness 25
Plastic (Solohill)	crosslinked polystyrene	none	none	1.02	125 - 212
Plastic Plus (Solohill)	crosslinked polystyrene	none	+	1.026 +/- 0.004	125 - 212
Glas (Solohill)	crosslinked polystyrene	high silica glass	none	1.026 +/- 0.004	125 - 212
Hillex II (Solohill)	modified polystyrene	cationic trimethyl ammo-nium	+	1.09 - 1.15	160 - 200

For microscopic monitoring, cells were fluorescently labeled at different days of expansion in order to estimate cell attachment and growth on the different microcarriers (s. Table 5). For both UC and AM MSCs, cell attachment was low and the majority of microcarriers remained cell-free 1 d after inoculation (Figure 10). UC MSCs attached well to Cytodex 1, 2D Microhex, and Glas microcarriers whereas no or only very rare cell adhesion to Hillex II, Plastic, or Plastic Plus microcarriers was observed. At the end of expansion (day 9), UC MSC proliferation was highest on Cytodex 1 microcarriers. Cell proliferation on Glas microcarriers resulted in formation of microcarrier-cell aggregates (Figure 10, day 9). Cell growth on 2D Microhex microcarriers was very low. For AM MSCs, no cell attachment and/or proliferation was observed on Hillex II, Plastic Plus, Glas, and 2D Microhex microcarriers (Figure 10B). Few cells attached to Plastic microcarriers. As for UC MSCs, attachment and proliferation for AM MSCs was highest on Cytodex 1 microcarriers.

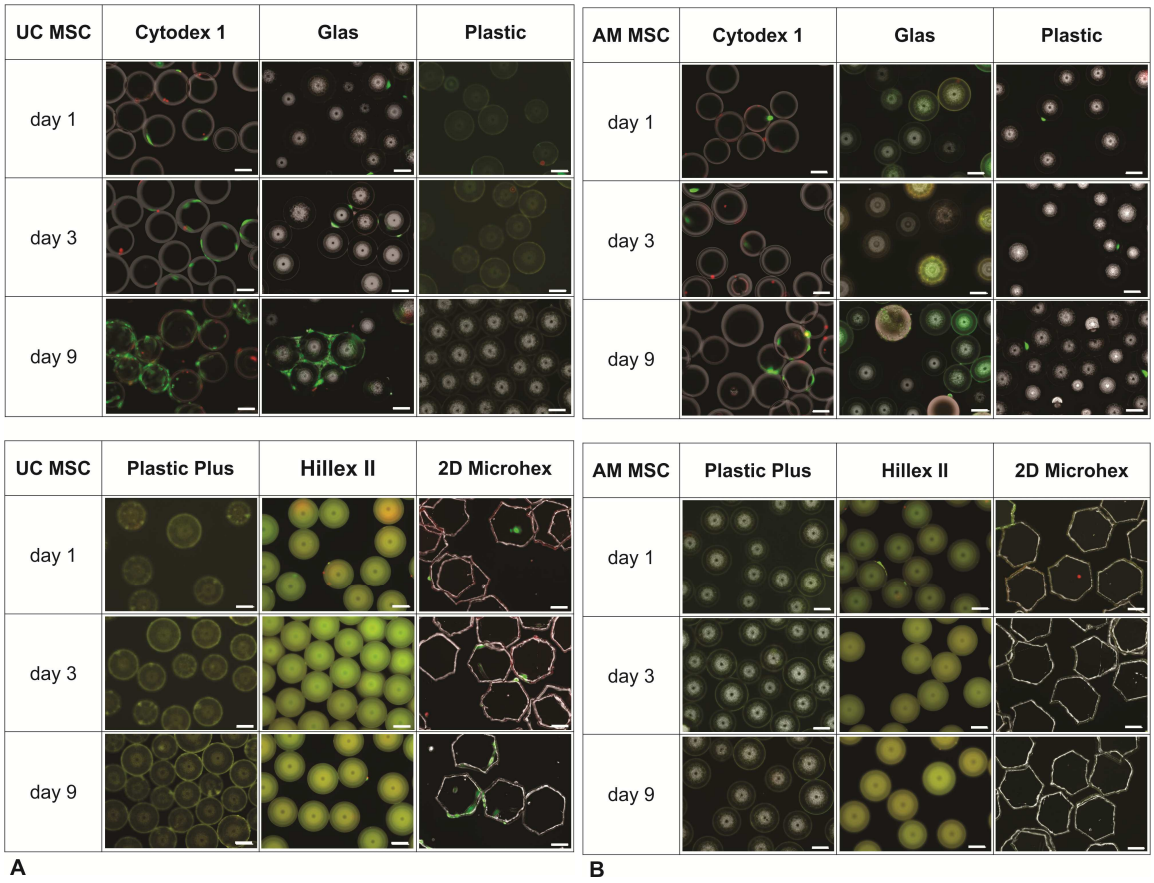

Figure 10: Microscopic evaluation of cell proliferation on six different microcarriers. UC (A) or AM (B) MSCs were expanded on microcarriers in spinner flasks. On day 1, 3, and 7 after inoculation, a homogenous sample of the respective cell-microcarrier suspension was drawn and cells were stained using the fluorescent dyes calcein (living cells, green) and ethidium homodimer (dead cells, red). Hillex II microcarriers showed unspecific fluorescence. Scale bar: 100 µm.

The microscopic observations are in accordance with measurements of metabolic activity using AlamarBlue®. As only viable cells can metabolize the AlamarBlue® dye, this assay allows correlating fluorescence intensity and cell viability (Schreer et al., 2005). As depicted in Figure 11, the highest number of metabolic active and hence viable UC MSCs was observed using Cytodex 1 microcarriers, followed by 2D Microhex and Glas microcarriers. For AM MSCs, viability was highest for cells expanded on Cytodex 1 and Plastic microcarriers. The AlamarBlue® Assay was not applicable with Hillex II microcarriers as these microcarriers absorbed the assay's dye.

Cell number determination after 9 days of expansion revealed similar cell counts for UC MSCs expanded on Cytodex 1 and Glas microcarriers (Figure 11; 5200 cells/cm² and 5400 cells/cm², respectively) whereas only 2100 cells/cm² cells were counted on 2D Microhex microcarriers. For AM MSCs, cell numbers after 10 days were in general much

lower compared to UC MSCs. Cell count was highest for AM MSCs expanded on Plastic microcarriers (660 cells/cm²) followed by Cytodex1 microcarriers (220 cells/cm²).

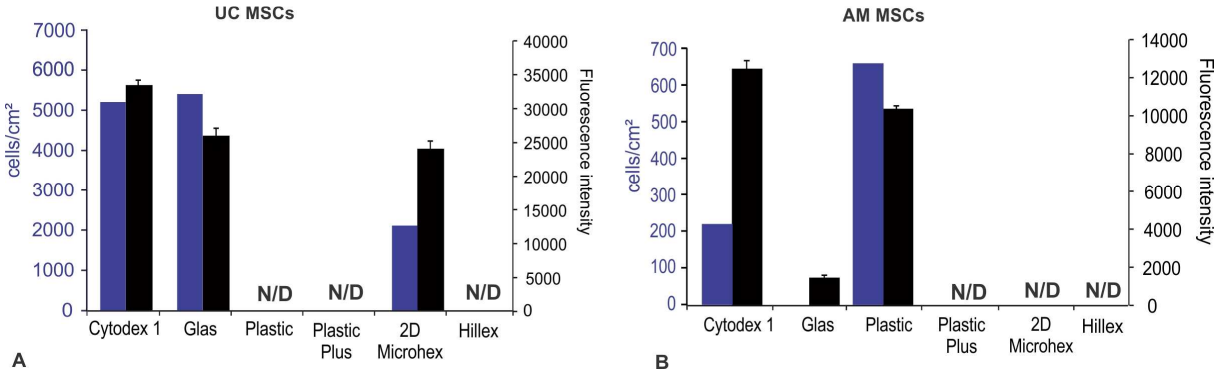

Figure 11: Cell number and metabolic activity of cells expanded on six different microcarriers. Cell numbers (blue) of UC MSCs (A) or AM MSCs (B) cultivated on Cytodex 1, Glas, Plastic, Plastic Plus, Hillex II, or 2D Microhex microcarriers were determined by enzymatic detachment and subsequent counting of cells. Metabolic activity (black) of MSCs expanded on microcarriers was evaluated by measuring the fluorescence intensity resulting from reduction of resazurin (AlamarBlue®). Fluorescence intensities were determined on day 6 after inoculation by excitation at 535 nm, emission at 590 nm. Intensities were background-corrected (medium only). AlamarBlue® measurements were performed in triplicates. N/D not determined due to too low cell number or intensity below background.

Determination of cell numbers on microcarriers was hampered by a relatively high loss of cells during the harvest procedure. Thus, an additional method to monitor cell growth which does not require enzymatic cell detachment was employed. As cell numbers correlate with glucose consumption and lactate production rates (Meuwly et al., 2006, Zhang et al., 2011), both parameters were calculated for UC and AM MSCs. In accordance with previous results from cell counts and metabolic activity, the glucose consumption rate was highest for UC MSCs expanded on Cytodex 1 (60 µmol/l/h) and Glas microcarriers (57 µmol/l/h), followed by 2D Microhex microcarriers (45 µmol/l/h). Virtually no glucose consumption was observed for the remaining microcarriers. In addition, production of the metabolite lactate was also highest for cells expanded on Cytodex 1 (107 µmol/l/h) and Glas microcarriers (94 µmol/l/h), followed by 2D Microhex microcarriers (82 µmol/l/h). As the previous data suggests, glucose consumption as well as lactate production of AM MSCs were only observed for cells expanded on Plastic and Cytodex 1 microcarriers (7 µmol/l/h, 16 µmol/l/h and 3 µmol/l/h, 11 µmol/l/h, respectively). Compared to UC MSCs, glucose consumption and lactate production rates were rather low, indicating that MSCs isolated from AM grew considerably slower than MSCs from UC.

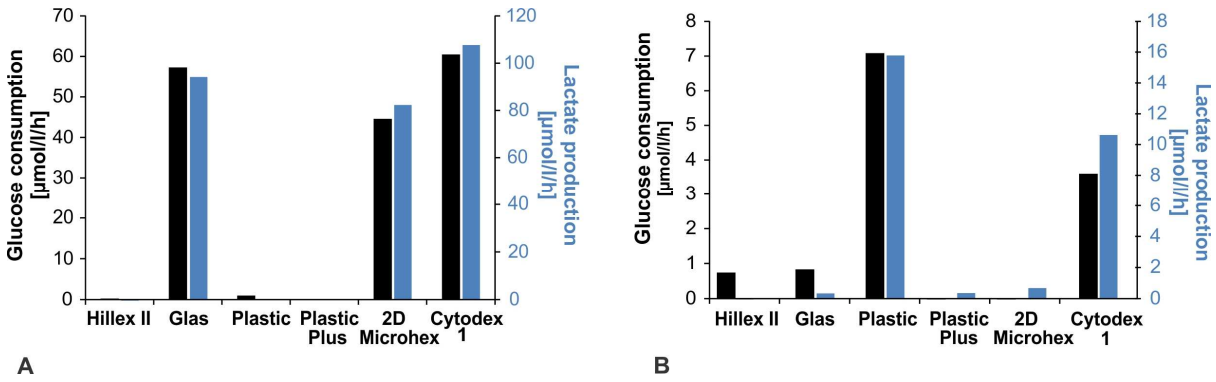

Figure 12: Glucose and lactate consumption rates of MSC on different microcarriers. Average glucose and lactate consumption rates from day 6 to 9 (UC MSCs, A) or day 6 to 10 (AM MSCs, B) were calculated according to Equation 4 for MSCs grown on different microcarriers.

In summary, these results indicated that Cytodex 1 microcarriers were best suitable for expansion of UC and AM MSCs. Therefore, all following experiments were performed using Cytodex 1 microcarriers.

3.1.2 Process Optimization: Inoculation of MSCs

As noted previously by different authors, initial cell attachment is a crucial step for obtaining high cell yields from microcarrier-based expansion processes (Yuan et al., 2012, Eibes et al., 2010, Frauenschuh et al., 2007, Shiragami et al., 1997). To optimize attachment of MSCs to Cytodex 1 microcarriers, different inoculation procedures were evaluated: I) 3 h intermitted stirring followed by continuous stirring, II) 1h intermitted stirring followed by overnight static cultivation, III) stirring for 2 min at 40 rpm followed by overnight static cultivation. The intermitted stirring step consisted of stirring at 40 rpm for 2 min followed by 30 min static cultivation for the respective time intervals for all three inoculation procedures. The effect of the different inoculation procedures was monitored microscopically, by determination of metabolic active and therefore viable cells, metabolite measurements, and cell count. Exemplary, inoculation was optimized using UC MSCs.

Cell attachment after one day was too low to determine differences between the three inoculation procedures by microscopic observation. However, after 4 d and especially after 7 d of expansion, differences between the procedures were observed (Figure 13). A static overnight incubation (II and III) resulted in higher cell proliferation compared to procedure I. Between procedures II and III, using single, 2 min stirring (procedure III) led to higher cell numbers than an initial 1 h intermitted stirring protocol (procedure II). These observations were confirmed by the total cell count and glucose consumption rates. Using procedure III resulted in highest cell yield (10×10^5 cells) and glucose consumption (45 µmol/l/h), followed by procedure II and I (Figure 13). In correlation to the glucose consumption rates, lactate production rates were also highest for procedure III.

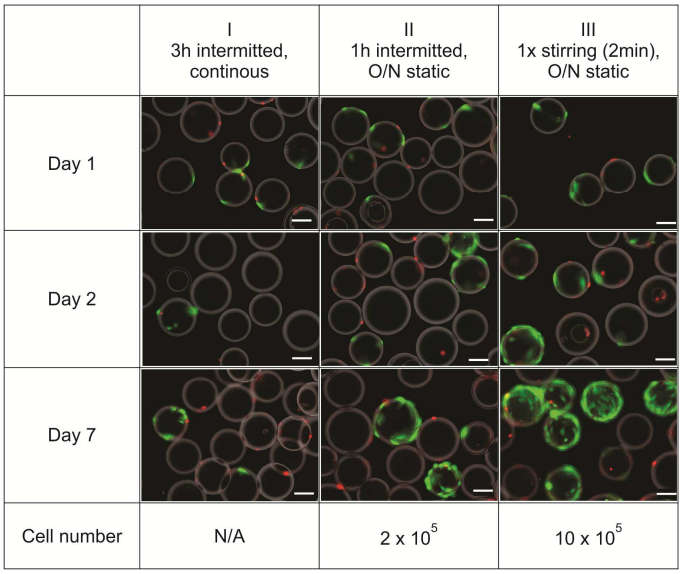

Figure 13: Evaluation of different inoculation procedures. UC MSCs were seeded at equal densities on Cytodex 1 microcarriers using three different inoculation procedures: I) 3 h intermitted stirring followed by continuous stirring, II) 1h intermitted stirring followed by overnight static cultivation, III) stirring for 2 min at 40 rpm followed by overnight static cultivation. Cells were stained using the fluorescent dyes calcein (living cells, green) and ethidiumhomodimer (dead cells, red). N/A = cell number too low for conclusive counting. Scale bar: 100 µm.

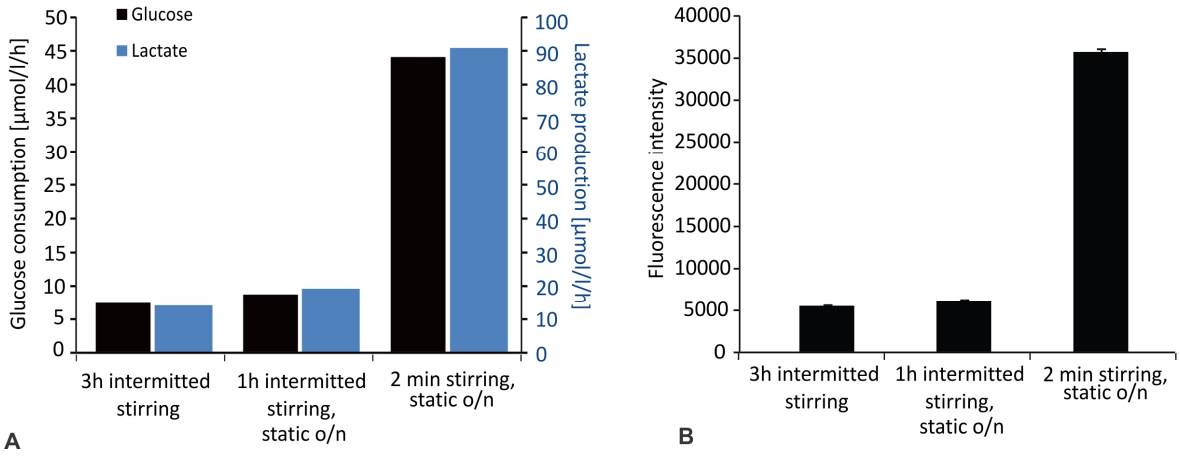

Figure 14: Influence of the inoculation procedure: Cell metabolism and metabolic activity. The average glucose consumption and lactate production rates from day 4 to day 7 of UC MSCs (n = 1) using different inoculation procedures were calculated (A). Cellular embolic activity, correlating with viability, was determined using the AlamarBlue® assay (B). Measurements were performed as technical triplicates on day 7. Fluorescence intensity resulting from reduction of resazurin (Alamar Blue) was determined by excitation at 535 nm, emission at 590 nm.

In addition, metabolic activity of cells on microcarriers was evaluated using the Alamar Blue assay. In accordance with the previous findings, inoculation procedure III led to the highest fluorescence intensity, with an approx. 7-fold increase compared to inoculation procedure I and II. This showed that procedure III (static overnight incubation after initial short stirring) did not only lead to the highest number of cells but that these cells were also viable.

In summary, an initial, 2 min stirring followed by static incubation (procedure III) led to better cell attachment and proliferation compared to strategies using an intermitted stirring profile followed by continuous stirring (procedure I) or static incubation (procedure II). Therefore, procedure III was employed for all following experiments.

3.2 MSC Expansion on Cytodex 1 Microcarriers: Characterization of the Cultivation Process

For developing a biopharmaceutical production process, characterization of basic cultivation parameters is essential. As it is widely acknowledged that the expansion process influences quality and properties of the final product, a comparative analysis of the microcarrier and flask expansion process was performed.

MSCs isolated from UC or AM were expanded on microcarriers in spinner flasks (stirring) or standard cell culture flasks (static). For both expansion methods, equal cell densities (1200 cells/cm²) and feeding regimes (50% medium exchange every other day) were applied. Based on previous results (see 3.1), expansions were performed using Cytodex 1 microcarriers and an inoculation procedure consisting of 2 min stirring followed by overnight static cultivation. For both cell sources, cells from three donors were evaluated during three independent cultivation runs to address run- and donor-dependent variations. UC and AM MSCs were isolated from the same donors (i.e. same genetic background). Figure 15 exemplary shows one cultivation run of UC and AM MSCs on Cytodex 1 microcarriers from all three donors. Keeping the ratio of cells per surface equal to flask expansion (1200 cells/cm²), microcarriers were inoculated with MSCs using a calculated ratio of about 1.2 cells/microcarrier, However, a majority of microcarriers remained cell-free after inoculation, even though the improved inoculation procedure (see 3.1.2) was used. Towards the end of cultivation, a higher fraction of microcarriers tended to be occupied by MSCs. Furthermore, cell-microcarrier aggregates started to form towards the end of the culture period. Cells were harvested preferably before severe aggregation was observed, as cells within aggregates may be deprived from sufficient nutrient and oxygen supply and might change their biological properties due to 3D growth (Datta et al., 2006). A second criterion for cell harvest was reaching of 80% cell confluence on the majority of cell-bearing microcarriers. For UC MSCs, this was on day 7 (donor 3), day 8 (donor 2) and day 10 (donor 1). AM MSCs were harvested on day 8 (donor 3), day 9 (donor 1) and day 10 (donor 2).

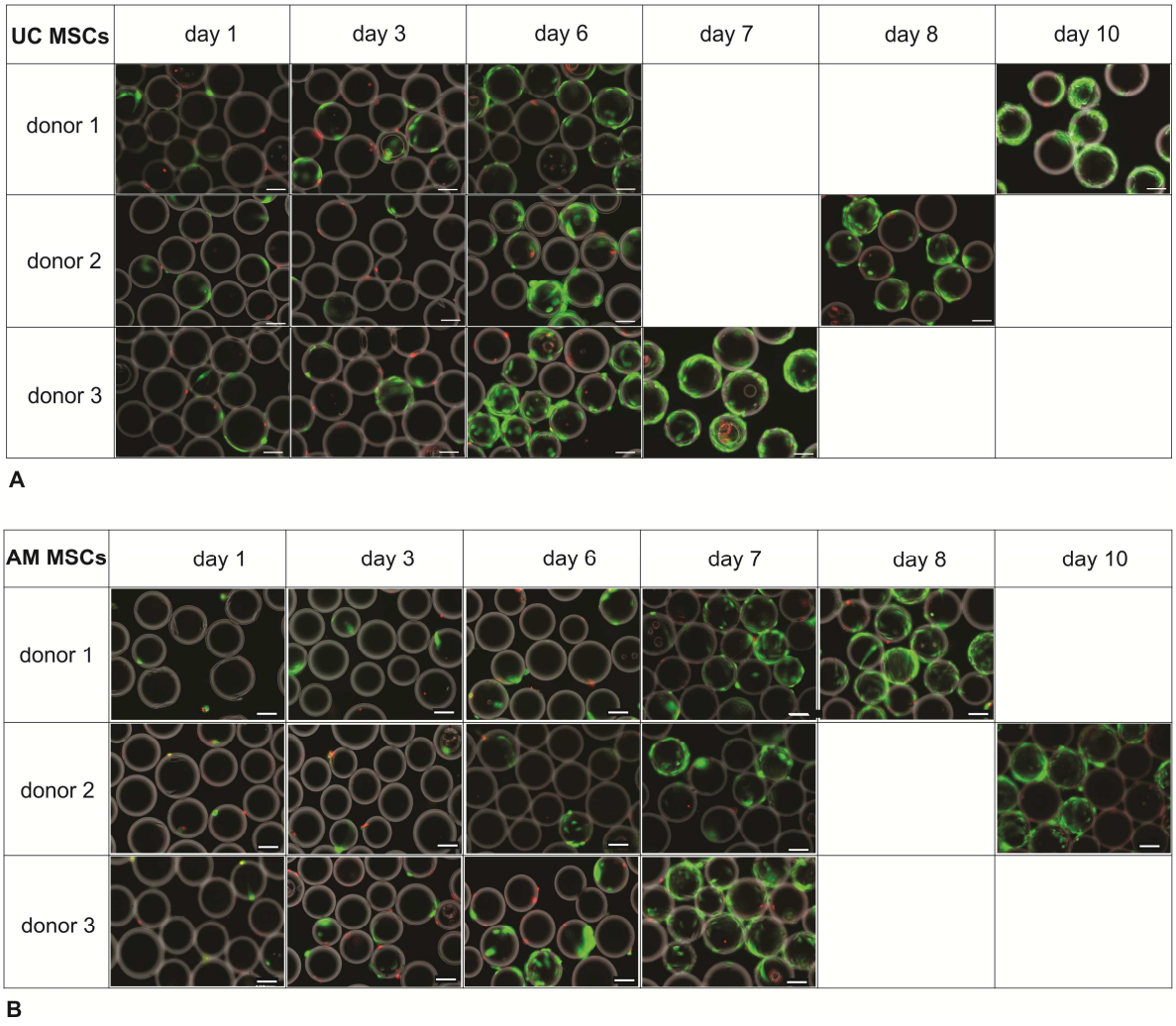

Figure 15: Expansion of MSCs Cytodex 1 microcarriers. UC (A) or AM MSCs (B) from three different donors were seeded at equal densities on Cytodex 1 microcarriers. Cells were stained on the respective days using the fluorescent dyes calcein (living cells, green) and ethidiumhomodimer (dead cells, red). Scale bar: 100 µm.

3.2.1 Cell Numbers, Population Doublings, and Doubling Time

Growth curves obtained for microcarrier-expanded UC and AM MCS showed an initial lag phase followed by an exponential phase (Figure 16). The lag phase is caused by cell attachment and adaption to culture conditions (Léo et al., 2008). For both sources, this phase is considerably long (3 to 4 days), probably due to the use of freshly thawed MSCs which require an elongated adjustment phase after inoculation. Cells did not enter the stationary phase, indicating that cultivation time was not long enough to lead to growth inhibition due to toxic metabolites or contact inhibition. As indicated by the standard deviation bars, variance between different expansions runs was rather high.

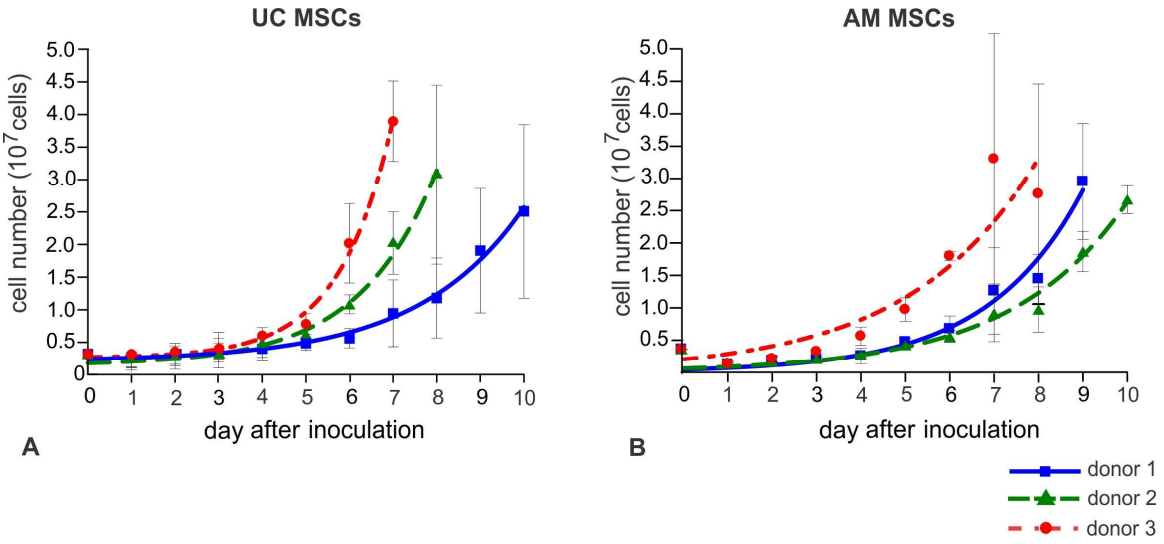

Figure 16: Growth of MSCs on Cytodex 1 microcarriers over time. Three donors of UC MSCs (A) and AM MSCs (B) were cultivated for the indicated times on Cytodex 1 microcarriers in spinner flasks. Cell numbers were determined by LDH measurements and growth curves were fitted using XLfit. Depicted are mean values with standard deviations of three independent expansions.

Based on the cell numbers, population doublings and doubling time for UC and AM MSCs of three different donors were calculated. Figure 17 and Figure 18 depict the calculated parameters of three independent cultivation runs for microcarrier- and flask-expanded cells of each donor. Comparing the two cell sources, differences in population doublings and doubling time were observed: UC MSCs showed faster cell growth than AM MSCs for both cultivation methods. Donor 3 showed the fastest growth parameters for both sources. In contrast, donor 2 of UC MSCs grew faster than donor 1, whereas for AM MSCs, cells from donor 1 grew faster than donor 2. Concerning the two different expansion methods, doubling times and population doublings of MSCs were generally comparable for microcarrier and flask expansions.

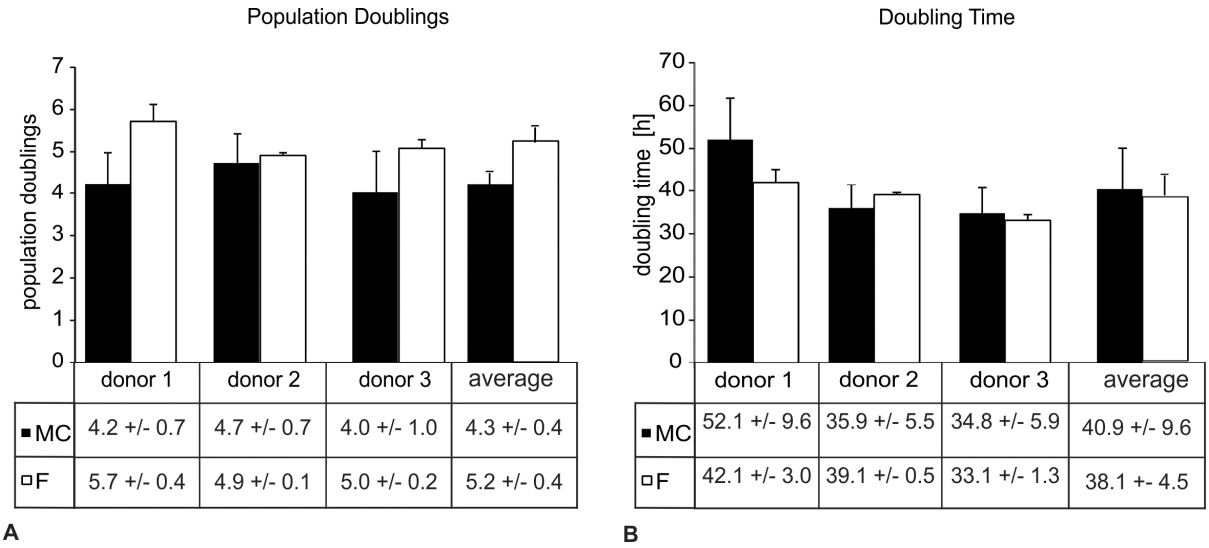

Figure 17: Population doublings and doubling time of UC MSCs. Comparison of population doubling (A) and doubling time (B) of microcarrier (MC)- and flask (F)-expanded cells. Black bars represent MC-expanded MSCs, white bars flask-expanded cells. Depicted are means with standard deviations of three independent runs per donor. Average values are calculated from all three donors.

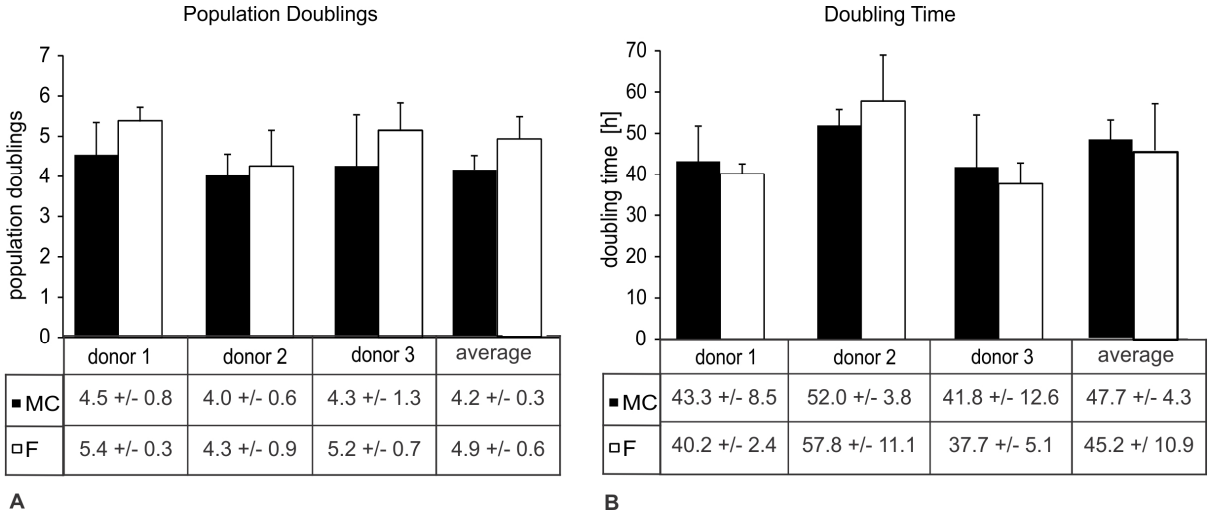

Figure 18: Population doublings and doubling time of AM MSCs. Comparison of population doubling (A) and doubling time (B) of microcarrier (MC)- and flask (F)-expanded cells. Black bars represent MC-expanded MSCs, white bars flask-expanded cells. Depicted are means with standard deviations of three independent runs per donor. Average values are calculated from all three donors.

3.2.2 pH Value and Osmolality

For process control, pH value and osmolality of the cultivation medium were monitored daily. For all three donors and both cultivation methods, the pH value decreased during the expansion period (Figure 19). For UC MSCs, no differences in the pH decrease between microcarrier and flask-expansion was observed. For AM MSCs, however, microcarrier expansion

tended to lead to a higher pH decrease than flask expansion. The drop in pH values correlated with the accumulation of lactate in the culture medium (see 3.2.3).

The osmolality of culture medium from both UC and AM MSCs was rather constant throughout the expansion period (Figure 20), ranging from 270 to 340 mOsmol/kg, thereby remaining in the osmolality range described for *in vitro* cultivation of mammalian cells (Waymouth, 1970, Lindl and Gstraunthaler, 2008a). These findings apply to both microcarrier- and flask-expanded MSCs of both cell sources.

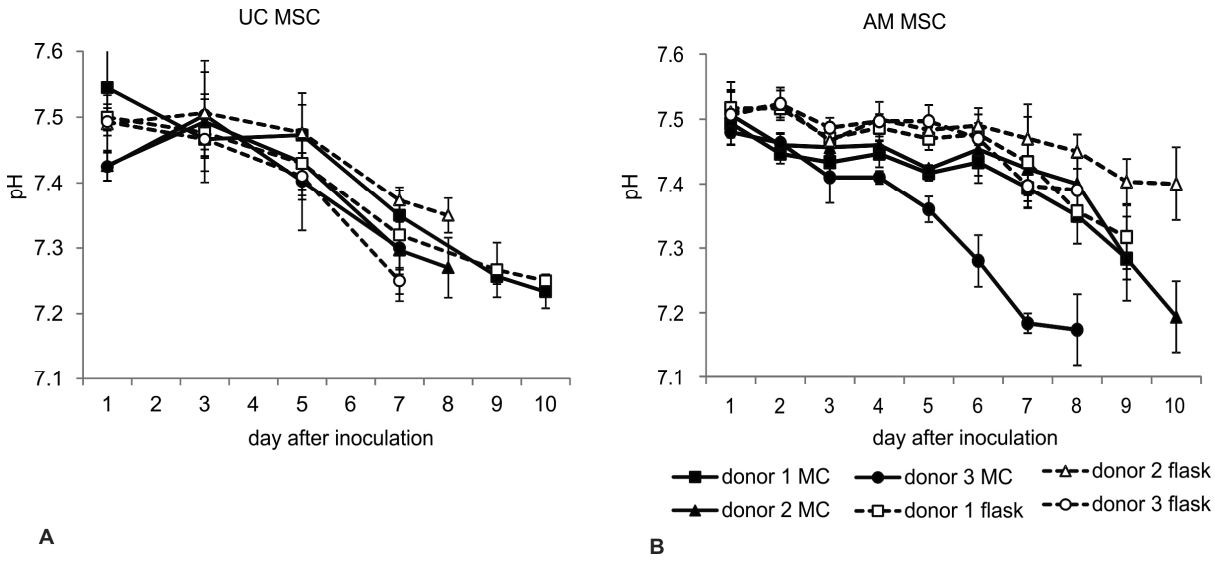

Figure 19: Analysis of pH values during expansion of microcarrier- and flask-expanded MSCs. (A) UC MSCs, (B) AM MSCs. Depicted are mean values +/- standard deviation of three independent runs per donor.

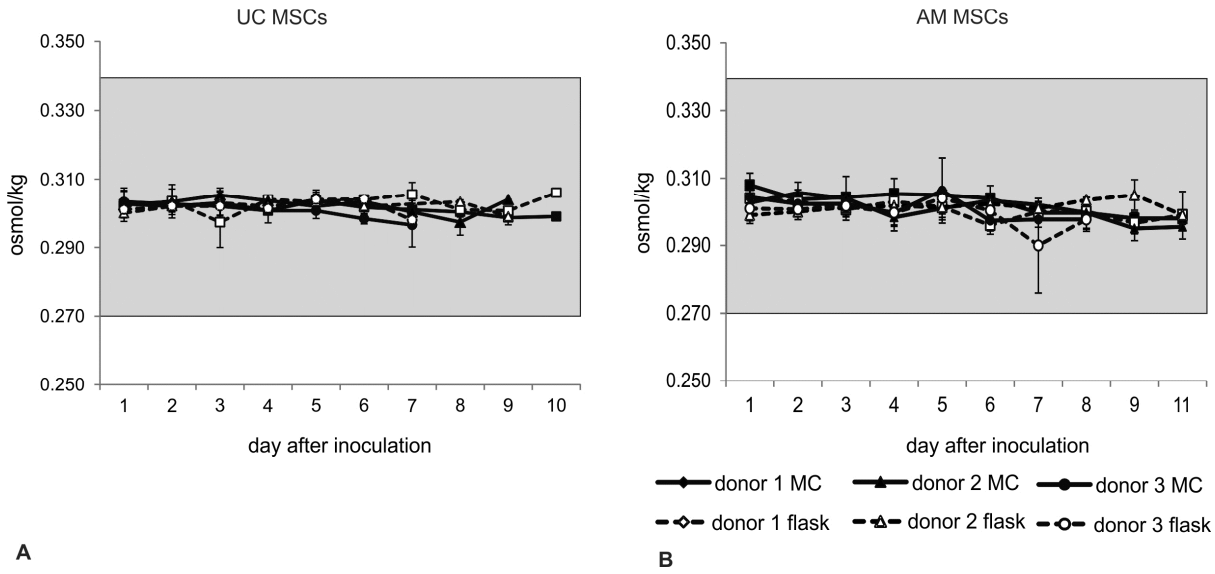

Figure 20: Analysis of osmolality of culture medium during expansion of microcarrier- and flask-expanded MSCs. (A) UC MSCs, (B) AM MSCs. Depicted are mean values +/- standard deviations of three independent runs per donor. Shading illustrates range commonly applied in mammalian cell culture.

3.2.3 Nutrients and Metabolites

Cellular metabolism was evaluated for UC and AM MSCs of three different donors during expansion on microcarriers or in cell culture flasks. Concentrations of glucose, lactate, ammonia, glutamate, sodium, and potassium in the culture medium were monitored over time (Figure 21 and Figure 22). For both cell sources and all donors, glucose concentrations decreased over cultivation time, correlating with an increase in lactate and the increase in cell numbers (see 3.2.1). Glucose concentrations in cell culture medium from microcarrier-expanded MSCs tended to be lower than concentrations from flask expansion, which is due to the higher cell concentration per medium volume in microcarrier expansion. During the end of cultivation, glucose concentrations tended to decrease below the detection limit. This indicated that, even though part of the medium was exchanged every other day, nutrient supply was not sufficient and additional glucose should be provided during cultivation.

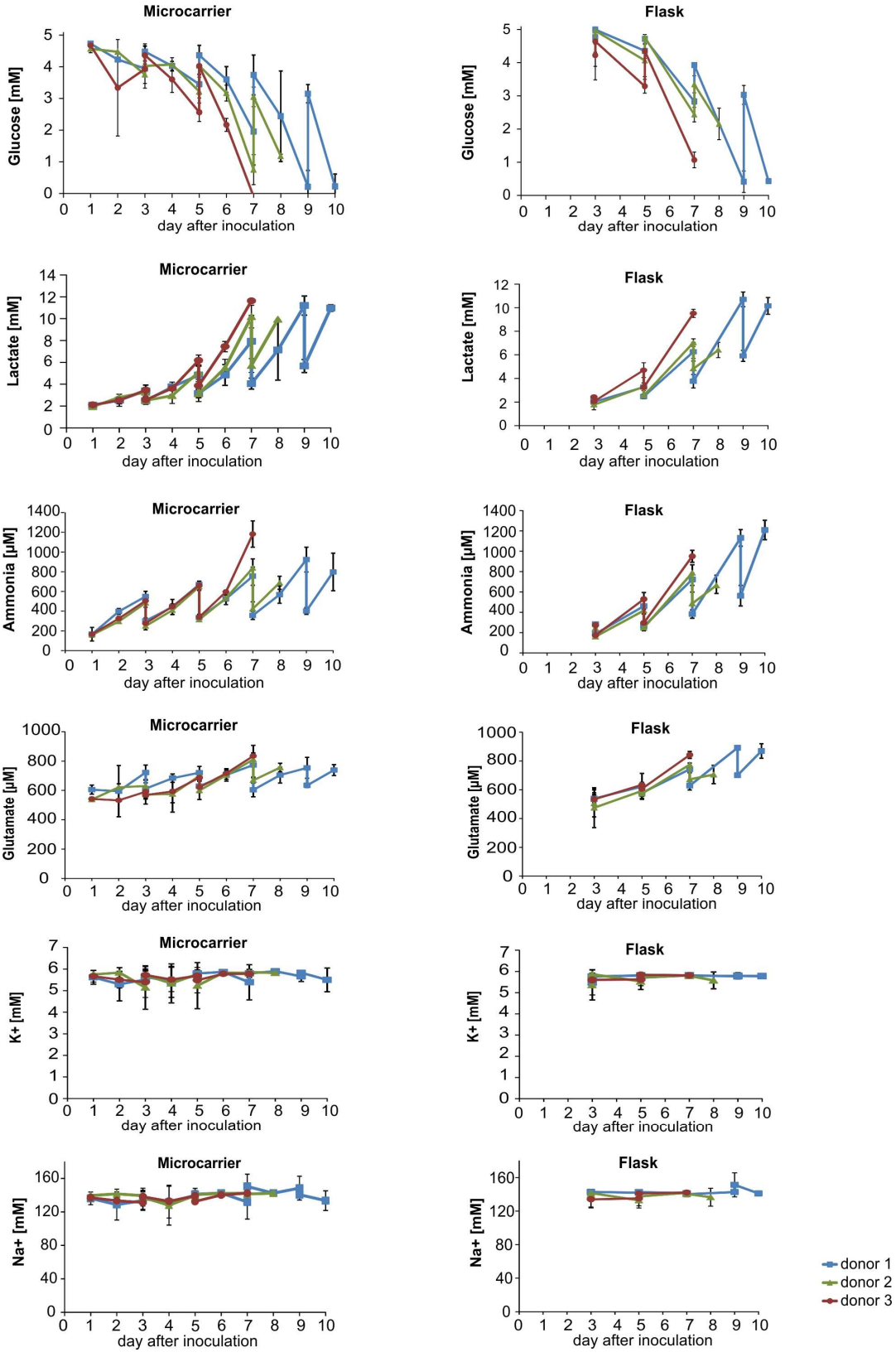

Figure 21: UC MSC metabolism. Glucose, lactate, ammonia, glutamate, potassium, and sodium concentrations were determined in microcarrier cultures (left) or flask cultures (right) for three different donors. For each donor, three independent expansion runs were performed. Depicted are mean concentrations with standard deviations.

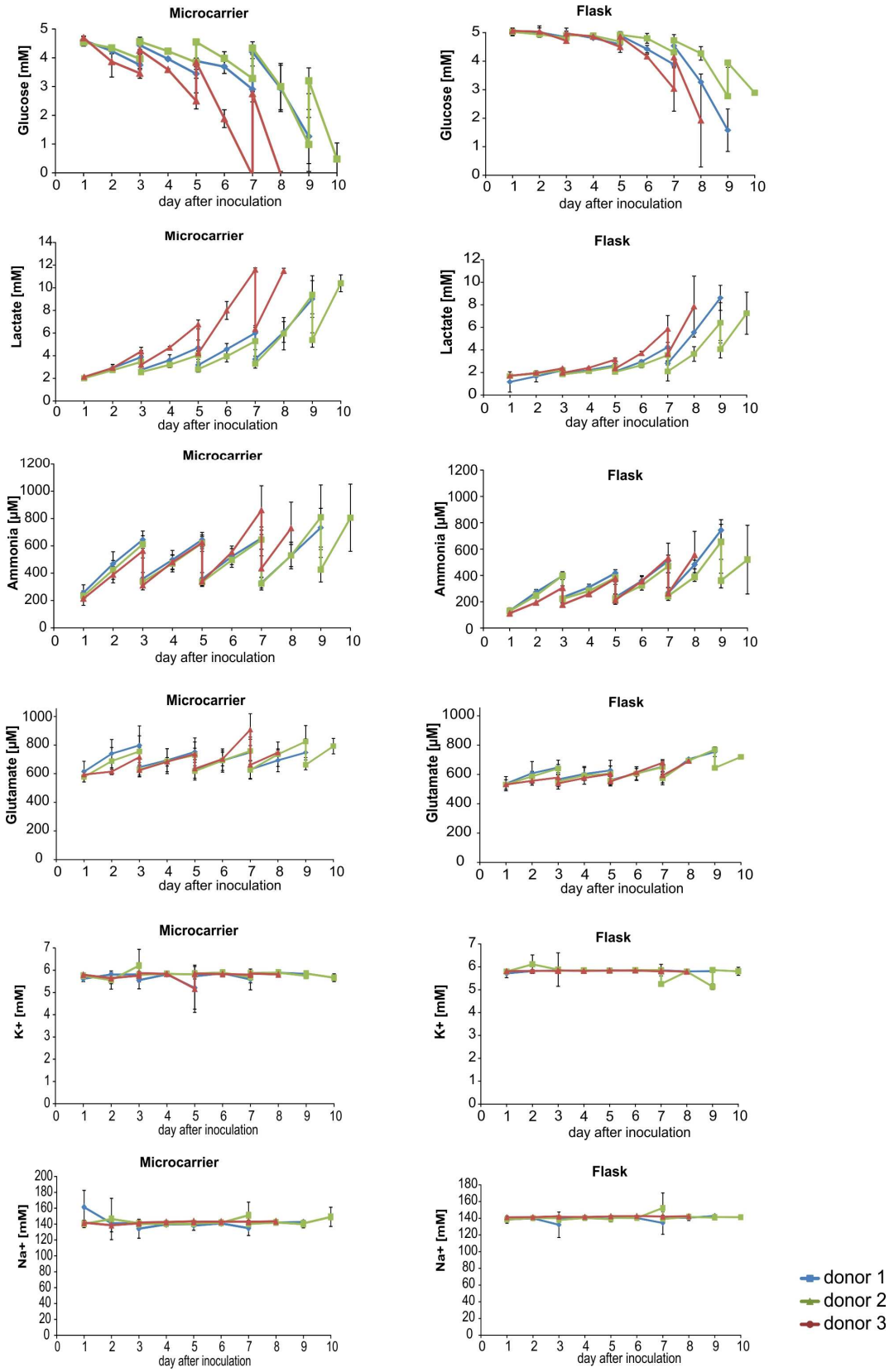

Figure 22: AM MSC metabolism. Glucose, lactate, ammonia, glutamate, potassium, and sodium concentrations were determined in microcarrier cultures (left) or flask cultures (right) for three different donors. For each donor, three independent expansion runs were performed. Depicted are mean concentrations with standard deviations.

Specific glucose consumption and lactate production rates were calculated for all three UC and AM MSC donors (Figure 23). In accordance with previous observations, high variance between donors and cells from the two different sources was observed. Glucose consumption and lactate production from UC MSCs were generally about 2-fold increased compared to AM MSCs (average rates of 4.9 pmol/h/cell and 6.6 pmol/h/cell for AM MSCs, compared to 6.3 pmol/h/cell and 12 pmol/h/cell, respectively) (Figure 23), correlating with the previously noted faster growth of UC MSCs (see 3.2.1). The only exception to this observation was the relatively high glucose consumption rate of donor 3 AM MSCs (8.5 pmol/h/cell compared to 3.2 pmol/h/cell for UC MSCs of the same donor). Remarkably, this did not correlate with an increase of the lactate production rate, which was comparable for AM and UC MSCs from donor 3. The reason for this discrepancy remains elusive and was not further evaluated in this work.

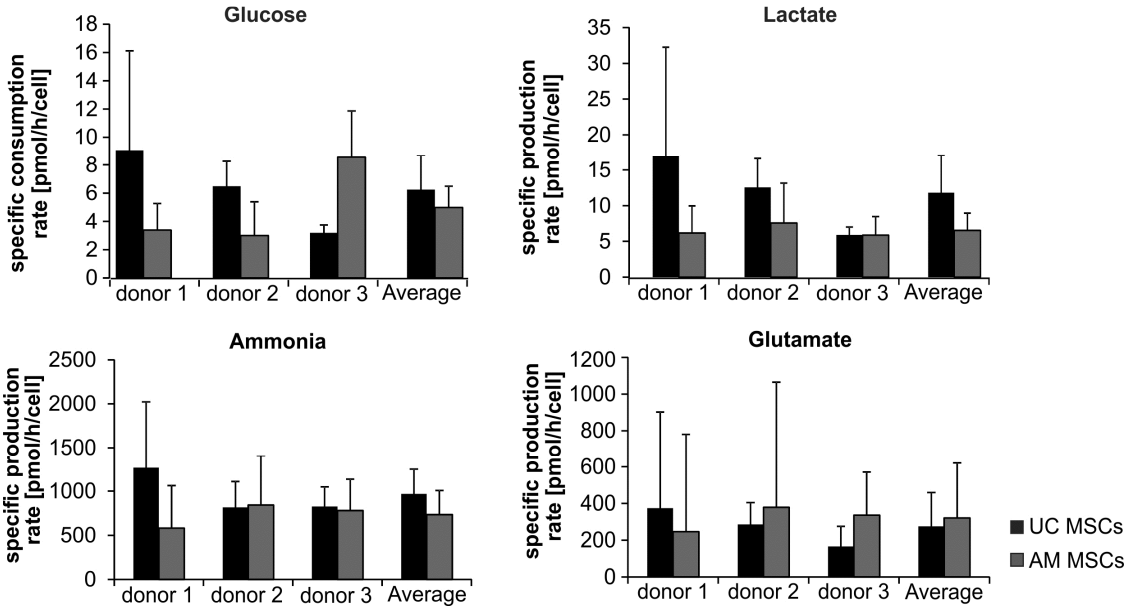

Figure 23: Specific consumption or production rates. Mean glucose consumption and lactate, ammonia, and glutamate production rates from day 6 to 7 calculated for three donors of UC MSCs (black) or AM MSCs (grey). For each donor, three independent cultivation runs were performed. Average values were calculated from all three donors and are shown with standard deviations.

Yields of lactate from glucose ($Y_{lac/glc}$) were around 2 for both UC and AM MSCs. Again, AM MSCs showed higher donor-to-donor-variation (Table 6). $Y_{lac/glc}$ can be used to estimate which metoblic pathway cells use to gain energy (Schop et al., 2009a, Higuera et al., 2009) and $Y_{lac/glc}$ of up to 2 is connected to glucose metabolism via glycolysis (Glacken, 1988, Newsholme et al., 1985).

Table 6: Yields of lactate from glucose ($Y_{lac/glc}$). $Y_{lac/glc}$ for three donors of UC and AM MSCs at day 6 to 7. Calculated are mean yields +/- standard deviations from three independent expansion runs and average values from all three donors.

$Y_{lac/glc}$ [mol/mol]	Donor 1	Donor 2	Donor 3	Average
UC MSCs	1.8 +/- 0.6	1.9 +/- 0.2	1.8 +/- 0.1	1.9 +/- 0.1
AM MSCs	1.8 +/- 0.5	2.5 +/- 0.4	0.7 +/- 0.9	1.7 +/- 0.9

Ammonium and glutamate are produced by consumption of glutamine which is, besides glucose, the second important energy source for mammalian cells. Concentrations of both metabolites increased with growing cell numbers during expansion and showed similar concentrations for all three donors of UC and AM MSCs, independent of the cultivation method (Figure 21 and Figure 22). Measurements of glutamine concentrations were impaired due to the use of GlutaMAX^{TM}, a stable dipeptide from L-glutamine and L-alanyl-L-glutamine, which could not be measured directly using the COBAS Integra 400. Therefore, yields of ammonia from glutamine, which may have provided more insight into the metabolic pathway routes of UC and AM MSCs, could not be calculated. In this context, studies of Schop et al. have already indicated that glutamine is not a major source for generation of energy in BM MSCs (Schop et al., 2009b). Like lactate, ammonium is a toxic metabolite produced during cell culture (Schneider et al., 1996). For human MSCs, concentrations of 2.4 mM were shown to inhibit cell proliferation (Schop et al., 2009a).

Sodium and potassium are important for maintenance of the membrane potential and also contribute to the osmotic pressure of the culture medium. Concentrations commonly used for mammalian cell culture are 137 – 155 mM and 3 – 4 mM for sodium and potassium, respectively (Lindl and Gstraunthaler, 2008b). Throughout flask and microcarrier cultivation and for both AM and UC MSCs, sodium and potassium concentrations remained constant and within this concentration range (Figure 21 and Figure 22).

3.2.4 Cell Yield, Viability, and Harvest Efficiency

Cell yield, viability, and harvest efficiency of microcarrier-expanded MSCs were determined for three different donors after three independent cultivation runs and compared to cell yield obtained from standard flask expansion (Table 7).

Table 7: Cell yield and harvest efficiency. Cell yield and viability of microcarrier- or flask-expanded UC (top) and AM (bottom) MSC from three different donors. For each donor, three independent expansions were evaluated. Harvest efficiency was calculated for microcarrier-expanded MSCs only.

UC MSCs	Microcarrier				Flask			
	Donor 1	Donor 2	Donor 3	Average	Donor 1	Donor 2	Donor 3	Average
10^3 cells/cm²	8.0 +/- 2.5	5.1 +/- 2.5	7.2 +/- 2.4	6.7 +/- 1.5	64.9 +/- 16.9	36.2 +/- 1.6	34.9 +/- 6.2	45.3 +/- 17.0
10^5 cells/ml medium	2.0 +/- 0.6	1.3 +/- 0.6	1.8 +/-0.6	1.7 +/- 0.6	3.2 +/- 0.8	1.8 +/- 0.1	1.7 +/- 0.3	2.3 +/- 0.9
Viability	96% +/- 1%	94% +/- 3%	96% +/- 2%	95% +/- 1%	82% +/- 10%	91% +/- 6%	93% +/- 2%	89% +/- 6%
Harvest efficiency	74% +/- 18%	51% +/- 24%	56% +/- 21%	61% +/- 12%				

AM MSCs	Microcarrier				Flask			
	Donor 1	Donor 2	Donor 3	Average	Donor 1	Donor 2	Donor 3	Average
10^3 cells/cm²	10.8 +/- 10.6	6.7 +/- 3.8	8.2 +/- 2.4	8.6 +/- 2.0	51.3 +/- 12.2	26.4 +/- 17.5	45.9+/- 10.2	41.2 +/- 13.1
10^5 cells/ml medium	2.7 +/- 2.6	1.7 +/- 0.9	2.1 +/- 0.6	2.1 +/- 0.5	2.6 +/- 0.6	1.3 +/- 0.9	2.2 +/- 1	2.1 +/- 0.7
Viability	94% +/- 5%	90% +/- 6%	93% +/- 5%	92% +/- 2%	96% +/- 1%	92% +/- 4%	95% +/- 3%	94% +/-2%
Harvest efficiency	87% +/- 81%	70% +/- 51%	99% +/- 70%	85% +/- 14%				

For both MSC sources, cell yield per surface area was higher for flask-expanded than microcarrier-expanded MSCs. On average, cell yield/cm² was almost 7-fold higher for flask-expanded compared to microcarrier-expanded UC MSCs (45.3×10^3 cells/cm² and 6.7×10^3 cells/cm², respectively) and almost 5-fold higher in flask-expanded compared to microcarrier-expanded AM MSCs (41.2×10^3 cells/cm² and 8.6×10^3 cells/cm²). This is in accordance with the observation that many microcarriers remained cell-free until the end of the cultivation process (see 3.2) whereas the flask surface was covered to 90% - 100% confluence. However, when comparing cell yields per volume of culture medium, comparable results were obtained for flask- and microcarrier-expanded cells: 1.7×10^5 cells/ml and 2.1 x cells/ml for microcarrier-expanded UC and AM MSCs and 2.3×10^5 cells/ml and 2.1×10^5 cells/ml for flask-expanded UC and AM MSCs, respectively. This was due to the higher surface area to volume ratio in the microcarrier expansion process.

To evaluate the efficiency of the harvest procedure of microcarrier-expanded MSCs, the number of cells after harvest was compared to the cell number determined by the daily LDH measurements performed at the same day. The harvest efficiency for the different UC and AM MSC donors is summarized in Table 7. On average, the harvest efficiency for AM MSCs was higher than for UC MSCs (85% compared to 61%). Furthermore, a high standard deviation of up to 81% was found for individual donors, indicating a high variance of the harvest procedure between the different runs.

3.3 Cell Characterization and Comparative Analysis of Microcarrier- and Flask-Expanded MSCs

To confirm basic MSC characteristics of expanded cells and to evaluate the influence of different bioprocessing technologies, i.e. microcarrier- and flask-based MSC expansion, a comprehensive analysis of MSC characteristics and functions was performed after the respective expansion periods.

3.3.1 Morphology

In order to evaluate UC and AM MSC morphology on Cytodex 1 microcarriers at high magnification, SEM analysis was performed. As depicted in Figure 24, MSCs expanded on microcarrier were small (about 10 µm in diameter) and showed a rather round morphology of both UC and AM MSCs. This was very different to their usual morphology in flask expansion, where they have a spread, flat and spindle-shaped morphology (see e.g. undifferentiated MSCs in Figure 28). Furthermore, flow cytometry analysis showed that microcarrier-expanded UC and AM MSCs were smaller in size, less granular, and more heterogenous as illustrated by decreased FSC and SSC intensities and more condensed MSC cloud in the FSC vs. SSC plot compared to flask-expanded MSCs. (Figure 25). In addition, calculating the forward scatter ratio of microcarrier-expanded to flask-expanded MSCs was used to quantify relative differences in cell size between the cultivation methods. These calculations revealed that cells expanded on microcarriers were smaller than those from flasks (FSC ratio < 1), an observation consistent with the microscopic evaluation (Figure 25B). This observation was MSC source-dependent; the effect on cell size was more pronounced for UC MSCs, as shown by the higher FSC ratio for AM MSCs.

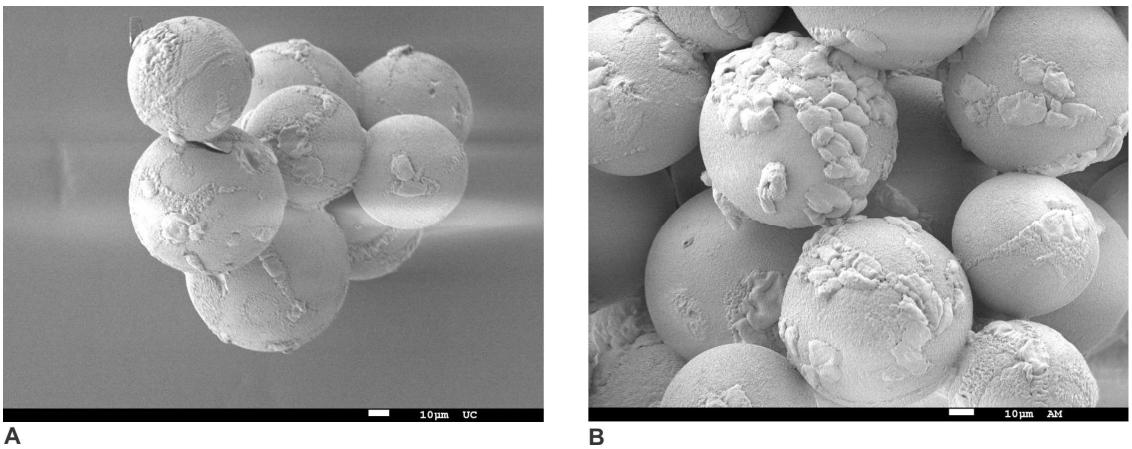

Figure 24: SEM of MSCs on Cytodex 1 microcarriers. Pictures kindly provided by Katia Rodewald. Pictures are shown in 450-fold (A) or 550-fold (B) magnification. Scale bar: 10 µm.

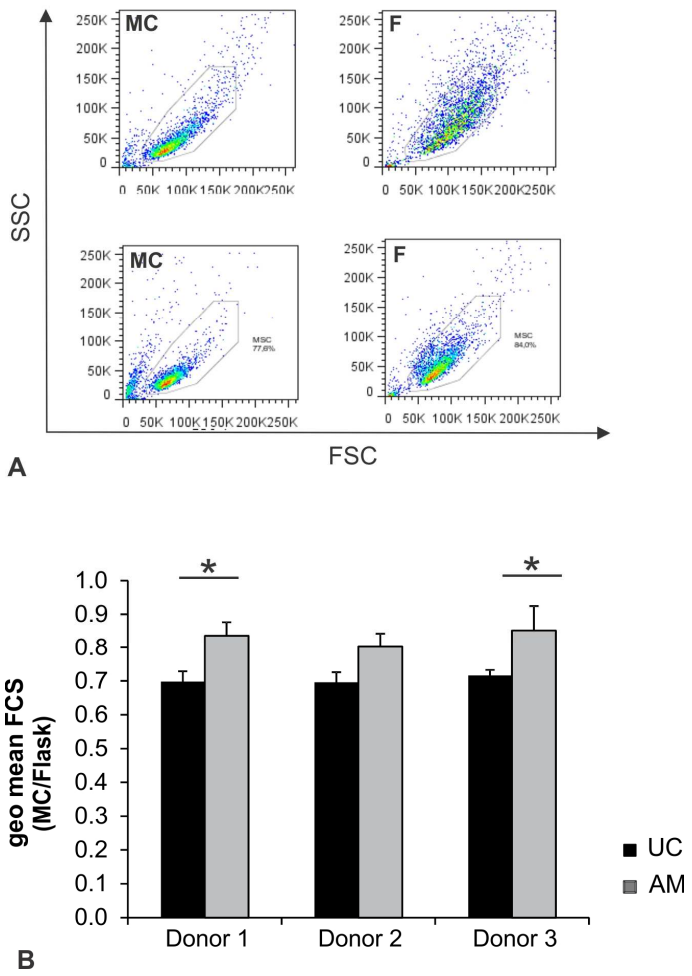

Figure 25: Differences in size and granularity of microcarrier- and flask-expanded MSCs. (A) FSC vs. SSC scatter plot of UC (top) and AM (bottom) MSCs expanded on microcarriers (MC, left) or flasks (F, right). (B) Ratio of FCS of microcarrier compared to flask-expanded MSCs for three independent expansions per donor. Depicted are mean values and standard deviations of three independent expansions. FSC forward scatter; SSC side scatter. * indicates $p < 0.05$.

3.3.2 Phenotype

To evaluate the influence of culture conditions on surface marker expression, expanded cells were analyzed by flow cytometry for expression of ISCT-defined MSC markers and additional MSC-related markers that have been described in the literature. For all three donors, UC and AM MSC displayed the classical MSC phenotype as defined by the ISCT (Dominici et al., 2006) independent of the applied cultivation method (Figure 26). Cells stained positive for surface markers CD73, CD90, and CD105 and negative for the haematopoietic cell markers CD14, CD19, CD34, CD45, and HLA-DR.

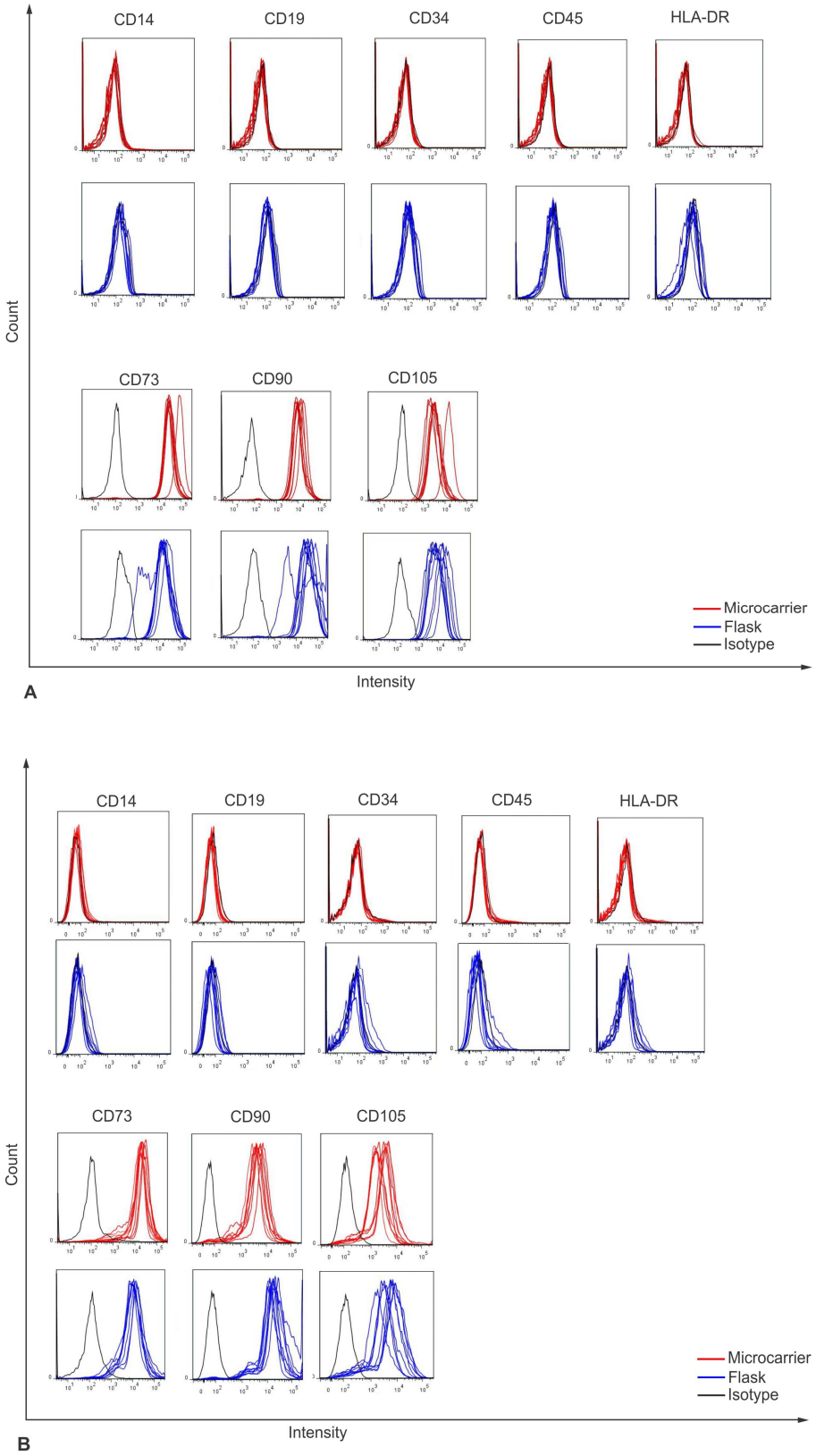

Figure 26: ISCT-defined surface marker expression of expanded MSCs. Analysis of MSC phenotype by flow cytometery. Histograms show fluorescence labeled markers on UC (A) or AM (B) MSCs expanded on microcarriers (red) or flask (blue) compared to representative isotype control (black). Depicted are analysis of MSCs from three different donors and three independent runs per donor.

In addition to the surface markers defined by the ISCT, a number of alternative surface molecules were analyzed (Figure 27). These molecules were chosen based on literature findings indicating a role of these surface markers in phenotype characterization, migration, or immune modulation. UC and AM MSCs from all donors expressed integrin subunit alpha4 /CD49d (Parolini et al., 2008), coagulation factor II/CD142 (Moll et al., 2012), activated leukocyte cell adhesion molecule ALCAM/CD166 (Pittenger et al., 1999), human epidermal growth factor receptors HER1 and HER2 (Buhring et al., 2007), melanoma-associated chondroitin sulfate protein MCSP (Kozanoglu et al., 2009), and hepatocyte growth factor receptor c-Met (Chacko et al., 2010, Son et al., 2006). Orexin receptor type 2/CD200 (Pietila et al., 2012) was differently expressed depending on the cell source: all UC MSCs expressed CD200 whereas AM MSCs showed variable expression. Melanoma cell adhesion molecular MCAM/CD146 (Crisan et al., 2008, Schugar et al., 2009) was expressed by all MSCs, except for microcarrier-expanded UC MSCs from donor 3.

UC and AM MSCs did not express platelet endothelial cell adhesion molecule PECAM/CD31 (Ishige et al., 2009) and nerve growth factor receptor NGFR/CD271 (Kuci et al., 2010). In addition, with the exception of a weak expression on flask-expanded AM MSCs from donor 1, all MSCs lacked expression of macrophage stimulating 1 receptor/CD136. Expression of angiotensin converting enzyme/CD143 (Zambidis et al., 2008) was also not detectable on UC and AM MSCs expanded on microcarriers, and flask-expanded MSCs only showed weak to moderate expression in one donor.

Remarkably, expression of frizzled-9/ CD349, a G-protein-coupled receptor involved in Wnt signaling (Buhring et al., 2007, Karasawa et al., 2002), showed distinct differences depending on the cultivation method for all three donors of both cell sources. Microcarrier-expanded cells did not express CD349 whereas flask-expanded cells stained positive for CD349 (Figure 27B).

UC MSC	MC			Flask		
	donor 1	donor 2	donor 3	donor 1	donor 2	donor 3
CD31	-	-	-	-	-	-
CD49d	++	++	+	++	++	+
CD136	-	-	-	-	-	-
CD142	++	++	++	+	+	++
CD143	-	-	-	++	-	-
CD146	+	+	-	++	+	+
CD166	++	+++	++	++	++	++
CD200	++	++	++	++	++	++
CD271	-	-	-	-	-	-
CD349	-	-	-	+	++	++
HER1	+++	+++	+++	++	++	+++
Her2	+	+	+	+	+	+
MCSP	++	+++	++	+++	+++	+++
c-Met	++	++	+	+	+	+

AM MSC	MC			Flask		
	donor 1	donor 2	donor 3	donor 1	donor 2	donor 3
CD31	-	-	-	-	-	-
CD49d	++	+	+	++	+	+
CD136	-	-	-	+	-	-
CD142	+	+++	++	++	++	++
CD143	-	-	-	+	-	-
CD146	+	+	+	+	+	+
CD166	++	++	++	++	++	++
CD200	-	++	-	-	+	-
CD271	-	-	-	-	-	-
CD349	-	-	-	+	+	+
HER1	++	+++	++	++	++	++
Her2	+	++	++	+	++	++
MCSP	++	++	++	++	+++	++
c-Met	++	+	+	+	+	+

A

Symbol	MFI sample/isotype control
-	<2
+	>2<10
++	>10<50
+++	>50

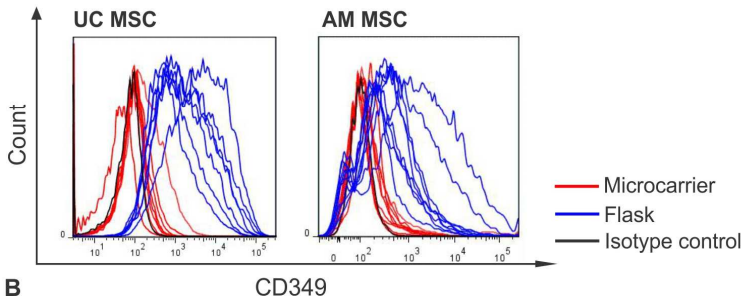

B

Figure 27: Surface marker analysis revealed distinct marker expression. (A) Flow cytometery analysis of surface markers of UC (left) or AM (right) MSCs expanded on microcarriers or standard cell culture flasks. Marker expression was normalized to isotype control and ranged on the depicted scale from no (-) to high (+++) expression. For each donor, average expression of three independent expansions is depicted. (B) Histograms show CD349 expression of microcarriers (red) or flask (blue) expanded UC and AM MSCs from three independent expansions of three donors. Representative isotype control is shown in black. MFI mean fluorescence intensity.

3.3.3 Differentiation of MSCs into Adipogenic, Osteogenic, and Chondrogenic Lineages

MSCs are multipotent adult stem cells which can differentiate into different cell types. In particular, tri-lineage differentiation potential into adipocytes, osteoblasts and chondroblasts is an ISCT criterion for MSC characterization. Therefore, UC and AM MSCs were differentiated into these three lineages after microcarrier or flask expansion.

Independent of the cultivation method UC and AM MSCs from all three donors demonstrated differentiation potential into adipocytes as assessed by Oil Red O staining of intracellular li-

pid droplets (Figure 28). During Oil Red O staining of differentiated AM MSCs the dye tended to precipitate. These precipitates, however, could be clearly distinguished from the stainings of lipid droplets as indicated in Figure 28B. Osteogenic differentiation of MSCs was assessed by Alzarin Red staining of mineralized extracellular matrix (Figure 29). UC and AM MSCs from all three donors and both cell sources showed osteogenic differentiation, without any influence of the cultivation method. In addition, expanded UC and AM MSCs were differentiated into chondroblasts in 3D spheroid cultures. All differentiated MSCs stained positive for extracellular matrix proteoglycans of cartilage (Figure 30). Some of the undifferentiated MSCs samples also showed chondrogenic differentiation, which was, however, only weak and locally identifiable compared to differentiated MSCs.

In summary, MSCs from both sources and all three donors demonstrated tri-lineage differentiation potential. No effect of the expansion process on MSC differentiation was observed.

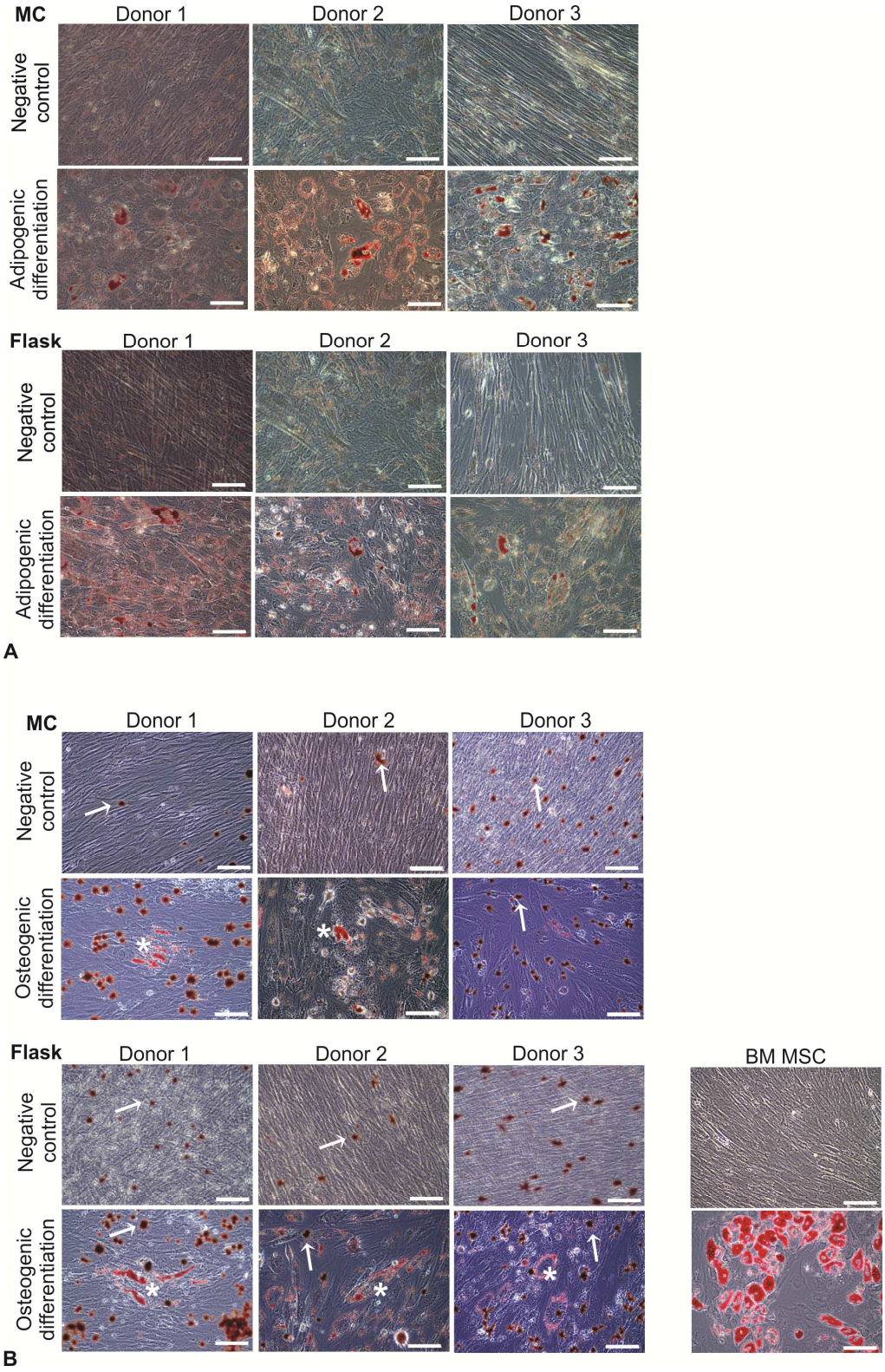

Figure 28: Adipogenic differentiation of expanded MSC. UC (A) or AM (B) MSCs expanded on microcarriers or flasks were differentiated into adipocytes. Representative phase contrast microscopic pictures of 3 donors are shown. BM MSCs with known tri-lineage differentiation potential served as positive controls. Lipid droplets are stained with Red Oil O. Abbreviations: MC microcarrier; BM bone marrow. Arrows point to dye precipitates, * indicate stained lipid droplets. Scale bar: 100 µm.

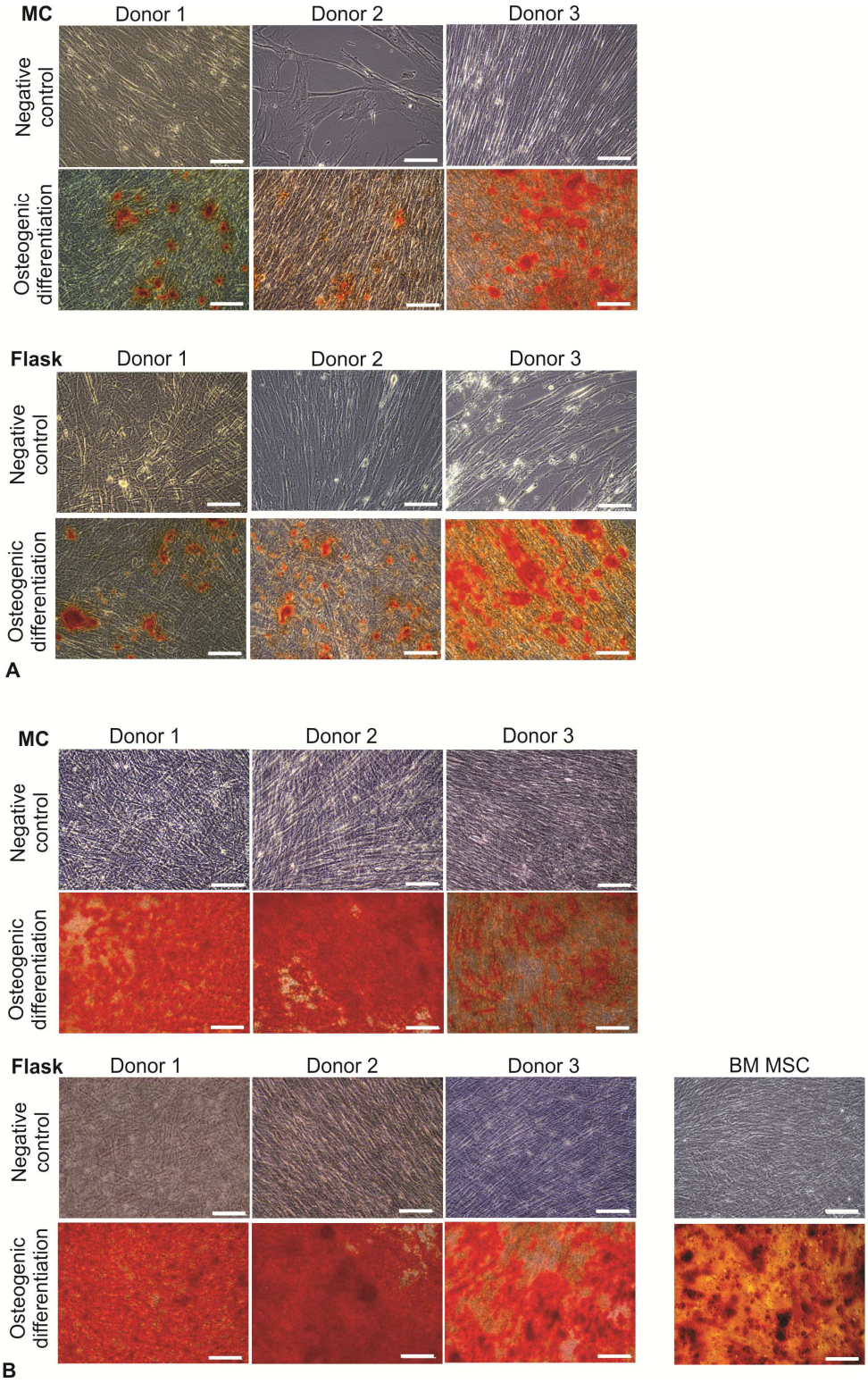

Figure 29: Osteogenic differentiation of expanded MSC. UC (A) or AM (B) MSCs expanded on microcarrier or flasks were differentiated into osteoblasts. Representative phase contrast microscopic pictures of three donors are shown. BM MSCs with known tri-lineage differentiation potential served as positive controls. Calcium phosphate precipitates are stained with Alizarin Red S. Abbreviations: MC microcarrier; BM bone marrow. Scale bar: 100 µm.

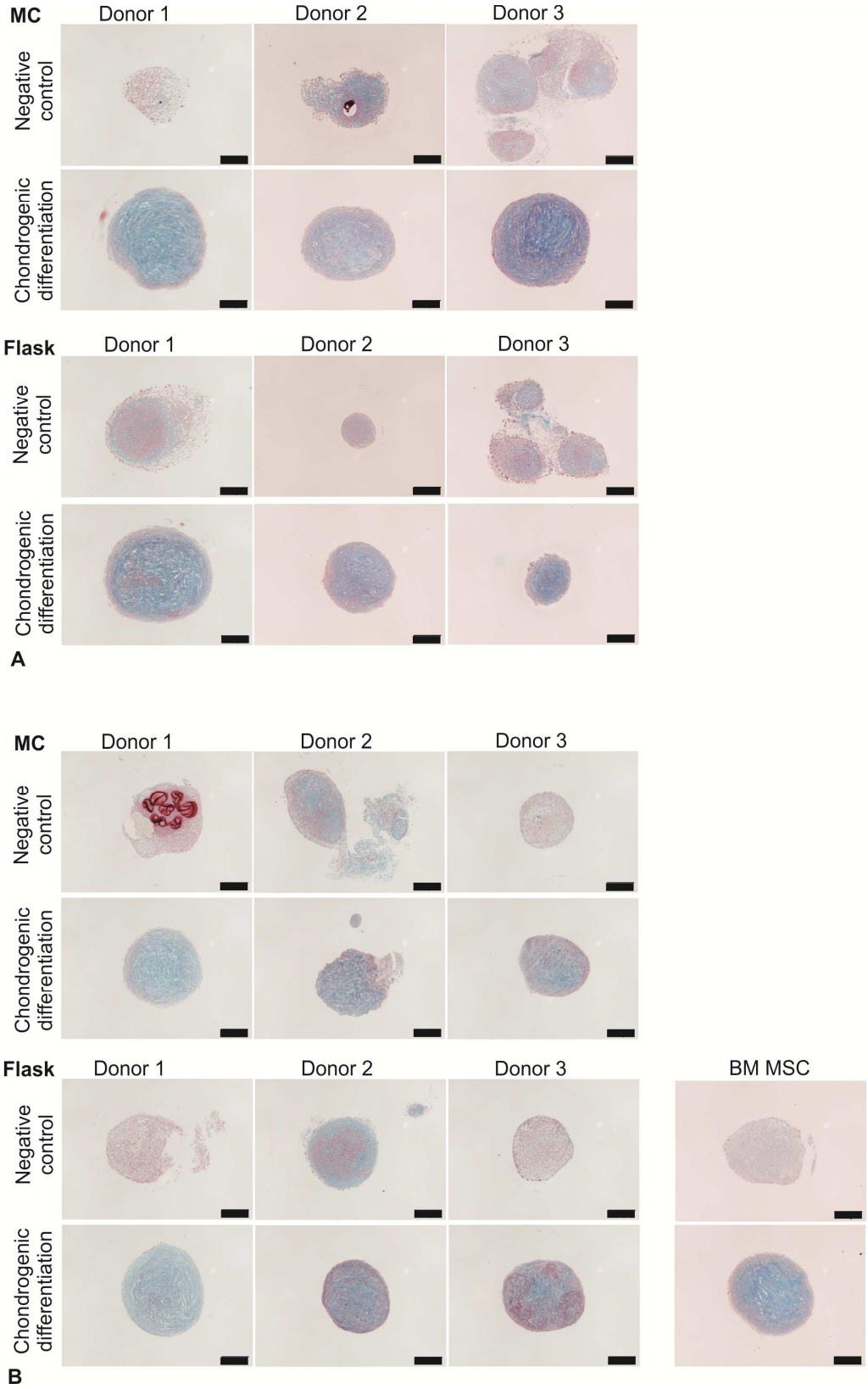

Figure 30: Chondrogenic differentiation of expanded MSC. UC (A) or AM (B) MSCs expanded on microcarriers or flasks were differentiated into chondroblasts. Representative pellet sections of three donors are shown. Cartilage proteoglycans are stained with Alcian Blue. Abbreviations: MC microcarrier; BM bone marrow. Scale bar: 200 µm.

3.3.4 Immunosuppressive Capacity of Microcarrier- and Flask-expanded MSCs

MSCs have an inhibitory effect on various immune cells, including inhibition of T lymphocyte proliferation (Ramasamy et al., 2008, Marigo and Dazzi, 2011). This inhibitory function has been described to be further increased after cytokine stimulation of MSCs (Ren et al., 2009, Crop et al., 2010). Therefore, the immunosuppressive capacity of expanded MSCs was studied *in vitro* by evaluating their effect on PBMC proliferation in the absence and presence of cytokines. UC and AM MSCs significantly ($p < 0.05$) inhibited PBMC proliferation with the exception of UC MSCs from donor 1 (both microcarrier- and flask-expanded) and flask-expanded UC MSCs from donor 2 (Figure 31). Overall, cytokine stimulation further increased the inhibition of PBMC proliferation (Figure 31B, E). However, a significant effect of stimulated compared to non-stimulated MSCs was only observed for microcarrier- and flask-expanded UC MSCs ($p< 0.05$, Figure 31C) whereas stimulated AM MSCs showed a non-significant tendency of increased PBMC inhibition (Figure 31F). Except for non-stimulated UC MSCs, no significant difference in PBMC inhibition between microcarrier- and flask-expanded UC or AM MSCs was observed.

Concerning predictability of this *in vitro* immunomodulatory effect of MSCs to *in vivo* conditions, it should be noted that no correlation between *in vitro* and *in vivo* effects has been established (Singer and Caplan, 2011).

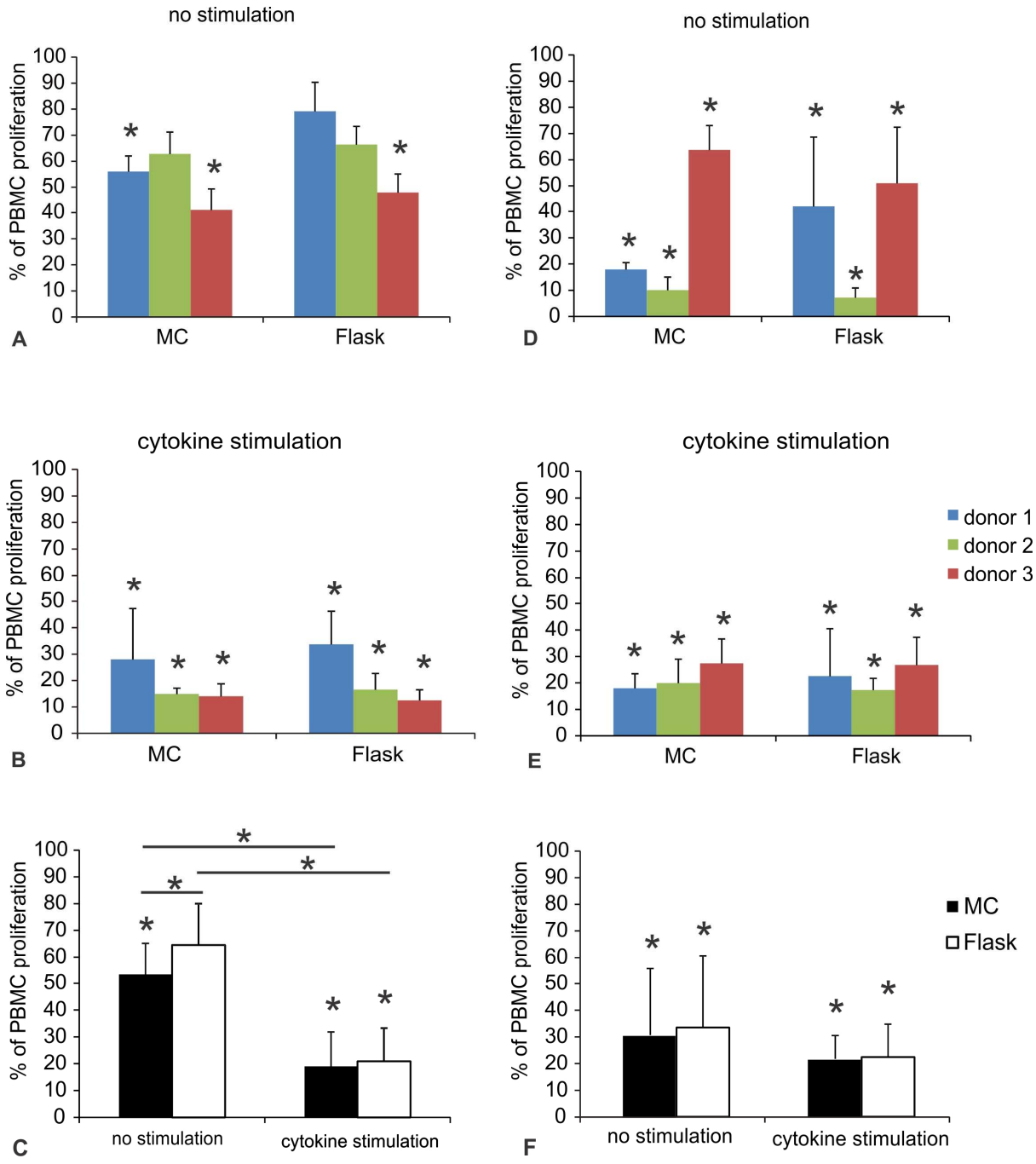

Figure 31: Comparative *in vitro* analysis of immunosuppressive properties of microcarrier- and flask-expanded MSCs. PBMCs were co-cultivated with IFN-γ and TNF-α-stimulated or non-stimulated UC (A-C) and AM (D-F). MSCs from three different donors to assess immunosuppressive properties of MSCs. Data depicted is normalized to control (PBMCs in absence of MSCs). Depicted is immunosuppression of expanded MSCs averaged over three independent expansions (A, B, D, E) or averaged over three donors for UC (C) and AM (F) MSCs. * indicates p-value <0.05 compared to control or, when underlined, compared to respective sample.

3.3.5 Cytokine Secretion of Microcarrier- and Flask-expanded MSCs

MSCs have been described to mediate their mode of action through secretion of paracrine and endocrine factors with immunomodulatory, anti-apoptotic, angiogenic, anti-fibrotic, chemoattractive or hematopoiesis-supportive function (Meirelles Lda et al., 2009). To evaluate potential influences of the expansion process on this function, the secretion profile of eight different factors from microcarrier- and flask-expanded UC and AM MSCs was quantified (Figure 32 and Figure 33). Remarkably, VEGF, a mitogen and pro-angiogenic factor (Bautch, 2012), was only secreted by cytokine-stimulated UC MSCs which had been expanded on microcarriers but not by flask-expanded cells (figure 23). FGF-2, also an angiogenic cytokine, showed a trend for higher secretion by microcarrier-expanded UC MSCs. However, this trend was not significant compared to flask-expanded cells. Secretion of Il-1ra, an anti-inflammatory and anti-fibrotic factor (Ortiz et al., 2007), and SDF-1, involved in migration and hematopoiesis-supportive (Sugiyama et al., 2006, Liu et al., 2011), were also significantly higher in stimulated microcarrier-expanded cells compared to flask-expanded UC MSCs. NGF (neuroprotective and anti-apoptotic (Hsiao et al., 2012)), M-CSF (supporting hematopoiesis (Majumdar et al., 2000)), and MCP-1 (involved in angiogenesis and immunomodulation (Hung et al., 2007)) did not show a significant change in secretion between the different cultivation methods. Secretion of HGF (immunomodulatory, anti-apoptotic and anti-fibrotic function (Togel et al., 2007, Di Nicola et al., 2002, Suga et al., 2009)) was significantly higher in non-stimulated flask-expanded UC MSCs than microcarrier-expanded cells but did not show different secretion in stimulated cells.

Similar to UC MSCs, AM MSCs cultivated on microcarriers also showed significantly higher VEGF secretion than flask-expanded cells (Figure 33). Remarkably, basal VEGF secretion of non-stimulated AM MSCs was even higher than secretion of non-stimulated AM MSCs, whereas for non-stimulated UC MSCs, VEGF secretion was not detectable. Microcarrier-expanded AM MSCs additionally showed significantly higher secretion of FGF-2 (both in stimulated and non-stimulated cells). IL-1ra and SDF-1a, which were found to be higher secreted by microcarrier-expanded UC MSCs, also showed a trend for higher secretion by microcarrier-expanded AM MSCs. NGF secretion tended to be higher in flask-expanded AM MSCs, but this difference was only significant for non-stimulated cells. M-CSF, MCP-1, and HGF were secreted significantly higher by stimulated microcarrier-expanded AM MSCs.

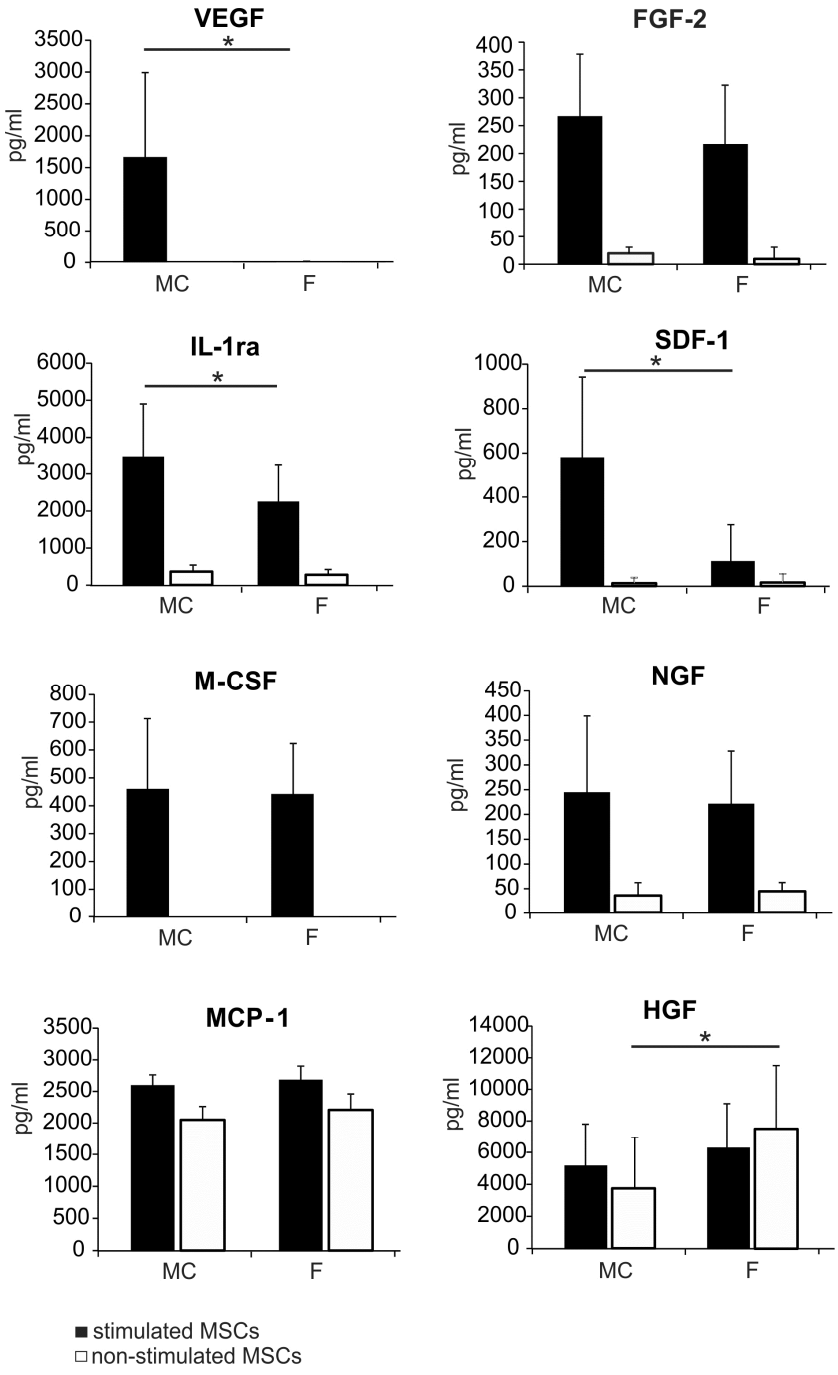

Figure 32: Comparative analysis of selected cytokines, chemokines, and growth factors secreted by UC MSCs. Concentration of factors secreted by TNF-α- and INF-γ-stimulated or non-stimulated UC MSCs expanded on microcarriers (MC) or standard cell culture flasks (F). Depicted are average concentrations and standard deviations calculated from three donors and three independent expansions per donor. * indicates p-value < 0.05.

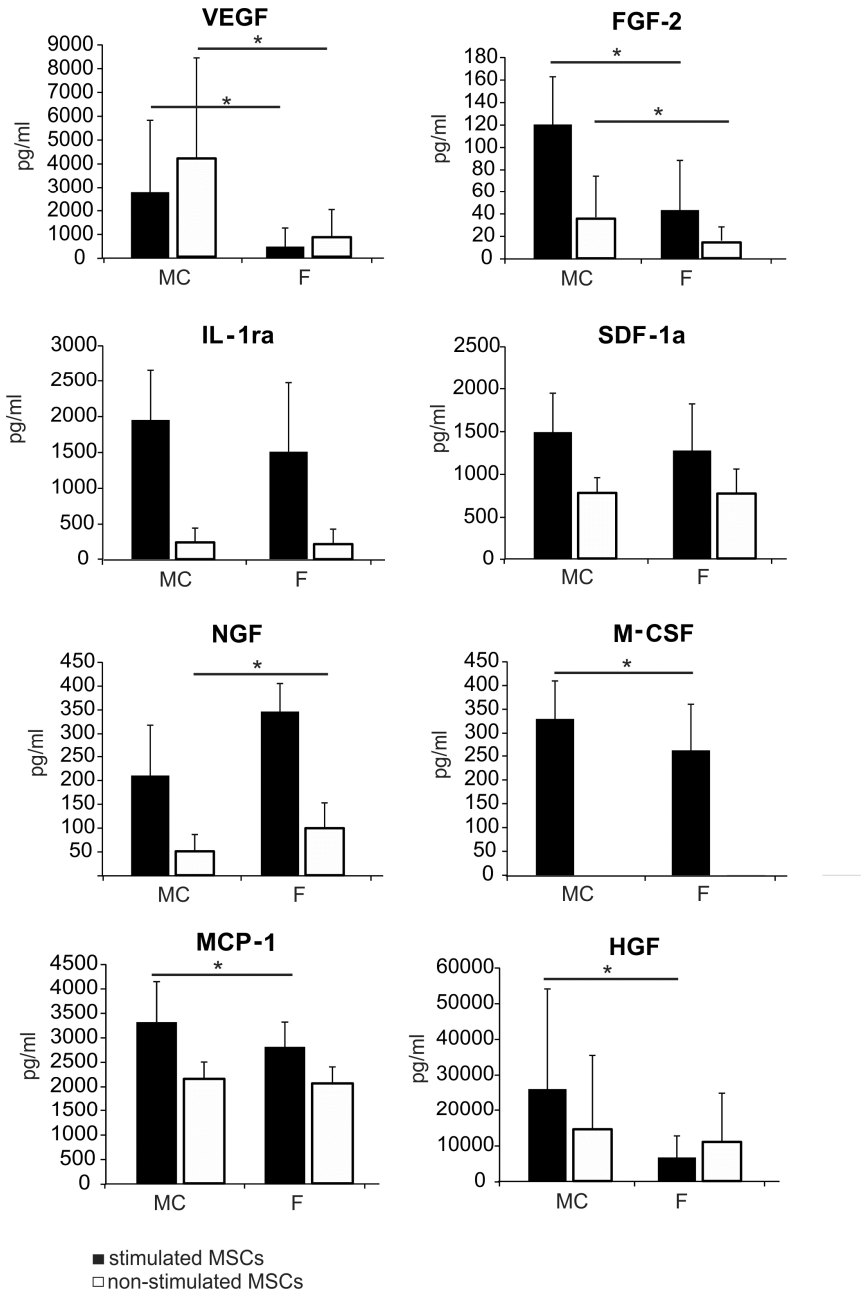

Figure 33: Comparative analysis of selected cytokines, chemokines and growth factors secreted by AM MSCs. Concentration of factors secreted by TNF-α- and INF-γ-stimulated or non-stimulated AM MSCs expanded on microcarriers (MC) or standard cell culture flasks (F). Depicted are average concentrations and standard deviations calculated from three donors and three independent expansions per donor. * indicates p-value < 0.05.

3.3.6 Gene Expression Patterns of Microcarrier- and Flask-expanded MSCs

To obtain better knowledge of functional differences arising from the cultivation process, gene expression analysis of UC MSCs expanded on microcarrier in stirred, regulated bioreac-

tors and standard cell culture flasks was performed. 371 genes were selected based on general cellular and MSC-related functions and analyzed in a customized RT-PCR assay. An overview of selected genes is provided in Supplementary Table 10.

Hierarchical, agglomerative clustering and principle component analysis (PCA) were performed to analyze whether cell source, cell donor and/or the expansion process led to similarities in MSC gene expression patterns. Based on the selected gene panel, both methods revealed that UC and AM MSCs primarily clustered depending on the cultivation process (Figure 34). The dendrogram showed that microcarrier- and flask-expanded MSCs clearly clustered in two different groups. Within these groups, MSCs tended to be more similar depending on their cell source than the individual cell donor; all flask-expanded UC MSCs clustered close together which was also found for all AM MSCs with the exception of donor 2, who was more similar to UC MSCs. Similar results were observed for microcarrier-expanded cells: With the exception of AM MSC donor 2 and UC MSCs donor 3, which cluster close together, MSCs from different donors cluster according to their cell source within the microcarrier group.

PCA is a classical method to reduce the multi-dimensionality of a data set (Jolliffe, 2002). Using PCA, high dimensional data, such as gene expression data, can be reduced into two dimensions which then account for most of the variance in the data set. Based on the gene expression profile of the 371 selected genes, PCA showed that, despite the usually high variability between different cell sources and donors, microcarrier- and flask-expanded UC and AM MSCs can be separated into different groups according to their cultivation process (Figure 34B).

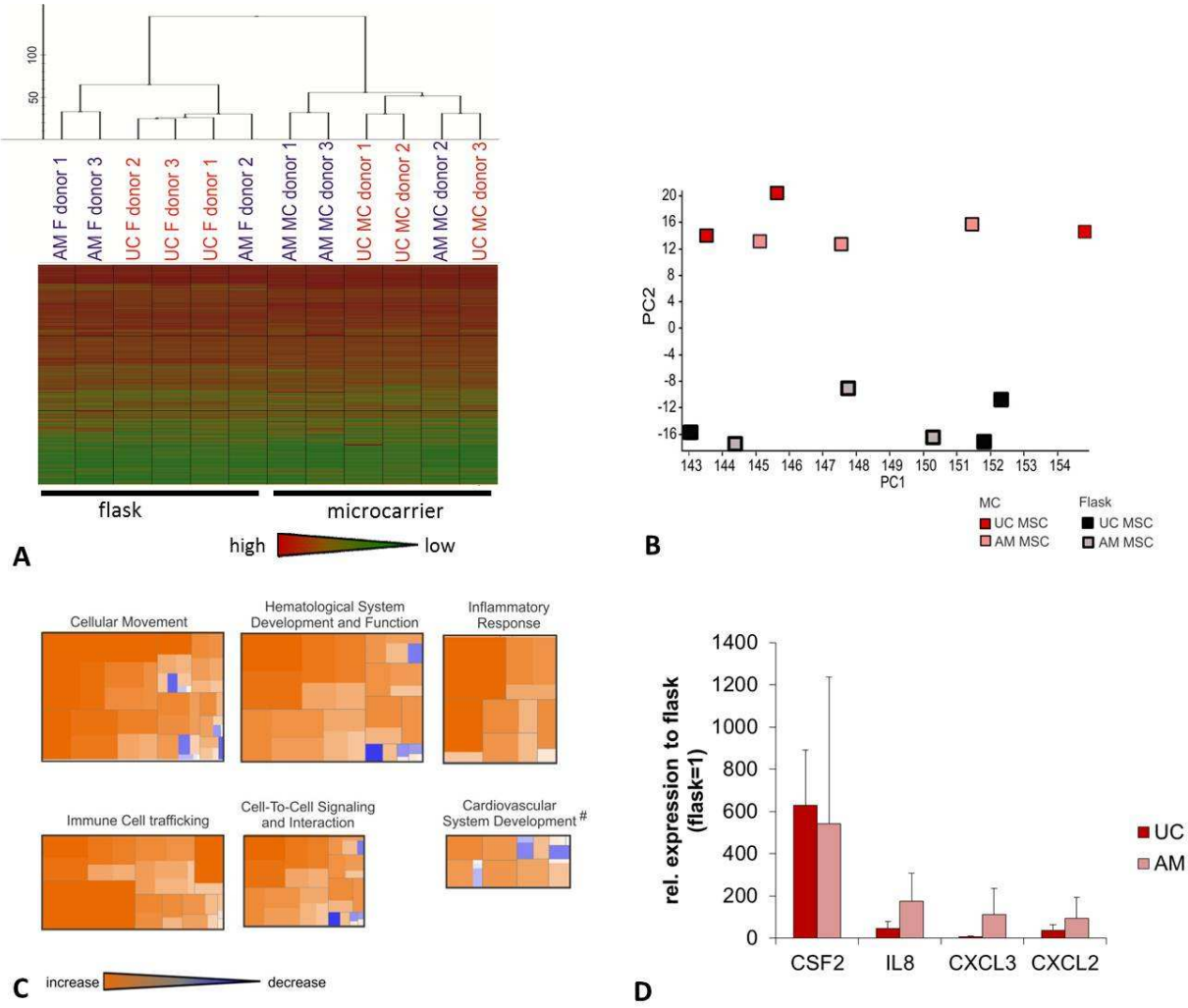

Figure 34 Comparative gene expression analysis of MSCs expanded on microcarriers or flasks. Based on gene expression of microcarrier (MC)- and flask (F)-expanded UC and AM MSCs from three different donors. (A) Hierarchical clustering; (B) Principle Component Analysis (PCA); (C) Pathway analysis based on differentially expressed genes in microcarrier-expanded MSCs relative to flask-expanded cells. Depicted are heatmaps of biological functions in which different pathways were found to be affected by differentially expressed genes. Heatmaps colored by z-score.; #: z-score < 2. (D) Expression level of selected, differentially expressed genes. Depicted are average values of three independent expansions from three donors.

In summary, both cluster analysis and PCA revealed that, based on their gene expression, MSCs cultivated with the same expansion method were more similar to each other than MSCs from the same donor or cell source. Gene expression of microcarrier-expanded UC and AM MSCs was compared to flask-expanded MSCs. Out of the 371 gene panel, 104 genes were found to be differently expressed ($p < 0.05$) in microcarrier-expanded MSCs compared to flask-expanded MSCs (Supplementary Table 1). To evaluate functional implications of the cultivation processes, pathway analysis was performed using Ingenuity Pathway Analysis

(IPA). Based on the Ingenuity Knowledge database, IPA identifies biological functions and pathways that are most significant to the input dataset. It should be noted that this analysis was not performed on whole genome data and pathway analysis was likely to be biased due to the pre-selection of specific genes.

IPA mainly identified the following functional groups to be affected by cultivation-based changes in gene expression: Cellular movement, immune cell trafficking, hematological system development and function, cell-to-cell signaling, and inflammatory response (Figure 34C). Within these groups, pathways affecting the immune system were significantly increased in microcarrier-expanded MSCs. These up-regulated functions included the mobilization, attraction, and/or recruitment of myeloid cells such as neutrophils, granulocytes, phagocytes, and macrophages. In particular, the mRNA expression level of CSF2, IL8, CXCL 2 and 3, all of which are associated with immune responses, were significantly up-regulated in microcarrier-expanded MSCs compared to flask-expanded MSCs (Figure 34D).

In addition, pathway analysis identified the functional group of “cardiovascular system development” to be increased in microcarrier-expanded MSCs (Figure 34). Among others, this group consisted of increased functions concerning angiogenesis and tubulation of endothelial cells, involving angiogenesis-related genes such as IL8, FGF2, VEGFA or CCL7. This finding correlates with previous results which suggested improved angiogenic properties of microcarrier-expanded MSCs (see 3.3.2 and 3.3.5). However, significance of these functions was not given as the z-score remained below 2, the significant threshold defined by IPA. This may be due to the pre-selection of genes which may have resulted in an insufficient number of genes involved in the relevant pathways.

3.4 Scale-up of MSC Expansion on Microcarriers: Cultivation under Regulated Conditions

Microcarrier-based expansion provides excellent means for scale-up. To evaluate the scale-up feasibility of the microcarrier-based MSCs technology, the process established in spinner flasks (see above) was transferred to bioreactors with a working volume of up to 1.5 l. As of today, the vast majority of microcarrier studies with MSCs used bioreactor working volumes ranging from 25 ml to 250 ml (Table 4). In contrast to spinner flask expansion, large-scale bioreactors allow online monitoring and regulation of the culture process. Process control is essential for robust, reproducible expansion as it can influence product properties and quality. In fact, previous experiments have already demonstrated the need for regulation of pH value (see 3.2.2) or nutrients (3.2.3) for microcarrier-based MSC expansion.

In preliminary experiments, two different bioreactor systems, different gas spargers for aeration, pH values, pO_2 concentrations, nutrient and metabolite concentrations, and seeding density were evaluated (see Supplements Fermentation). Based on these experiments, UC MSCs from three different donors were cultivated at pH 7.35 and 20% O_2 in stirred, 2 L Quad glass vessel bioreactors adapted to a bioreactor control unit (Biostat® B-DCU) as described in Supplementary Table 7. Glucose concentration was maintained at 1 g/l. UC MSCs were harvested at about 80% confluence, followed by a detailed cell characterization and comparison to flask-expanded UC MSCs. All experiments concerning large-scale cell expansion, monitoring of culture parameters and cell harvest were performed by the group of Dr. Ingo Gorr (see Supplements Fermentation) and harvested cells were then characterized as part of this work. In parallel, MSC expansion on standard cell culture flasks was performed using equal cell densities for inoculation.

3.4.1 Phenotype

To evaluate the influence of the cultivation process on surface marker expression, expanded cells were analyzed by flow cytometry for expression of ISCT-defined MSC markers and additional MSC-related markers that have been described in the literature. Analysis of surface marker expression showed that cells from all three donors fulfilled the ISCT criteria (Dominici et al., 2006) (Figure 35). Analysis of additional surface markers revealed an expression profile similar to MSC expanded in spinner flasks (see 3.3.2) with the following exceptions: CD142 and c-Met were not expressed on UC MSCs expanded on microcarrier in a regulated bioreactor whereas cells expanded under non-regulated conditions in spinner flasks stained positive for these two markers. Concerning the expression of CD349 (frizzled-9), mi-

crocarrier-expanded UC MSCs from two donors showed weaker expression than flask-expanded cells (Figure 35B). However, in contrast to MSCs expanded in spinner-flasks, UC MSCs from donor 1, which were expanded under regulated conditions in a bioreactor, showed CD349 expression levels comparable to flask-expanded cells. As only one expansion run for each donor was performed, this could also be due to measurement inaccuracy. On average, however, expansion on microcarrier led to a weaker CD349 expression compared to flask expansion.

	Microcarrier			Flask		
	donor 1	donor 4	donor 5	donor 1	donor 4	donor 5
CD14	-	-	-	-	-	-
CD19	-	-	-	-	-	-
CD34	-	-	-	-	-	-
CD45	-	-	-	-	-	-
HLA-DR	-	-	-	-	-	-
CD73	+++	+++	+++	+++	+++	+++
CD90	+++	+++	+++	+++	+++	+++
CD105	++	+	+	++	++	++
CD31	-	-	-	-	-	-
CD49d	++	+	+	++	++	++
CD136	-	-	-	-	-	-
CD142	-	-	-	++	++	+
CD143	-	-	-	-	-	-
CD146	+	+	+	++	++	++
CD166	++	++	++	++	++	++
CD200	++	+	+	++	+	++
CD271	-	-	-	-	-	-
CD349	+	-	+	++	+	++
Her1	+	++	++	+++	++	++
Her2	+	+	+	+	+	+
MCSP	++	+	++	+++	+++	+++
c-Met	-	-	-	++	+	+

Symbol	MFI sample/isotype control
-	<2
+	>2<10
++	>10<50
+++	>50

A

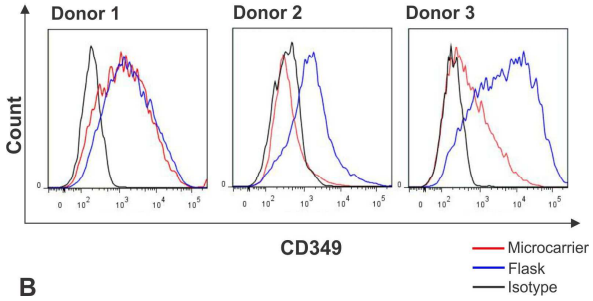

B

Figure 35: MSC phenotype. Flow cytometery analysis of surface markers of UC MSCs expanded on microcarriers or standard cell culture flasks. (A) Marker expression was normalized to isotype control and ranged on the depicted scale from no (-) to high (+++) expression. One expansion run for was performed for each donor. ISCT criteria are highlighted by blue frame. (B) Histograms show CD349 expression of microcarrier- (red) or flask- (blue) expanded UC MSCs from three donors. Isotype control is shown in black.

3.4.2 Immunosuppressive Capacity of MSCs

As described previously for MSCs expanded under non-regulated conditions in spinner flasks (see 3.3.4), the immunosuppressive capacity of expanded MSCs was studied *in vitro* by evaluating their effect on PBMC proliferation in the absence and presence of cytokines. UC MSCs expanded on microcarriers in regulated bioreactors inhibited PBMC proliferation comparable to flask-expanded MSCs from the same donors (Figure 36). Notably, variability

of PBMC proliferation inhibition was smaller for MSCs expanded under regulated conditions in bioreactors than for cells expanded under non-regulated conditions in flasks.

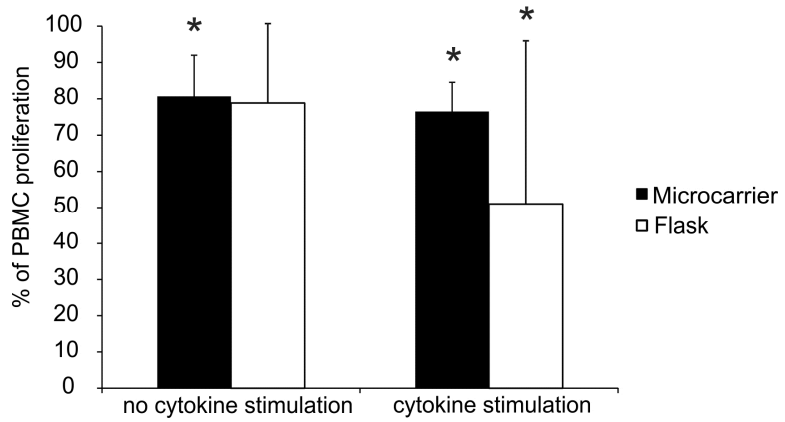

Figure 36: Comparative *in vitro* analysis of immunosuppressive properties. To assess the immunosupressive function of UC MSCs expanded on microcarriers in bioreactors (black) or standard cell culture flasks (white), PBMCs were co-cultivated with IFN-γ and TNF-α-stimulated or non-stimulated UC MSCs from three different MSC donors. Averaged data from three donors (one expansion run per donor) is depicted normalized to control (PBMCs in absence of MSCs). * indicates p-value <0.05 compared to control.

3.4.3 Cytokine Secretion

MSCs have been described to mediate their mode of action through secretion of paracrine and endocrine factors with immunomodulatory, anti-apoptotic, angiogenic, anti-fibrotic, chemoattractive, or hematopoiesis-supportive function (Meirelles Lda et al., 2009). To evaluate a potential influence arising from bioreactor or flask expansion, secretion of eight different factors from stimulated and non-stimulated UC MSCs was quantified (Figure 37). Except for NGF expression in non-stimulated UC MSCs, no significant differences between microcarrier-based bioreactor and flask expansion was observed for secretion of VEGF, FGF-2, IL-1ra, SDF1, M-CSF, MCP-1, or HGF. In accordance with previous findings in spinner flasks, VEGF was only secreted by stimulated UC MSCs. Furthermore, microcarrier-expanded MSCs showed a trend of higher VEGF secretion than flask-expanded cells.

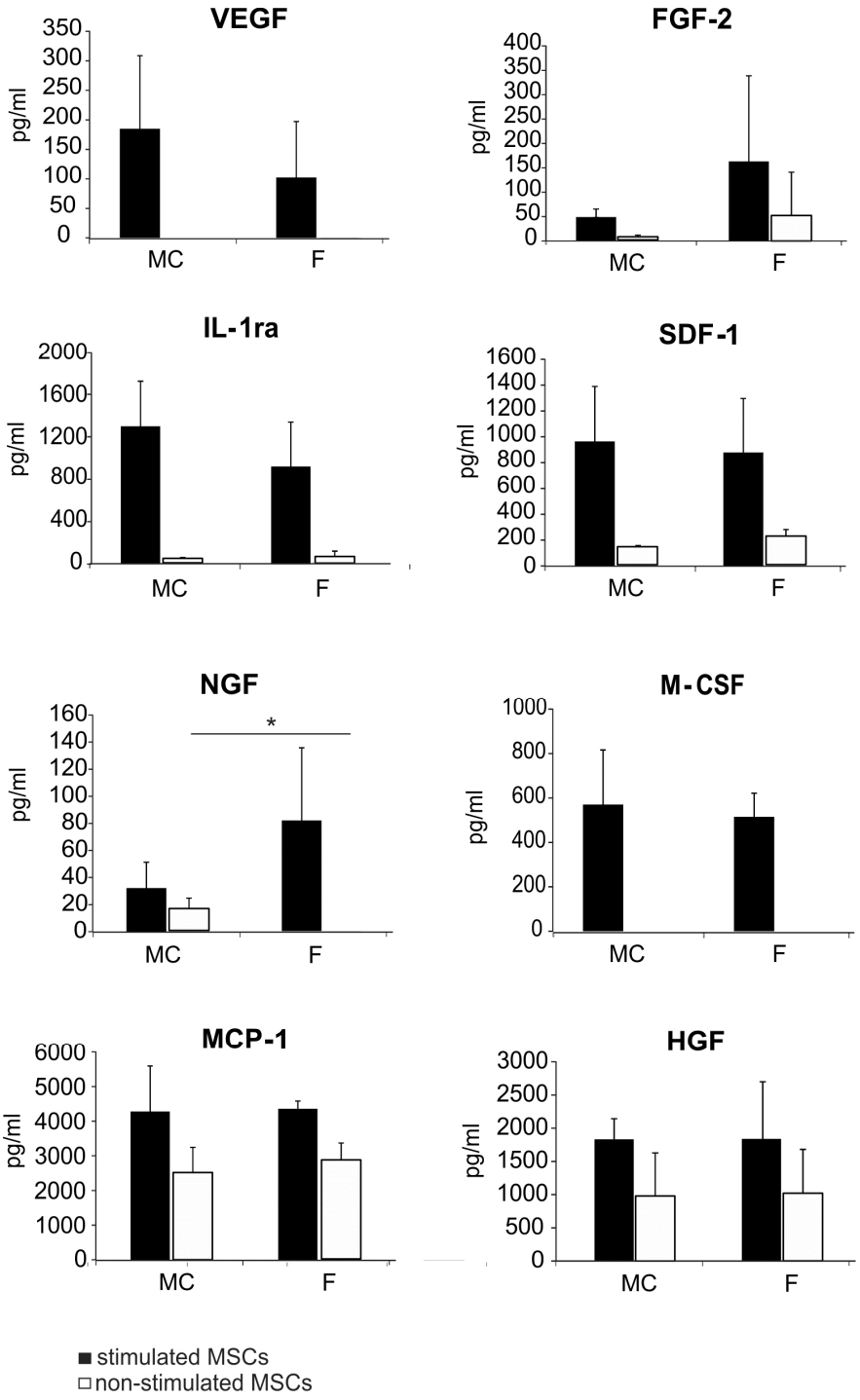

Figure 37: Comparative analysis of selected cytokines, chemokines, and growth factors. Concentration of factors secreted by TNF-α- and INF-γ-stimulated or non-stimulated UC MSCs (three donors) expanded on microcarriers under regulated conditions in bioreactors or standard cell culture flasks. Depicted are average concentrations and standard deviations calculated from three donors. * indicates p-value < 0.05.

3.4.4 Gene Expression Analysis

To obtain better knowledge of functional differences arising from the different cultivation processes, gene expression analysis of UC MSCs expanded on microcarrier in stirred, regulated bioreactors and standard cell culture flasks was performed. 371 genes were selected based on general cellular and MSC-related functions and analyzed in a customized RT-PCR assay. An overview of selected genes is provided in Supplementary Table 10.

In order to not only evaluate differences between microcarrier and flask expansion but to also uncover possible differences between the cultivation under regulated (bioreactor) and non-regulated (spinner flask) conditions, data from the previously described small scale experiments in spinner flasks was also added to the analysis. Hierarchical clustering showed that microcarrier-expanded MSCs (both from regulated and non-regulated conditions) and flask-expanded MSCs can be separated into two different groups according to the expansion process (see Figure 38A). PCA showed that UC MSCs cultivated on microcarrier in regulated bioreactors clustered very close together whereas MSCs cultivated under non-regulated conditions on microcarrier and flasks showed higher variability (Figure 38B).

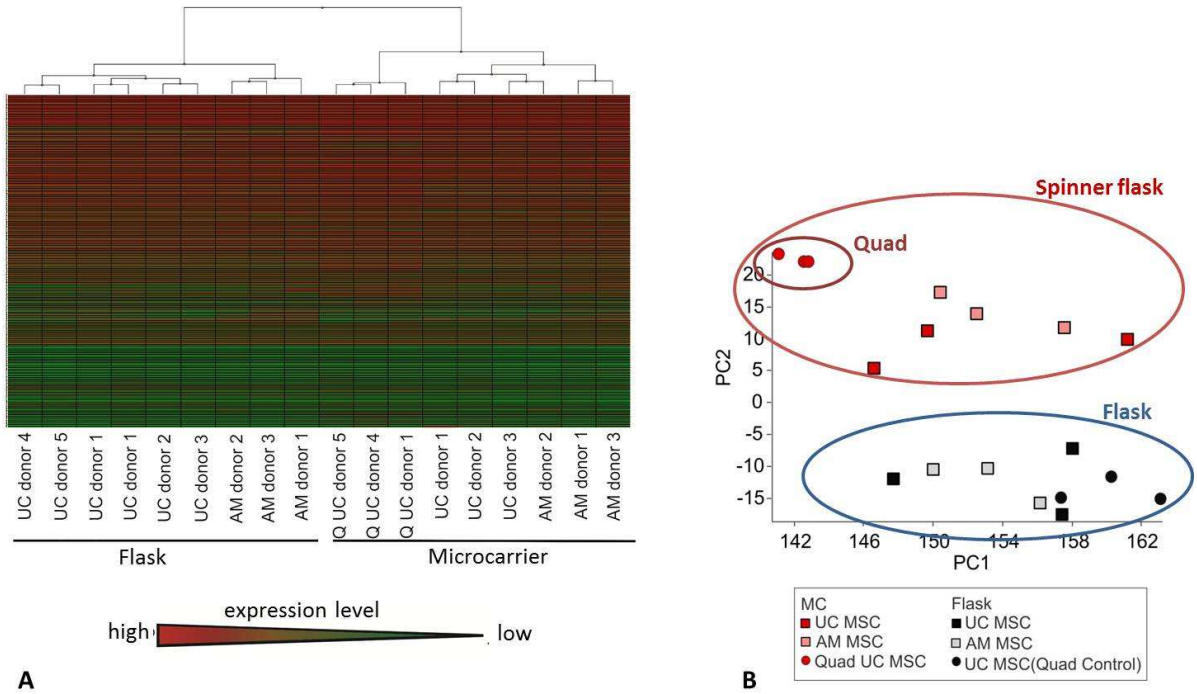

Figure 38: Comparative gene expression analysis of microcarrier- and flask-expanded MSCs. Hierarchical clustering (A) and PCA (B) was performed based on gene expression of microcarrier- and flask-expanded UC and AM MSCs. Microcarrier expansion was performed under regulated conditions in bioreactors (Quads Q) (3 donors, 1 expansion run per donor) or spinner flasks (3 donors, 3 runs per donor). Donors and replicates for flask controls according to microcarrier expansions.

3.5 Cultivation of MSCs on Thermoresponsive Surfaces

Anchorage-dependent MSCs are usually harvested from surfaces by enzymatic treatment. A major disadvantage of enzymatic detachment is that it can destroy cell surface molecules, damage cells, or impair cellular functions (Yang et al., 2012). To avoid harsh enzymatic treatment, cells can be cultivated on thermoresponsive surfaces and detached by temperature reduction (Yamada et al., 1990, Okano et al., 1993, Shi et al., 2010). MSC detachment from the commercially available thermoresponsive UpCell^{TM} surface was evaluated. Moreover, thermoresponsive surfaces made of novel biomaterials were developed by Dr. Ning Zhang, at the department of Prof. Dr. Rieger, aiming to optimize MSC detachment properties.

3.5.1 Cultivation of MSCs on UpCell^{TM} Surface

The commercially available, poly(N-isopropylacrylamide) (PNIPAAM)-based UpCell^{TM} surface (Nunc, ThermoScientific) was evaluated regarding MSC proliferation and detachment. At 37 °C, MSCs attached and proliferated on this surface. The crucial characteristic of the UpCell^{TM} surface, however, is cell detachment at temperatures below the LCST (32 °C). Therefore, UC MSCs detachment was evaluated by reducing the temperature and incubation in cell culture medium at room temperature (Figure 39A). After prolonged incubation at room temperature (RT), MSCs started to slowly detach. Yet, only poor cell detachment was observed within 2 h. According to the manufacturer's instructions, detachment should occur within 40 min (personal communication and manufacturer's protocol). As controls, MSCs cultivated on standard cell culture surface were treated likewise and did not show cell detachment upon cooling and incubation at RT (Figure 39A). Furthermore, cell detachment at different cell densities was evaluated using BM MSCs (Figure 39B). At high cell densities (10,000 MSCs/cm²), cells detached in cell aggregates whereas at low cell densities (500 MSCs/cm²), detachment as single cells was observed.

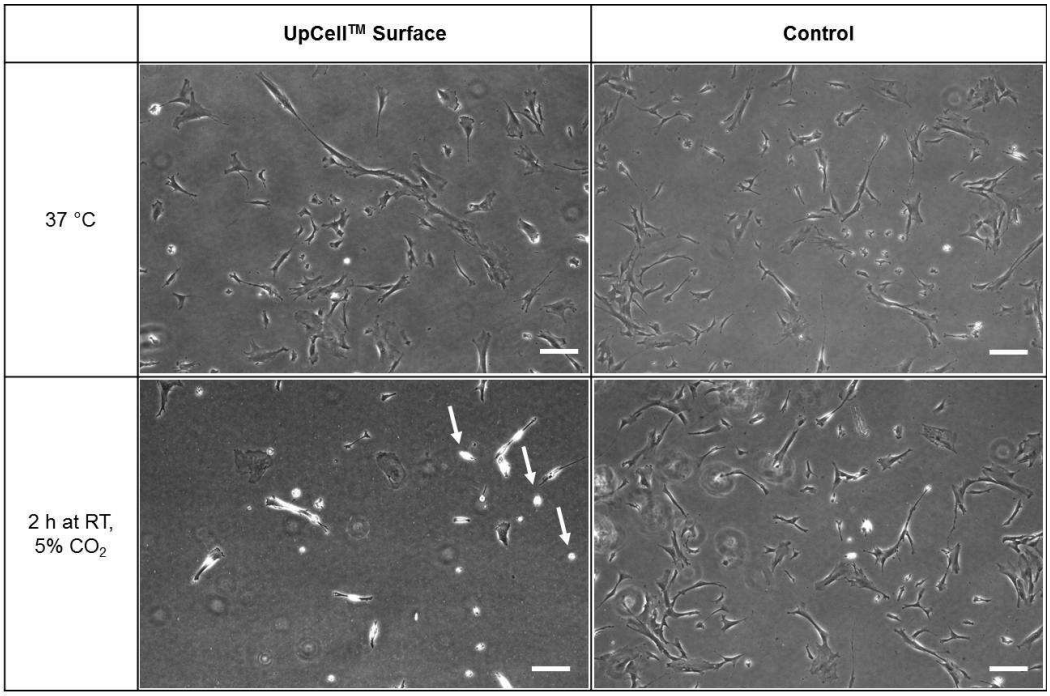

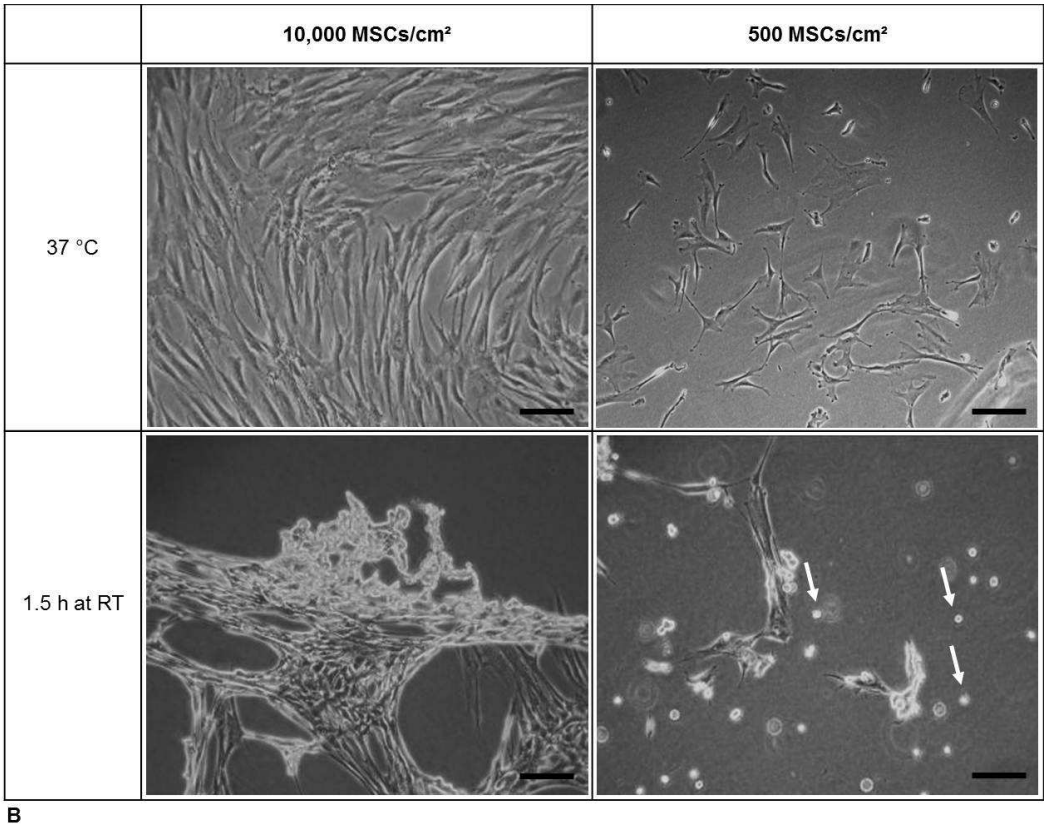

Figure 39. MSC detachment from UpCell™ surface. UC MSCs were cultivated on thermoresponsive UpCell surfaces and detached by cooling. (A) Comparison of UC MSC detachment from UpCell™ surface and standard cell culture surface (tissue culture treated polystyrene, control). UC MSCs were seeded at 1000 cells/cm², cultivated for 4 d at 37 °C and detached by cooling to room temperature (RT). (B) Influence of different cell densities on BM MSC detachment. Arrows point to detached cells. Scale bar: 200 µm.

3.5.2 Cultivation of MSCs on Non-Commercial, Thermoresponsive Surfaces

Temperature-induced detachment of MSCs from the commercially available UpCell™ surfaces was very slow with many cells still attaching to the surface after 2 h of incubation at reduced temperature (see above). Aiming to improve MSCs detachment, new thermoresponsive surfaces, with improved surface properties regarding MSCs detachment, were developed by Dr. Ning Zhang at the department of Prof. Dr. Rieger (TUM).

All polymers and polymer-coated surfaces were developed, synthesized and kindly provided by Dr. Ning Zhang.

3.5.2.1 Toxicity Screening

An essential prerequisite for new polymer-coated surfaces is the lack of toxicity of the respective polymers. To identify polymers suitable for use in MSC culture, BM MSCs were cultured in the absence or presence of different polymer solutions. Inhibitory or toxic effects of polymers were evaluated by cell number determination after 3 d of cultivation (Figure 40). As controls, MSCs were cultured under toxic conditions (2% DMSO, positive control) or left untreated (negative control). As reference, MSCs were additionally cultured in the presence of PNIPAAM, the LCST polymer used for commercially available UpCell™ sufaces. Polymer concentrations were based on literature descriptions (Yamada et al., 1990, Takezawa et al., 1990). Different batches of poly(diethyl vinylphosphonate) (PDEVP) did not inhibit MSC proliferation when used in low concentrations (3 mg/ml), resulting in cell numbers comparable to untreated controls and low doses of PNIPAAM (Figure 40). Yet, at higher concentrations of PDEVP (30 mg/ml), cell proliferation was inhibited as illustrated by the decrease in cell numbers. This, however, was comparable to the inhibition of cell growth by high concentrations of PNIPAAM. Additionally, two poly(2-alkyl-2-oxazline)s (POx) were tested. Poly(2-metyl-2-oxazline) (PMeOx) and poly(2-n-propyl-2-oxazline) (PnPrOx) already inhibited MSC proliferation at low concentrations (3 mg/ml and 2 mg/ml, respectively, Figure 40). It should be noted that precipitation of some polymers (marked with # in Figure 40), in particular low and high doses of PnPrOx, led to complete coverage of cells, thus potentially impairing cells from sufficient nutrient and oxygen supply. This is likely to inhibit cell proliferation, making it impossible to distinguish whether inhibition of cell proliferation was due to coverage with polymer, toxic properties of the polymer or a combination of both.

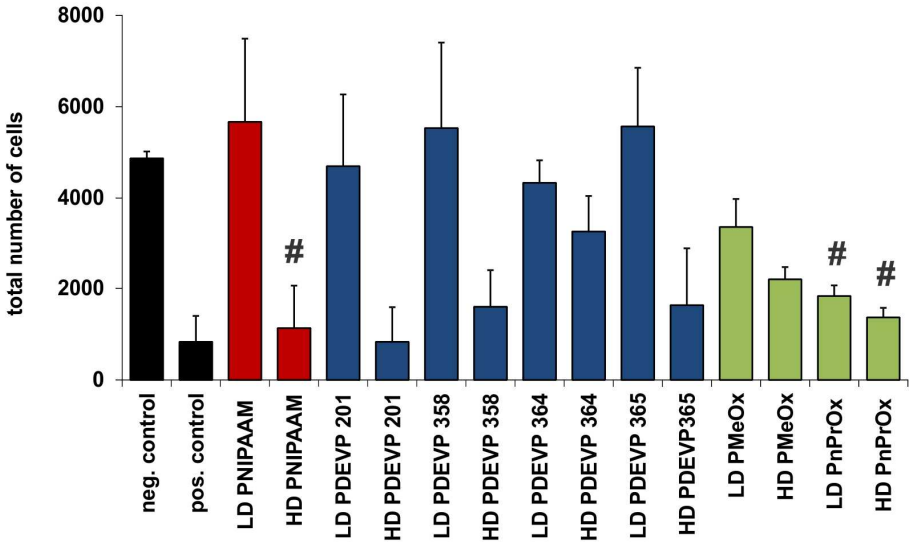

Figure 40. Toxicity of different polymer solutions. BM MSCs were cultured for 3 days in the presence of low (LD) or high doses (HD) of different polymers. Negative controls were left untreated. Positive controls were cultured in medium containing 2% DMSO. Cells from three different wells were counted. Depicted are mean values with standard deviations. LD = 3 mg/ml (except for 2 mg/ml for PNIPAAM and PnPrOx), HD = 30 mg/ml (except for 20 mg/ml for PNIPAAM and PnPrOx), # = polymer precipitate overlaid cells. Abbreviations: PNIPAAM poly(N-isopropylacrylamide); PDEVP poly(diethyl vinylphosphonate); PMeOx poly(2-metyl-2-oxazline); PnPrOx poly(2-n-propyl-2-oxazline).

In summary, PDEVP seemed to be suitable for MSC cultivation, comparable to the commercially used PNIPAAM. The tested poly(2-oxazoline)s inhibited cell proliferation even at low concentrations. However, on temperature-responsive surfaces, polymers will be bound to substrate and not be present in solution, which may alter the observed toxic properties of these polymers. Hence, poly(2-oxazoline)s may be evaluated as an alternative to poly(vinylphosphonate)s for coating of cell culture substrates.

3.5.2.2 MSCs Cultivation on PDAVP-coated Surfaces

Besides lack of polymer toxicity, an essential requirement for MSCs cultivation on thermoresponsive surfaces is MSC attachment and proliferation on the respective polymer-coated surfaces. To provide such surfaces for evaluation in cell culture experiments Zhang et al. developed a novel method for controlled, homogenous, and covalent coating of (silicon) substrates with poly(dialkyl vinylphosphonate) (PDAVP) brushes (Zhang et al., 2012a). Using rare earth catalysts, surface-initiated group transfer polymerization was used for surface graft-

ing, leading to polymer-coated substrates with controllable thickness and thermoresponsive properties (see Figure 41) (Zhang et al., 2012b, Zhang et al., 2012a). Polymer layer thickness can be regulated by extending UV polymerizations time (increases thickness of poly(ethylene glycol dimethacrylate) (PEGDM) cross-layer), increasing DAVP monomer/catalyst ratio or prolonging SI-GTP time (see Zhang et al., 2012a). Furthermore, Zhang et al. found that the LCST of polymer-coated surfaces can be easily regulated by copolymerization. For example, copolymerization of DEVP and DPVP allowed for LCST adjustment to physiological relevant regions around and below 37 °C (Zhang et al., 2012b).

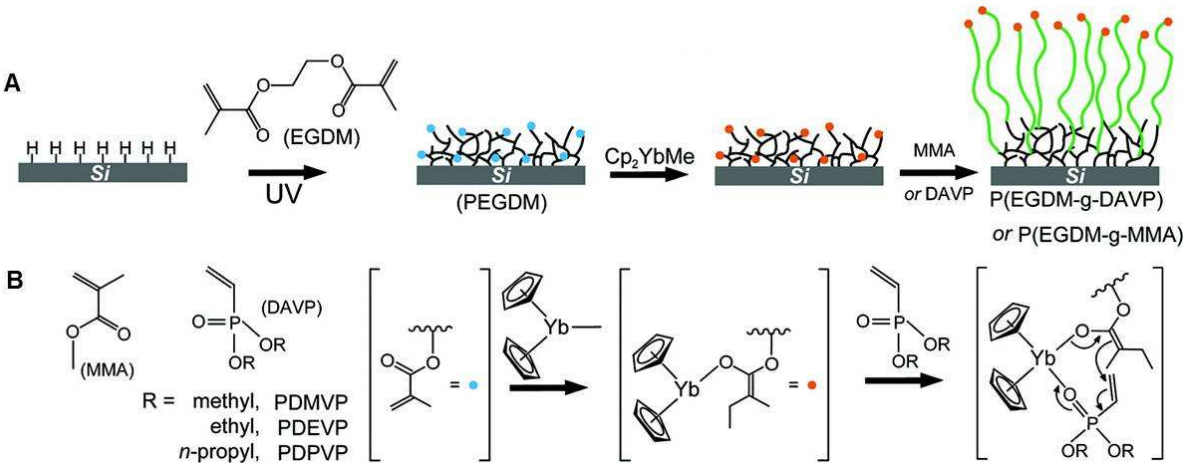

Figure 41: Preparation of poly(vinylphosphonate)-coated substrates. (A) Hydrogen-terminated silicon substrates are pre-coated with a cross-linked PEGDM layer using UV polymerization. Then rare earth metal catalyst-mediated surface-initiated group transfer polymerization (SI-GTP) of DAVP is applied for grafting of DAVP on PEGDM layer. (B) Molecular structure of MMA and DAVP (left) and reaction mechanism of SI-GTP (initiation and chain growth). Abbreviations: EGDM ethylene glycol dimethacrylate; DAVP diethyl vinylphosphonate; Cp2YbMe bis(cyclopentadienyl)methylytterbium (catalyst); MMA methyl methacrylate. Adopted from Zhang et al., 2012a.

First, MSC adhesion and proliferation on different polymer-coated surfaces was evaluated at cultivation temperature (37 °C). Tested substrates varied in polymer layer thickness, copolymer composition and theoretical LCST. Generally, MSCs attached and proliferated on PDAVP-coated substrate as exemplary shown in Figure 42 for UC MSCs cultivation on a P(DEVP-co-DPVP)-coated glass surface. Compared to cell attachment and proliferation on standard cell culture surfaces (tissue culture treated polystyrene), cell attachment was slightly decreased, correlation to a lower cell density after 3 d of cultivation (Figure 42).

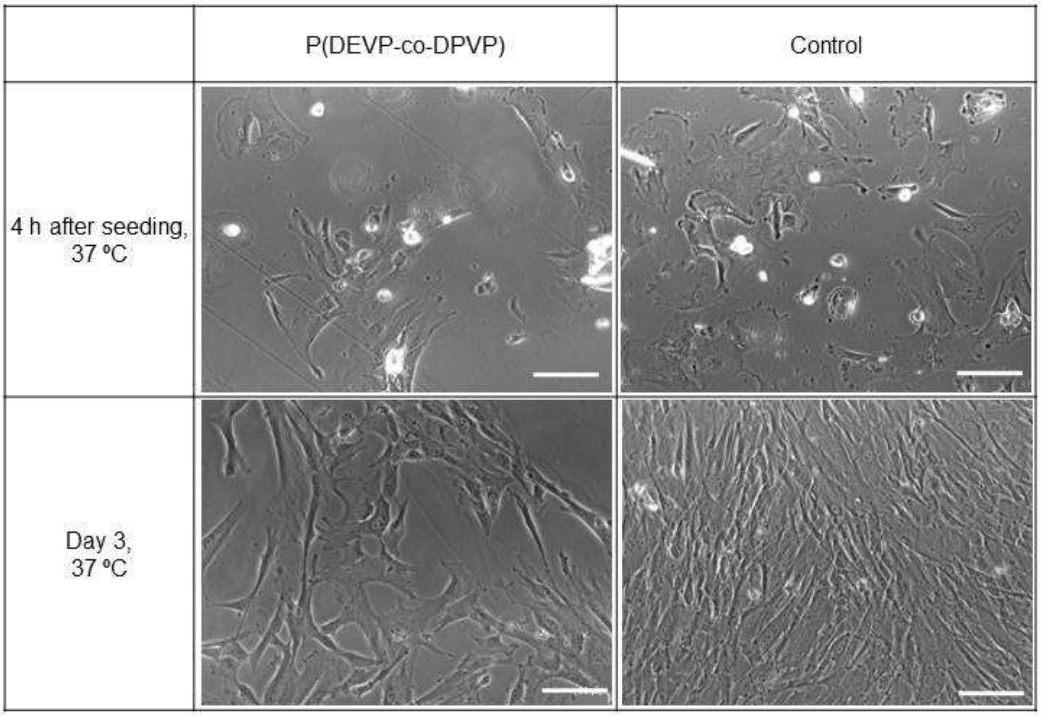

Figure 42: Cell adhesion and proliferation on PDAVP-grafted surfaces. UC MSCs were seeded at equal densities on P(DEVP-co-DPVP)-coated glass surfaces or standard cell culture surfaces (tissue culture treated polystyrene, control). Cell attachment 4 h after seeding and cell proliferation after 3 days were evaluated. Lower critical solution temperature (LCST) of P(DEVP-co-DPVP): 34 °C. Abbreviation: P(DEVP-co-DPVP) poly(diethl vinylphosphonate-co-dipropyl vinylphosphonate). Scale bar: 100 µm.

Next, the key property of polymer-coated surfaces, i.e. temperature-induced cell detachment, was assessed. In principal, two different aspects were evaluated during these experiments, namely the influence of polymer layer thickness and copolymer composition. For this, UC MSCs were cultivated for 2 to 4 d on polymer-coated substrates at 37 °C. Then, temperature was reduced by medium exchange with cold medium (4 °C) and incubation at RT (~21 °C) for various time periods.

PDEVP-coated surfaces grafted with low (11 nm) and high (152 nm) polymer layer thickness were evaluated regarding temperature-induced MSC detachment. In both samples, contact angles changed by approximately 10° upon temperature reduction from 40 °C to 22 °C (data provided by Dr. Ning Zhang, see Supplementary Figure 1), showing a hydrophobic-hydrophilic switch comparable to PNIPAAM-coated UpCell^{TM} surfaces (Okano et al., 1993, Plunkett et al., 2006). However, no cell detachment from either surface was observed upon temperature reduction from 37 °C to RT (Figure 43).

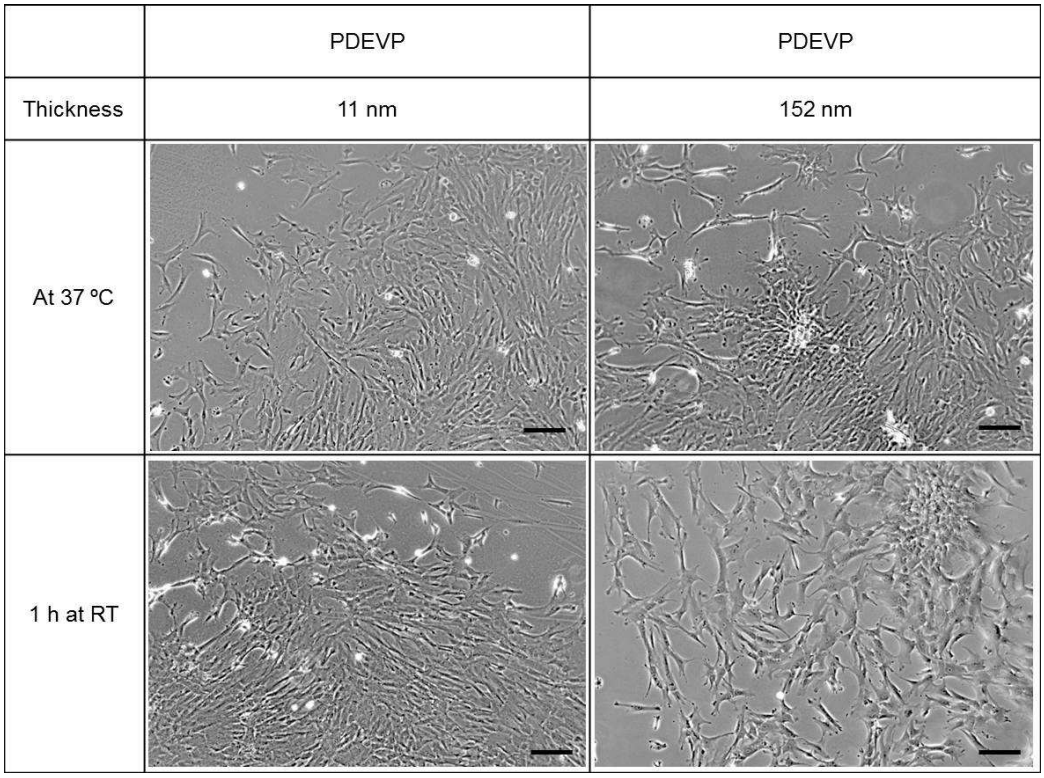

Figure 43: Microscopic observation of MSC behavior on PDEVP-grafted surfaces upon temperature reduction. UC MSCs were seeded at equal densities on PDEVP-grafted glass surfaces with different polymer layer thickness (11 nm, left and 152 nm, right) and cultured for 2 days at 37 °C (top row). MSC behavior upon cooling and incubation at RT was observed (bottom row). Abbreviations: PDEVP poly(diethyl vinylphosphonate); RT room temperature. Scale bar: 200 µm.

As the LCST of PDAVPs can be adjusted by copolymerization (Zhang et al., 2012b), substrates grafted with different copolymer ratios were synthesized. Again, cells were first cultured at 37 °C and then temperature was reduced and cells were incubated for designated time periods at RT. Figure 44 depicts representative results for some of these substrates. Upon temperature reduction, UC MSCs cultivated on P($DEVP_{90}$-co-$DPVP_9$) showed notable morphology changes. Whereas MSCs possessed their characteristic spindle-shape like morphology at 37 °C, cells started to condense, obtaining a rounder shape at reduced temperature. A very small number of cells detached as round spheroids from the surface (see Figure 44A, left column). Yet, detachment was slow with only few cells detaching after 2 h at RT. The described morphological changes were observed for polymer-coated surface with an LCST well below the standard cultivation temperature of 37 °C (here: LCST of 34 °C in bulk solution), but less prominent or not observable on polymer-coated surfaces with higher LCST (here: 38 °C and 49 °C; Figure 44). As a control, MSCs cultivated on standard cell culture surfaces were used and did not show detachment and/or morphological changes upon temperature reduction (data not shown).

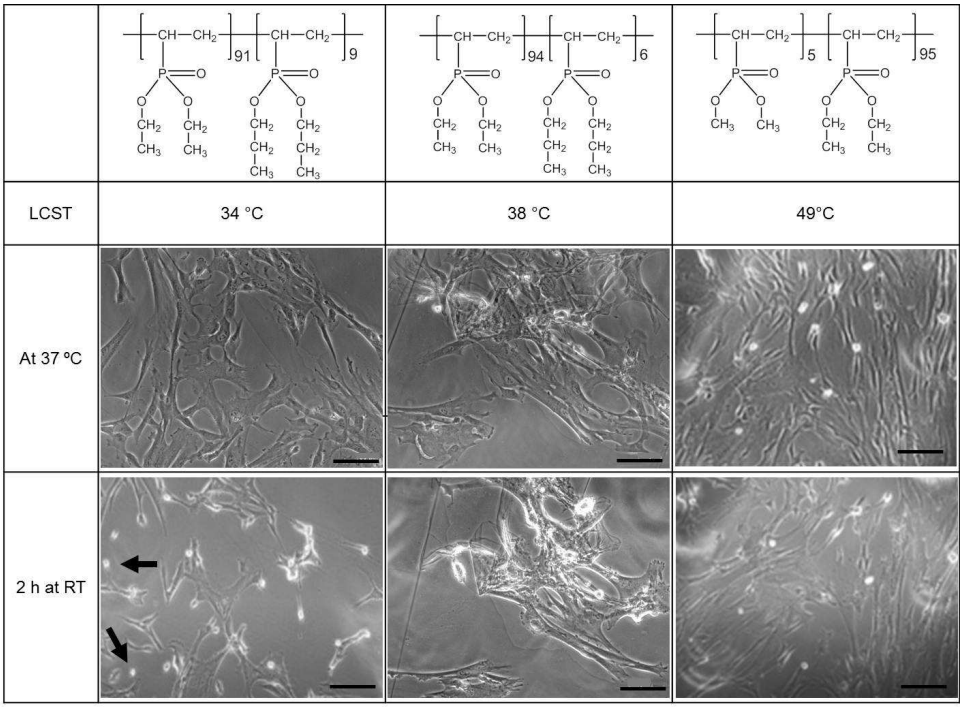

A

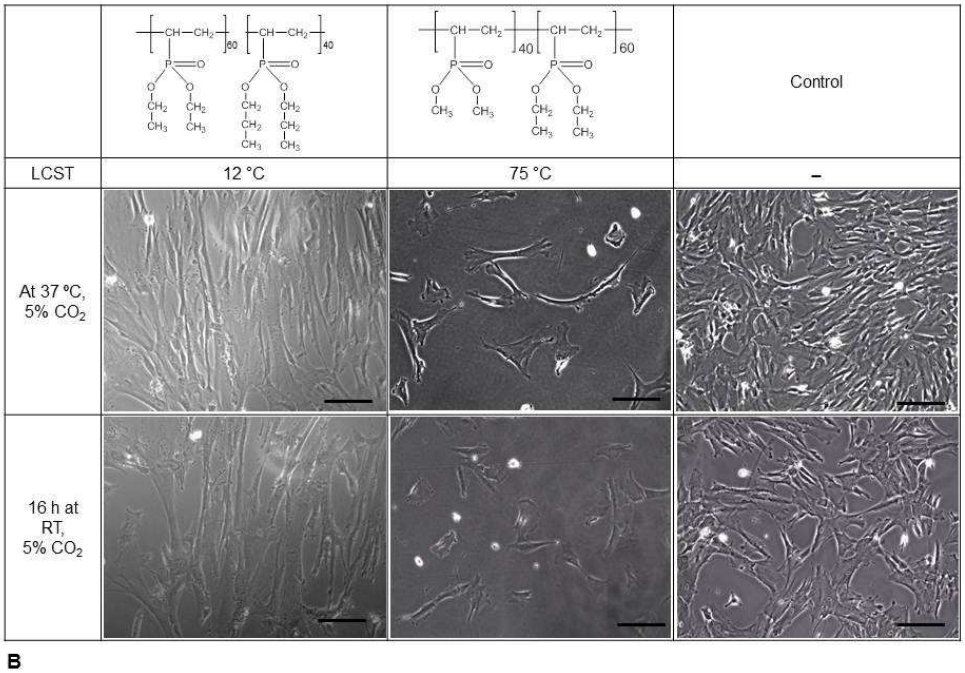

B

Figure 44: Microscopic observation of MSC behavior upon temperature reduction on different polymer-coated surfaces. UC MSCs were seeded at equal densities on P(DEVP$_{90}$-co-DPVP$_9$)-, P(DEVP$_{94}$-co-DPVP$_6$)-, P(DEVP$_5$-co-DPVP$_{95}$)-coated glass substrates (A, from left to right) and cultured for 3 d at 37 °C. MSC behavior upon cooling and incubation at RT and atmospheric air (~0.04% CO_2) was evaluated (A, bottom row). Similar to A, UC MSCs in B were seeded on P(DEVP$_{60}$-co-DPVP$_{40}$)- and P(DMVP$_{60}$-co-DEVP$_{40}$)-coated glass surfaces or standard tissue culture treated polystyrene surface (control) (left to right) and cultivated at 37 °C. In contrast to A, incubation at RT was performed at 5% CO_2 (bottom row). Abbreviations: RT room temperature, LCST lower critical solution temperature (as determined in bulk solution). Scale bar: 100 µm.

It should be noted that the incubations at reduced temperature noted above were performed in atmospheric air, i.e. at approximately 0.04% CO_2 (Beck, 2007) and not under standard controlled cultivation conditions which contain 5% CO_2. The CO_2 decrease leads to a pH increase of the sodium bicarbonate buffered culture medium. Hence, the observed cell detachment could have also occurred due to these pH changes. To eliminate a potential pH effect, cell detachment studies were performed at RT and 5% CO_2. As shown for P($DEVP_{60}$-co-$DPVP_{40}$)- and P($DMVP_{60}$-co-$DEVP_{40}$)-coated substrate, no relevant cell detachment could be detected under these conditions even after 16 h incubation at RT (Figure 44, left column). Remarkably, UC MSCs also attached to the rather hydrophilic P($DMVP_{60}$-co-$DEVP_{40}$)-coated surface (LCST 75 °C in bulk solution), even if cell attachment was reduced compared to P($DEVP_{60}$-co-$DPVP_{40}$)-coated and standard cell culture surface (Figure 44B).

4 Discussion

Hematopoietic stem cell therapy has been successfully applied for many decades, saving the lives of thousands of patients who suffer from leukemia or other blood diseases (Appelbaum, 2012). Mesenchymal stem cells (MSCs) have emerged as a promising candidate for cell therapy due to their unique therapeutic characteristics (Ma, 2012, Huss, 2010, Parekkadan and Milwid, 2010). They are currently being evaluated in numerous clinical trials for treatment of diseases with high unmet medical needs such as graft-versus-host disease (GvHD), myocardial infarction, multiple sclerosis, bone and cartilage damage, diabetes, and critical limb ischemia (http://www.clinicaltrials.gov). Therapeutic application of MSCs requires large amount of cells: 10^6 to 10^7 cells are commonly administered as a single dose (Ringden et al., 2006, Sato et al., 2010, Subbanna, 2007). This demand for high cell numbers is opposed by the limited number of MSCs that can be isolated from tissue. Therefore, an efficient, GMP-compliant cell expansion process is a key technology for manufacturing of a biopharmaceutical "off-the shelf" cell therapy product. Moreover, manufacturing of biopharmaceuticals is a complex process and it is commonly acknowledged that "the process is the product," i.e. that slight changes of the manufacturing process can influence properties of the final product with respect to its clinical safety and efficacy (Roger, 2006). Hence, special considerations have to be given to the cell manufacturing process to ensure maintenance of MSC characteristics and therapeutic relevant function and to ensure production of a reproducible, high quality cell-based medicinal product. State of the art cell culture technologies using flask or cell stack expansions have several drawbacks which make them unfavorable for large-scale expansion of a clinical MSC product. These limitations can be overcome by an innovative MSC expansion technology which allows not only for superior cell cultivation under good manufacturing practice (GMP) but also holds the potential to modulate MSCs towards tailored functions, thus priming them for the treatment of distinct diseases.

4.1 MSC Cultivation on Microcarriers: Process Development, Optimization, and Scale-up

Microcarrier-based cultivation in stirred bioreactors provides excellent means for expansion of a therapeutic cell product in a GMP-compliant process. It does not only offer a large culture surface area in small volume for cost-efficient production of adherent cells but also allows reproducible expansion in a closed, automated, regulated, and scalable process. During the establishment of a microcarrier-based expansion process, numerous parameters (such as medium composition, inoculation procedure, stirring speed, optimal pH and pO_2 values) can

be optimized. For various reasons, cell attachment is a critical step in the expansion process. First, it determines the initial cell density, a parameter described to influence MSC proliferation and function (McBride and Knothe Tate, 2008, Colter et al., 2000, Hu et al., 1985). Additionally, as the amount of MSCs isolated from tissue is limited, efficient cell attachment is highly desired. Therefore, the main parameter addressed for optimization in this work was efficient cell attachment through a) identifying the most suitable microcarrier format and b) improving the seeding procedure.

Judging from the different findings in the literature, it can be assumed that certain microcarrier formats may be more suitable for certain types of MSCs (Frauenschuh et al., 2007, Sart et al., 2012, Sart et al., 2010, Weber et al., 2007). To my knowledge, no study has so far evaluated UC and AM MSC expansion on microcarriers (see Table 4). In contrast to other studies using ear MSCs (Sart et al., 2012) or rat BM MSCs (Yang et al., 2007b), human UC and AM MSCs employed in the presented work attached most efficiently to Cytodex 1 microcarriers. Cell adhesion to substrate surface is mediated through focal adhesions consisting of cell surface receptors, mainly integrins, which bind to extracellular matrix (ECM) proteins absorbed to the surface (Berrier and Yamada, 2007). Various surface material properties such as chemical composition and surface topography have been described to influence cell adhesion in a cell-type dependent manner (Chang and Wang, 2011, Kim et al., 2010, Cavalcanti-Adam et al., 2007). Different biomaterials are used for microcarrier production. For MSC expansion, Cytodex and CultiSpher are most commonly employed (see Table 4 of introduction) consisting of modified dextran or gelatin. Dextran is a biocompatible, branched, α-D-1,6-glucose-linked glucan (www.dextran.net). Gelatin, which is obtained by hydrolysis of collagen, is a commonly used coating in adherent cell culture (Salacinski et al., 2001). Both UC and AM MSCs used in this study showed best attachment to positively charged Cytodex 1 microcarriers. However, this preference is not solely due to the microcarriers' charge, as other tested microcarrier types were also positively charged, but displayed notably lower cell adhesion. Charge density is also known to influence cell adhesion (Curtis and Buultjens, 1973), but it is unknown if and how the various microcarrier types differ regarding this parameter. It can be assumed that a combination of factors such as surface charge, charge density, chemical composition, and hydrophobicity have mediated the observed superior attachment to Cytodex 1 microcarriers.

Besides surface material composition, the inoculation procedure itself can influence cell attachment. Different inoculation procedures have been described in the literature ranging from

static inoculation to continuous stirring throughout the whole process (Shiragami et al., 1997, Yuan et al., 2012). In theory, static inoculation may lead to better cell adhesion due to the prolonged cell-microcarrier contact time, whereas inoculation under stirring conditions may result in more homogenous cell distributions. In this work, static overnight inoculation with only a short, initial mixing of the cell-microcarrier suspension initiated the best MSC attachment and subsequent proliferation. A negative effect on homogeneity of the cell distribution was not observed compared to procedures consisting of longer stirring periods. Despite the improved protocol and a theoretical concentration of 1.2 cells/microcarrier, many microcarriers remained cell-free after inoculation, revealing further room for optimization. As an example, different seeding densities could be evaluated. Indeed, other investigators usually used higher concentrations of cells/microcarrier and the microcarrier manufacturers also recommend higher cell densities for inoculation (Yuan et al., 2012, Elseberg et al., 2012, Healthcare, 2005). MSC seeding densities should be carefully chosen since they were found to be inversely related to proliferation and multilineage differentiation potential (Sekiya et al., 2002). Other strategies to improve cell attachment could be provided by surface engineering, for example, through coating of microcarrier surfaces with ECM proteins like laminin or fibronectin or through incorporation of RDG peptides to improve integrin-ECM binding (Spatz and Geiger, 2007).

Concerning cell distributions on microcarriers, it was striking that cells did not attach and proliferate homogenously on the microcarriers. In particular, many microcarriers were still cell-free at the end of the cultivation process whereas others showed up to 100% confluence. Bead-to-bead transfer of cells has been previously reported (Wang and Ouyang, 1999, Sart et al., 2009, Schop et al., 2008) but may not be sufficient for a more homogenous cell distribution in this case. Furthermore, upon reaching higher cell densities, cell-microcarrier aggregates tended to form, which is in accordance to previous observations from other authors (Schop et al., 2008, Eibes et al., 2010, Frauenschuh et al., 2007, Ferrari et al., 2012). The formation of aggregates leads to heterogeneity of the cell population with impaired nutrient and oxygen supply of cells within the aggregate and differences in the microenvironment are known to influence MSC fate and function (Gregory et al., 2005). Aggregation could be avoided by increasing stirring speed (considering, however, that higher stirring speed leads to increased shear stress) or reducing serum and/or Mg^{2+} and Ca^{2+} concentrations (GE Healthcare, 2005). Addition of fresh microcarriers has also been shown to limit aggregation which has been explained by bead-to-bead transfer (Ferrari et al., 2012, Schop et al., 2010).

A further crucial point for optimization is the harvest procedure. Efficient separation of microcarrier and MSCs is a crucial point for obtaining a cell product that can be applied clinically. In this work, a size-based separation of microcarriers and cells using filter systems was employed. However, this method has two major drawbacks. First, a substantial amount of cells is lost during the harvest procedure, resulting in harvest efficiencies as low as 61%. Second, microcarriers could not be completely removed from the cell product (data not shown). Poor cell harvest from Cytodex 1 microcarriers has been reported in the literature (Timmins et al., 2012). To improve cell recovery and purity, more sophisticated harvest procedures could be employed. For example, the use of magnetic carriers would facilitate a more efficient separation of microcarriers from cells. Preliminary experiments using magnetized Cytodex 1 microcarrier showed that generally, MSC expansion on magnetic microcarriers is possible (data not shown). The question of whether the magnetization of microcarriers influences cell characteristics and function remains to be elucidated.

Even though medium optimization was not part of this work, it should be noted that medium composition and optimal nutrient supply are critical parameters in cell expansion. Glucose and glutamine are the main energy source for animal cells (Glacken, 1988). Especially at the end of cultivation, glucose consumption of MSCs in spinner flasks was high, resulting in complete glucose depletion (the concentration dropped below the detection limit). Therefore, additional glucose should be provided and this point was addressed in the large-scale bioreactor experiments in this work. Glucose consumption rates were found to be similar to previously reported rates of 2 – 8 pmol/h/cell in BM MSCs studies (Schop et al., 2010). Metabolism of glucose and glutamine results in production of the toxic metabolites lactate and ammonia which accumulate in the culture medium and can inhibit cell growth (Hassell et al., 1991). Lactate can lower the pH value of the culture medium whereas NH_3 can diffuse through the cell membranes, disrupting the pH levels of intracellular compartments and causing cell death (Schneider et al., 1996, Martinelle et al., 1996). These toxic metabolites were at least partly removed by refreshing half of the culture medium, thereby keeping lactate concentrations below 12 mM and ammonia concentrations below 1.2 mM. These concentrations should not be growth limiting according to previous studies which reported on inhibiting concentrations equal to or greater than 35 mM and 2.4 mM, respectively (Schop et al., 2009a).

The yield of lactate from glucose ($Y_{lac/glc}$) can be used to estimate which metabolic pathway cells use to gain energy (Schop et al., 2009a, Higuera et al., 2009). The observed $Y_{lac/glc}$ of up to 2 is connected to glucose metabolism via glycolysis instead of the more energy efficient

oxidative phosphorylation (Glacken, 1988, Newsholme et al., 1985). Calculated $Y_{lac/glc}$ and glucose consumption rates are comparable to those obtained from studies on BM MSCs (Schop et al., 2009a). In accordance with results presented here, previous studies also found that MSCs primarily use the anaerobic glycolysis pathway, even when cultivated under normoxic (21% O_2) conditions (Schop et al., 2010, Pattappa et al., 2011). This phenomenon, i.e. glycolytic metabolism and high production levels of lactate despite the presence of sufficient levels of oxygen, is called the Warburg effect (Krebs, 1972).

While lab-scale experiments in spinner flasks are a useful tool to develop and optimize basic steps in a microcarrier-based expansion process, they do not provide the means for expansion in a controlled and regulated environment. In contrast, larger bioreactor systems allow for appropriate regulation of the microenvironment through online control of all basic culture parameters such as pH, pO_2, pCO_2 values, or nutrient levels. The microcarrier-based expansion process is well suitable for scale-up to controlled and regulated stirred bioreactors. Regarding MSC expansion, however, maximum culture volumes used so far commonly remain below 500 ml. Only two studies use culture volumes of 1 l or above (Elseberg et al., 2012, Sart et al., 2009) and only one of them employs controlled and regulated bioreactor conditions (Elseberg et al., 2012). Within this thesis, the MSCs expansion process on Cytodex 1 microcarrier was successfully scaled up to 1.5 l (exemplary for UC MSCs). Moreover, detailed analysis of bioreactor-expanded cells revealed that MSC characteristics were maintained and comparable to flask-expanded cells. Interestingly, PCA indicated that controlled and regulated bioreactor conditions lead to a less heterogeneous gene expression pattern: Like spinner flask-expanded cells, MSCs expanded in controlled bioreactors were clearly distinguishable from flask-expanded cells, but in contrast to spinner flask-expanded cells, they showed very close clustering. This illustrates that MSC expansion under controlled, regulated conditions can help to reduce variability between different donors, leading to a more homogenous cell product. In fact, this addresses one frequently uttered objection regarding therapeutic use of MSCs, namely the high variability and heterogeneity of expanded cells (Wagner and Ho, 2007, Bieback et al., 2012). Reproducible, homogenous cell quality is a critical point for a therapeutic cell product. In accordance with regulatory requirements, findings presented here clearly underline the need for a controlled, regulated manufacturing process. As the “the process is the product,” the manufacturing process can have crucial influence on the final product with respect to its clinical safety and efficacy. In the biopharmaceutical industry, this paradigm is

already widely acknowledged regarding the production of monoclonal antibodies and other recombinant proteins (Schneider, 2008, Heinemann and Hompesch, 2011).

4.2 Source and Donor Variability

Regarding development of an "off-the-shelf" clinical cell product, standardized, reproducible manufacturing of the active pharmaceutical ingredient (API), in this case MSCs, is required. Yet, heterogeneity of cells due to different sources, donors, or cultivation methods is high and represents one of the major hurdles in the field (Bieback et al., 2012, Wagner and Ho, 2007). Source- and donor-related variability and the influence of the expansion process will be discussed in the following.

While BM remains the most widely used source for MSC isolation, MSCs can be isolated from virtually all postnatal tissues of the body (da Silva Meirelles et al., 2006). Although cells isolated from different sources are commonly characterized as "MSCs," it can be assumed that these cells are not identical regarding their biological function (Prockop and Oh, 2012, Prockop, 2009). MSCs from perinatal tissues such as UC and AM have been described as advantageous compared to adult tissue-derived MSCs regarding cell age, proliferative capacity, simplicity of isolation, and quantity of isolated cells (Hass et al., 2011, Ilancheran et al., 2009). Comparative studies of MSCs from various sources are scarce but have reported on differences in cell morphology, surface markers, cytokine secretion, or proliferation capacity *in vitro* (Lv et al., 2012, Hass et al., 2011, Barlow et al., 2008) and alterations in therapeutic protective mechanisms *in vivo* (Hauser et al., 2010).

In this work, UC and AM MSCs were isolated from the same donors (three donors total), therefore sharing the same genetic background. Hence, observed differences between UC and AM MSCs, such as higher proliferation capacity of UC MSCs (illustrated by the lower doubling times of UC MSCs) or distinct cytokine secretion, are most likely source-dependent and independent of the genetic background or donor variability. The high variation in growth rates between MSCs from different sources and different donors has already been described by others (Siddappa et al., 2007, Phinney et al., 1999) and was confirmed for UC and AM MSCs by this data. Since the comparison of different sources was not a focus of this work, these differences shall not be further discussed.

Furthermore, donor-to-donor variability is commonly high and has been shown to lead to altered cytokine secretion (Zhukareva et al., 2010) or expansion potential of MSCs (Koller et

al., 1996). In particular, AM MSCs have been previously found to show remarkably high inter-donor variability regarding growth characteristics, immunomodulatory capacity, secreted cytokine profile, and gene expression (unpublished data from our laboratory). Besides different cell sources and donors, independent expansion runs turned out to be an additional source for variability as shown in this work. The resulting variability is illustrated by large standard deviations as observed for cell numbers, immunomodulatory capacity or secreted cytokines, for example. Remarkably, despite variability resulting from different donors, sources and expansion runs, hierarchical clustering and PCA revealed that MSCs clearly clustered based on the cultivation method, indicating that the biological variability contributed less to variance than the expansion process. In other words, the effect of different cultivation methods on gene expression is higher than the effect of cell source or donor. This stresses the high influence of the cultivation technique on MSC fate. Interestingly, gene expression analysis indicated that variability between different MSC donors can be reduced by transferring the microcarrier-based expansion process to regulated conditions in bioreactors (see also discussion 4.1 above). This may help to overcome one of the major challenges regarding therapeutic use of MSCs, namely the high variability and heterogeneity of expanded cells.

4.3 Influence of Culture Conditions on MSC Characteristics and Function

It is well known that both *in vivo* and in *vitro*, cell fate is determined by the microenvironment of the cells (Eshghi and Schaffer, 2008, Wagner and Ho, 2007, Ema and Suda, 2012, Moore and Lemischka, 2006). *In vitro*, different culture conditions influence cell characteristics and functions: Besides biochemical factors and cell-cell interactions, mechanical stimuli- and surface topography and composition have been reported to influence cell morphology and function (Discher et al., 2009, Adamo and Garcia-Cardena, 2011, Dado et al., 2012, Gregory et al., 2005, Chang and Wang, 2011). Therefore, it stands to reason that dynamic expansion of MSCs on spherical, microporous, positively charged dextran Cytodex 1 microcarrier will also influence MSC morphology and function compared to standard static expansion on flat, solid, polystyrene-based surfaces. Yet, the effect of microcarrier-based expansion on MSCs is only sparsely evaluated in the literature with most studies addressing only minimal MSC characteristics: Phenotype of unspecific cell surface markers and tri-lineage differentiation potential (Eibes et al., 2010, Ferrari et al., 2012, Santos et al., 2011, Frauenschuh et al., 2007, Sart et al., 2009). This work provides a detailed comparative analysis of microcarrier- and flask-expanded UC and AM MSCs from three different donors. Analysis revealed an ef-

fect of the different cultivation processes on MSC morphology and characteristics, suggesting that MSC functions can be modulated and tailored by the expansion process. This is an important fact as different therapeutic indications will require specialized MSC characteristics and, in fact, different approaches using complex genetic or biochemical manipulation have been applied to optimize MSC efficacy (Wagner et al., 2009).

First of all, it should be noted that independent of the cultivation process, expanded cells showed MSC-typical characteristics and fulfilled ISCT minimal criteria (Dominici et al., 2006). They were plastic adherent, showed tri-lineage differentiation capacity and expression of defined surface molecules. In addition, immunosuppressive capacity of expanded MSCs was assessed and shown to be independent of the cultivation method (3.3.4).

MSCs expanded under different culture conditions showed differences in morphology: MSCs expanded under stirring conditions on microcarriers were smaller (3.3.1) and also less granular compared to flask-expanded cells. Morphological changes may result from the different microenvironments that cells are exposed to during dynamic cultivation on microcarrier or static incubation on cell culture flasks: Besides shear stress (Adamo and Garcia-Cardena, 2011, Chang and Wang, 2011) and surface chemistry and topography, cell densities have also been reported to be crucial for MSCs morphology (Colter et al., 2000). Moreover, links between cell morphology and function have been described previously. For example, studies of Prockop and co-workers suggested that morphological changes can alter proliferative capacity: Populations of smaller, agranular cells were shown to divide more rapidly whereas larger, more granular cells were connected to stationary cultures (Colter et al., 2000, Colter et al., 2001). In this work neither a change in doubling time nor in differentiation potential between the smaller, microcarrier-expanded and larger, flask-expanded MSCs could be shown. This, however, is in accordance with previous reports showing that, while having an anti-apoptotic effect, shear stress did not promote MSC proliferation but rather delivered cell cycle arrest (Luo et al., 2011) or even led to a decrease in cell number (Maul et al., 2011).

Besides regulation of proliferation, cell shape has also been reported to regulate tri-lineage differentiation of MSCs mediated by the actin cytoskeleton organization and activity of the RhoGTPase RhoA (McBeath et al., 2004, Mathieu and Loboa, 2012). Whereas other studies have reported an increased osteogenic and chondrogenic differentiation potential in response to shear stress (through modulated cell morphology/cytoskeleton organization) (Kreke et al., 2005, Sharp et al., 2009, Arnsdorf et al., 2009, Kreke et al., 2008, Li et al., 2004, Zuscik et al., 2008, Yeatts et al., 2012), an altered differentiation potential was not observed in this work.

However, most of the studies employed laminar shear stress and investigated the differentiation potential while both shear stress and differentiation-inducing biochemicals are applied simultaneously (see e.g. Kreke et al., 2005, Kreke et al., 2008, Yeatts et al., 2012). In contrast, in this work turbulent shear stress was applied and differentiation was chemically induced after harvest from microcarriers, i.e. after shear stress had been applied. Regarding the influence of stress mediated by microcarrier-based expansion, controversial results have been reported. Most microcarrier-based MSC expansion studies lack comparison to static flask expansion of MSCs (Schop et al., 2008, Ferrari et al., 2012, Santos et al., 2011, Boo et al., 2011), but a comparative study of Tseng at al. showed an induction of osteogenesis in microcarrier-cultured BM MSC, as compared to flask-expanded cells, even in the absence of biochemical stimulus (Tseng et al., 2012). However, similar to results presented here, Timmins and co-workers did not find altered MSC differentiation of stirred microcarrier cultures compared to static flask-expanded cells (Timmins et al., 2012). Regarding these controversial findings, it is important to consider that the influence of the microenvironment on MSC fate is multifactorial and complex, consisting not only of shear stress, but also other factors such as substrate topography or chemical composition of microcarriers.

In addition to morphological changes, cultivation-dependent differences were revealed by analysis of cytokine secretion and surface molecule expression. First, MSCs expanded on microcarrier secreted more VEGF than flask-expanded MSCs, an effect significant for both AM and UC MSCs and especially pronounced in UC MSCs which did not express any measurable VEGF when expanded in flasks (3.3.5). Moreover, significantly increased FGF-2 secretion was observed in microcarrier-expanded AM MSCs (trend in UC MSCs). VEGF and FGF-2 are known mitogens for endothelial cells with pro-angiogenic and anti-apoptotic function (Byrne et al., 2005, Kajdaniuk et al., 2011). SDF-1, was also found to be increased in microcarrier-expanded MSCs (statistically significant in UC MSCs, trend in AM MSCs) Interestingly, SDF-1 has been previously described to increase mRNA expression of cytokines such as FGF and VEGF in BM MSCs (Liu et al., 2011). This suggests a possible cross talk and feed-forward loop of SDF-1 and VEGF/FGF in UC and AM MSCs which could be further evaluated in future studies.

MSCs and MSC-like adult stem cell lines have previously been shown to secrete angiogenesis-promoting cytokines (Boomsma and Geenen, 2012, Huss et al., 2004). The data presented here shows that secretion of such cytokines can be further increased by a suitable microenvironment mediated through appropriate cultivation processes. In accordance with findings pre-

sented here, other studies on BM MSCs have reported on an increase of VEGF secretion through mechanotransductive signaling induced by laminar shear stress (Kreke et al., 2008) or dragging forces (Kasten et al., 2010).

Furthermore, additional evidence suggesting an increased angiogenic potential of microcarrier-expanded MSCs was the lack of CD349/frizzled-9 expression on microcarrier-expanded MSCs. Frizzled-9 is a seven transmembrane-spanning G-protein coupled receptor involved in Wnt/β-catenin signaling (Karasawa et al., 2002). In MSCs, Wnt signaling was found to regulate lineage specification and self-renewal (Ling et al., 2009, Etheridge et al., 2004). Interestingly, Tran et al have reported previously that CD349 negative human placenta-derived MSCs, in contrast to CD349 positive cells, positively affect blood flow recovery after vascular occlusion (Tran et al., 2011). Remarkably, the authors did not find a significant increase of VEGF mRNA expression in CD349 negative cells but rather correlated the described pro-angiogenic effect to increases in FGF-2 and PDGF expression (Tran et al., 2011). In contrast to their findings, this work showed a significantly increased VEGF expression on the protein level of CD349 negative, microcarrier-expanded cells. On the mRNA level, neither FGF, VEGF, nor PDGF expression changed significantly compared to CD349 positive, flask-expanded MSCs (see Supplementary Table 1). Discrepancies between mRNA and protein expression levels, however, are known and may be due to translational regulation, post-transcriptional modifications and/or different half-lives of proteins and mRNAs (Vogel and Marcotte, 2012).

Supporting evidence, suggesting an increase in angiogenic potential of microcarrier-expanded MSCs, was also revealed by gene expression and pathway analysis. This analysis showed an increase in functions connected to the category “cardiovascular system development” compared to flask-expanded MSCs. Within this category, several genes and pathways related to angiogenesis were increased in microcarrier-expanded MSCs. The fact that this increase was not significant might be explained by the pre-selection of a panel of 371 genes, likely resulting in an insufficient number of genes involved in the respective pathways.

In future studies, the indications for improved pro-angiogenic function of microcarrier-expanded MSCs clearly need to be confirmed by functional assays. For this, *in vitro* angiogenesis assays, such as HUVEC sprouting assay (Korff and Augustin, 1999), tube formation assays (Madri et al., 1988) or rat aortic ring assay (Nicosia and Ottinetti, 1990), could be used. Ultimately, such tests should be performed *in vivo.* Possible assays include cornea angiogenesis assays performed in mice’ or rabbits’ eyes (Muthukkaruppan and Auerbach, 1979,

Gimbrone et al., 1972) or chorioallantoic membrane assays performed on chick embryos (Brooks et al., 1999). Furthermore, for therapeutic applications of such pre-conditioned MSCs, efficacy would have to be demonstrated in appropriate animal disease models. As the data presented here suggests an improved pro-angiogenic function of microcarrier-expanded MSCs, these cells may have a higher potential/efficacy in therapeutic applications requiring re-vascularization or neo-angiogenesis. For example, previous studies have reported on a VEGF-mediated therapeutic effect of MSCs in rat models of acute kidney injury (Tögel et al., 2009), Parkinson disease (Xiong et al., 2011), or myocardial infarction (Kim et al., 2011), and an adult stem cell line was shown to support angiogenesis in a murine model of hind-limb ischemia (Conrad and Huss, 2005), which is a long-term complication in diabetic patients (Pedrajas et al., 2012).

Pathway analysis revealed further biological functions that were influenced by the different culture conditions. As a general remark, it should be noted that gene expression analysis was not performed on whole genome data and, therefore, analysis is likely to be biased due to the pre-selection of specific genes. Nevertheless, a significant increase in functions regarding the immune system, including the mobilization, attraction and/or recruitment of myeloid cells, such as neutrophils, granulocytes, phagocytes, and macrophages, was found in microcarrier-expanded UC and AM MSCs compared to flask-expanded cells. Previous studies have already revealed an increase of genes involved in immune system development and function in MSCs from perinatal tissue (i.e. AM and UC) compared to adult BM MSCs using standard flask expansion (unpublished data from our laboratory). Remarkable, in the work presented here, a further increase regarding these functions has been observed when AM or UC MSCs were cultivated under stirred conditions on microcarriers. This suggests that appropriate culture conditions can further prime UC and AM MSCs towards specific immunomodulatory functions, possibly also increasing their efficacy in relevant therapeutic applications.

In particular, the mRNA expression levels of CSF2, IL8, CXCL 2, and 3, all of which are associated with the immune response, were shown to be increased in microcarrier-expanded MSCs (Figure 34). CSF2 is mainly associated with the differentiation of monocytes (Gordon and Martinez, 2010). Like CXCL 2 and 3, the chemoattractive molecule IL8 (also known as CXCL 8) is a member of the CXC chemokine family, mainly connected to chemotaxis of neutrophils (Spanaus et al., 1997). Interestingly, studies of Carrero et al. found that CFS2, IL8, and CXC chemokine expression was highly induced in MSCs in a pro-inflammatory as mimicked *in vitro* by cytokine IL-1β stimulation. (Carrero et al., 2012). IL-1β in turn was al-

so increased in microcarrier-expanded MSCs in this work (among the ten genes with highest fold change of expression) and, in accordance with this finding, has previously been reported to be increased in response to shear stress (Glossop and Cartmell, 2009). This suggests that dynamic microcarrier-based expansion mimics elements of an inflammatory, IL-1β-induced environment. With regard to the above suggested pro-angiogenic potential of microcarrier-expanded MSCs, it is interesting to note that, besides their chemoattractive function, CXC chemokines have additional biological activities including potent angiogenic effects (Strieter et al., 1995b, Koch et al., 1992, Strieter et al., 1995a). In fact, the angiogenic activity is mediated through their shared, structural ERL (glutamate-arginine-leucine) motif (Strieter et al., 1995b). This dual role could account for the observed increases in functions related to both the immune response and angiogenesis in microcarrier-expanded MSCs.

In conclusion, this work strongly indicates that certain biological function of MSCs can be modulated by the expansion process. Data showed increased pro-angiogenic properties and immunmodulatory functions of microcarrier-expanded MSCs as compared to conventionally cultured MSCs from flasks. These findings do not only stress the importance and influence of the cellular microenvironment and cultivation conditions, but also suggest that, by using appropriate cultivation conditions, MSC function may be primed towards specific therapeutic applications.

4.4 MSC Cultivation on Thermoresponsive Surfaces

A major advantage of thermoresponsive surfaces is that, in contrast to traditional enzymatic harvest, temperature-induced cell detachment preserves cell surface molecules and ECM proteins yielding viable and healthier cells (Canavan et al., 2005a, Yang et al., 2012). In particular, since high-quality, efficacious MSCs are required for therapeutic applications, an enzyme-free detachment method would be beneficial regarding a cell expansion process for a therapeutic MSC product. As discussed above, microcarrier-based cultivation process offers excellent means for large-scale expansion of adherent cells and manufacturing of a clinical MSC product. Therefore, coating of microcarriers with thermoresponsive polymers would provide an innovative technology for cell expansion. In fact, very few studies have evaluated cell expansion on thermoresponsive microcarriers so far (Tamura et al., 2012a, Tamura et al., 2012b, Tamura et al., 2012c, Yang et al., 2010a) and only the study of Yang et. al. employed MSC which were derived from BM. All of the mentioned studies used microcarriers coated with poly(N-isopropylacrylamide) (PNIPAAM) or PNIPAAM co-polymers. In the work presented here, novel polymers were evaluated regarding their suitability for MSC expansion with the aim to improve and optimize MSC detachment. First, however, MSC detachment from commercially available PNIPAAM-coated UpCell^{TM} surfaces was evaluated.

Temperature-induced MSC detachment from PNIPAAM-coated surfaces was found to be very slow (see 3.5.1). Detachment was associated with a very slow change in MSC morphology from spread, fibroblast-like to round morphology. As noted by other authors, it is known that cooling-induced cell detachment is an active, ATP-dependent process involving cytoskeletal rearrangement (Yamato et al., 1999, Chen et al., 2008). However, this change was apparently too slow for efficient MSC detachment, in contrast to other reports using BM MSCs (Yang et al., 2010a, Shi et al., 2010). This could be due to different types of MSCs employed in these studies. Furthermore, MSCs were found to detach in aggregates or cell layers, especially at high cell densities. This is in accordance with findings from other authors (Yang et al., 2005, Yang et al., 2007a) and can be explained by the fact that cell-cell contacts, which are formed more extensively at high cell densities, are not dissociated by the temperature-dependent cell detachment from the culture surface. In fact, this property is essential for one of the main applications of UpCell^{TM} surfaces, namely tissue engineering, for which production of intact cell sheets is required (Kushida et al., 1999, Yamato et al., 2001, Nagase et al., 2009). In contrast, therapeutic application of MSCs requires administration of MSCs in single cell suspension, in particular as MSCs were found to be trapped in the lung after intra-

venous injection, a potential risk for pulmonary embolism (Fischer et al., 2009, Ankrum and Karp, 2010). To minimize cell aggregates, two basic strategies are possible. First, cell-cell interactions can be split after harvest. For this, gentle pipetting or enzymatic treatment can be employed. However, the former is highly dependent on cell type and strength of established cell-cell interaction and was not effective for MSCs grown to high densities (data not shown). The latter is unfavorable as it re-introduces enzymatic treatment and its drawbacks. Another strategy can focus on prevention of cell-cell interactions. Indeed, this idea is used for so-called RepCell™ surface which have recently been developed by a Japanese company (http://www.cellseed.com). Otherwise similar to the UpCell™ surface, RepCell™ is equipped with grids which functions as a barrier between cells, thus improving harvest of single cells.

To address the slow cell detachment from commercially available PNIPAAM-coated surfaces, an aim of this project was to develop surfaces with optimized detachment properties. While PNIPAAM's LCST of 32 °C makes it an attractive polymer for cell culture applications, it was found to have a broad transition range during the cooling process (Lutz et al., 2006). This slow transition may explain the observed slow cell detachment. Poly(dialkyl vinylphosphonate)s (PDAVPs) and their copolymers which have been synthesized for this project showed a fast thermoresponsive switch with narrow transition range (Zhang et al., 2012b). Furthermore, an important consideration for biomedical and cell culture application is the influence of salts or complex media on thermoresponsive behavior (Zhang et al., 2005, Lutz et al., 2006). PDAVPs and their copolymers were found to be relatively insensitive to the addition of physiological concentrations of salt and medium supplements: Observed salting-out effects on LCST were smaller or comparable to PNIPAAM (Zhang et al., 2012b). This, and their biocompatibility, make PDAVP attractive thermoresponsive polymers for cell culture application.

Yet, MSC detachment form PDAVP-coated substrate was found to be slow and inefficient. It is known from the literature that polymer thickness influences cell detachment behavior with polymer brushes thinner than approximately 15 nm impairing cell detachment (Mizutani et al., 2008). This has been explained by weakened compression of thin polymer brushes upon temperature-induced brush swelling resulting in a reduced detachment force f_{cell} and, therefore, inefficient cell detachment (Halperin and Kroger, 2012) (see also Figure 9). Together with the possibility that cells might have interacted with uncoated substrate at low grafting density, this could explain why no cell detachment was observed from thin, 11 nm polymer layers.

However, increasing the polymer layer thickness (152 nm) did not improve cell detachment. Interestingly, it was observed that at very high thickness, polymer brushes did not swell significantly upon cooling (see Supplementary Figure 2), suggesting that coil-globule transition was impaired due to steric hindrance when polymer grafting was very dense and thick. This hypothesis is supported by other authors who have also reported on impaired chain collapse and protein absorption on densely grafted polymer brushes (Xue et al., 2011), which in turn would lead to hindered cell detachment. Possibly, the ideal grafting density and polymer brush thickness for MSC detachment lies somewhere between 11 nm to 152 nm (see Figure 45). As the newly developed grafting-method by Zhang et al. allows for regulation of polymer thickness through different polymerization times (Zhang et al., 2012a), substrates coated with layers of different thickness could be easily tested in future experiments.

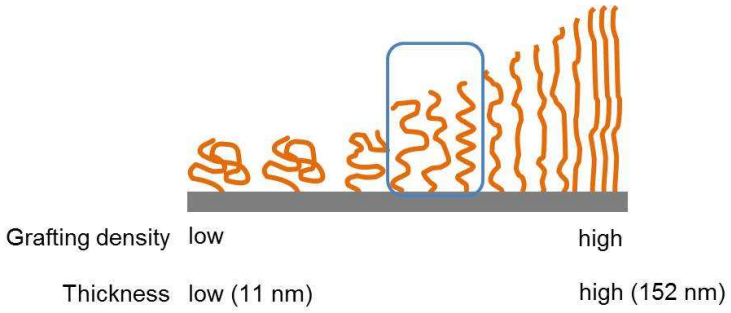

Figure 45. Variation of grafting density and layer thickness. The ideal grafting density (marked in blue) for cell detachment may lie between the tested thicknesses of 11 nm and 152 nm. (Modified figure kindly provided by Dr. Ning Zhang).

A second aspect that might lead to impaired cell detachment is an insufficient thermo-switching behavior due to inappropriate LCST of the coated surfaces. Yet, contact angle measurements revealed that PDAVP-grafted surfaces undergo a hydrophobic-hydrophilic switch upon cooling (Supplementary Figure 1). To adjust the LCST, PDAVPs with different copolymer ratios were synthesized and grafted on substrates, but no improved cell detachment was observed. In particular, a strategy to facilitate cell detachment is copolymerization with more hydrophilic polymers. While this strategy has been successfully employed by others (Hyeong Kwon et al., 2003), copolymerization of DEVP and the very hydrophilic DMVP did not improve MSC detachment under the tested conditions. Remarkably, UC MSCs still attached to these rather hydrophilic surfaces (LCSTs in bulk solution well above 37 °C), indicating that this type of MSCs has a preference for more hydrophilic surfaces (see discussion of biological reasons below). Surface hydration after cooling is crucial for fast and efficient cell detachment. Thus, future studies could also evaluate the effect of porous membranes,

which improve water access to the polymer-grafted surface and which have been previously shown to accelerate cell detachment (Kwon et al., 2000).

Besides surface-related reasons, biological reasons may also account for the impaired MSC detachment. It is generally accepted that cell attachment to surfaces is mediated through absorption of extracellular matrix (ECM) proteins such as collagen, laminin, and fibronectin. These ECM proteins are deposited by cells or derived from serum proteins and cell adhesion is mediated through interaction of ECM proteins and cell surface molecules, most prominently integrins (Carré and Lacarrière, 2009, Schwarz and Gardel, 2012, Barczyk et al., 2010, Geiger et al., 1987, Gumbiner, 1996, Berrier and Yamada, 2007). It has been shown for thermoresponsive surfaces that ECM remains partially attached to the surface whereas parts of the ECM are detached together with cells upon temperature reduction (Canavan et al., 2005a, Canavan et al., 2005b, Kushida et al., 1999). As ECM composition differs depending on the cell type, cell detachment was also found to be cell type-dependent (Kushida et al., 2005). This cell type influence may be the reason for impaired UC MSCs detachment from thermoresponsive surfaces, in contrast to other MSC studies which have reported on successful detachment of BM MSCs from PNIPAAM-coated surfaces (Cho et al., 2004, Shi et al., 2010, Yang et al., 2012, Yang et al., 2010a). Moreover, findings of this study showed that UC MSCs have the ability to attach to hydrophilic surfaces (e.g. to surfaces grafted with P($DMVP_{60}$-co-$DEVP_{40}$) which has an LCST of 75 °C in bulk solution). Therefore, the cooling-induced switch from hydrophobic to hydrophilic surface properties may not be sufficient for UC MSCs detachment. Previous studies have reported of cell type-dependent attachment preferences to hydrophilic or hydrophobic surfaces (Saltzman, 2000), with some cell types such as fibroblasts even attaching to extremely hydrophilic surfaces (contact angles close to 0°) (Ishizaki et al., 2010).

For a complete discussion of parameters that may affect cell release, it should be noted that cell detachment was found to be influenced by the medium composition and temperature under which it is performed (Reed et al., 2008, Okano et al., 1995). For example, it is well-known that the presence of divalent Mg^{2+} and Ca^{2+} ions support cell attachment to substrates whereas detachment is facilitated in their absence (Takeichi and Okada, 1972, Heng et al., 2009). Mg^{2+}-, Ca^{2+}-free PBS was found to improve cooling-induced detachment of MSCs from thermoresponsive surfaces (data not shown). However, detachment was not due to thermoresponsive properties of the surface, because under the same conditions, MSC also detached from standard cell culture surfaces. Regarding the optimal detachment temperature, it

should be well below the LCST but, as cell detachment was shown to be ATP-dependent, also high enough to allow for sufficient cellular metabolism (Okano et al., 1995). To ensure efficient cellular activity, room temperature was employed for cell detachment experiments. As other authors also reported on efficient cell detachment even at low (4 °C) temperature (Reed et al., 2008), the influence of different temperatures (4 °C vs. room temperature) was evaluated but no effect on UC MSC detachment was observed (data not shown).

In summary, a novel, poly(vinylphosphonate)-coated thermoresponsive surface which allows for efficient MSC attachment and proliferation has been developed (Zhang et al., 2012b, Zhang et al., 2012a). Polymer layer thickness and LCST of grafted polymers can be easily adjusted. However, properties of the polymer-grafted surface could not be improved to a level that allowed for efficient cooling-induced cell detachment, but some parameters that can be addressed for optimization in future work are discussed above. Once an efficient cell detachment is established, future studies should also assess the effect of enzyme-free, temperature-induced detachment on MSC characteristics and function which may be altered due to different surface topography and treatment. Indeed, the few studies performed on detachment of MSCs from thermoresponsive surfaces reported on improved proliferation, viability, and differentiation potential compared to trypsin-treated MSCs from control surfaces (Shi et al., 2010, Yang et al., 2012). After efficient cell detachment is achieved on planar surfaces, future work could also focus on transfer of the polymer-coating to spheroid microcarriers.

5 Summary and Outlook

Hematopoietic stem cell therapy has been successfully applied for many decades, saving the lives of thousands of patients who suffer from leukemia or other diseases of the hematopoietic system (Appelbaum, 2012). More recently, mesenchymal stem cells (MSCs) have emerged as a promising tool for cell therapy due to their unique therapeutic characteristics (Ma, 2012, Huss, 2010, Parekkadan and Milwid, 2010). Clinical application of MSCs requires administration of large cell doses, a need which is opposed by the limited number of MSCs that can be isolated from tissues (Santos et al., 2013). Therefore, extensive cell expansion in an efficient, reproducible, and scalable process under GMP-compliant conditions is a crucial step regarding the development of a biopharmaceutical "off-the shelf" cell therapy product. Moreover, tight process control and monitoring is essential as the manufacturing process determines properties and quality of the biopharmaceutical product, which is often acknowledged with the term "the process is the product" (Polastro, 2001, Zuniga and Calvo, 2009). Hence, it needs to be assured that the manufacturing process does not impaired MSC characteristics and therapeutic relevant functions. State-of-the-art cell culture technologies, such as flasks or cell stacks, have several drawbacks and limitations which make them unfavorable for large-scale expansion of a clinical cell product. On the other hand, microcarrier-based cultivation in stirred bioreactors provides an excellent method for scalable and efficient expansion of adhesion-dependent MSCs.

In this work, a microcarrier-based MSC expansion process was developed and successfully scaled up to the bioreactor level (1.5 l). Cytodex 1 microcarriers were identified as the most suitable microcarrier format for MSC expansion. Further process optimization regarding the inoculation procedure led to improved cell attachment and consequently higher cell yield. While it is well known that culture conditions alter cell fate and function (see 1.3), previous studies on MSC expansion on microcarriers addressed this topic only sparsely. In this work, a detailed comparative analysis of microcarrier- and flask-expanded umbilical cord and amniotic membrane MSCs from three different donors was performed. Independent of the cultivation method, expanded cells shared similar doubling times, basic MSC characteristics, and comparable immunosuppressive capacity *in vitro*. Interestingly, despite the commonly high biological variability due to different cell sources and donors, gene expression analysis and subsequent principal component analysis (PCA) showed cultivation-dependent gene expression patterns and clustering of microcarrier- and flask-expanded MSCs. Remarkably, further results indicated that variability between different MSC donors can be reduced by transfer-

ring the microcarrier-based expansion process to regulated conditions in bioreactors (3.4.4). This addresses one frequently uttered challenge regarding therapeutic use of MSCs, namely the high variability and heterogeneity of expanded cells (Bieback et al., 2012), and emphasizes the need for controlled, regulated manufacturing processes for production of reproducible, homogenous cell-based therapeutic products.

Dynamic cultivation of MSCs on spheroid microcarriers significantly altered MSC morphology and function compared to standard static cultivation on cell culture. Microcarrier-expanded MSCs were found to be smaller and less granular compared to flask-expanded cells. Most interestingly, microcarrier-expanded MSCs showed increased secretion of VEGF and FGF-2, which are both potent angiogenic factors. In addition, these cells lacked expression of CD349/frizzled 9, which has previously been reported to positively affect re-endothelialization (Tran et al., 2011). Therefore, these findings strongly indicate that microcarrier-expanded MSCs have an increased pro-angiogenic potential. Furthermore, gene expression and pathway analysis revealed an increase in functions connected to angiogenesis and the immune system. In conclusion, these findings stress the high influence of culture conditions on cell characteristics and functions and suggest that MSCs may be primed for specific therapeutic applications through an appropriate expansion process. This hypothesis needs to be confirmed by future functional *in vitro* and *in vivo* studies.

Furthermore, a crucial point regarding the expansion process of adhesion-dependent MSC is the need for cell dissociation from the culture surface for cell harvest. Due to the cell damaging effect of traditional enzymatic or mechanical detachment methods, cell harvest may have deleterious effects on quality and properties of the final cell product. Thermoresponsive surfaces allow for gentle, temperature-dependent cell detachment. Combining the thermoresponsive polymer technology and microcarrier-based MSC expansion offers a promising approach for an innovative manufacturing process. In this work, thermoresponsive, planar surfaces were evaluated for MSC cultivation. MSC detachment from the commercially available poly(N-isopropylacrylamid)-coated UpCell^{TM} surface (Nunc) was found to be poor and slow. Thus, novel thermoresponsive, poly(vinylphosphonate)-coated surfaces were developed by the group of Prof. Rieger, TU Munich, which should provide means for optimized MSC detachment. While MSCs were found to attach and proliferate on PDAVP-grafted surfaces, MSC detachment could not be optimized in the limited time of this project. Future work should focus on identifying the ideal polymer grafting density and polymer layer thickness for efficient MSC detachment.

6 Zusammenfassung und Ausblick

Hämatopoetische Stammzelltherapie wird seit mehreren Jahrzehnten erfolgreich angewandt und rettet das Leben tausender Patienten, die an Leukämie oder anderen Erkrankungen des blutbildenden Systems leiden. Mesenchymale Stammzellen (MSCs) stellen aufgrund ihrer einzigartigen therapeutischen Charakteristika eine vielversprechende zelltherapeutische Modalität dar (Ma, 2012, Huss, 2010, Parekkadan and Milwid, 2010). Die klinische Anwendung von MSCs erfordert das Verabreichen hoher Zelldosen. Demgegenüber steht allerdings eine begrenzte Anzahl an MSCs, die aus Geweben isoliert werden kann (Santos et al., 2013). Ein entscheidender Schritt für die Entwicklung eines biopharmazeutischen, gebrauchsfertigen Zellproduktes ist daher die Zellexpansion in einem effizienten, reproduzierbaren und skalierbaren Prozess, welcher auf Bedingungen „Guter Herstellungspraxis“ (Good Manufacturing Practice, GMP) übertragbar ist. Darüber hinaus ist eine strenge Kontrolle und Überwachung des Herstellungsprozesses essenziell, da der Prozess Eigenschaften und Qualität des biopharmazeutischen Produktes bestimmt. Dies wird mit dem Ausdruck „der Prozess ist das Produkt“ beschrieben (Polastro, 2001, Zuniga and Calvo, 2009). Zellkulturtechnologien wie Flaschen- und Wannenstapelkulturen, die dem Stand der Technik entsprechen, haben verschiedenste Nachteile und Einschränkungen, wodurch sie für Expansionen eines klinischen Zellprodukts im Großmaßstab nicht geeignet sind. Die Kultivierung von adhärenten MSCs auf Microcarriern bietet hingegen hervorragende Möglichkeiten für eine GMP-kompatible, skalierbare und effiziente Expansion.

In dieser Arbeit wurde ein auf Microcarriern basierender Expansionsprozess für MSCs entwickelt und erfolgreich auf den Bioreaktormaßstab (1,5 l) transferiert. Dabei wurden Cytodex 1 Microcarrier als geeignete Microcarrier für die Expansion von MSCs bestimmt. Darüber hinaus konnte der Expansionsprozess durch eine verbesserte Inokulationsmethode optimiert werden, wodurch die Zelladhäsion und Ausbeute gesteigert wurden. Obwohl bekannt ist, dass Kulturbedingungen die Eigenschaften und Funktionen von Zellen verändern können (siehe 1.3), haben sich bisherige Microcarrier-basierte MSC Studien kaum mit diesem Thema befasst. In dieser Arbeit wurde eine detaillierte, vergleichende Analyse von auf Microcarriern oder in Flaschen expandierten Zellen durchgeführt. Dazu wurden aus Nabelschnur oder Amnionmembran isolierte MSCs von drei verschiedenen Spendern untersucht. Unabhängig vom Kultivierungsprozess besaßen die expandierten Zellen ähnliche Verdopplungszeiten, wesentliche MSC Charakteristika und vergleichbares immunsuppressives Verhalten *in vitro*. Trotz der allgemein hohen Variabilität aufgrund von verschiedenen Zellquellen und Spendern zeig-

ten Genexpressionsanalysen und die daraus resultierende Hauptkomponentenanalyse (PCA) abhängig von der Kultivierungsmethode unterschiedliche Genexpressionsmuster und Gruppierung der auf Microcarriern oder in Flaschen expandierten MSCs. Weitere Ergebnisse wiesen bemerkenswerterweise darauf hin, dass die Variabilität zwischen verschiedenen MSC Spendern durch den Transfer des Expansionsprozesses in kontrollierte Bioreaktoren vermindert werden kann (siehe 3.4). Dies spricht eine der großen Herausforderungen in der Entwicklung von MSC Therapien an, nämlich die hohe Variabilität und Heterogenität der expandierten Zellen (Bieback et al., 2012), und unterstreicht die Wichtigkeit eines kontrollierten, regulierten Herstellungsprozesses, um ein reproduzierbares, homogenes Zellprodukt herzustellen.

Die dynamische Kultivierung von MSCs auf spheroiden Microcarriern änderte die Morphologie und Funktion der MSCs signifikant im Vergleich zur statischen Standardkultivierung auf flachen Zellkulturoberflächen. Microcarrier-expandierte MSCs waren kleiner und weniger granulär im Vergleich zu in Flaschen expandierten Zellen. Interessanterweise wiesen Microcarrier-expandierte MSCs eine erhöhte Sekretion von VEGF und FGF-2 auf, welches beide hochwirksame angiogene Faktoren sind. Zudem exprimierten diese Zellen kein CD349/frizzled 9. Diese fehlende Expression wurde zuvor in Verbindung mit einem positiven Effekt auf die Re-Endothelialisierung beschrieben (Tran et al., 2011). Diese Beobachtungen deuten daher stark auf ein erhöhtes angiogenes Potential von auf Microcarriern expandierten Zellen hin. Des Weiteren zeigte die Genexpressionsanalyse in diesen Zellen eine Hochregulation von Funktionen, die mit Angiogenese und Immunmodulation in Verbindung stehen. Im Fazit betonen diese Ergebnisse den großen Einfluss der Kulturbedingungen auf Zelleigenschaften und Funktionen und weisen darauf hin, dass MSCs durch entsprechende Kulturbedingungen für spezifische therapeutische Indikationen konditioniert werden können. Diese Hypothese muss durch zukünftige funktionelle *in vitro* und *in vivo* Studien bestätigt werden.

Ein weiterer kritischer Punkt bezüglich der Expansion von adhärenten MSCs ist die Zellernte und die damit verbundene Zellablösung. Konventionelle enzymatische oder mechanische Methoden führen zu Zellschäden und können dadurch Qualität und Eigenschaften des finalen Zellprodukts negativ beeinflussen. Thermoresponsive Oberflächen hingegen ermöglichen ein sanftes, temperaturabhängiges Zellablösen. Eine Kombination der thermoresponsiven Polymertechnologie mit der Microcarrier-basierten MSC Expansion stellt einen vielversprechenden Ansatz für einen innovativen Herstellungsprozess dar. In dieser Arbeit wurden thermo-

responsive Oberflächen für die Expansion von MSCs evaluiert. Da das Ablösen von MSCs von kommerziellen, mit Poly(N-isopropylacrylamid)-beschichteten UpCell^{TM} Oberflächen sehr langsam und ineffizient war, wurden neue, thermoresponsive Poly(vinylphosphonat)-beschichtete Oberflächen in der Gruppe von Prof. Rieger (TU München) entwickelt. Diese sollten die Möglichkeit für ein optimiertes Ablösen der MSCs bieten. Während MSCs auf diesen Oberflächen adhärierten und proliferierten, konnte das Ablösen der Zellen in der begrenzten Zeit des Projektes nicht optimiert werden. Künftige Arbeiten sollten den Schwerpunkt haben, die für effizientes Ablösen der MSCs benötigte ideale Dichte und Dicke der Polymerschicht zu finden.

7 Material and Methods

7.1 Material

6-well plates Nunclon Vita (Nunc, cat. no. 145380)

6-well plates, Tissue culture Treated (BD Falcon, cat. no. 353046)

12-well plates CellBIND Surface (Corning, cat. no. 3336)

24-well plates, tissue culture treated (Corning, cat. no. 3526)

96-well plate (Becton Dickinson, cat. no. 351177)

BD FACS Canto II (BD Bioscience)

BD Vacutainer, 0.105 M buffered sodium citrate (Becton Dickinson, cat. no.367714)

Buechner funnel, 70 ml (Duran, cat. no. 213412207)

Cedex XS Analyzer (Innovatis Systems, Roche Applied Science)

Cell Strainer, 70 µm and 100 µm (BD Bioscience, cat. no. 352350 and 352360)

Cobas Integra® 400 plus Analyzer (Roche Diagnostics)

Conical centrifuge tubes, Polypropylene, 15ml (BD Biosciences, cat. no. 352097)

FACS tubes (BD Falcon, cat. no. 352052)

Filter discs, PETEX, 47 mm diameter, mesh opening 80 µm (SEFAR, cat. no. D061-0020-157-00)

Hemocytometer (Neubauer chamber, Paul Marienfeld GmbH & Co KG, cat. no. 0640110)

Heracell 150i Incubator (Thermo Scientific, cat. no. 51026283)

Heracell 240 Incubator (Thermo Scientific, cat. no. 51026332)

Heraeus Multifuge X3R Centrifuge (Thermo Scientific, cat. no. 75004515)

Infinite 200 Pro (Tecan Goup Ltd)

Laminar flow (Herasafe, Thermo Scientific and BDK Luft-und Reinraumtechnik GmbH)

LightCycler 480 II (Roche Applied Science)

Mastercycler Pro S (Eppendorf, cat. no. 6325000.510)

“Mr. Frosty” freezing container (Nalgene, cat. no. 5100-0001)

Nano Drop 2000 (Thermo Scientific, cat. no. ND2000)

Osmomat 030 (Gonotec, cat. no. 30.9.1010)

pH Meter 330i (WTW, cat. no. 9.774 365)

Spinner flasks, 125 ml (Corning, cat. no. 4500-125)

Syringe filter 0.2 µm (Sartorius Stedim Biotech, cat. no. 17764)

Table centrifuge 5424R (Eppendorf, cat. no. 5424 000.010)

Tissue Culture Flasks, 175 cm² (BD Falcon, cat. no. 353112)

Tissue Culture Flasks, 25 cm² (BD Falcon, cat. no. 353014)

UpCell™ 6-well Multidish (Nunc, cat. no. 174901)

Varioklav Dampfsterilisator Typ 500 (H+P Labortechnik)

Water bath Type I TW8 (Julabo Labortechnik GmbH)

Zeiss Microscope, Observer Z1 (Zeiss)

7.1.1 Microcarrier

2D Microhex microcarrier (Nunc, cat. no. 139106)

Cytodex 1 microcarrier (GE Healthcare, cat. no. 17-0448-02)

Glas microcarrier (Solohill Engineering, cat. no. G102-1521)

Hillex II® (Solohill Engineering, cat. no. H112-170)

Plastic microcarrier (Solohill Engineering, cat. no. P102-1521)

Plastic Plus microcarrier (Solohill Engineering, cat. no. PP102-1521)

7.1.2 Antibodies

Table 8: Primary and secondary antibodies

Target	Species	Isotype	Clone	Format	Supplier	Cat. no.
CD14	human	IgG2a, κ	M5E2	FITC	BD	555397
CD19	human	IgG1, κ	4G7	FITC	BD	345776
CD31	human	IgG1, κ	WM59	PE	BD	555446
CD34	human	IgG1, κ	581	FITC	BD	555821
CD45	human	IgG1, κ	HI30	FITC	BD	555482
CD49d	human	IgG1, κ	9F10	APC	BD	559881
CD73	human	IgG1, κ	AD2	PE	BD	550257
CD90	human	IgG1, κ	E510	FITC	BioLegend	328108
CD105	human	IgG1, κ	266	PE	BD	560839
CD136	mouse	IgG1, κ	MM0478-10F24	-	Abcam	AB90243
CD142	human	IgG1, κ	HTF-1	PE	BD	550312
CD143	human	IgG1, κ	5-369	PE	BioLegend	344203
CD146	mouse	IgG1, κ	HLDA8	PE	Miltenyi	130-092-853
CD166	human	IgG_1, κ	3A6	PE	BD	559263
CD200	human	IgG1, κ	MRC OX-104	PE	BD	552475
CD271	mouse	IgG1, κ	ME20.4-1.H4	FITC	Miltenyi	130-091-917
CD349	human	IgM, κ	W3C4E11	AF647	BioLegend	326705
HLA-DR	human	IgG2a, κ	L243 (G46-6)	PE	BD	555812
HER1	mouse	IgG1, κ	H11	-	DakoCytomation	M3563
HER2	mouse	IgG1, κ	TA1		CalBiochem	OP39
MCSP	human	IgG1, κ	LC007	-	In-house	-
C-Met	human	IgG1, κ	Met Mab_3	-	In-house	-

Table 9: Isotype control antibodies

Isotype controls	Isotype	Clone	Format	Supplier	Cat. no.
Mouse	IgG1, κ	MOPC-21	FITC	BD Pharmigen	555748
Mouse	IgG2a, κ	G155-178	FITC	BD	555573
Mouse	IgG1, κ	MOPC-21	PE	BD	555749
Mouse	IgG1, κ	MOPC-31C	purified	BD	557273
Mouse	IgG1, κ	MOPC	APC	BD	555751
Mouse	IgG1, κ	MOPC-21	FITC	BioLegend	400110
Mouse	IgG1. κ	IS5-21F5	FITC	Miltenyi	130-092-213
Mouse	IgG2a, κ	G155-178	PE	BD	555574
Mouse	IgG1, κ	IS5-21F5	PE	Miltenyi	130-092-212
Mouse	IgG1, κ	MOPC-21	PE	BioLegend	400112
Human	IgG1 κ	I5154	-	Sigma-Aldrich	I5154
Mouse	IgM, κ	MM-30	AF647	BioLegend	401618

7.1.3 Kits

480 Probes Master (Roche Applied Science, cat. no. 04887301001)

Agilent RNA 6000 Nano Kit (Agilent, cat. no. 5067-1511)

Bio-Plex Pro™ Human Cytokine assays, Group I and II (Biorad, cat. no. M50-OKCAFO, MFO-005KMII)

Cytotoxicity Detection Kit (LDH) (Roche Applied Science, cat. no. 11644793001)

First Strand cDNA Synthesis Kit (Roche Applied Science, cat. no. 11483188001)

High pure RNA Isolation Kit (Roche Applied Science, cat. no. 11828665001)

QIAquick PCR Purification Kit (Qiagen, cat. no. 28104)

Roche RealTime Ready Costum Panel 384- 384+ (Roche Applied Science, cat. no. 05582644001)

7.1.4 Reagents

0.05% Trypsin-EDTA (Gibco, cat. no. 25300054)

0.25% Trypsin-EDTA (Gibco, cat. no. 25200056)

2-Propanol, p.a. (Sigma-Aldrich, cat. no. 33539)

5(6)-Carboxy-fluorescein-diacetat-N-succinimidylester (CFSE) (Sigma-Aldrich, cat. no. 21888)

Adipogenic induction medium (Lonza, cat. no. PT-3102B)

Adipogneic induction single quots (Lonza, cat. no. PT-4135)

AlamarBlue (Invitrogen, cat. no. DAL1025)

Alizarin red S (Sigma-Aldrich, cat. no. A5533)

Alpha MEM without glutamine (Lonza, cat. no. BE12-169F)

BSA fraction V IgG free (Gibco, cat. no. 30036578)

Calibration Standard 300 mOsmol/kg (Gonotec, cat. no. 30.9.0020)

Chondrogenic differentiation basal medium (Lonza, cat. no. PT-3925)

Chondrogenic induction single quots (Lonza, cat. no. PT-4121)

Collagnease type CLS1 (Biochrom, cat. no. C1-22)

DNase I (Sigma-Aldrich, cat. no. DN25)

DMSO (Sigma-Aldrich, cat. no. D2650)

DPBS without Mg^{2+}, Ca^{2+} (Lonza, cat. no. BE17-512F)

DPBS with Mg^{2+}, Ca^{2+} (Lonza, cat. no. BE17-513F)

EMEM (Lonza, cat. no. 12-136F)

Eukitt® (Sigma-Aldrich, cat. no. 03989)

Ethanol, p.a. (Merck Milipore, cat. no. 100983)

FCS (Gibco, cat. no. 10270 Lot 41F3491K)

Ficoll-Paque Plus (GE Healthcare, cat. no. 17-1440-02)

Formaldehyd 37% p.a. (Roth, cat. no. 4979.1)

GlutaMax-I (Gibco, cat. no. 35050-038)

Glutaraldehyde solution, 8% (Sigma-Aldrich, cat. no. G7526)

HBSS (Invitrogen, cat. no.14175)

Hyaluronidase (Applichem, cat. no.A1937.0001)

IFN-γ (Roche Applied Science, cat. no. 11040596001)

Methanol, p.a. (Merck, cat. no. 1060091000)

Oil Red O (Sigma-Aldrich, cat. no. O0625)

Osmiumtetroxide solution, 2% (Sigma-Aldrich, cat. no. 75633)

Osteogenic differentiation basal medium (Lonza, cat. no. PT-3924)

Osteogenic induction sinlge quots (Lonza, cat. no. PT-4120)

Penicillin-Streptomycin (Gibco, cat. no. 15140122)

PHA-L (Roche, cat. no. 11249738001)

RPMI 1640 (Lonza, cat. no. BE12-167F)

TGF-β3 (Lonza, cat. no. PT-4124)

TNF-α (Roche, cat. no. 11371843001

Trypan Blue Solution, 0.4% (Sigma-Aldrich, cat. no. T8154)

7.1.5 Software

Bio-Plex Manager version 6.1 (Bio-Rad)

Diva version 6.1.3 (BD Bioscience)

FlowJo version7.6.4 (Treestar)

GenEX version 5.3.6 (MultiD Analysis AB)

IPA version 14197757 (Ingenuity Systems Inc.)

LightCycler 480 Software version 1.5 (Roche Applied Science)

Magellan version 7.0 (Tecan Group Ltd)

Microsoft Office Professional Plus 2010, version 14.0 (Microsoft Corporation)

R version 2.15.0 (R Foundation for Statistical Computing, http://www.R-project.org)

7.2 Methods

7.2.1 Isolation of MSCs from Umbilical Cord and Amniotic Membrane

Umbilical cord (UC) and amniotic membrane (AM) were obtained during caesarian sections from human term placentas and purchased from the Red Cross Blood Transfusion Service of Upper Austria. A written informed consent approved by ethical committees was signed by all donors. AM MSCs were isolated as described previously with some modifications (Kita et al., 2010, Marongiu et al., 2010). All isolation steps were performed under aseptic conditions using sterile tools. Amniotic membrane was washed thoroughly three times in ice cold HBSS to remove blood clots and then cut into pieces and digested with 0.05% trypsin-EDTA containing 25 mg/ml DNase I (2 ml trypsin digestion solution per ml wet tissue) for 1 h at 37 °C in a shaking water bath. The membrane was vigorously shaken every 10 min to release amniotic epithelial cells. After 1 h, the membrane was washed four times with HBSS and moved to a clean tube. Collagenase digestion solution (EMEM containing 265 U/ml Collagenase type CLS I and 25µg/ml DNase I) was added using 1 ml solution per ml wet tissue. The membrane was digested for 45 min to 1.5 h at 37 °C in a shaking water bath until completely dissociated. The digested tissue was passed through a 100 µm cell strainer and AM MSCs were sedimented by centrifugation for 5 min at 300 g. Cells were washed using HBSS, counted and seeded at a density of 20,000 cells/cm² in standard culture medium (alpha-MEM supplemented with 10%°FCS, 100 U/ml Penicillin, 100 µg/ml Streptomycin and 2 mM Glutamax).

UC MSCs were isolated as described previously with some modifications (Seshareddy et al., 2008). First, remaining blood was removed. Then, the UC was cut into small pieces and washed in cold DPBS. The UC pieces were digested for 6 h at 37 °C in a shaking water bath using Mg^{2+}- and Ca^{2+}-free DPBS supplemented with 530 U/mL Collagenase CLS I, 674 U/mL Hyaluronidase, and 25 µg/mL DNase I. The UC tube was vigorously shaken every 1 h. The digested tissue was passed through a 100 µm cell strainer, UC MSCs were sedimented by centrifugation at 300 g for 5 min, washed in DPBS and seeded at a density of 20,000 cells/cm² in standard culture medium. Culture medium was exchanged after 1 day for both AM and UC MSC isolations.

7.2.2 Cell Culture and Expansion

Cultivation was performed at 37 °C, 5% CO_2 in a humidified atmosphere. Unless otherwise noted, all MSC cultivations were performed in standard cell culture medium using alpha-

MEM supplemented with 10% FCS, 100 U/ml Penicillin, 100 µg/ml Streptomycin and 2 mM GlutaMAX™. This cell culture medium is termed “medium“ in the following descriptions.

7.2.2.1 Thawing, Cultivation, and Cryo-preservation of MSCs

Cells were thawed for 90 s at 37 °C in a water bath and transferred quickly to 10 ml medium. After centrifugation for 5 min at 300 g, supernatant was discarded and cells were re-suspended in a designated volume of medium. Cells were plated in appropriate cell numbers on cell culture dishes or flasks. For general cell expansion, cells were seeded in regular tissue culture flasks at 500 - 1,000 cells/cm² and 2,500 – 5,000 MSCs/ml unless otherwise noted. Medium was exchanged every 3 - 4 days. Reaching 70% - 90% confluence, cells were washed once with Mg^{2+}-, Ca^{2+}-free DPBS and detached using 0.05% Trypsin-EDTA (7 ml per 175cm² flask, 5 min, 37 °C). Trypsin was inactivated by adding 2.3-fold volume of medium. Cell numbers and viability were determined using the trypan blue exclusion method and a hemocytometer or Cedex XS Analyzer for cell counting. For passaging, cells were re-seeded on new cell culture flasks. For freezing, cells were sedimented by centrifugation (5 min at 300 g), carefully re-suspended in ice cold cryomedium (90% FCS and 10% DMSO) to concentrations of 1 x 10^6 – 5 x 10^6 cells/ml and 1 ml of cell suspension was transferred to cryovials. Then, cells were immediately transferred to pre-cooled (4 °C) freezing containers and stored at -80 °C overnight, which allowed for cell freezing at a constant cooling rate of 1 °C/min. The following day, cells were transferred to storage in liquid nitrogen.

7.2.2.2 Calculation of Population Doublings and Doubling Times

Population doublings (PD) and doubling times (DT) were calculated using the following equations:

$$PD = \log_2 \frac{C_{tx}}{C_{t1}} \qquad \text{Equation 2}$$

where C_{t1} is the cell number (cells/cm²) at day 1 and C_{tx} the cell number (cells/cm²) at the day of harvest

$$DT = \frac{\Delta t}{PD} \qquad \text{Equation 3}$$

where Δt is the cultivation time.

7.2.2.3 Cultivation of MSCs on Microcarriers

Unless otherwise noted, Cytodex 1, 2D Microhex, Hillex II, Plastic, Plastic Plus and Glas microcarriers corresponding to a surface area of 2500 cm² were prepared and, if necessary, autoclaved according to the manufacturer's instructions. Before cell inoculation, microcarriers were washed twice with cell culture medium. Then, microcarriers were re-suspended in a total volume of 45 ml and transferred to spinner flasks. Frozen MSCs of passage 3 were thawed as noted above and used directly for inoculation of spinner flasks. Spinner flasks were inoculated with 1200 cells/cm² to a final culture volume of 50 ml. As controls for cell growth, regular cell culture flasks were inoculated with equal cell densities. Different inoculation procedures were evaluated in this work. After inoculation and unless otherwise noted, 50 ml cell culture medium were added to obtain a final culture volume of 100 ml and the culture was stirred continuously at 40 rpm using an external magnetic stirring system for agitation. Unless otherwise noted, medium exchange was performed every 3 – 4 days by gravity-mediated settling of the cell-microcarrier complexes and subsequent exchange of 50% of the medium with fresh medium. Cells were cultivated for the indicated time periods and then harvested by enzymatic detachment. For this, the cell-microcarrier complexes were washed twice with Mg^{2+}, Ca^{2+}-free DPBS and then cells were detached by incubation in 0.25% Trypsin-EDTA for 7 min on an orbital shaker at 50 rpm. The enzymatic reaction was stopped by adding serum-containing medium. For complete cell harvest, the solution was subsequently passed through a 80 µm mesh filter placed in a Buechner funnel for separation of cells from microcarriers. Microcarriers on top of the filter were washed twice with 10 ml medium to increase cell yield. For cell counting, not all cells were harvested and only a designated volume of cell-microcarrier suspension was passed through a 70 µm cell strainer. Cell numbers and viability were determined using the trypan blue exclusion method and Cedex XS analyzer.

As controls, regular cell culture flasks (175cm²/flask) were inoculated with equivalent cell densities (1200 cells/cm²) using 35 ml culture medium. Corresponding to microcarrier-cultivation, 50% medium was exchanged every 3-4 days or as noted otherwise.

7.2.2.4 Indirect Cell Counting and Growth Analysis of MSCs on Microcarriers

Daily determination of cell numbers in spinner flasks was performed by measuring total intracellular lactate dehydrogenase (LDH) content after forced cell lysis. LDH content of the lysate correlates with cell number (Wolterbeek and van der Meer, 2005) and absolute quantification was performed using a calibration curve.

1 ml homogenous cell-microcarrier suspension was drawn from cultures in spinner flasks. Microcarriers were allowed to settle for 5 min, supernatant was removed and replaced with an equal volume of Mg^{2+}-, Ca^{2+}- containing DPBS to wash the microcarriers. Microcarriers were allowed to settle and supernatant was removed. Cells were lysed for 15 min at 4 °C, rotating in 1%°Triton X solution. Cell debris and microcarriers were sedimented by centrifugation at 1000 g for 10 min at 4 °C and LDH content of the lysate was determined based on colorimetric LDH detection using the "Cytotoxicity Detection Kit" (LDH) according to the manufacturer's protocol. Absorbance measurements at 450 nm were performed using the Infinite 200 Pro Reader. Cell numbers were determined daily. Growth curves were fitted using the Excel add-in XLfit.

7.2.2.5 Cultivation of MSCs on Thermoresponsive Surfaces

7.2.2.5.1 Toxicity Screening

All polymers except for PNIPAAM were provided by Dr. Ning Zhang (AG Rieger, TUM). Polymers were dissolved in standard cell culture medium which was subsequently sterile filtered by passing through a 0.2 µm filter. BM MSCs were seeded in 24-well plates at a density of 1000 cells/cm². After one day, cell culture medium was removed and replaced with medium containing designated polymer concentrations. As controls, cells were treated with 2% DMSO (positive control) or left untreated (negative control). All treatments were performed in triplicates. After 3 days, cells were detached using 0.25% trypsin and cell numbers were determined using a Neubauer chamber.

7.2.2.5.2 Cultivation of MSCs on Thermoresponsive UpCell™ Surface

In principle, cultivation of MSCs on UpCell™ surfaces was performed as described for regular cell culture surfaces above. For cell detachment, temperature was lowered by replacing the cell culture medium with 4 °C cell culture medium instead of using trypsin. Then, cells were incubated for the indicated time periods at room temperature (RT).

7.2.2.5.3 Cultivation on Newly Developed Surfaces

All polymer-coated glass samples were synthesized and provide by Dr. Ning Zhang (AG Rieger, TUM). Before use in cell culture, samples were put in 70% ethanol and treated by ultrasonic sound for 1 min. Afterwards, samples were thoroughly washed 5 times in DPBS. For cell culture, the polymer-coated samples were glued onto 10 cm glass petri dishes using Eukitt®. After drying overnight, the petri dishes were washed thoroughly three times with

DPBS. Passage 3 or 4 UC MSCs were seeded at a density of 13,000 cells/cm² in 15 ml standard cell culture medium and cultured for 3 to 4 d. Unless otherwise noted, temperature was then lowered for cell detachment by replacing the cell culture medium with 4 °C cell culture medium and cells were incubated for the indicated time periods at RT. As controls, cells were cultured on standard cell culture surfaces (tissue culture treated polystyrene) and treated analogous to polymer-coated surfaces.

7.2.3 Microscopic Analysis of MSCs on Microcarriers

7.2.3.1 Live/Dead Viability Staining

To observe cell attachment and proliferation on microcarriers, fluorescent cell staining using the "Live/Dead Viability/Cytotoxicity Kit" was performed. The kit contains the non-flourescent and cell permeable dye calcein AM which is enzymatically converted to the fluorescent dye calcein, staining living cells green, and ethidium homodimer, which only passes through damaged cell membranes and whose fluorescence highly increases upon binding to nucleic acids, resulting in a red staining of dead cells. In principle, the stainings were performed as described in the manufacturer's protocol. A homogenous cell-microcarrier sample was drawn, washed once in Mg^{2+}-, Ca^{2+}-containing DPBS and stained by rotation for 10 min at 37 °C using 2 µM calcein AM and 2 µM ethidium homodimer-1. The cell-microcarrier suspension was washed once with Mg^{2+}-, Ca^{2+}-containing DPBS and analysis was performed on microscope slides under a fluorescence microscope.

7.2.3.2 SEM Analysis

For sample preparation and cell fixation on microcarrier, 5 ml samples were drawn from spinner flask cultures and washed once with Mg^{2+}-, Ca^{2+}-containing DPBS. Cells were pre-fixed for 15 min using 2.5% glutaraldehyde in DPBS and subsequently fixed overnight at 4 °C in 10% formaldehyde. Samples were washed twice with DPBS and cross-linked with 2% osmium tetroxide for 1 h at RT. Cells were extensively washed with DPBS and dehydrated using the following gradient, incubating with each concentration for 30 min at RT: 20% ethanol, 30% ethanol, 50% ethanol, 75% ethanol, 85% ethanol, 95% ethanol, 2 x 100% ethanol. Then, samples were dried at RT. SEM analysis was performed by Katia Rodewald (TUM).

7.2.4 AlamarBlue® Assay

Metabolic active cells convert the AlamarBlue® reagent into a fluorescent dye. Therefore, this assay allows assessing cell viability. Furthermore, the produced fluorescence signal also correlates with cell number (Gloeckner et al., 2001). For this assay, 1 ml homogenous cell-microcarrier suspension was drawn from spinner flasks. 100 µl AlamarBlue® staining solution were added and the solution was incubated for 3 h at 37 °C, 5% CO_2. As a reference, 1 ml cell-free medium was incubated with AlamarBlue® in the same way. After incubation and centrifugation for 3 min at 12,000 g, 200 µl microcarrier-free supernatant were transferred to black 96-well plates. Measurements were performed in triplicates using the Infinite 200 Pro Reader. Excitation wavelength was 535 nm, and fluorescence emission was measured at 590 nm using optimal amplification. To correct for background noise, fluorescence intensities obtained from cell-free medium were subtracted.

7.2.5 Medium Analysis

7.2.5.1 Nutrients and Metabolites

Glucose, lactate, ammonia, glutamine, glutamate, sodium, and potassium concentrations in cell culture supernatant were measured using the Cobas Integra 400 instrument. For this, supernatant was drawn from cultures under aseptic conditions. Supernatant drawn from microcarrier cultures was passed through a 70 µm cell strainer before further use. To remove cell debris, supernatant was centrifuged for 10 min at 4000 g and the supernatant was transferred to a fresh tube. Samples were stored at -20 °C until measurements were performed.

Glucose consumption rates (qGlc) and likewise lactate, ammonia, and glutamate production rates were calculated with the following equation:

$$qGlc = \frac{C_{Glc}\,(t2) - C_{Glc}(t1)}{t2 - t1} \qquad \text{Equation 4}$$

where $C_{Glc}(t2)$ and $C_{Glc}(t1)$ are the glucose concentrations at time points t2 and t1. A negative q represents consumption, a positive q production.

Cell-specific glucose consumption rates and likewise lactate, ammonia and glutamate specific production rates were calculated with the following equation:

$$q_s Glc = \frac{C_{Glc}\,(t2) - C_{Glc}(t1)}{(t2 - t1) * (C_x(t2) - C_X(t1)} \qquad \text{Equation 5}$$

where $C_x(t2)$ and $C_x(t1)$ are cell numbers at time points t2 and t1.

The yield of lactate from glucose was calculated using the following equation:

$$Y_{Lac/Glc} = \frac{\Delta Lac}{\Delta Glc} \qquad \text{Equation 6}$$

where ΔLac is the lactate production in a specific time interval and ΔGlc the glucose consumption in the same time interval.

7.2.5.2 Osmolality

0.5 ml supernatant was removed from cultures under aseptic conditions. Supernatant drawn from microcarrier cultures was passed through a 70 µm cell strainer before further use. To remove cell debris, supernatant was centrifuged for 10 min at 4000 g and the supernatant was transferred to a fresh tube. Osmolality of supernatants was determined using the Osmomat 030 instrument. Based on the principle of freezing point depression, the instrument determined osmolality by comparing the freezing point of the sample to the freezing point of pure water.

7.2.5.3 pH Value

pH value of cell culture medium was determined using the pH 330i instrument. Supernatant was drawn from cultures under aseptic conditions and measured immediately.

7.2.6 Cell Characterization after Expansion

7.2.6.1 Tri-lineage Differentiation of MSCs

UC and AM MSCs were differentiated into adipocytes, osteoblasts, and chondrocytes. As positive controls, differentiation of BM MSCs which had previously shown tri-lineage differentiation was performed. In principle, differentiation was performed as previously described (Pittenger et al., 1999). For adipogenic and osteogenic differentiation, MSCs were seeded in 1 ml standard culture medium into 12-well CellBinding plates at 2 x 10^4 cells/cm². To obtain cell spheroids for chondrogenic differentiation, 2.5 x 10^5 cells were centrifuged for 5 min at 150 g in a 15 ml conical polypropylene centrifugation tube and kept overnight in 1 ml standard cell culture medium. Then, cells were exposed to adipogenic induction medium (basal medium + adipogenic induction quots), osteogenic induction medium (basal medium + osteogenic induction quots) or chondrogenic induction medium (basal medium + chondrogenic induction quots + 10 ng/ml TGFβ3, added immediately before use). As negative controls, cells were maintained in standard cell culture medium. All media were ex-

changed every 3 - 4 days and after 3 weeks, cells were fixed overnight in 4% formaldehyde. Prior to the following stainings, fixation solution was removed by washing three times with DPBS. For analysis of adipogenic differentiation, lipid droplets of differentiated cells were stained using Red Oil O. For this, a 0.3% solution of Red Oil O in 60% isopropanol was passed through a 0.2 µm filter. Cells were than stained for 2 h with this solution, washed three times with DPBS and microscopically analyzed. For analysis of osteogenic differentiation, cells were stained in aqueous 2% Alizarin Red S solution that had previously been passed through a 0.2 µm filter. Alizarin Red S stains calcium deposits of osteoblasts (Puchtler et al., 1969). After staining for 20 min, cells were washed four times and microscopically analyzed. Regarding chondrogenic differentiation, histological sections and stainings of fixed cell spheroids were performed by Jürgen Funk and Christelle Zundel (F. Hoffmann-La Roche AG, Basel). Briefly, fixed cells were embedded in paraffin, sections were slide-mounted and stained with Alcian Blue. Alcian Blue stains proteoglycans deposits of chondrocytes (Hassell and Horigan, 1982).

7.2.6.2 Immunosuppressive Properties of MSCs *in vitro*

In vitro evaluation of immunosuppressive properties of MSCs was performed based on previously described protocols (Hartmann et al., 2010, Quah et al., 2007). MSCs were co-cultured in direct contact with allogeneic, human peripheral blood mononuclear cells (PBMCs). The influence on PBMC proliferation was assessed by monitoring the fluorescent dye carboxyfluorescein succinimidyl ester (CFSE). Initially present as carboxyfluorescein diacetate succinimidyl ester, the dye is non-fluorescent, but once inside the cells its acetate groups are enzymatically removed, yielding fluorescent CFSE which is trapped inside the cell due to its reduced membrane permeability. Upon cell division CFSE is equally distributed between daughter cells (Quah et al., 2007).

For this assay, cell cultivation was performed using RPMI medium containing 10% FCS, 100 U/mL Penicillin, and 100µg/mL Streptomycin. MSCs were seeded at 1.58×10^4 cells/cm² in 24-well plates and stimulated over night with RPMI medium containing 20 ng/ml IFN-γ and 20 ng/ml TNF-α to mimic a pro-inflammatory environment. For non-stimulated controls, the corresponding volume of 0.1% BSA in DPBS was added as a solvent control. To exclude an influence of residual cytokines control wells without MSCs were also incubated overnight with cytokine solution.

On day after MSCs seeding, PBMCs were isolated from peripheral blood of healthy donors using 5 mL vacutainer tubes containing 12.35 mg sodium citrate and 2.21 mg citric acid.

PBMCs were isolated by gradient density centrifugation for which the peripheral blood was overlaid onto Ficoll-Paque PLUS and centrifuged for 20 min at 1200 g using no break for deceleration to maintain the different gradient phases. Then, the PBMC-containing Ficoll-plasma interface was carefully removed and washed with sterile DPBS. 1 - 50 x 10^6 cells were centrifuged at 400 g for 5 min and re-suspended in 1 ml DPBS containing 5% FCS for CFSE labeling. PBMCs were stained by quickly adding CFSE to the cell suspension, obtaining a final concentration of 5 µM CFSE. To induce their proliferation, PBMCs were stimulated with 0.5 µg/ml phytohemagglutinin-L (PHA-L). For non-stimulated controls, the corresponding amount of sterile water was added as solvent control. PBMCs were added in a ratio of 10:1 to MSCs, which had been previously washed once with DPBS to remove cytokines. As references, PBMCs were also cultured in the absence of MSCs. After cultivation for 6 days at 37 °C and 5% CO_2, the PBMC-containing supernatant was removed, washed and re-suspended in DPBS containing 2% FCS. PBMCs were analyzed by flow cytometry (FACS Canto II) using the FITC/CFSE channel. Subsequent data analysis was performed with FlowJo software. PBMC proliferation in the absence of MSCs from three technical replicates was averaged. Similarly, PHA-induced PBMC proliferation in the presence of MSCs from three technical replicates was averaged and then normalized to the calculated PBMC proliferation in the absence of MSCs. PBMC proliferation in the absence of MSCs was set to 100%.

7.2.6.3 Flow Cytometric Analysis

After enzymatic cell detachment, cells were sedimented, re-suspended in DPBS containing 2% FCS and passed through a 70 µm cell strainer. 1 x 10^5 MSCs suspended in 100 µL DPBS containing 2% FCS were stained with the appropriate antibody or corresponding isotype control for 20 minutes at 4 °C (see Table 8 and Table 9). If necessary, cells were incubated with 1 µg of the respective secondary antibody for 20 minutes at 4 °C after washing twice with DPBS containing 2% FCS. After incubation, cells were washed twice and re-suspended in 250 µl DPBS containing 2% FCS and analyzed by flow cytometry using FACS Canto II. Data analysis was performed using FlowJo software.

7.2.6.4 Quantification of Secreted Factors

Different cytokines, chemokines and growth factors secreted from MSCs were quantified using Bio-Plex Pro™ immunoassays. Based on distinct colored magnetic beads, these immunassays allow the quantification of multiple proteins in, for example, cell culture supernatants. For this assay, MSCs were seeded in standard culture medium at a density of 5.2 x 10^4 cells/cm^2. After 24 h, when cells were confluent, MSCs were washed twice with

culture medium without FCS. Cells were stimulated using FCS-free medium containing 20 ng/mL TNF-α and 20 ng/mL INF-γ. Non-stimulated controls were incubated with FCS-free standard cell culture medium containing the corresponding volumes of solvent control (0.1% BSA in DPBS). After 24 h, supernatants were collected and debris were sedimented by centrifugation at 1,000 g, 4 °C for 10 min. Using Bio-Plex Pro™ assays, hepatocyte growth factor (HGF), basic fibroblast growth factor (FGF-2), vascular endothelial growth factor (VEGF), monocyte chemotactic protein-1 (MCP-1), stromal cell-derived factor 1-alpha (SDF-1a), interleukin 1 receptor antagonist (IL-1ra), nerve growth factor (NGF), macrophage colony-stimulating factor (M-CSF) were quantified according to the manufacturer's protocol.

7.2.6.5 Gene Expression Analysis

7.2.6.5.1 RNA Extraction

For RNA extraction, MSCs were harvested as described above. 3 x 10^6 cells were sedimented by centrifugation at 300 g, 5 min and washed once with cold (4 °C) DPBS. DPBS was discarded, sedimented cells were shock frozen in liquid nitrogen and stored at -80 °C until total RNA was isolated from MSCs using the "High Pure RNA Isolation Kit" (Roche Applied Science) according to the manufacturer's protocol. Using this kit, cells were lysed, RNases inactivated and nucleic acids bound to glass fibers inside of the kit's test tubes. DNA was digested by DNase I and after washing, RNA is eventually eluted from the glass fibers. RNA concentrations were determined using the NanoDrop spectrophotometer which calculates nucleic acid concentrations based on the Beer-Lambert Law

$$c = \frac{A * e}{l} \qquad \text{Equation 7}$$

where c is the nucleic acid concentration, A the absorbance at 260 nm, e the extinction coefficient and l the path length.

RNA quality was determined using the Agilent 6000 Nano Kit and Agilent 2100 bioanalyzer. It is important to ensure RNA integrity as RNA degradation may impair further analysis. For quality assessment, the Agilent chip technology provides the RNA integrity number (RIN) algorithm (Schroeder et al., 2006). Samples were prepared according to the manufacturer's protocol. RNA samples with RIN > 9 were utilized further analysis and stored at -80 °C.

7.2.6.5.2 cDNA Synthesis

cDNA was synthesized using the "Transcription First Strand cDNA Synthesis Kit". The kit utilizes the recombinant enzyme Transcriptor Reverse Transcriptase for reverse transcription of RNA into single-stranded cDNA. As primers, random hexamer primers, which allow priming throughout the full length of the RNA template and equal transcription of all RNA sequences, and oligo(dT)18 primer, which bind to the beginning of the poly(A) tail, were used. Using 2 µg RNA as input material, the reverse transcription (RT) was performed according to the manufacturer's manual with the following modification: the recommended standard reaction volume was scaled up 5 times to obtain sufficient amounts of cDNA. A two-step RT-PCR was performed using the following settings:

Table 10: cDNA synthesis RT-PCR protocol

Step 1	Template denaturation	65 °C, 10 min
	Cooling and addition of enzyme	4 °C
Step 2	RT reaction	55 °C, 30 min
	RT inactivation	85 °C, 5 min
	Cooling	4 °C

After synthesis, cDNA was purified using the QiaQuick Purification kit (Qiagen) according to the manufacturer's instructions to remove residual nucleotides. The kit is based on DNA binding to silica membrane while contaminants are washed away. cDNA concentrations were determined using the NanoDrop spectrophotometer.

7.2.6.5.3 Quantitative Real-Time PCR (qRT-PCR)

qRT-PCR was performed using customized RealTime ready 384 Panels (Roche Applied Science). The assay is provided with the respective primer and probes dried in wells of a LightCycler® 480 multiwell plate. For each cDNA, qRT-PCR was performed in duplicates according to the following table on the LightCycler® 480 instrument:

Table 11: qRT-PCR setup

Components	**1x**		
LightCycler® 480 Probes Master (2x)	5 µl		
cDNA (1ng/µl)	2 µl		
H2O, PCR grade	3 µl		
Final volume	20 µl		
PCR Protocol	**Temperature**	**Time**	**Ramp rate**
Pre-incubation	95 °C	10 min	4.8 °C/s
Amplification 45 cycles	95 °C	10 s	4.8 °C/s
	60 °C	30 s	2.5 °C/s
	72 °C	1 s	4.8 °C/s
Cooling	40 °C	30 s	2.5 °C/s

Genes included in the customized panel are listed in Supplementary Table 10.

Using the GenEX software, Cq values were normalized with the following, previously experimentally selected housekeeping genes: ACTB (actin β), GAPDH (glyceraldehyde-3-phosphate dehydrogenase), G6PD (glucose-6-phosphate dehydrogenase), IPO8 (importin 8), RPL13A (small nucleolar RNA, C/D box 32A ribosomal protein L13a), SDHA (succinate dehydrogenase complex, subunit A), TBP (TATA box binding protein), YWHAZ (tyrosine 3-monooxygenase/tryptophan 5-monooxygenase activation protein, zeta polypeptide) (Wiechmann et al., 2011). Relative mRNA levels were calculated with the $2^{-\Delta\Delta Ct}$ method. For principle component analysis (PCA) and hierarchical clustering, normalized gene expression values were converted to linear scale, technical duplicates were merged and log2 transformed.

7.2.6.5.4 Pathway Analysis

Pathway analysis was performed using the Ingenuity Pathway Analysis (IPA) software. For comparison of microcarrier- and flask- expanded MSCs, gene expression data was first normalized with 8 housekeeping genes as described above and then further normalized to gene expression of flask-expanded cells. Expression values were log2 transformed and average values for microcarrier- and flask- expanded cells were calculated. With this data and using a cut-off value of 1, IPA's core analysis was performed with a focus on biological functions. Based on the differentially regulated genes in the dataset, IPA identifies biological functions that are expected to be increased or decreased. As a statistical measure for the correlation between gene expression (user input data) and the described direction of relationship (IPA knowledge database of literature findings), z-scores are calculated. By definition, z-scores ≥ 2

or ≤ 2 indicate a significant increase or decrease of the function. In addition, p-values are calculated which indicate the likelihood that a gene is related to a specific function by chance only. P-values were calculated using the right-tailed Fisher's exact test based on the number of differently expressed genes (user input data) and the total number of genes measured in the experiment. P-values ≤ 0.05 were considered as statistically significant.

7.2.7 Statistical Analysis

Unless otherwise noted, statistical analysis was performed using R (R Team, 2012). Data was tested for normal distribution using the Shapiro-Wilk normality test. When data was normal distributed, p-values were calculated using the unpaired, two-sided Student's t-test. Otherwise the non-parametric Wilcoxon rank sum test was applied. P-values < 0.05 were considered as statistically significant.

8 References

ADAMO, L. & GARCIA-CARDENA, G. 2011. Directed stem cell differentiation by fluid mechanical forces. *Antioxidants & redox signaling,* 15**,** 1463-73.

ANKRUM, J. & KARP, J. M. 2010. Mesenchymal stem cell therapy: Two steps forward, one step back. *Trends in molecular medicine,* 16**,** 203-9.

APPELBAUM, F. R. 2012. Retrospective. E. Donnall Thomas (1920-2012). *Science,* 338**,** 1163.

ARNSDORF, E. J., TUMMALA, P., KWON, R. Y. & JACOBS, C. R. 2009. Mechanically induced osteogenic differentiation--the role of RhoA, ROCKII and cytoskeletal dynamics. *J Cell Sci,* 122**,** 546-53.

BAJPAI, A. K., SHUKLA, S. K., BHANU, S. & KANKANE, S. 2008. Responsive polymers in controlled drug delivery. *Progress in Polymer Science,* 33**,** 1088-1118.

BANFI, A., MURAGLIA, A., DOZIN, B., MASTROGIACOMO, M., CANCEDDA, R. & QUARTO, R. 2000. Proliferation kinetics and differentiation potential of ex vivo expanded human bone marrow stromal cells: Implications for their use in cell therapy. *Exp Hematol,* 28**,** 707-15.

BARCZYK, M., CARRACEDO, S. & GULLBERG, D. 2010. Integrins. *Cell and tissue research,* 339**,** 269-80.

BARKER, S. L., ROSS, D., TARLOV, M. J., GAITAN, M. & LOCASCIO, L. E. 2000. Control of flow direction in microfluidic devices with polyelectrolyte multilayers. *Anal Chem,* 72**,** 5925-9.

BARLOW, S., BROOKE, G., CHATTERJEE, K., PRICE, G., PELEKANOS, R., ROSSETTI, T., DOODY, M., VENTER, D., PAIN, S., GILSHENAN, K. & ATKINSON, K. 2008. Comparison of human placenta- and bone marrow-derived multipotent mesenchymal stem cells. *Stem cells and development,* 17**,** 1095-107.

BARTOSH, T. J., YLOSTALO, J. H., MOHAMMADIPOOR, A., BAZHANOV, N., COBLE, K., CLAYPOOL, K., LEE, R. H., CHOI, H. & PROCKOP, D. J. 2010. Aggregation of human mesenchymal stromal cells (MSCs) into 3D spheroids enhances their antiinflammatory properties. *Proceedings of the National Academy of Sciences of the United States of America,* 107**,** 13724-9.

BATISTA, U., GARVAS, M., NEMEC, M., SCHARA, M., VERANIC, P. & KOKLIC, T. 2010. Effects of different detachment procedures on viability, nitroxide reduction kinetics and plasma membrane heterogeneity of V-79 cells. *Cell biology international,* 34**,** 663-8.

BAUER, P., HANCOCK, L., RATHMAN, J. & CHALMERS, J. J. 2000. Cell-microcarrier adhesion to gas-liquid interfaces and foam. *Biotechnology progress,* 16**,** 125-32.

BAUTCH, V. L. 2012. VEGF-directed blood vessel patterning: from cells to organism. *Cold Spring Harb Perspect Med,* 2**,** a006452.

BECK, E. G. 2007. 180 years of atmospheric CO2 gas analysis by chemical methods. *Energy & Environment,* 18.

BERRIER, A. L. & YAMADA, K. M. 2007. Cell-matrix adhesion. *J Cell Physiol,* 213**,** 565-73.

BI, B., SCHMITT, R., ISRAILOVA, M., NISHIO, H. & CANTLEY, L. G. 2007. Stromal cells protect against acute tubular injury via an endocrine effect. *J Am Soc Nephrol,* 18**,** 2486-96.

BIEBACK, K., WUCHTER, P., BESSER, D., FRANKE, W., BECKER, M., OTT, M., PACHER, M., MA, N., STAMM, C., KLUTER, H., MULLER, A., HO, A. D. & CONSORTIUM, S.-M. 2012. Mesenchymal stromal cells (MSCs): science and f(r)iction. *J Mol Med (Berl),* 90**,** 773-82.

BLUM, B. & BENVENISTY, N. 2008. The tumorigenicity of human embryonic stem cells. *Adv Cancer Res,* 100**,** 133-58.

BOA-SAN, H., BAI-YONG, S., RUI, Z., ZHAO-HAI, W., ZHI-YONG, D., DONG-FENG, C., MIN-MIN, S., HONG-WEI, L. & CHENG-HONG, P. 2009. Microcarrier cytodex3 culture technique for amlification of a large amount of adult bone morrow mesenchymal stem cells. *J.Clinical Rehabilitative Tissue Engineering Research,* 13**,** 1996-2000.

BOBIS, S., JAROCHA, D. & MAJKA, M. 2006. Mesenchymal stem cells: characteristics and clinical applications. *Folia histochemica et cytobiologica / Polish Academy of Sciences, Polish Histochemical and Cytochemical Society,* 44**,** 215-30.

BOO, L., SELVARATNAM, L., TAI, C. C., AHMAD, T. S. & KAMARUL, T. 2011. Expansion and preservation of multipotentiality of rabbit bone-marrow derived mesenchymal stem cells in dextran-based microcarrier spin culture. *J.Mater.Sci.Mater.Med.,* 22**,** 1343-1356.

BOOMSMA, R. A. & GEENEN, D. L. 2012. Mesenchymal Stem Cells Secrete Multiple Cytokines That Promote Angiogenesis and Have Contrasting Effects on Chemotaxis and Apoptosis. *PLoS ONE,* 7**,** e35685.

BOUTRIS, C., CHATZI, E. G. & KIPARISSIDES, C. 1997. Characterization of the LCST behaviour of aqueous poly(N-isopropylacrylamide) solutions by thermal and cloud point techniques. *Polymer,* 38**,** 2567-2570.

BROOKS, P. C., MONTGOMERY, A. M. & CHERESH, D. A. 1999. Use of the 10-day-old chick embryo model for studying angiogenesis. *Methods Mol Biol,* 129**,** 257-69.

BRUDER, S. P., JAISWAL, N. & HAYNESWORTH, S. E. 1997. Growth kinetics, self-renewal, and the osteogenic potential of purified human mesenchymal stem cells during extensive subcultivation and following cryopreservation. *J Cell Biochem,* 64**,** 278-94.

BUHRING, H. J., BATTULA, V. L., TREML, S., SCHEWE, B., KANZ, L. & VOGEL, W. 2007. Novel markers for the prospective isolation of human MSC. *Annals of the New York Academy of Sciences,* 1106**,** 262-71.

BYRNE, A. M., BOUCHIER-HAYES, D. J. & HARMEY, J. H. 2005. Angiogenic and cell survival functions of vascular endothelial growth factor (VEGF). *J Cell Mol Med,* 9**,** 777-94.

CANAVAN, H. E., CHENG, X., GRAHAM, D. J., RATNER, B. D. & CASTNER, D. G. 2005a. Cell sheet detachment affects the extracellular matrix: a surface science study comparing thermal liftoff, enzymatic, and mechanical methods. *J Biomed Mater Res A,* 75**,** 1-13.

CANAVAN, H. E., CHENG, X., GRAHAM, D. J., RATNER, B. D. & CASTNER, D. G. 2005b. Surface characterization of the extracellular matrix remaining after cell detachment from a thermoresponsive polymer. *Langmuir,* 21**,** 1949-55.

CAPLAN, A. I. 1991. Mesenchymal stem cells. *Journal of Orthopaedic Research,* 9**,** 641-650.

CAPLAN, A. I. 2009. Why are MSCs therapeutic? New data: new insight. *J Pathol,* 217**,** 318-24.

CARRÉ, A. & LACARRIÈRE, V. 2009. Relationship between cell adhesion and protein adsorption. *In:* G. ANDERSON, E. (ed.) *Proceedings of the 32nd Annual Meeting.*

CARRERO, R., CERRADA, I., LLEDO, E., DOPAZO, J., GARCIA-GARCIA, F., RUBIO, M. P., TRIGUEROS, C., DORRONSORO, A., RUIZ-SAURI, A., MONTERO, J. A. & SEPULVEDA, P. 2012. IL1beta induces mesenchymal stem cells migration and leucocyte chemotaxis through NF-kappaB. *Stem cell reviews,* 8**,** 905-16.

CAVALCANTI-ADAM, E. A., VOLBERG, T., MICOULET, A., KESSLER, H., GEIGER, B. & SPATZ, J. P. 2007. Cell spreading and focal adhesion dynamics are regulated by spacing of integrin ligands. *Biophysical journal,* 92**,** 2964-74.

CHACKO, S. M., AHMED, S., SELVENDIRAN, K., KUPPUSAMY, M. L., KHAN, M. & KUPPUSAMY, P. 2010. Hypoxic preconditioning induces the expression of prosurvival and proangiogenic markers in mesenchymal stem cells. *Am J Physiol Cell Physiol,* 299**,** C1562-70.

CHANG, H. & WANG, Y. 2011. Cell Responses to Surface and Architecture of Tissue Engineering Scaffolds. *In:* (ED.), D. E. (ed.) *Regenerative Medicine and Tissue Engineering - Cells and Biomaterials.* http://www.intechopen.com/books/regenerative-medicine-and-tissue-engineering-cells-and-biomaterials/cell-responses-to-surface-and-architecture-of-tissue-engineering-scaffolds: InTech.

CHASE, L., LAKSHMIPATHY, U., SOLCHAGA, L., RAO, M. & VEMURI, M. 2010. A novel serum-free medium for the expansion of human mesenchymal stem cells. *Stem Cell Research & Therapy,* 1**,** 8.

CHEN, A. K., CHEN, X., CHOO, A. B., REUVENY, S. & OH, S. K. 2011. Critical microcarrier properties affecting the expansion of undifferentiated human embryonic stem cells. *Stem cell research,* 7**,** 97-111.

CHEN, B., XU, F. J., FANG, N., NEOH, K. G., KANG, E. T., CHEN, W. N. & CHAN, V. 2008. Engineering cell de-adhesion dynamics on thermoresponsive poly(N-isopropylacrylamide). *Acta Biomater.,* 4**,** 218-229.

CHEN, X., XU, H., WAN, C., MCCAIGUE, M. & LI, G. 2006. Bioreactor expansion of human adult bone marrow-derived mesenchymal stem cells. *Stem Cells,* 24**,** 2052-2059.

CHERRY, R. S. & PAPOUTSAKIS, E. T. 1988. Physical mechanisms of cell damage in microcarrier cell culture bioreactors. *Biotechnology and bioengineering,* 32**,** 1001-14.

CHO, J. H., KIM, S. H., PARK, K. D., JUNG, M. C., YANG, W. I., HAN, S. W., NOH, J. Y. & LEE, J. W. 2004. Chondrogenic differentiation of human mesenchymal stem cells using a thermosensitive poly(N-isopropylacrylamide) and water-soluble chitosan copolymer. *Biomaterials,* 25**,** 5743-5751.

CHRIST, B. & DOLLINGER, M. M. 2010. The generation of hepatocytes from mesenchymal stem cells and engraftment into the liver. *Curr Opin Organ Transplant.*

COLTER, D. C., CLASS, R., DIGIROLAMO, C. M. & PROCKOP, D. J. 2000. Rapid expansion of recycling stem cells in cultures of plastic-adherent cells from human bone marrow. *Proceedings of the National Academy of Sciences of the United States of America,* 97**,** 3213-8.

COLTER, D. C., SEKIYA, I. & PROCKOP, D. J. 2001. Identification of a subpopulation of rapidly self-renewing and multipotential adult stem cells in colonies of human marrow stromal cells. *Proceedings of the National Academy of Sciences of the United States of America,* 98**,** 7841-5.

CONRAD, C. & HUSS, R. 2005. Adult stem cell lines in regenerative medicine and reconstructive surgery. *J Surg Res,* 124**,** 201-8.

CRESPY, D. & ROSSI, R. N. 2007. Temperature-responsive polymers with LCST in the physiological range and their applications in textiles. *Polymer International,* 56**,** 1461-1468.

CRISAN, M., YAP, S., CASTEILLA, L., CHEN, C. W., CORSELLI, M., PARK, T. S., ANDRIOLO, G., SUN, B., ZHENG, B., ZHANG, L., NOROTTE, C., TENG, P. N., TRAAS, J., SCHUGAR, R., DEASY, B. M., BADYLAK, S., BUHRING, H. J., GIACOBINO, J. P., LAZZARI, L., HUARD, J. & PEAULT, B. 2008. A Perivascular Origin for Mesenchymal Stem Cells in Multiple Human Organs. *Cell Stem Cell,* 3**,** 301-313.

CROP, M. J., BAAN, C. C., KOREVAAR, S. S., IJZERMANS, J. N., PESCATORI, M., STUBBS, A. P., VAN IJCKEN, W. F., DAHLKE, M. H., EGGENHOFER, E., WEIMAR, W. & HOOGDUIJN, M. J. 2010. Inflammatory conditions affect gene expression and function of human adipose tissue-derived mesenchymal stem cells. *Clinical and experimental immunology,* 162**,** 474-86.

CRUZ, H. J., MOREIRA, J. L. & CARRONDO, M. J. 1999. Metabolic shifts by nutrient manipulation in continuous cultures of BHK cells. *Biotechnol Bioeng,* 66**,** 104-13.

CURTIS, A. S. & BUULTJENS, T. E. 1973. Cell adhesion and locomotion. *Ciba Found Symp,* 14**,** 171-86.

CURTIS, A. S., FORRESTER, J. V., MCINNES, C. & LAWRIE, F. 1983. Adhesion of cells to polystyrene surfaces. *J Cell Biol,* 97**,** 1500-6.

DA SILVA MEIRELLES, L., CAPLAN, A. I. & NARDI, N. B. 2008. In search of the in vivo identity of mesenchymal stem cells. *Stem Cells,* 26**,** 2287-99.

DA SILVA MEIRELLES, L., CHAGASTELLES, P. C. & NARDI, N. B. 2006. Mesenchymal stem cells reside in virtually all post-natal organs and tissues. *J Cell Sci,* 119**,** 2204-13.

DA SILVA MEIRELLES, L., FONTES, A. M., COVAS, D. T. & CAPLAN, A. I. 2009. Mechanisms involved in the therapeutic properties of mesenchymal stem cells. *Cytokine and Growth Factor Reviews,* 20**,** 419-427.

DADO, D., SAGI, M., LEVENBERG, S. & ZEMEL, A. 2012. Mechanical control of stem cell differentiation. *Regenerative medicine,* 7**,** 101-16.

DATTA, N., PHAM, Q. P., SHARMA, U., SIKAVITSAS, V. I., JANSEN, J. A. & MIKOS, A. G. 2006. In vitro generated extracellular matrix and fluid shear stress synergistically enhance 3D osteoblastic differentiation. *Proceedings of the National Academy of Sciences of the United States of America,* 103**,** 2488-93.

DEWEZ, J. L., LHOEST, J. B., DETRAIT, E., BERGER, V., DUPONT-GILLAIN, C. C., VINCENT, L. M., SCHNEIDER, Y. J., BERTRAND, P. & ROUXHET, P. G. 1998. Adhesion of mammalian cells to polymer surfaces: from physical chemistry of surfaces to selective adhesion on defined patterns. *Biomaterials,* 19**,** 1441-5.

DI NICOLA, M., CARLO-STELLA, C., MAGNI, M., MILANESI, M., LONGONI, P. D., MATTEUCCI, P., GRISANTI, S. & GIANNI, A. M. 2002. Human bone marrow stromal cells suppress T-lymphocyte proliferation induced by cellular or nonspecific mitogenic stimuli. *Blood,* 99**,** 3838-43.

DIEHL, C. & SCHLAAD, H. 2009. Thermo-Responsive Polyoxazolines with Widely Tuneable LCST. *Macromolecular Bioscience,* 9**,** 157-161.

DISCHER, D. E., MOONEY, D. J. & ZANDSTRA, P. W. 2009. Growth factors, matrices, and forces combine and control stem cells. *Science,* 324**,** 1673-7.

DOMINICI, M., LE, B. K., MUELLER, I., SLAPER-CORTENBACH, I., MARINI, F., KRAUSE, D., DEANS, R., KEATING, A., PROCKOP, D. & HORWITZ, E. 2006. Minimal criteria for defining multipotent mesenchymal stromal cells. The International Society for Cellular Therapy position statement. *Cytotherapy.,* 8**,** 315-317.

DOUCET, C., ERNOU, I., ZHANG, Y., LLENSE, J. R., BEGOT, L., HOLY, X. & LATAILLADE, J. J. 2005. Platelet lysates promote mesenchymal stem cell expansion: a safety substitute for animal serum in cell-based therapy applications. *J.Cell Physiol,* 205**,** 228-236.

EIBES, G., DOS SANTOS, F., ANDRADE, P. Z., BOURA, J. S., ABECASIS, M. M. A., DA SILVA, C. L. & CABRAL, J. M. S. 2010. Maximizing the ex vivo expansion of human mesenchymal stem cells using a microcarrier-based stirred culture system. *Journal of Biotechnology,* 146**,** 194-197.

EIBL, R., KAISER, S., LOMBRISER, R. & EIBL, D. 2010. Disposable bioreactors: the current state-of-the-art and recommended applications in biotechnology. *Appl Microbiol Biotechnol,* 86**,** 41-9.

ELSEBERG, C. L., LEBER, J., SALZIG, D., WALLRAPP, C., KASSEM, M., KRAUME, M. & CZERMAK, P. 2012. Microcarrier-based expansion process for hMSCs with high vitality and undifferentiated characteristics. *Int J.Artif.Organs,* 35**,** 93-107.

EMA, H. & SUDA, T. 2012. Two anatomically distinct niches regulate stem cell activity. *Blood,* 120**,** 2174-81.

ENGLER, A. J., SEN, S., SWEENEY, H. L. & DISCHER, D. E. 2006. Matrix elasticity directs stem cell lineage specification. *Cell,* 126**,** 677-89.

ERICES, A., CONGET, P. & MINGUELL, J. J. 2000. Mesenchymal progenitor cells in human umbilical cord blood. *Br J Haematol,* 109**,** 235-42.

ESHGHI, S. & SCHAFFER, D. V. 2008. Engineering microenvironments to control stem cell fate and function. *StemBook.* Cambridge (MA).

ETHERIDGE, S. L., SPENCER, G. J., HEATH, D. J. & GENEVER, P. G. 2004. Expression profiling and functional analysis of wnt signaling mechanisms in mesenchymal stem cells. *Stem cells,* 22**,** 849-60.

FEKETE, N., ROJEWSKI, M. T., FURST, D., KREJA, L., IGNATIUS, A., DAUSEND, J. & SCHREZENMEIER, H. 2012. GMP-compliant isolation and large-scale expansion of bone marrow-derived MSC. *PloS one,* 7**,** e43255.

FERRARI, C., BALANDRAS, F., GUEDON, E., OLMOS, E., CHEVALOT, I. & MARC, A. 2012. Limiting cell aggregation during mesenchymal stem cell expansion on microcarriers. *Biotechnol.Prog.*

FISCHER, U. M., HARTING, M. T., JIMENEZ, F., MONZON-POSADAS, W. O., XUE, H., SAVITZ, S. I., LAINE, G. A. & COX, C. S., JR. 2009. Pulmonary passage is a major obstacle for intravenous stem cell delivery: the pulmonary first-pass effect. *Stem cells and development,* 18**,** 683-92.

FRAUENSCHUH, S., REICHMANN, E., IBOLD, Y., GOETZ, P. M., SITTINGER, M. & RINGE, J. 2007. A microcarrier-based cultivation system for expansion of primary mesenchymal stem cells. *Biotechnol.Prog.,* 23**,** 187-193.

FRIEDENSTEIN, A. J., DERIGLASOVA, U. F., KULAGINA, N. N., PANASUK, A. F., RUDAKOWA, S. F., LURIA, E. A. & RUADKOW, I. A. 1974. Precursors for

fibroblasts in different populations of hematopoietic cells as detected by the in vitro colony assay method. *Exp Hematol,* 2**,** 83-92.

FRIEDENSTEIN, A. J., PETRAKOVA, K. V., KUROLESOVA, A. I. & FROLOVA, G. P. 1968. Heterotopic of bone marrow. Analysis of precursor cells for osteogenic and hematopoietic tissues. *Transplantation,* 6**,** 230-47.

FRITH, J. E., THOMSON, B. & GENEVER, P. G. 2010a. Dynamic three-dimensional culture methods enhance mesenchymal stem cell properties and increase therapeutic potential. *Tissue Eng Part C Methods,* 16**,** 735-49.

FRITH, J. E., THOMSON, B. & GENEVER, P. G. 2010b. Dynamic Three-Dimensional Culture Methods Enhance Mesenchymal Stem Cell Properties and Increase Therapeutic Potential *Tissue Engineering Part C: Methods,* 16**,** 735-749.

GAO, J. & CAPLAN, A. I. 2003. Mesenchymal stem cells and tissue engineering for orthopaedic surgery. *Chir Organi Mov,* 88**,** 305-16.

GEIGER, B., VOLK, T., VOLBERG, T. & BENDORI, R. 1987. Molecular interactions in adherens-type contacts. *J Cell Sci Suppl,* 8**,** 251-72.

GIL, E. S. & HUDSON, S. M. 2004. Stimuli-reponsive polymers and their bioconjugates. *Progress in Polymer Science,* 29**,** 1173-1222.

GIMBRONE, M. A., JR., LEAPMAN, S. B., COTRAN, R. S. & FOLKMAN, J. 1972. Tumor dormancy in vivo by prevention of neovascularization. *J Exp Med,* 136**,** 261-76.

GLACKEN, M. W. 1988. Catabolic Control of Mammalian Cell Culture. *Nat Biotech,* 6**,** 1041-1050.

GLICKLIS, R., MERCHUK, J. C. & COHEN, S. 2004. Modeling mass transfer in hepatocyte spheroids via cell viability, spheroid size, and hepatocellular functions. *Biotechnology and Bioengineering,* 86**,** 672-680.

GLOECKNER, H., JONULEIT, T. & LEMKE, H. D. 2001. Monitoring of cell viability and cell growth in a hollow-fiber bioreactor by use of the dye Alamar Blue. *Journal of immunological methods,* 252**,** 131-8.

GLOSSOP, J. R. & CARTMELL, S. H. 2009. Effect of fluid flow-induced shear stress on human mesenchymal stem cells: differential gene expression of IL1B and MAP3K8 in MAPK signaling. *Gene Expr Patterns,* 9**,** 381-8.

GOODWIN, T. J., SCHROEDER, W. F., WOLF, D. A. & MOYER, M. P. 1993. Rotating-wall vessel coculture of small intestine as a prelude to tissue modeling: aspects of simulated microgravity. *Proc Soc Exp Biol Med,* 202**,** 181-92.

GORDON, S. & MARTINEZ, F. O. 2010. Alternative activation of macrophages: mechanism and functions. *Immunity,* 32**,** 593-604.

GREGORY, C. A., YLOSTALO, J. & PROCKOP, D. J. 2005. Adult bone marrow stem/progenitor cells (MSCs) are preconditioned by microenvironmental "niches" in culture: a two-stage hypothesis for regulation of MSC fate. *Science's STKE : signal transduction knowledge environment,* 2005**,** pe37.

GRIFFIN, M. D., RITTER, T. & MAHON, B. P. 2010. Immunological aspects of allogeneic mesenchymal stem cell therapies. *Hum Gene Ther,* 21**,** 1641-55.

GUILAK, F., COHEN, D. M., ESTES, B. T., GIMBLE, J. M., LIEDTKE, W. & CHEN, C. S. 2009. Control of stem cell fate by physical interactions with the extracellular matrix. *Cell stem cell,* 5**,** 17-26.

GUMBINER, B. M. 1996. Cell adhesion: the molecular basis of tissue architecture and morphogenesis. *Cell,* 84**,** 345-57.

HALPERIN, A. & KROGER, M. 2012. Theoretical considerations on mechanisms of harvesting cells cultured on thermoresponsive polymer brushes. *Biomaterials*.

HAMILTON, W. G. & HAM, R. G. 1977. Clonal growth of chinese hamster cell lines in protein-free media. *In Vitro,* 13**,** 537-47.

HARICHANDAN, A. & BUHRING, H. J. 2011. Prospective isolation of human MSC. *Best Pract Res Clin Haematol,* 24**,** 25-36.

HARTMANN, I., HOLLWECK, T., HAFFNER, S., KREBS, M., MEISER, B., REICHART, B. & EISSNER, G. 2010. Umbilical cord tissue-derived mesenchymal stem cells grow best under GMP-compliant culture conditions and maintain their phenotypic and functional properties. *J Immunol Methods,* 363**,** 80-9.

HASS, R., KASPER, C., BOHM, S. & JACOBS, R. 2011. Different populations and sources of human mesenchymal stem cells (MSC): A comparison of adult and neonatal tissue-derived MSC. *Cell Commun Signal,* 9**,** 12.

HASSELL, J. R. & HORIGAN, E. A. 1982. Chondrogenesis: A model developmental system for measuring teratogenic potential of compounds. *Teratogenesis, Carcinogenesis, and Mutagenesis,* 2**,** 325-331.

HASSELL, T., GLEAVE, S. & BUTLER, M. 1991. Growth inhibition in animal cell culture. The effect of lactate and ammonia. *Appl Biochem Biotechnol,* 30**,** 29-41.

HAUSER, P. V., DE FAZIO, R., BRUNO, S., SDEI, S., GRANGE, C., BUSSOLATI, B., BENEDETTO, C. & CAMUSSI, G. 2010. Stem cells derived from human amniotic fluid contribute to acute kidney injury recovery. *American Journal of Pathology,* 177**,** 2011-2021.

HAYFLICK, L. & MOORHEAD, P. S. 1961. The serial cultivation of human diploid cell strains. *Exp Cell Res,* 25**,** 585-621.

GE HEALTHCARE, 2005. *Microcarrier Cell Culture: Principles and Methods*, GE Healthcare/Amersham Biosciences.

HEINEMANN, L. & HOMPESCH, M. 2011. Biosimilar insulins: how similar is similar? *J Diabetes Sci Technol,* 5**,** 741-54.

HENG, B. C., COWAN, C. M. & BASU, S. 2009. Comparison of enzymatic and non-enzymatic means of dissociating adherent monolayers of mesenchymal stem cells. *Biol.Proced.Online.,* 11**,** 161-169.

HEWITT, C. J., LEE, K., NIENOW, A. W., THOMAS, R. J., SMITH, M. & THOMAS, C. R. 2011. Expansion of human mesenchymal stem cells on microcarriers. *Biotechnol Lett,* 33**,** 2325-35.

HIGUERA, G., SCHOP, D., JANSSEN, F., VAN DIJKHUIZEN-RADERSMA, R., VAN BOXTEL, T. & VAN BLITTERSWIJK, C. A. 2009. Quantifying in vitro growth and metabolism kinetics of human mesenchymal stem cells using a mathematical model. *Tissue engineering. Part A,* 15**,** 2653-63.

HOLTORF, H. L., JANSEN, J. A. & MIKOS, A. G. 2005. Flow perfusion culture induces the osteoblastic differentiation of marrow stroma cell-scaffold constructs in the absence of dexamethasone. *Journal of biomedical materials research. Part A,* 72**,** 326-34.

HONG, Y., GONG, Y., GAO, C. & SHEN, J. 2008. Collagen-coated polylactide microcarriers/chitosan hydrogel composite: injectable scaffold for cartilage regeneration. *J Biomed Mater Res A,* 85**,** 628-37.

HORWITZ, E. M. & DOMINICI, M. 2008. How do mesenchymal stromal cells exert their therapeutic benefit? *Cytotherapy,* 10**,** 771-4.

HORWITZ, E. M., LE BLANC, K., DOMINICI, M., MUELLER, I., SLAPER-CORTENBACH, I., MARINI, F. C., DEANS, R. J., KRAUSE, D. S., KEATING, A. & INTERNATIONAL SOCIETY FOR CELLULAR, T. 2005. Clarification of the nomenclature for MSC: The International Society for Cellular Therapy position statement. *Cytotherapy,* 7**,** 393-5.

HSIAO, S. T., ASGARI, A., LOKMIC, Z., SINCLAIR, R., DUSTING, G. J., LIM, S. Y. & DILLEY, R. J. 2012. Comparative analysis of paracrine factor expression in human adult mesenchymal stem cells derived from bone marrow, adipose, and dermal tissue. *Stem cells and development,* 21**,** 2189-203.

HU, W. S., MEIER, J. & WANG, D. I. 1985. A mechanistic analysis of the inoculum requirement for the cultivation of mammalian cells on microcarriers. *Biotechnology and bioengineering,* 27**,** 585-95.

HUNG, S. C., POCHAMPALLY, R. R., CHEN, S. C., HSU, S. C. & PROCKOP, D. J. 2007. Angiogenic effects of human multipotent stromal cell conditioned medium activate the PI3K-Akt pathway in hypoxic endothelial cells to inhibit apoptosis, increase survival, and stimulate angiogenesis. *Stem cells,* 25**,** 2363-70.

HUSS, R. 2010. Stem cell therapeutics: hope for patients and biopharma! *Stem cells and development,* 19**,** 593-4.

HUSS, R., HEIL, M., MOOSMANN, S., ZIEGELHOEFFER, T., SAGEBIEL, S., SELIGER, C., KINSTON, S. & GOTTGENS, B. 2004. Improved arteriogenesis with simultaneous skeletal muscle repair in ischemic tissue by SCL(+) multipotent adult progenitor cell clones from peripheral blood. *J Vasc Res,* 41**,** 422-31.

HYEONG KWON, O., KIKUCHI, A., YAMATO, M. & OKANO, T. 2003. Accelerated cell sheet recovery by co-grafting of PEG with PIPAAm onto porous cell culture membranes. *Biomaterials,* 24**,** 1223-32.

ILANCHERAN, S., MOODLEY, Y. & MANUELPILLAI, U. 2009. Human Fetal Membranes: A Source of Stem Cells for Tissue Regeneration and Repair? *Placenta,* 30**,** 2-10.

ISHIGE, I., NAGAMURA-INOUE, T., HONDA, M. J., HARNPRASOPWAT, R., KIDO, M., SUGIMOTO, M., NAKAUCHI, H. & TOJO, A. 2009. Comparison of mesenchymal stem cells derived from arterial, venous, and Wharton's jelly explants of human umbilical cord. *Int J Hematol,* 90**,** 261-9.

ISHIZAKI, T., SAITO, N. & TAKAI, O. 2010. Correlation of cell adhesive behaviors on superhydrophobic, superhydrophilic, and micropatterned superhydrophobic/superhydrophilic surfaces to their surface chemistry. *Langmuir,* 26**,** 8147-54.

IWANAGA, Y., BRAUN, D. & FROMHERZ, P. 2001. No correlation of focal contacts and close adhesion by comparing GFP-vinculin and fluorescence interference of Dil. *Eur Biophys J,* 30**,** 17-26.

JOLLIFFE, I. T. 2002. *Principle Component Analysis,* New York, Springer Verlag New York, Inc.

JORDI JOAN, C. & FRANCESC, G. 2005. Cell Metabolism. *Cell Culture Technology for Pharmaceutical and Cell-Based Therapies.* CRC Press.

JUNG, S., PANCHALINGAM, K. M., ROSENBERG, L. & BEHIE, L. A. 2012a. Ex vivo expansion of human mesenchymal stem cells in defined serum-free media. *Stem cells international,* 2012**,** 123030.

JUNG, S., PANCHALINGAM, K. M., WUERTH, R. D., ROSENBERG, L. & BEHIE, L. A. 2012b. Large-scale production of human mesenchymal stem cells for clinical applications. *Biotechnol Appl Biochem,* 59**,** 106-120.

JUNG, Y. J., JU, S. Y., YOO, E. S., CHO, S., CHO, K. A., WOO, S. Y., SEOH, J. Y., PARK, J. W., HAN, H. S. & RYU, K. H. 2007. MSC-DC interactions: MSC inhibit maturation and migration of BM-derived DC. *Cytotherapy,* 9**,** 451-8.

KAJDANIUK, D., MAREK, B., FOLTYN, W. & KOS-KUDLA, B. 2011. Vascular endothelial growth factor (VEGF) - part 1: in physiology and pathophysiology. *Endokrynol Pol,* 62**,** 444-55.

KARASAWA, T., YOKOKURA, H., KITAJEWSKI, J. & LOMBROSO, P. J. 2002. Frizzled-9 is activated by Wnt-2 and functions in Wnt/beta -catenin signaling. *The Journal of biological chemistry,* 277**,** 37479-86.

KARP, J. M. & LENG TEO, G. S. 2009. Mesenchymal stem cell homing: the devil is in the details. *Cell Stem Cell,* 4**,** 206-16.

KASTEN, A., MULLER, P., BULNHEIM, U., GROLL, J., BRUELLHOFF, K., BECK, U., STEINHOFF, G., MOLLER, M. & RYCHLY, J. 2010. Mechanical integrin stress and magnetic forces induce biological responses in mesenchymal stem cells which depend on environmental factors. *J Cell Biochem,* 111**,** 1586-97.

KEDONG, S., XIUBO, F., TIANQING, L., MACEDO, H. M., LILI, J., MEIYUN, F., FANGXIN, S., XUEHU, M. & ZHANFENG, C. 2010. Simultaneous expansion and harvest of hematopoietic stem cells and mesenchymal stem cells derived from umbilical cord blood. *J.Mater.Sci.Mater.Med.,* 21**,** 3183-3193.

KEESE, C. R. & GIAEVER, I. 1983. Cell growth on liquid microcarriers. *Science,* 219**,** 1448-9.

KELLEY, B. 2007. Very Large Scale Monoclonal Antibody Purification: The Case for Conventional Unit Operations. *Biotechnology Progress,* 23**,** 995-1008.

KERN, S., EICHLER, H., STOEVE, J., KLUTER, H. & BIEBACK, K. 2006. Comparative analysis of mesenchymal stem cells from bone marrow, umbilical cord blood, or adipose tissue. *Stem Cells,* 24**,** 1294-1301.

KIM, M. H., KINO-OKA, M. & TAYA, M. 2010. Designing culture surfaces based on cell anchoring mechanisms to regulate cell morphologies and functions. *Biotechnol Adv,* 28**,** 7-16.

KIM, S. H., MOON, H. H., KIM, H. A., HWANG, K. C., LEE, M. & CHOI, D. 2011. Hypoxia-inducible vascular endothelial growth factor-engineered mesenchymal stem cells prevent myocardial ischemic injury. *Mol Ther,* 19**,** 741-50.

KITA, K., GAUGLITZ, G. G., PHAN, T. T., HERNDON, D. N. & JESCHKE, M. G. 2010. Isolation and characterization of mesenchymal stem cells from the sub-amniotic human umbilical cord lining membrane. *Stem cells and development,* 19**,** 491-502.

KNORR, M. & DENK, P. O. 2002. Verätzungen und Verbrennungen. *In:* ROHRBACH, J. M., STEUHL, K.-P., KNORR, M. & KIRCHHOF, B. (eds.) *Ophthalmologische Traumatologie: Textbuch und Atlas.* Stuttgart, Germany: Schattauer.

KNOTHE, S. & NEUBAUER, M. 2013. GMP Requirements and Quality Management of Cellular Products. *In:* LOREDANA DE BARTOLO, A. B. (ed.) *Biomaterials for Stem Cell Therapy.* Crc Press Inc.

KOCAOEMER, A., KERN, S., KLUTER, H. & BIEBACK, K. 2007. Human AB serum and thrombin-activated platelet-rich plasma are suitable alternatives to fetal calf serum for the expansion of mesenchymal stem cells from adipose tissue. *Stem Cells,* 25**,** 1270-1278.

KOCH, A., POLVERINI, P., KUNKEL, S., HARLOW, L., DIPIETRO, L., ELNER, V., ELNER, S. & STRIETER, R. 1992. Interleukin-8 as a macrophage-derived mediator of angiogenesis. *Science,* 258**,** 1798-1801.

KOLIOS, G. & MOODLEY, Y. 2013. Introduction to stem cells and regenerative medicine. *Respiration,* 85**,** 3-10.

KOLLER, M. R., MANCHEL, I., BROTT, D. A. & PALSSON, B. 1996. Donor-to-donor variability in the expansion potential of human bone marrow cells is reduced by accessory cells but not by soluble growth factors. *Exp Hematol,* 24**,** 1484-93.

KOPEN, G. C., PROCKOP, D. J. & PHINNEY, D. G. 1999. Marrow stromal cells migrate throughout forebrain and cerebellum, and they differentiate into astrocytes after injection into neonatal mouse brains. *Proceedings of the National Academy of Sciences of the United States of America,* 96**,** 10711-6.

KORFF, T. & AUGUSTIN, H. G. 1999. Tensional forces in fibrillar extracellular matrices control directional capillary sprouting. *J Cell Sci,* 112 (Pt 19)**,** 3249-58.

KOZANOGLU, I., BOGA, C., OZDOGU, H., SOZER, O., MAYTALMAN, E., YAZICI, A. C. & SAHIN, F. I. 2009. Human bone marrow mesenchymal cells express NG2: possible increase in discriminative ability of flow cytometry during mesenchymal stromal cell identification. *Cytotherapy,* 11**,** 527-33.

KRAMPERA, M., GLENNIE, S., DYSON, J., SCOTT, D., LAYLOR, R., SIMPSON, E. & DAZZI, F. 2003. Bone marrow mesenchymal stem cells inhibit the response of naive and memory antigen-specific T cells to their cognate peptide. *Blood,* 101**,** 3722-9.

KREBS, H. A. 1972. The Pasteur effect and the relations between respiration and fermentation. *Essays Biochem,* 8**,** 1-34.

KREKE, M. R., HUCKLE, W. R. & GOLDSTEIN, A. S. 2005. Fluid flow stimulates expression of osteopontin and bone sialoprotein by bone marrow stromal cells in a temporally dependent manner. *Bone,* 36**,** 1047-55.

KREKE, M. R., SHARP, L. A., LEE, Y. W. & GOLDSTEIN, A. S. 2008. Effect of intermittent shear stress on mechanotransductive signaling and osteoblastic differentiation of bone marrow stromal cells. *Tissue engineering. Part A,* 14**,** 529-37.

KUCI, S., KUCI, Z., KREYENBERG, H., DEAK, E., PUTSCH, K., HUENECKE, S., AMARA, C., KOLLER, S., RETTINGER, E., GREZ, M., KOEHL, U., LATIFI-PUPOVCI, H., HENSCHLER, R., TONN, T., VON LAER, D., KLINGEBIEL, T. & BADER, P. 2010. CD271 antigen defines a subset of multipotent stromal cells with immunosuppressive and lymphohematopoietic engraftment-promoting properties. *Haematologica,* 95**,** 651-9.

KUSHIDA, A., YAMATO, M., ISOI, Y., KIKUCHI, A. & OKANO, T. 2005. A noninvasive transfer system for polarized renal tubule epithelial cell sheets using temperature-responsive culture dishes. *Eur Cell Mater,* 10**,** 23-30; discussion 23-30.

KUSHIDA, A., YAMATO, M., KONNO, C., KIKUCHI, A., SAKURAI, Y. & OKANO, T. 1999. Decrease in culture temperature releases monolayer endothelial cell sheets together with deposited fibronectin matrix from temperature-responsive culture surfaces. *J.Biomed.Mater.Res.,* 45**,** 355-362.

KWON, O. H., KIKUCHI, A., YAMATO, M., SAKURAI, Y. & OKANO, T. 2000. Rapid cell sheet detachment from poly(N-isopropylacrylamide)-grafted porous cell culture membranes. *J Biomed Mater Res,* 50**,** 82-9.

LE BLANC, K., FRASSONI, F., BALL, L., LOCATELLI, F., ROELOFS, H., LEWIS, I., LANINO, E., SUNDBERG, B., BERNARDO, M. E., REMBERGER, M., DINI, G., EGELER, R. M., BACIGALUPO, A., FIBBE, W., RINGDEN, O., DEVELOPMENTAL COMMITTEE OF THE EUROPEAN GROUP FOR, B. & MARROW, T. 2008. Mesenchymal stem cells for treatment of steroid-resistant, severe, acute graft-versus-host disease: a phase II study. *Lancet,* 371**,** 1579-86.

LE BLANC, K., SAMUELSSON, H., GUSTAFSSON, B., REMBERGER, M., SUNDBERG, B., ARVIDSON, J., LJUNGMAN, P., LONNIES, H., NAVA, S. & RINGDEN, O. 2007. Transplantation of mesenchymal stem cells to enhance engraftment of hematopoietic stem cells. *Leukemia,* 21**,** 1733-8.

LE BLANC, K., TAMMIK, C., ROSENDAHL, K., ZETTERBERG, E. & RINGDEN, O. 2003. HLA expression and immunologic properties of differentiated and undifferentiated mesenchymal stem cells. *Exp Hematol,* 31**,** 890-6.

LÉO, P., GALESI, A. L., SUAZO, C. A. & MORAES, A. M. 2008. Animal Cells: Basic Concepts. *In:* CASTILHO, L. R., MORAES, A. M. & EAUGUSTO, E. F. P. (eds.) *Animal Cell Technology: From Biopharmaceuticals to Gene Therapy.* Taylor & Francis.

LEPPERDINGER, G., BRUNAUER, R., JAMNIG, A., LASCHOBER, G. & KASSEM, M. 2008. Controversial issue: is it safe to employ mesenchymal stem cells in cell-based therapies? *Exp.Gerontol.,* 43**,** 1018-1023.

LI, S. C. & ZHONG, J. F. 2009. Twisting immune responses for allogeneic stem cell therapy. *World journal of stem cells,* 1**,** 30-5.

LI, Y. J., BATRA, N. N., YOU, L., MEIER, S. C., COE, I. A., YELLOWLEY, C. E. & JACOBS, C. R. 2004. Oscillatory fluid flow affects human marrow stromal cell proliferation and differentiation. *J Orthop Res,* 22**,** 1283-9.

LI, Z., GUO, X., PALMER, A. F., DAS, H. & GUAN, J. 2012. High Efficiency Matrix Modulus-Induced Cardiac Differentiation of Human Mesenchymal Stem Cells inside a Thermosensitive Hydrogel. *Acta biomaterialia*.

LINDL, T. & GSTRAUNTHALER, G. 2008a. Physiologische Zellkulturparameter. *Zell- und Gewebekultur.* Heidelberg: Spektrum Akademischer Verlag.

LINDL, T. & GSTRAUNTHALER, G. 2008b. Zellkulturmedien. *Zell- und Gewebekultur.* Heidelberg: Spektrum Akademischer Verlag.

LINDROOS, B., BOUCHER, S., CHASE, L., KUOKKANEN, H., HUHTALA, H., HAATAJA, R., VEMURI, M., SUURONEN, R. & MIETTINEN, S. 2009. Serum-free, xeno-free culture media maintain the proliferation rate and multipotentiality of adipose stem cells in vitro. *Cytotherapy.,* 11**,** 958-972.

LING, L., NURCOMBE, V. & COOL, S. M. 2009. Wnt signaling controls the fate of mesenchymal stem cells. *Gene,* 433**,** 1-7.

LIU, X., DUAN, B., CHENG, Z., JIA, X., MAO, L., FU, H., CHE, Y., OU, L., LIU, L. & KONG, D. 2011. SDF-1/CXCR4 axis modulates bone marrow mesenchymal stem cell apoptosis, migration and cytokine secretion. *Protein & cell,* 2**,** 845-54.

LÜLLAU, E. & FENGE, C. 2005. Cell Culture Bioreactors. *Cell Culture Technology for Pharmaceutical and Cell-Based Therapies.* CRC Press.

LUO, W., XIONG, W., ZHOU, J., FANG, Z., CHEN, W., FAN, Y. & LI, F. 2011. Laminar shear stress delivers cell cycle arrest and anti-apoptosis to mesenchymal stem cells. *Acta Biochim Biophys Sin (Shanghai),* 43**,** 210-6.

LUTZ, J. F., AKDEMIR, O. & HOTH, A. 2006. Point by point comparison of two thermosensitive polymers exhibiting a similar LCST: is the age of poly(NIPAM) over? *J Am Chem Soc,* 128**,** 13046-7.

LV, F., LU, M., CHEUNG, K. M., LEUNG, V. Y. & ZHOU, G. 2012. Intrinsic properties of mesemchymal stem cells from human bone marrow, umbilical cord and umbilical cord blood (comparing the different sources of msc). *Current stem cell research & therapy*.

MA, T. 2012. Mesenchymal Stem Cell Expansion for Therapeutic Application. *In:* HAYAT, M. A. (ed.) *Stem Cells and Cancer Stem Cells, Volume 7.* Springer Netherlands.

MADRI, J. A., PRATT, B. M. & TUCKER, A. M. 1988. Phenotypic modulation of endothelial cells by transforming growth factor-beta depends upon the composition and organization of the extracellular matrix. *J Cell Biol,* 106**,** 1375-84.

MAHARJAN, P., WOONTON, B. W., BENNETT, L. E., SMITHERS, G. W., DESILVA, K. & HEARN, M. T. W. 2008. Novel chromatographic separation — The potential of smart polymers. *Innovative Food Science & Emerging Technologies,* 9**,** 232-242.

MAJUMDAR, M. K., THIEDE, M. A., HAYNESWORTH, S. E., BRUDER, S. P. & GERSON, S. L. 2000. Human marrow-derived mesenchymal stem cells (MSCs) express hematopoietic cytokines and support long-term hematopoiesis when differentiated toward stromal and osteogenic lineages. *Journal of hematotherapy & stem cell research,* 9**,** 841-8.

MAKINO, S., FUKUDA, K., MIYOSHI, S., KONISHI, F., KODAMA, H., PAN, J., SANO, M., TAKAHASHI, T., HORI, S., ABE, H., HATA, J., UMEZAWA, A. & OGAWA, S. 1999. Cardiomyocytes can be generated from marrow stromal cells in vitro. *J Clin Invest,* 103**,** 697-705.

MARIGO, I. & DAZZI, F. 2011. The immunomodulatory properties of mesenchymal stem cells. *Seminars in immunopathology,* 33**,** 593-602.

MARONGIU, F., GRAMIGNOLI, R., SUN, Q., TAHAN, V., MIKI, T., DORKO, K., ELLIS, E. & STROM, S. C. 2010. Isolation of amniotic mesenchymal stem cells. *Current protocols in stem cell biology,* Chapter 1**,** Unit 1E 5.

MARTINELLE, K., WESTLUND, A. & HAGGSTROM, L. 1996. Ammonium ion transport-a cause of cell death. *Cytotechnology,* 22**,** 251-4.

MATHER, J. P. 1998. Laboratory scaleup of cell cultures (0.5-50 liters). *Methods Cell Biol,* 57**,** 219-27.

MATHIEU, P. S. & LOBOA, E. G. 2012. Cytoskeletal and focal adhesion influences on mesenchymal stem cell shape, mechanical properties, and differentiation down osteogenic, adipogenic, and chondrogenic pathways. *Tissue engineering. Part B, Reviews,* 18**,** 436-44.

MAUL, T. M., CHEW, D. W., NIEPONICE, A. & VORP, D. A. 2011. Mechanical stimuli differentially control stem cell behavior: morphology, proliferation, and differentiation. *Biomech.Model.Mechanobiol.,* 10**,** 939-953.

MCBEATH, R., PIRONE, D. M., NELSON, C. M., BHADRIRAJU, K. & CHEN, C. S. 2004. Cell shape, cytoskeletal tension, and RhoA regulate stem cell lineage commitment. *Dev Cell,* 6**,** 483-95.

MCBRIDE, S. H. & KNOTHE TATE, M. L. 2008. Modulation of stem cell shape and fate A: the role of density and seeding protocol on nucleus shape and gene expression. *Tissue engineering. Part A,* 14**,** 1561-72.

MEIRELLES LDA, S., FONTES, A. M., COVAS, D. T. & CAPLAN, A. I. 2009. Mechanisms involved in the therapeutic properties of mesenchymal stem cells. *Cytokine & growth factor reviews,* 20**,** 419-27.

MEUWLY, F., PAPP, F., RUFFIEUX, P. A., BERNARD, A. R., KADOURI, A. & VON STOCKAR, U. 2006. Use of glucose consumption rate (GCR) as a tool to monitor and control animal cell production processes in packed-bed bioreactors. *J Biotechnol,* 122**,** 122-9.

MEUWLY, F., RUFFIEUX, P. A., KADOURI, A. & VON STOCKAR, U. 2007. Packed-bed bioreactors for mammalian cell culture: bioprocess and biomedical applications. *Biotechnol Adv,* 25**,** 45-56.

MIMEAULT, M., HAUKE, R. & BATRA, S. K. 2007. Stem cells: a revolution in therapeutics-recent advances in stem cell biology and their therapeutic applications in regenerative medicine and cancer therapies. *Clin Pharmacol Ther,* 82**,** 252-64.

MITALIPOV, S. & WOLF, D. 2009. Totipotency, pluripotency and nuclear reprogramming. *Adv Biochem Eng Biotechnol,* 114**,** 185-99.

MIZUTANI, A., KIKUCHI, A., YAMATO, M., KANAZAWA, H. & OKANO, T. 2008. Preparation of thermoresponsive polymer brush surfaces and their interaction with cells. *Biomaterials,* 29**,** 2073-81.

MOLL, G., RASMUSSON-DUPREZ, I., VON BAHR, L., CONNOLLY-ANDERSEN, A. M., ELGUE, G., FUNKE, L., HAMAD, O. A., LONNIES, H., MAGNUSSON, P. U., SANCHEZ, J., TERAMURA, Y., NILSSON-EKDAHL, K., RINGDEN, O., KORSGREN, O., NILSSON, B. & LE BLANC, K. 2012. Are therapeutic human mesenchymal stromal cells compatible with human blood? *Stem cells,* 30**,** 1565-74.

MOORE, K. A. & LEMISCHKA, I. R. 2006. Stem cells and their niches. *Science,* 311**,** 1880-5.

MUTHUKKARUPPAN, V. & AUERBACH, R. 1979. Angiogenesis in the mouse cornea. *Science,* 205**,** 1416-8.

NAGASE, K., KOBAYASHI, J. & OKANO, T. 2009. Temperature-responsive intelligent interfaces for biomolecular separation and cell sheet engineering. *J.R.Soc.Interface,* 6 Suppl 3**,** S293-S309.

NEMETH, K., LEELAHAVANICHKUL, A., YUEN, P. S. T., MAYER, B., PARMELEE, A., DOI, K., ROBEY, P. G., LEELAHAVANICHKUL, K., KOLLER, B. H., BROWN, J. M., HU, X., JELINEK, I., STAR, R. A. & MEZEY, E. 2009. Bone marrow stromal cells attenuate sepsis via prostaglandin E 2-dependent reprogramming of host macrophages to increase their interleukin-10 production. *Nature Medicine,* 15**,** 42-49.

NEUSS, S., BECHER, E., WOLTJE, M., TIETZE, L. & JAHNEN-DECHENT, W. 2004. Functional expression of HGF and HGF receptor/c-met in adult human mesenchymal stem cells suggests a role in cell mobilization, tissue repair, and wound healing. *Stem Cells,* 22**,** 405-14.

NEWSHOLME, E. A., CRABTREE, B. & ARDAWI, M. S. 1985. The role of high rates of glycolysis and glutamine utilization in rapidly dividing cells. *Biosci Rep,* 5**,** 393-400.

NICOSIA, R. F. & OTTINETTI, A. 1990. Growth of microvessels in serum-free matrix culture of rat aorta. A quantitative assay of angiogenesis in vitro. *Lab Invest,* 63**,** 115-22.

NISHIDA, K., YAMATO, M., HAYASHIDA, Y., WATANABE, K., YAMAMOTO, K., ADACHI, E., NAGAI, S., KIKUCHI, A., MAEDA, N., WATANABE, H., OKANO, T. & TANO, Y. 2004. Corneal reconstruction with tissue-engineered cell sheets composed of autologous oral mucosal epithelium. *N Engl J Med,* 351**,** 1187-96.

OHLSTEIN, B., KAI, T., DECOTTO, E. & SPRADLING, A. 2004. The stem cell niche: theme and variations. *Curr Opin Cell Biol,* 16**,** 693-9.

OKANO, T., YAMADA, N., OKUHARA, M., SAKAI, H. & SAKURAI, Y. 1995. Mechanism of cell detachment from temperature-modulated, hydrophilic-hydrophobic polymer surfaces. *Biomaterials,* 16**,** 297-303.

OKANO, T., YAMADA, N., SAKAI, H. & SAKURAI, Y. 1993. A novel recovery system for cultured cells using plasma-treated polystyrene dishes grafted with poly(N-isopropylacrylamide). *J.Biomed.Mater.Res.,* 27**,** 1243-1251.

ORTIZ, L. A., DUTREIL, M., FATTMAN, C., PANDEY, A. C., TORRES, G., GO, K. & PHINNEY, D. G. 2007. Interleukin 1 receptor antagonist mediates the antiinflammatory and antifibrotic effect of mesenchymal stem cells during lung injury. *Proceedings of the National Academy of Sciences of the United States of America,* 104**,** 11002-7.

OWEN, M. 1988. Marrow stromal stem cells. *J Cell Sci Suppl,* 10**,** 63-76.

PAPOUTSAKIS, E. T. 1991. Fluid-mechanical damage of animal cells in bioreactors. *Trends Biotechnol,* 9**,** 427-37.

PAREKKADAN, B. & MILWID, J. M. 2010. Mesenchymal stem cells as therapeutics. *Annu Rev Biomed Eng,* 12**,** 87-117.

PARK, J. S., HASHI, C. & LI, S. 2010. Culture of bone marrow mesenchymal stem cells on engineered matrix. *Methods Mol Biol,* 621**,** 117-37.

PAROLINI, O., ALVIANO, F., BAGNARA, G. P., BILIC, G., BUHRING, H. J., EVANGELISTA, M., HENNERBICHLER, S., LIU, B., MAGATTI, M., MAO, N., MIKI, T., MARONGIU, F., NAKAJIMA, H., NIKAIDO, T., PORTMANN-LANZ, C. B., SANKAR, V., SONCINI, M., STADLER, G., SURBEK, D., TAKAHASHI, T. A., REDL, H., SAKURAGAWA, N., WOLBANK, S., ZEISBERGER, S., ZISCH, A. & STROM, S. C. 2008. Concise review: isolation and characterization of cells from human term placenta: outcome of the first international Workshop on Placenta Derived Stem Cells. *Stem cells,* 26**,** 300-11.

PATTAPPA, G., HEYWOOD, H. K., DE BRUIJN, J. D. & LEE, D. A. 2011. The metabolism of human mesenchymal stem cells during proliferation and differentiation. *Journal of cellular physiology,* 226**,** 2562-70.

PEDRAJAS, F. G., CAFASSO, D. E. & SCHNEIDER, P. A. 2012. Endovascular therapy: is it effective in the diabetic limb? *Semin Vasc Surg,* 25**,** 93-101.

PHINNEY, D. G., KOPEN, G., RIGHTER, W., WEBSTER, S., TREMAIN, N. & PROCKOP, D. J. 1999. Donor variation in the growth properties and osteogenic potential of human marrow stromal cells. *J Cell Biochem,* 75**,** 424-36.

PIETILA, M., LEHTONEN, S., TUOVINEN, E., LAHTEENMAKI, K., LAITINEN, S., LESKELA, H. V., NATYNKI, A., PESALA, J., NORDSTROM, K. & LEHENKARI, P. 2012. CD200 positive human mesenchymal stem cells suppress TNF-alpha secretion from CD200 receptor positive macrophage-like cells. *PloS one,* 7**,** e31671.

PITTENGER, M. F., MACKAY, A. M., BECK, S. C., JAISWAL, R. K., DOUGLAS, R., MOSCA, J. D., MOORMAN, M. A., SIMONETTI, D. W., CRAIG, S. & MARSHAK, D. R. 1999. Multilineage potential of adult human mesenchymal stem cells. *Science,* 284**,** 143-7.

PLUNKETT, K. N., ZHU, X., MOORE, J. S. & LECKBAND, D. E. 2006. PNIPAM chain collapse depends on the molecular weight and grafting density. *Langmuir,* 22**,** 4259-66.

POLASTRO, E. 2001. The Future of Biogenerics. *Contract Pharma,* 3**,** 40-50.

PROCKOP, D. J. 1997. Marrow stromal cells as stem cells for nonhematopoietic tissues. *Science,* 276**,** 71-4.

PROCKOP, D. J. 2009. Repair of tissues by adult stem/progenitor cells (MSCs): controversies, myths, and changing paradigms. *Mol.Ther,* 17**,** 939-946.

PROCKOP, D. J., BRENNER, M., FIBBE, W. E., HORWITZ, E., LE, B. K., PHINNEY, D. G., SIMMONS, P. J., SENSEBE, L. & KEATING, A. 2010a. Defining the risks of mesenchymal stromal cell therapy. *Cytotherapy.,* 12**,** 576-578.

PROCKOP, D. J., BRENNER, M., FIBBE, W. E., HORWITZ, E., LE BLANC, K., PHINNEY, D. G., SIMMONS, P. J., SENSEBE, L. & KEATING, A. 2010b. Defining the risks of mesenchymal stromal cell therapy. *Cytotherapy,* 12**,** 576-8.

PROCKOP, D. J. & OH, J. Y. 2012. Medical therapies with adult stem/progenitor cells (MSCs): a backward journey from dramatic results in vivo to the cellular and molecular explanations. *J Cell Biochem.,* 113**,** 1460-1469.

PUCHTLER, H., MELOAN, S. N. & TERRY, M. S. 1969. On the history and mechanism of alizarin and alizarin red S stains for calcium. *J Histochem Cytochem,* 17**,** 110-24.

QUAH, B. J., WARREN, H. S. & PARISH, C. R. 2007. Monitoring lymphocyte proliferation in vitro and in vivo with the intracellular fluorescent dye carboxyfluorescein diacetate succinimidyl ester. *Nat Protoc,* 2**,** 2049-56.

RAMASAMY, R., FAZEKASOVA, H., LAM, E. W., SOEIRO, I., LOMBARDI, G. & DAZZI, F. 2007. Mesenchymal stem cells inhibit dendritic cell differentiation and function by preventing entry into the cell cycle. *Transplantation,* 83**,** 71-6.

RAMASAMY, R., TONG, C. K., SEOW, H. F., VIDYADARAN, S. & DAZZI, F. 2008. The immunosuppressive effects of human bone marrow-derived mesenchymal stem cells target T cell proliferation but not its effector function. *Cellular immunology,* 251**,** 131-6.

RATAJCZAK, M. Z., ZUBA-SURMA, E., KUCIA, M., RECA, R., WOJAKOWSKI, W. & RATAJCZAK, J. 2006. The pleiotropic effects of the SDF-1-CXCR4 axis in organogenesis, regeneration and tumorigenesis. *Leukemia,* 20**,** 1915-24.

REED, J. A., LUCERO, A. E., COOPERSTEIN, M. A. & CANAVAN, H. E. 2008. The effects of cell culture parameters on cell release kinetics from thermoresponsive surfaces. *J Appl Biomater Biomech,* 6**,** 81-8.

REN, G., SU, J., ZHANG, L., ZHAO, X., LING, W., L'HUILLIE, A., ZHANG, J., LU, Y., ROBERTS, A. I., JI, W., ZHANG, H., RABSON, A. B. & SHI, Y. 2009. Species variation in the mechanisms of mesenchymal stem cell-mediated immunosuppression. *Stem cells,* 27**,** 1954-62.

REN, G., ZHANG, L., ZHAO, X., XU, G., ZHANG, Y., ROBERTS, A. I., ZHAO, R. C. & SHI, Y. 2008. Mesenchymal stem cell-mediated immunosuppression occurs via concerted action of chemokines and nitric oxide. *Cell Stem Cell,* 2**,** 141-50.

RINGDEN, O., UZUNEL, M., RASMUSSON, I., REMBERGER, M., SUNDBERG, B., LONNIES, H., MARSCHALL, H. U., DLUGOSZ, A., SZAKOS, A., HASSAN, Z., OMAZIC, B., ASCHAN, J., BARKHOLT, L. & LE BLANC, K. 2006. Mesenchymal stem cells for treatment of therapy-resistant graft-versus-host disease. *Transplantation,* 81**,** 1390-7.

RIVKIN, R., BEN-ARI, A., KASSIS, I., ZANGI, L., GABERMAN, E., LEVDANSKY, L., MARX, G. & GORODETSKY, R. 2007. High-yield isolation, expansion, and differentiation of murine bone marrow-derived mesenchymal stem cells using fibrin microbeads (FMB). *Cloning Stem Cells,* 9**,** 157-175.

RODRIGUES, C. A., FERNANDES, T. G., DIOGO, M. M., DA SILVA, C. L. & CABRAL, J. M. 2011. Stem cell cultivation in bioreactors. *Biotechnol Adv,* 29**,** 815-29.

ROGER, S. D. 2006. Biosimilars: How similar or dissimilar are they? (Review Article). *Nephrology,* 11**,** 341-346.

SALACINSKI, H. J., TIWARI, A., HAMILTON, G. & SEIFALIAN, A. M. 2001. Cellular engineering of vascular bypass grafts: Role of chemical coatings for enhancing endothelial cell attachment. *Medical and Biological Engineering and Computing,* 39**,** 609-618.

SALEM, H. K. & THIEMERMANN, C. 2010. Mesenchymal stromal cells: current understanding and clinical status. *Stem Cells,* 28**,** 585-96.

SALTZMAN, W. M. 2000. Cell Interactions with Polymers. *In:* LANZA, R. P., LANGER, R. & VACANTI, J. (eds.) *Principles of Tissue Engineering.* Academic Press.

SANCHEZ, J. C. & LOPEZ-ZAPATA, D. F. 2010. Effects of osmotic challenges on membrane potential in human articular chondrocytes from healthy and osteoarthritic cartilage. *Biorheology,* 47**,** 321-31.

SANTOS, F. D., ANDRADE, P. Z., ABECASIS, M. M., GIMBLE, J. M., CHASE, L. G., CAMPBELL, A. M., BOUCHER, S., VEMURI, M. C., SILVA, C. L. & CABRAL, J. M. 2011. Toward a Clinical-Grade Expansion of Mesenchymal Stem Cells from Human Sources: A Microcarrier-Based Culture System Under Xeno-Free Conditions. *Tissue Eng Part C.Methods*.

SANTOS, F. D., ANDRADE, P. Z., SILVA, C. L. & CABRAL, J. M. S. 2013. Scaling-up Ex Vivo Expansion of Mesenchymal Stem/Stromal Cells for Cellular Therapies. *In:* CHASE, L. G. & VEMURI, M. C. (eds.) *Mesenchymal Stem Cell Therapy*. Humana Press.

SART, S., ERRACHID, A., SCHNEIDER, Y. J. & AGATHOS, S. N. 2012. Modulation of mesenchymal stem cell actin organization on conventional microcarriers for proliferation and differentiation in stirred bioreactors. *Journal of tissue engineering and regenerative medicine*.

SART, S., SCHNEIDER, Y. J. & AGATHOS, S. N. 2009. Ear mesenchymal stem cells: an efficient adult multipotent cell population fit for rapid and scalable expansion. *J.Biotechnol.,* 139**,** 291-299.

SART, S., SCHNEIDER, Y. J. & AGATHOS, S. N. 2010. Influence of culture parameters on ear mesenchymal stem cells expanded on microcarriers. *J.Biotechnol.,* 150**,** 149-160.

SATIJA, N. K., SINGH, V. K., VERMA, Y. K., GUPTA, P., SHARMA, S., AFRIN, F., SHARMA, M., SHARMA, P., TRIPATHI, R. P. & GURUDUTTA, G. U. 2009. Mesenchymal stem cell-based therapy: a new paradigm in regenerative medicine. *J Cell Mol Med,* 13**,** 4385-402.

SATO, K., OZAKI, K., MORI, M., MUROI, K. & OZAWA, K. 2010. Mesenchymal stromal cells for graft-versus-host disease : basic aspects and clinical outcomes. *J Clin Exp Hematop,* 50**,** 79-89.

SCHNEIDER, C. K. 2008. Monoclonal Antibodies - Regulatory Challenges. *Curr Pharm Biotechnol,* 9**,** 431-438.

SCHNEIDER, M., MARISON, I. W. & VON STOCKAR, U. 1996. The importance of ammonia in mammalian cell culture. *J Biotechnol,* 46**,** 161-85.

SCHOP, D., JANSSEN, F. W., BORGART, E., DE BRUIJN, J. D. & VAN DIJKHUIZEN-RADERSMA, R. 2008. Expansion of mesenchymal stem cells using a microcarrier-based cultivation system: growth and metabolism. *J.Tissue Eng Regen.Med.,* 2**,** 126-135.

SCHOP, D., JANSSEN, F. W., VAN RIJN, L. D., FERNANDES, H., BLOEM, R. M., DE BRUIJN, J. D. & VAN DIJKHUIZEN-RADERSMA, R. 2009a. Growth, metabolism, and growth inhibitors of mesenchymal stem cells. *Tissue engineering. Part A,* 15**,** 1877-86.

SCHOP, D., JANSSEN, F. W., VAN RIJN, L. D., FERNANDES, H., BLOEM, R. M., DE BRUIJN, J. D. & VAN DIJKHUIZEN-RADERSMA, R. 2009b. Growth, metabolism, and growth inhibitors of mesenchymal stem cells. *Tissue Eng Part A,* 15**,** 1877-86.

SCHOP, D., VAN DIJKHUIZEN-RADERSMA, R., BORGART, E., JANSSEN, F. W., ROZEMULLER, H., PRINS, H. J. & DE BRUIJN, J. D. 2010. Expansion of human mesenchymal stromal cells on microcarriers: growth and metabolism. *J.Tissue Eng Regen.Med.,* 4**,** 131-140.

SCHREER, A., TINSON, C., SHERRY, J. P. & SCHIRMER, K. 2005. Application of Alamar blue/5-carboxyfluorescein diacetate acetoxymethyl ester as a noninvasive cell viability assay in primary hepatocytes from rainbow trout. *Analytical biochemistry,* 344**,** 76-85.

SCHROEDER, A., MUELLER, O., STOCKER, S., SALOWSKY, R., LEIBER, M., GASSMANN, M., LIGHTFOOT, S., MENZEL, W., GRANZOW, M. & RAGG, T. 2006. The RIN: an RNA integrity number for assigning integrity values to RNA measurements. *BMC Mol Biol,* 7**,** 3.

SCHUGAR, R. C., CHIRIELEISON, S. M., WESCOE, K. E., SCHMIDT, B. T., ASKEW, Y., NANCE, J. J., EVRON, J. M., PEAULT, B. & DEASY, B. M. 2009. High harvest yield, high expansion, and phenotype stability of CD146 mesenchymal stromal cells from whole primitive human umbilical cord tissue. *J Biomed Biotechnol,* 2009**,** 789526.

SCHWARZ, U. S. & GARDEL, M. L. 2012. United we stand: integrating the actin cytoskeleton and cell-matrix adhesions in cellular mechanotransduction. *Journal of cell science,* 125**,** 3051-60.

SEKIYA, I., LARSON, B. L., SMITH, J. R., POCHAMPALLY, R., CUI, J. G. & PROCKOP, D. J. 2002. Expansion of human adult stem cells from bone marrow stroma: conditions that maximize the yields of early progenitors and evaluate their quality. *Stem Cells,* 20**,** 530-541.

SENSEBE, L., BOURIN, P. & TARTE, K. 2011. Good manufacturing practices production of mesenchymal stem/stromal cells. *Hum Gene Ther,* 22**,** 19-26.

SERRA, M., BRITO, C., LEITE, S. B., GORJUP, E., VON, B. H., CARRONDO, M. J. & ALVES, P. M. 2009. Stirred bioreactors for the expansion of adult pancreatic stem cells. *Ann.Anat.,* 191**,** 104-115.

SESHAREDDY, K., TROYER, D. & WEISS, M. L. 2008. Method to isolate mesenchymal-like cells from Wharton's Jelly of umbilical cord. *Methods in cell biology,* 86**,** 101-19.

SHARP, L. A., LEE, Y. W. & GOLDSTEIN, A. S. 2009. Effect of low-frequency pulsatile flow on expression of osteoblastic genes by bone marrow stromal cells. *Ann Biomed Eng,* 37**,** 445-53.

SHI, D., MA, D., DONG, F., ZONG, C., LIU, L., SHEN, D., YUAN, W., TONG, X., CHEN, H. & WANG, J. 2010. Proliferation and multi-differentiation potentials of human mesenchymal stem cells on thermoresponsive PDMS surfaces grafted with PNIPAAm. *Biosci.Rep.,* 30**,** 149-158.

SHIRAGAMI, N., HAKODA, M., ENOMOTO, A. & HOSHINO, T. 1997. Hydrodynamic effect on cell attachment to microcarriers at initial stage of microcarrier culture. *Bioprocess Engineering,* 16**,** 399-401.

SHUKLA, A. A. & GOTTSCHALK, U. 2012. Single-use disposable technologies for biopharmaceutical manufacturing. *Trends Biotechnol*.

SIDDAPPA, R., LICHT, R., VAN BLITTERSWIJK, C. & DE BOER, J. 2007. Donor variation and loss of multipotency during in vitro expansion of human mesenchymal stem cells for bone tissue engineering. *J Orthop Res,* 25**,** 1029-41.

SINANAN, A. C., HUNT, N. P. & LEWIS, M. P. 2004. Human adult craniofacial muscle-derived cells: neural-cell adhesion-molecule (NCAM; CD56)-expressing cells appear to contain multipotential stem cells. *Biotechnol Appl Biochem,* 40**,** 25-34.

SINGER, N. G. & CAPLAN, A. I. 2011. Mesenchymal Stem Cells: Mechanisms of Inflammation. *Annual Review of Pathology: Mechanisms of Disease,* 6**,** 457-478.

SMITH, G. D. & BEDROV, D. 2003. Roles of Enthalpy, Entropy, and Hydrogen Bonding in the Lower Critical Solution Temperature Behavior of Poly(ethylene oxide)/Water Solutions. *The Journal of Physical Chemistry B,* 107**,** 3095-3097.

SON, B. R., MARQUEZ-CURTIS, L. A., KUCIA, M., WYSOCZYNSKI, M., TURNER, A. R., RATAJCZAK, J., RATAJCZAK, M. Z. & JANOWSKA-WIECZOREK, A. 2006. Migration of bone marrow and cord blood mesenchymal stem cells in vitro is regulated by stromal-derived factor-1-CXCR4 and hepatocyte growth factor-c-met axes and involves matrix metalloproteinases. *Stem cells,* 24**,** 1254-64.

SOTIROPOULOU, P. A., PEREZ, S. A., SALAGIANNI, M., BAXEVANIS, C. N. & PAPAMICHAIL, M. 2006. Characterization of the optimal culture conditions for clinical scale production of human mesenchymal stem cells. *Stem Cells,* 24**,** 462-471.

SPAGGIARI, G. M., CAPOBIANCO, A., ABDELRAZIK, H., BECCHETTI, F., MINGARI, M. C. & MORETTA, L. 2008. Mesenchymal stem cells inhibit natural killer-cell proliferation, cytotoxicity, and cytokine production: role of indoleamine 2,3-dioxygenase and prostaglandin E2. *Blood,* 111**,** 1327-33.

SPANAUS, K. S., NADAL, D., PFISTER, H. W., SEEBACH, J., WIDMER, U., FREI, K., GLOOR, S. & FONTANA, A. 1997. C-X-C and C-C chemokines are expressed in the cerebrospinal fluid in bacterial meningitis and mediate chemotactic activity on peripheral blood-derived polymorphonuclear and mononuclear cells in vitro. *J Immunol,* 158**,** 1956-64.

SPATZ, J. P. & GEIGER, B. 2007. Molecular engineering of cellular environments: cell adhesion to nano-digital surfaces. *Methods in cell biology,* 83**,** 89-111.

SPIER, R. E. & GRIFFITHS, B. 1983. An examination of the data and concepts germane to the oxygenation of cultured animal cells. *Dev Biol Stand,* 55**,** 81-92.

STENDERUP, K., JUSTESEN, J., CLAUSEN, C. & KASSEM, M. 2003. Aging is associated with decreased maximal life span and accelerated senescence of bone marrow stromal cells. *Bone,* 33**,** 919-26.

STOLZING, A., COLEMAN, N. & SCUTT, A. 2006. Glucose-induced replicative senescence in mesenchymal stem cells. *Rejuvenation Res,* 9**,** 31-5.

STRIETER, R. M., POLVERINI, P. J., ARENBERG, D. A. & KUNKEL, S. L. 1995a. The role of CXC chemokines as regulators of angiogenesis. *Shock (Augusta, Ga.),* 4**,** 155-160.

STRIETER, R. M., POLVERINI, P. J., KUNKEL, S. L., ARENBERG, D. A., BURDICK, M. D., KASPER, J., DZUIBA, J., VAN DAMME, J., WALZ, A., MARRIOTT, D. & ET AL. 1995b. The functional role of the ELR motif in CXC chemokine-mediated angiogenesis. *J Biol Chem,* 270**,** 27348-57.

STUTE, N., HOLTZ, K., BUBENHEIM, M., LANGE, C., BLAKE, F. & ZANDER, A. R. 2004. Autologous serum for isolation and expansion of human mesenchymal stem cells for clinical use. *Exp Hematol,* 32**,** 1212-25.

SUBBANNA, P. K. 2007. Mesenchymal stem cells for treating GVHD: in-vivo fate and optimal dose. *Med Hypotheses,* 69**,** 469-70.

SUBRAMANIAN, K., PARK, Y., VERFAILLIE, C. M. & HU, W. S. 2011. Scalable expansion of multipotent adult progenitor cells as three-dimensional cell aggregates. *Biotechnol Bioeng,* 108**,** 364-75.

SUGA, H., ETO, H., SHIGEURA, T., INOUE, K., AOI, N., KATO, H., NISHIMURA, S., MANABE, I., GONDA, K. & YOSHIMURA, K. 2009. IFATS collection: Fibroblast growth factor-2-induced hepatocyte growth factor secretion by adipose-derived stromal cells inhibits postinjury fibrogenesis through a c-Jun N-terminal kinase-dependent mechanism. *Stem cells,* 27**,** 238-49.

SUGIYAMA, T., KOHARA, H., NODA, M. & NAGASAWA, T. 2006. Maintenance of the hematopoietic stem cell pool by CXCL12-CXCR4 chemokine signaling in bone marrow stromal cell niches. *Immunity,* 25**,** 977-88.

SUN, L. Y., HSIEH, D. K., SYU, W. S., LI, Y. S., CHIU, H. T. & CHIOU, T. W. 2010. Cell proliferation of human bone marrow mesenchymal stem cells on biodegradable microcarriers enhances in vitro differentiation potential. *Cell Prolif.,* 43**,** 445-456.

TAKAHASHI, K., TANABE, K., OHNUKI, M., NARITA, M., ICHISAKA, T., TOMODA, K. & YAMANAKA, S. 2007. Induction of pluripotent stem cells from adult human fibroblasts by defined factors. *Cell,* 131**,** 861-72.

TAKEICHI, M. & OKADA, T. S. 1972. Roles of magnesium and calcium ions in cell-to-substrate adhesion. *Exp Cell Res,* 74**,** 51-60.

TAKEZAWA, T., MORI, Y. & YOSHIZATO, K. 1990. Cell culture on a thermo-responsive polymer surface. *Biotechnology (N.Y.),* 8**,** 854-856.

TAMURA, A., KOBAYASHI, J., YAMATO, M. & OKANO, T. 2012a. Temperature-responsive poly(N-isopropylacrylamide)-grafted microcarriers for large-scale non-invasive harvest of anchorage-dependent cells. *Biomaterials*.

TAMURA, A., KOBAYASHI, J., YAMATO, M. & OKANO, T. 2012b. Thermally responsive microcarriers with optimal poly(N-isopropylacrylamide) grafted density for facilitating cell adhesion/detachment in suspension culture. *Acta Biomater,* 8**,** 3904-13.

TAMURA, A., NISHI, M., KOBAYASHI, J., NAGASE, K., YAJIMA, H., YAMATO, M. & OKANO, T. 2012c. Simultaneous enhancement of cell proliferation and thermally

induced harvest efficiency based on temperature-responsive cationic copolymer-grafted microcarriers. *Biomacromolecules,* 13**,** 1765-73.

R TEAM, 2012. R: A language and environment for statistical computing. . 2.15.0 ed. Vienna, Austria: R Foundation for Statistical Computing.

THARMALINGAM, T., SUNLEY, K., SPEARMAN, M. & BUTLER, M. 2011. Enhanced production of human recombinant proteins from CHO cells grown to high densities in macroporous microcarriers. *Mol Biotechnol,* 49**,** 263-76.

THOMSON, J. A., ITSKOVITZ-ELDOR, J., SHAPIRO, S. S., WAKNITZ, M. A., SWIERGIEL, J. J., MARSHALL, V. S. & JONES, J. M. 1998. Embryonic stem cell lines derived from human blastocysts. *Science,* 282**,** 1145-7.

TIMMINS, N. E., KIEL, M., GUENTHER, M., HEAZLEWOOD, C., DORAN, M. R., BROOKE, G. & ATKINSON, K. 2012. Closed system isolation and scalable expansion of human placental mesenchymal stem cells. *Biotechnology and Bioengineering***,** n/a-n/a.

TOGEL, F., WEISS, K., YANG, Y., HU, Z., ZHANG, P. & WESTENFELDER, C. 2007. Vasculotropic, paracrine actions of infused mesenchymal stem cells are important to the recovery from acute kidney injury. *American journal of physiology. Renal physiology,* 292**,** F1626-35.

TÖGEL, F., ZHANG, P., HU, Z. & WESTENFELDER, C. 2009. VEGF is a mediator of the renoprotective effects of multipotent marrow stromal cells in acute kidney injury. *J Cell Mol Med,* 13**,** 2109-2114.

TRAN, T. C., KIMURA, K., NAGANO, M., YAMASHITA, T., OHNEDA, K., SUGIMORI, H., SATO, F., SAKAKIBARA, Y., HAMADA, H., YOSHIKAWA, H., HOANG, S. N. & OHNEDA, O. 2011. Identification of human placenta-derived mesenchymal stem cells involved in re-endothelialization. *Journal of cellular physiology,* 226**,** 224-35.

TRITSCH, G. L. & MOORE, G. E. 1962. Spontaneous decomposition of glutamine in cell culture media. *Exp Cell Res,* 28**,** 360-4.

TSENG, P. C., YOUNG, T. H., WANG, T. M., PENG, H. W., HOU, S. M. & YEN, M. L. 2012. Spontaneous osteogenesis of MSCs cultured on 3D microcarriers through alteration of cytoskeletal tension. *Biomaterials,* 33**,** 556-564.

TWAITES, B. R., DE LAS HERAS ALARCON, C., LAVIGNE, M., SAULNIER, A., PENNADAM, S. S., CUNLIFFE, D., GORECKI, D. C. & ALEXANDER, C. 2005. Thermoresponsive polymers as gene delivery vectors: cell viability, DNA transport and transfection studies. *J Control Release,* 108**,** 472-83.

UCCELLI, A., MORETTA, L. & PISTOIA, V. 2008. Mesenchymal stem cells in health and disease. *Nat Rev Immunol,* 8**,** 726-36.

VAN DE VELDE, H., CAUFFMAN, G., TOURNAYE, H., DEVROEY, P. & LIEBAERS, I. 2008. The four blastomeres of a 4-cell stage human embryo are able to develop individually into blastocysts with inner cell mass and trophectoderm. *Hum Reprod,* 23**,** 1742-7.

VAN WEZEL, A. L. 1967. Growth of cell-strains and primary cells on micro-carriers in homogeneous culture. *Nature,* 216**,** 64-65.

VOGEL, C. & MARCOTTE, E. M. 2012. Insights into the regulation of protein abundance from proteomic and transcriptomic analyses. *Nat Rev Genet,* 13**,** 227-32.

WAGNER, J., KEAN, T., YOUNG, R., DENNIS, J. E. & CAPLAN, A. I. 2009. Optimizing mesenchymal stem cell-based therapeutics. *Curr Opin Biotechnol,* 20**,** 531-6.

WAGNER, W. & HO, A. D. 2007. Mesenchymal stem cell preparations--comparing apples and oranges. *Stem Cell Rev,* 3**,** 239-48.

WAGNER, W., HORN, P., CASTOLDI, M., DIEHLMANN, A., BORK, S., SAFFRICH, R., BENES, V., BLAKE, J., PFISTER, S., ECKSTEIN, V. & HO, A. D. 2008. Replicative senescence of mesenchymal stem cells: a continuous and organized process. *PloS one,* 3**,** e2213.

WANG, Y. & OUYANG, F. 1999. Bead-to-bead-transfer of vero cells in microcarrier culture. *Bioprocess Engineering,* 21**,** 211-213.

WARD, M. A. & GEORGIOU, T. K. 2011. Thermoresponsive Polymers for Biomedical Applications. *Polymers,* 3**,** 1215-1242.

WARNOCK, J. N. & AL-RUBEAI, M. 2006. Bioreactor systems for the production of biopharmaceuticals from animal cells. *Biotechnol Appl Biochem,* 45**,** 1-12.

WAUGH, A. 1999. Culturing Animal Cells in Fluidized Bed Reactors.

WAYMOUTH, C. 1970. Osmolality of mammalian blood and of media for culture of mammalian cells. *In vitro,* 6**,** 109-27.

WEBER, C., POHL, S., PORTNER, R., WALLRAPP, C., KASSEM, M., GEIGLE, P. & CZERMAK, P. 2007. Expansion and Harvesting of hMSC-TERT. *Open.Biomed.Eng J.,* 1**,** 38-46.

WEBER, C., FREIMARK, D., PORTNER, R., PINO-GRACE, P., POHL, S., WALLRAPP, C., GEIGLE, P. & CZERMAK, P. 2010. Expansion of human mesenchymal stem cells in a fixed-bed bioreactor system based on non-porous glass carrier--part A: inoculation, cultivation, and cell harvest procedures. *Int J.Artif.Organs,* 33**,** 512-525.

WIECHMANN, K., WALCH, H., SEILER, A., NEUBAUER, M. & WEGMEYER, H. 2011. Identifaction of Valid Endogenous References for Monitoring Gene Expression Changes in Human Multipotent Mesenchymal Stromal Cells using RealTime ready Assays. *RealTime ready Application Note No. 6* [Online]. Available: http://www.roche-applied-science.com/sis/realtimeready/RT_docs/fnr1286_RTR_AN_6_4ak.pdf.

WOLTERBEEK, H. T. & VAN DER MEER, A. J. 2005. Optimization, application, and interpretation of lactate dehydrogenase measurements in microwell determination of cell number and toxicity. *Assay and drug development technologies,* 3**,** 675-82.

WOODBURY, D., SCHWARZ, E. J., PROCKOP, D. J. & BLACK, I. B. 2000. Adult rat and human bone marrow stromal cells differentiate into neurons. *J Neurosci Res,* 61**,** 364-70.

XIONG, N., ZHANG, Z., HUANG, J., CHEN, C., JIA, M., XIONG, J., LIU, X., WANG, F., CAO, X., LIANG, Z., SUN, S., LIN, Z. & WANG, T. 2011. VEGF-expressing human umbilical cord mesenchymal stem cells, an improved therapy strategy for Parkinson's disease. *Gene Ther,* 18**,** 394-402.

XU, Q., YU, D., QIU, Y., ZHANG, H. & DING, Y. 2003. Function of a new internal bioartificial liver: an in vitro study. *Ann Clin Lab Sci,* 33**,** 306-12.

XUE, C., YONET-TANYERI, N., BROUETTE, N., SFERRAZZA, M., BRAUN, P. V. & LECKBAND, D. E. 2011. Protein adsorption on poly(N-isopropylacrylamide) brushes: dependence on grafting density and chain collapse. *Langmuir,* 27**,** 8810-8.

YAGI, H., SOTO-GUTIERREZ, A., PAREKKADAN, B., KITAGAWA, Y., TOMPKINS, R. G., KOBAYASHI, N. & YARMUSH, M. L. 2010. Mesenchymal stem cells: Mechanisms of immunomodulation and homing. *Cell Transplant,* 19**,** 667-79.

YAMADA, N., OKANO, T., SAKAI, H., KARIKUSA, F., SAWASAKI, Y. & SAKURAI, Y. 1990. Thermo-responsive polymeric surfaces; control of attachment and detachment of cultured cells. *Die Makromolekulare Chemie, Rapid Communications,* 11**,** 571-576.

YAMATO, M., AKIYAMA, Y., KOBAYASHI, J., YANG, J., KIKUCHI, A. & OKANO, T. 2007. Temperature-responsive cell culture surfaces for regenerative medicine with cell sheet engineering. *Progress in Polymer Science,* 32**,** 1123-1133.

YAMATO, M., OKUHARA, M., KARIKUSA, F., KIKUCHI, A., SAKURAI, Y. & OKANO, T. 1999. Signal transduction and cytoskeletal reorganization are required for cell detachment from cell culture surfaces grafted with a temperature-responsive polymer. *J Biomed Mater Res,* 44**,** 44-52.

YAMATO, M., UTSUMI, M., KUSHIDA, A., KONNO, C., KIKUCHI, A. & OKANO, T. 2001. Thermo-responsive culture dishes allow the intact harvest of multilayered keratinocyte sheets without dispase by reducing temperature. *Tissue Eng,* 7**,** 473-480.

YANG, H. S., JEON, O., BHANG, S. H., LEE, S. H. & KIM, B. S. 2010a. Suspension Culture of Mammalian Cells using Thermo-Sensitive Microcarrier that Allows Cell Detachment without Proteolytic Enzyme Treatment. *Cell Transplantation*.

YANG, H. S., JEON, O., BHANG, S. H., LEE, S. H. & KIM, B. S. 2010b. Suspension culture of mammalian cells using thermosensitive microcarrier that allows cell detachment without proteolytic enzyme treatment. *Cell Transplant.,* 19**,** 1123-1132.

YANG, J., YAMATO, M., KOHNO, C., NISHIMOTO, A., SEKINE, H., FUKAI, F. & OKANO, T. 2005. Cell sheet engineering: recreating tissues without biodegradable scaffolds. *Biomaterials,* 26**,** 6415-22.

YANG, J., YAMATO, M., SHIMIZU, T., SEKINE, H., OHASHI, K., KANZAKI, M., OHKI, T., NISHIDA, K. & OKANO, T. 2007a. Reconstruction of functional tissues with cell sheet engineering. *Biomaterials,* 28**,** 5033-43.

YANG, L., CHENG, F., LIU, T., LU, J. R., SONG, K., JIANG, L., WU, S. & GUO, W. 2012. Comparison of mesenchymal stem cells released from poly(N-isopropylacrylamide) copolymer film and by trypsinization. *Biomed.Mater.,* 7**,** 035003.

YANG, Y., ROSSI, F. M. & PUTNINS, E. E. 2007b. Ex vivo expansion of rat bone marrow mesenchymal stromal cells on microcarrier beads in spin culture. *Biomaterials,* 28**,** 3110-3120.

YEATTS, A. B., CHOQUETTE, D. T. & FISHER, J. P. 2012. Bioreactors to influence stem cell fate: Augmentation of mesenchymal stem cell signaling pathways via dynamic culture systems. *Biochimica et biophysica acta*.

YU, J., VODYANIK, M. A., SMUGA-OTTO, K., ANTOSIEWICZ-BOURGET, J., FRANE, J. L., TIAN, S., NIE, J., JONSDOTTIR, G. A., RUOTTI, V., STEWART, R., SLUKVIN, II & THOMSON, J. A. 2007. Induced pluripotent stem cell lines derived from human somatic cells. *Science,* 318**,** 1917-20.

YU, Y., LI, K., BAO, C., LIU, T., JIN, Y., REN, H. & YUN, W. 2009a. Ex vitro expansion of human placenta-derived mesenchymal stem cells in stirred bioreactor. *Appl.Biochem.Biotechnol.,* 159**,** 110-118.

YU, Y. Q., REN, H. Q., LI, K., BAO, C. Y., LIU, T. Q., JIN, Y. N., YUN, W. & DONG, B. 2009b. Large scale expansion of human placenta-derived mesenchymal cells in stirring bioreactor. *Chinese Journal of Biomedical Engineering,* 28**,** 749-753.

YUAN, Y., KALLOS, M. S., HUNTER, C. & SEN, A. 2012. Improved expansion of human bone marrow-derived mesenchymal stem cells in microcarrier-based suspension culture. *Journal of tissue engineering and regenerative medicine*.

ZAMBIDIS, E. T., PARK, T. S., YU, W., TAM, A., LEVINE, M., YUAN, X., PRYZHKOVA, M. & PEAULT, B. 2008. Expression of angiotensin-converting enzyme (CD143) identifies and regulates primitive hemangioblasts derived from human pluripotent stem cells. *Blood,* 112**,** 3601-14.

ZANGI, L., RIVKIN, R., KASSIS, I., LEVDANSKY, L., MARX, G. & GORODETSKY, R. 2006. High-yield isolation, expansion, and differentiation of rat bone marrow-derived mesenchymal stem cells with fibrin microbeads. *Tissue Eng,* 12**,** 2343-2354.

ZHANG, F., TIAN, J., WANG, L., HE, P. & CHEN, Y. 2011. Correlation between cell growth rate and glucose consumption determined by electrochemical monitoring. *Sensors and Actuators B: Chemical,* 156**,** 416-422.

ZHANG, N., SALZINGER, S., DEUBEL, F., JORDAN, R. & RIEGER, B. 2012a. Surface-initiated group transfer polymerization mediated by rare earth metal catalysts. *J Am Chem Soc,* 134**,** 7333-6.

ZHANG, N., SALZINGER, S. & RIEGER, B. 2012b. Poly(vinylphosphonate)s with Widely Tunable LCST: A Promising Alternative to Conventional Thermoresponsive Polymers. *Macromolecules,* 45**,** 9751-9758.

ZHANG, R., MJOSENG, H. K., HOEVE, M. A., BAUER, N. G., PELLS, S., BESSELING, R., VELUGOTLA, S., TOURNIAIRE, G., KISHEN, R. E., TSENKINA, Y., ARMIT, C., DUFFY, C. R., HELFEN, M., EDENHOFER, F., DE SOUSA, P. A. & BRADLEY, M. 2013. A thermoresponsive and chemically defined hydrogel for long-term culture of human embryonic stem cells. *Nature communications,* 4**,** 1335.

ZHANG, Y., FURYK, S., BERGBREITER, D. E. & CREMER, P. S. 2005. Specific Ion Effects on the Water Solubility of Macromolecules: PNIPAM and the Hofmeister Series. *J Am Chem Soc,* 127**,** 14505-14510.

ZHUKAREVA, V., OBROCKA, M., HOULE, J. D., FISCHER, I. & NEUHUBER, B. 2010. Secretion profile of human bone marrow stromal cells: donor variability and response to inflammatory stimuli. *Cytokine,* 50**,** 317-21.

ZUK, P. A., ZHU, M., MIZUNO, H., HUANG, J., FUTRELL, J. W., KATZ, A. J., BENHAIM, P., LORENZ, H. P. & HEDRICK, M. H. 2001. Multilineage cells from human adipose tissue: implications for cell-based therapies. *Tissue Eng,* 7**,** 211-28.

ZUNIGA, L. & CALVO, B. 2009. Global vision about the biological medicinal products: biosimilars (April, 2009). *Curr Pharm Biotechnol,* 10**,** 772-4.

ZUSCIK, M. J., HILTON, M. J., ZHANG, X., CHEN, D. & O'KEEFE, R. J. 2008. Regulation of chondrogenesis and chondrocyte differentiation by stress. *J Clin Invest,* 118**,** 429-38.

9 Supplements

Supplementary Table 1: Genes showing a significantly (p <0.05) higher expression (left) or lower expression (right) in microcarrier-expanded UC and AM MSCs relative to flask-expanded cells. Cut off: fold change <2

Gene	Assay ID	Fold change	p-Value
CSF2	110860	342.9	3.7E-08
IL8	103136	61.9	3.7E-08
CXCL3	103888	48.5	3.7E-08
CXCL1	137825	39.1	3.7E-08
CXCL1	105522	38.2	3.7E-08
CXCL2	103070	33.9	3.7E-08
TGFA	110787	30.5	3.7E-08
IL1B	100950	29.3	3.7E-08
MMP3	103167	17.2	2.0E-03
MMP1	103943	16.9	6.1E-03
STC1	116867	16.3	3.7E-08
CXCL5	110613	13.3	3.7E-08
CD24	139818	12.0	3.7E-08
AREG	111432	7.0	6.0E-09
ADAM8	109490	6.3	1.2E-04
ITGA6	113076	6.2	3.7E-08
PODXL	116328	5.4	2.0E-03
S100A4	110779	4.8	8.6E-03
ANPEP	108970	4.4	7.3E-04
NRG1	113134	4.1	1.1E-03
TFPI2	108032	3.9	2.0E-03
NRG1	139822	3.6	2.9E-03
TNFRSF1B	102682	3.5	2.0E-03
ROBO4	127380	3.4	7.7E-09
NT5E	105242	3.3	3.7E-08
CD274	104030	3.1	7.7E-09
DLGAP1	138553	3.0	1.4E-03
ITGA2	111263	2.9	4.7E-09
BCL2	100083	2.8	3.0E-02
CHN1	139743	2.8	7.3E-04
CCL7	110710	2.8	3.5E-03
ARHGAP29	122929	2.7	1.2E-02
CD44	110687	2.7	3.8E-04
SHC4	133970	2.6	8.6E-03
ADAM22	109117	2.5	1.4E-02
TGFBR2	104727	2.4	2.0E-04
CCL2	100240	2.3	5.1E-03
VEGFA	101034	2.3	9.7E-09
LIF	113007	2.3	8.6E-03
EPOR	140936	2.3	7.7E-09
NCAM1	111243	2.2	3.5E-02
FABP4	115237	2.2	1.0E-02
TNFRSF10A	101232	2.2	1.4E-02

Gene	Assay ID	Fold change	p-Value
ACAN	138057	-72.9	1.4E-02
ITGA11	140155	-27.9	3.7E-08
CCL5	113395	-26.0	7.7E-09
ACTA2	125175	-21.1	3.7E-08
VCAM1	103286	-20.1	1.7E-03
FGFR2	105812	-18.2	6.0E-09
FGF9	111498	-17.2	4.7E-09
ALPL	103448	-11.3	2.5E-04
MMP24	108460	-10.8	3.7E-08
ERBB3	106100	-10.7	3.7E-08
AOC3	115054	-8.5	6.0E-09
ALDH1A1	112320	-8.1	4.0E-02
COL1A1	100861	-7.5	3.7E-08
CDKN2B	101439	-7.4	2.5E-04
EGF	136007	-7.0	6.1E-03
NOTCH3	112380	-6.5	3.7E-08
WISP1	110191	-6.2	7.3E-03
COL1A2	103048	-5.8	3.7E-08
FBLIM1	126341	-5.7	1.2E-04
KIT	105674	-5.6	1.0E-02
NLGN3	126309	-5.2	2.0E-04
THBS1	104740	-4.8	2.9E-03
PDGFRB	105627	-4.7	4.1E-09
COL5A2	120754	-4.4	3.7E-08
ADAM12	140145	-4.4	7.7E-09
CXCL16	114685	-4.1	2.5E-04
CSF1R	105951	-4.1	4.3E-03
CTGF	100872	-3.8	1.7E-03
SDC2	113656	-3.7	3.7E-08
ITGB2	103578	-3.6	3.0E-02
FGF2	100912	-3.6	2.4E-03
CCDC80	115675	-3.5	7.7E-09
ADM2	137782	-3.5	8.6E-03
ACE	108903	-3.3	1.4E-02
MYH11	116429	-3.3	4.0E-02
CCND2	101384	-3.0	8.6E-03
SNAI1	112995	-2.9	4.7E-09
MCAM	105530	-2.8	1.2E-04
TGFBR1	104725	-2.8	1.2E-04
SERPINE2	103642	-2.7	2.0E-03
ITGA1	110762	-2.6	3.8E-04
CDH2	137066	-2.6	9.7E-09
ITGAV	110698	-2.5	3.7E-08

CDK1	101406	2.2	3.7E-08
MKI67	101512	2.2	2.0E-04
CCL2	141156	2.1	4.0E-02
CCNB1	101373	2.1	7.7E-09
GDNF	100445	2.1	5.1E-03
NRP1	111930	2.1	3.7E-08

CDH6	112143	-2.5	5.1E-03
PDGFA	110648	-2.4	1.9E-02
FAP	108274	-2.4	9.7E-09
KDR	105649	-2.4	2.6E-02
DDR1	110125	-2.3	2.0E-03
CDKN1A	102909	-2.3	3.1E-04
JAG1	108043	-2.3	2.3E-02
ATXN1	114769	-2.2	3.7E-08
MMP2	103899	-2.2	4.8E-04
PLEKHC1	103255	-2.2	4.7E-09
EFNB2	137312	-2.1	3.7E-08
THY1	116810	-2.1	2.0E-04

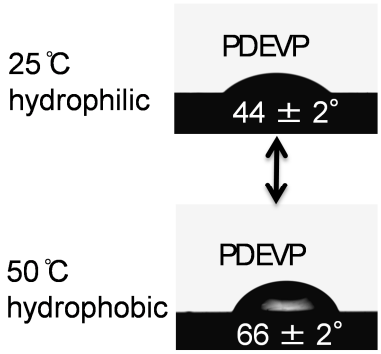

Supplementary Figure 1: Contact angle measurements of PDEVP-coated surface at different temperatures

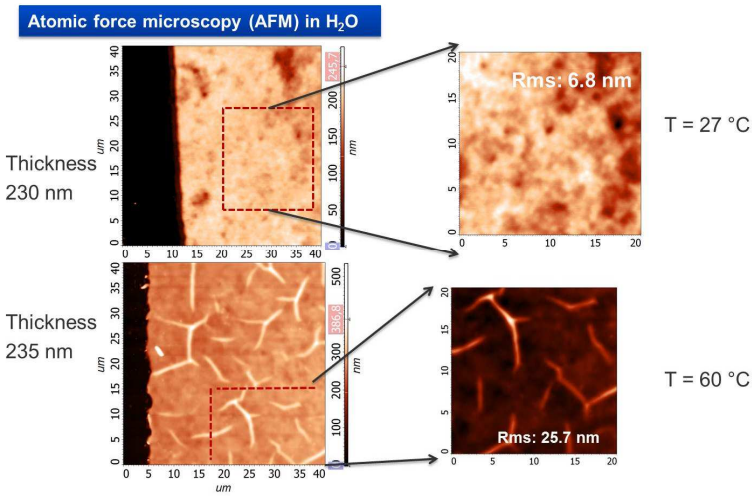

Supplementary Figure 2: Influence of temperature on polymer layer thickness. Figure provided by Dr. Ning Zhang.

Supplementary data: Fermentation

Experiments concerning large-scale cell expansion, monitoring of culture parameters and cell harvest were performed in the by Dr. Ingo Gorr, Christian Schwald, Manuel Meyer, and Alois Filgertshofer, Department of Large Molecule Research Penzberg. Data was kindly provided by Dr. Ingo Gorr. All experiments were performed using freshly thawed UC MSCs of passage 4. Control expansion on standard cell culture flasks was performed in parallel, using equal inoculation densities. 50% of culture medium was exchanged twice per week for both expansion technologies.

Run 1: Evaluation of bioreactor formats and sparging. A 1:2 split was performed at 80% confluence. For this, cells were trypsinized from microcarrier, fresh media-microcarrier suspension were added to a volume of 1000 ml. Harvest was performed at 80% confluence. MC: microcarrier, Glass reactor: Biostat® B-DCU 2 L Quad, glass vessel (Sartorius Stedim Biotech), Wave reactor: Biostat® CultiBag RM 2l optical (Sartorius Stedim Biotech).

Supplementary Table 2: Experimental set up run 1.

Glass Reactor	Volume (ml)	Technical Setup	MC (g)	pH	Cell density ($x10^6$)	pO_2	MSCs
1	750	Microsparger, pitched blade turbine	4.26 (~18.3 x 10^6 MC)	7.2 +/-0.05	22.5 (~1cell/MC)	20%	UC donor 1
2		Ringsparger, Rushton turbine					
Wave Reactor	**Volume (ml)**	**Technical Setup**	**MC (g)**	**pH**	**Cell density ($x10^6$)**	**pO_2**	**Cell line**
1	500	10 Rocks, Angle 7°	2.84 (~12.2x10^6 MC)	7.2 +/- 0.05	22.5 (~1cell/MC)	20%	UC donor 1
2				7.2 +/- 0.05	22.5 (~1cell/MC)	20%	

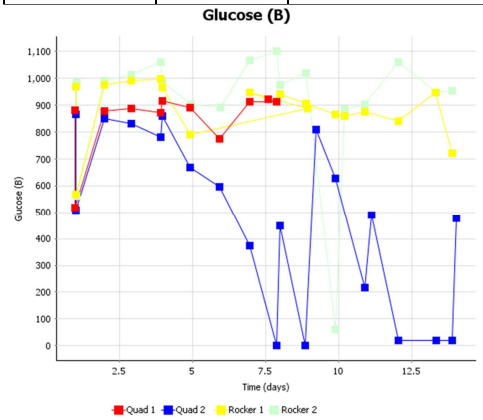

Supplementary Figure 3: Glucose concentrations run 1.

Supplementary Table 3: Cell yields run 1.

	Quad 1 Microsparger	**Quad 2 Ringsparger**	**Rocker 1 20% O_2**	**Rocker 2 5% O_2**
Total cell count inoculum ($x10^6$)	22.5	22.5	22.5	22.5
Total cell count harvest (day 15) ($x10^6$)	-	585	-	-
Amplification x - fold	-	26	-	-
Remark	Termination at day 8 due to lack of growth due to export of beads	Harvest at day 15	Termination at day 22 due to no growth	Termination at day 22 due to no growth

Run 2: Evaluation of different pH values. Length of pH-screen: 8 days; additional glucose feeding: 50% Glucose up to 1200 mg/l if consumption > 300 mg/l/day

Supplementary Table 4: Experimental set up run 2, pH evaluation.

Glass Reactor	**Volume (ml)**	**Technical Setup**	**MC (g)**	**pH**	**Cell density ($x10^6$)**	**pO_2**	**MSCs**
1	750	Ringsparger, Rushton turbine	4.26 (~18.3 x 10^6 MC)	7.2 +/- 0.05	22.5 (~1cell/mc)	20%	UC donor 1
2				7.3 +/- 0.05	22.5 (~1cell/mc)	20%	
3				7.4 +/- 0.05	22.5 (~1cell/mc)	20%	
4				7.5 +/- 0.05	22.5 (~1cell/mc)	20%	

Influence of pH, cell density and pO2 on cell growth. Additional glucose feeding: 50% Glucose up to 1200 mg/L if consumption > 300 mg/l/day

Supplementary Table 5: Experimental set up run 2, cell density and pO_2 evaluation.

Glass Reactor	**Volume (ml)**	**Technical Setup**	**MC (g)**	**pH**	**Cell density ($x10^6$)**	**pO_2**	**MSCs**
1	750	Ringsparger, Rushton turbine	4.26 (~18.3 x 10^6 MC)	7.5 +/- 0.05	90 (~4cells/mc)	20%	UC donor 1
2					90 (~4cells/mc)	5%	
3					22.5 (~1cell/mc)	20%	

Supplementary Table 6: Cell yields run 2, cell density and pO_2 evaluation.

	5% pO_2, high density	**20% pO_2, high density**	**20% pO_2, low density**
Total cell count inoculum ($x10^6$)	90	90	22.5
Total cell count harvest ($x10^6$)	241	325	98.5
Amplifikation x - fold	2.7	3.6	4.3

Run 3: Evaluation of different UC MSC donors. A 1:2 split was performed at 80% confluence: Half of the culture suspension was trypsinized from microcarrier, fresh media-microcarrier suspension was added to a volume of 750ml. Harvest was performed at 80% confluence.

Supplementary Table 7: Experimental set up run 3.

Glass Reactor	**Volume (ml)**	**Technical Setup**	**MC (g)**	**pH**	**Cell density ($x10^6$)**	**pO_2**	**MSCs**
1	750	Ringsparger, Rushton turbine	4.26 (~18.3x10^6 mc)	7.35 +/- 0.05	22.5 (~1cell/mc)	20% pO_2	UC donor 1
2				7.35 +/-0.05	22.5 (~1cell/mc)	20% pO_2	UC donor 4
3				7.35 +/-0.05	22.5 (~1cell/mc)	20% pO_2	UC donor 5

Cell yield after 15 days of culture (theoretical calculation to a culture volume of 1.5 l as cultures were halved during split).

Supplementary Table 8: Cell yields run 3.

	UC MSC donor 1	**UC MSC donor 4**	**UC MSC donor 5**
Total cell count inoculum ($x10^6$)	22.5	22.5	22.5
Total cell count day 15 ($x10^6$)	1,035	51	596
Amplifikation x - fold	46	2.3	26.5

Supplementary Table 9: Comparison cell yields run 1 - 3.

UC MSCs donor 1	Run 1 (Quad 2)	Run 2 (Quad 1)	Run3 (Quad 1)
Process Setup	pH 7.2, 20% pO_2 No feeding	pH 7.2, 20% pO_2 Feeding up to 1200 mg glucose/l	pH 7.35, 20% pO_2 Feeding up to 1200 mg glucose/l
Total cell count in-oculum ($x10^6$)	22.5	22.5	22.5
Total cell count day 15 ($x10^6$)	585	843	1,035
Amplifikation x - fold	26	37	46

Supplementary Table 10: Genes of customized qRT-PCR panel (RealTime ready)

Gene Symbol	Assay ID	Description	Note
ABCG2	101788	ATP-binding cassette, sub-family G (WHITE), member 2 [Source:HGNC Symbol;Acc:74]	
AC107016.2	114523	Keratin, type I cytoskeletal 18 (Cytokeratin-18)(CK-18)(Keratin-18)(K18)(Cell proliferation-inducing gene 46 protein) [Source:UniProtKB/Swiss-Prot;Acc:P05783]	
ACAN	138057	aggrecan [Source:HGNC Symbol;Acc:319]	
ACE	108903	angiotensin I converting enzyme (peptidyl-dipeptidase A) 1 [Source:HGNC Symbol;Acc:2707]	
ACTA2	125175	actin, alpha 2, smooth muscle, aorta [Source:HGNC Symbol;Acc:130]	
ACTB	101125	actin, beta [Source:HGNC Symbol;Acc:132]	Reference Gene
ADAM10	108628	ADAM metallopeptidase domain 10 [Source:HGNC Symbol;Acc:188]	
ADAM12	140145	ADAM metallopeptidase domain 12 [Source:HGNC Symbol;Acc:190]	
ADAM17	136024	ADAM metallopeptidase domain 17 [Source:HGNC Symbol;Acc:195]	
ADAM19	109730	ADAM metallopeptidase domain 19 [Source:HGNC Symbol;Acc:197]	
ADAM22	109117	ADAM metallopeptidase domain 22 [Source:HGNC Symbol;Acc:201]	
ADAM8	109490	ADAM metallopeptidase domain 8 [Source:HGNC Symbol;Acc:215]	
ADAM9	103838	ADAM metallopeptidase domain 9 [Source:HGNC Symbol;Acc:216]	
ADM	137818	adrenomedullin [Source:HGNC Symbol;Acc:259]	
ADM2	137782	adrenomedullin 2 [Source:HGNC Symbol;Acc:28898]	
AGTR1	100809	angiotensin II receptor, type 1 [Source:HGNC Symbol;Acc:336]	
ALCAM	117143	activated leukocyte cell adhesion molecule [Source:HGNC Symbol;Acc:400]	
ALDH1A1	112320	aldehyde dehydrogenase 1 family, member A1 [Source:HGNC Symbol;Acc:402]	

ALPL	103448	alkaline phosphatase, liver/bone/kidney [Source:HGNC Symbol;Acc:438]
ALPP	110208	alkaline phosphatase, placental [Source:HGNC Symbol;Acc:439]
ANGPT1	110625	angiopoietin 1 [Source:HGNC Symbol;Acc:484]
ANGPT1	140975	angiopoietin 1 [Source:HGNC Symbol;Acc:484]
ANPEP	108970	alanyl (membrane) aminopeptidase [Source:HGNC Symbol;Acc:500]
ANXA1	100033	annexin A1 [Source:HGNC Symbol;Acc:533]
ANXA1	107233	annexin A1 [Source:HGNC Symbol;Acc:533]
AOC3	115054	amine oxidase, copper containing 3 (vascular adhesion protein 1) [Source:HGNC Symbol;Acc:550]
APAF1	102892	apoptotic peptidase activating factor 1 [Source:HGNC Symbol;Acc:576]
AREG	111432	amphiregulin [Source:HGNC Symbol;Acc:651]
ARHGAP29	122929	Rho GTPase activating protein 29 [Source:HGNC Symbol;Acc:30207]
ATXN1	114769	ataxin 1 [Source:HGNC Symbol;Acc:10548]
BAD	104034	BCL2-associated agonist of cell death [Source:HGNC Symbol;Acc:936]
BCL2	100083	B-cell CLL/lymphoma 2 [Source:HGNC Symbol;Acc:990]
BDKRB2	113197	bradykinin receptor B2 [Source:HGNC Symbol;Acc:1030]
BDNF	100113	brain-derived neurotrophic factor [Source:HGNC Symbol;Acc:1033]
BMP2	104558	bone morphogenetic protein 2 [Source:HGNC Symbol;Acc:1069]
BMP7	104574	bone morphogenetic protein 7 [Source:HGNC Symbol;Acc:1074]
BST2	117914	bone marrow stromal cell antigen 2 [Source:HGNC Symbol;Acc:1119]

CASP8	100227	caspase 8, apoptosis-related cysteine peptidase [Source:HGNC Symbol;Acc:1509]
CASP9	100233	caspase 9, apoptosis-related cysteine peptidase [Source:HGNC Symbol;Acc:1511]
CCDC80	115675	coiled-coil domain containing 80 [Source:HGNC Symbol;Acc:30649]
CCL13	111292	chemokine (C-C motif) ligand 13 [Source:HGNC Symbol;Acc:10611]
CCL17	102711	chemokine (C-C motif) ligand 17 [Source:HGNC Symbol;Acc:10615]
CCL19	103845	chemokine (C-C motif) ligand 19 [Source:HGNC Symbol;Acc:10617]
CCL2	141156	chemokine (C-C motif) ligand 2 [Source:HGNC Symbol;Acc:10618]
CCL2	100240	chemokine (C-C motif) ligand 2 [Source:HGNC Symbol;Acc:10618]
CCL20	110753	chemokine (C-C motif) ligand 20 [Source:HGNC Symbol;Acc:10619]
CCL21	110668	chemokine (C-C motif) ligand 21 [Source:HGNC Symbol;Acc:10620]
CCL22	102713	chemokine (C-C motif) ligand 22 [Source:HGNC Symbol;Acc:10621]
CCL3	136214	chemokine (C-C motif) ligand 3 [Source:HGNC Symbol;Acc:10627]
CCL5	113395	chemokine (C-C motif) ligand 5 [Source:HGNC Symbol;Acc:10632]
CCL7	110710	chemokine (C-C motif) ligand 7 [Source:HGNC Symbol;Acc:10634]
CCL8	111343	chemokine (C-C motif) ligand 8 [Source:HGNC Symbol;Acc:10635]
CCNB1	101373	cyclin B1 [Source:HGNC Symbol;Acc:1579]
CCNB2	101376	cyclin B2 [Source:HGNC Symbol;Acc:1580]
CCND1	100844	cyclin D1 [Source:HGNC Symbol;Acc:1582]
CCND2	101384	cyclin D2 [Source:HGNC Symbol;Acc:1583]

CCR2	103019	chemokine (C-C motif) receptor 2 [Source:HGNC Symbol;Acc:1603]
CCR2	104065	chemokine (C-C motif) receptor 2 [Source:HGNC Symbol;Acc:1603]
CCR3	111241	chemokine (C-C motif) receptor 3 [Source:HGNC Symbol;Acc:1604]
CCR4	104068	chemokine (C-C motif) receptor 4 [Source:HGNC Symbol;Acc:1605]
CCR5	104069	chemokine (C-C motif) receptor 5 [Source:HGNC Symbol;Acc:1606]
CCR7	111317	chemokine (C-C motif) receptor 7 [Source:HGNC Symbol;Acc:1608]
CD24	139818	CD24 molecule
CD274	104030	CD274 molecule [Source:HGNC Symbol;Acc:17635]
CD34	113224	CD34 molecule [Source:HGNC Symbol;Acc:1662]
CD38	100250	CD38 molecule [Source:HGNC Symbol;Acc:1667]
CD44	110687	CD44 molecule (Indian blood group) [Source:HGNC Symbol;Acc:1681]
CD55	111910	CD55 molecule, decay accelerating factor for complement (Cromer blood group) [Source:HGNC Symbol;Acc:2665]
CD58	126215	CD58 molecule [Source:HGNC Symbol;Acc:1688]
CDH2	137066	cadherin 2, type 1, N-cadherin (neuronal) [Source:HGNC Symbol;Acc:1759]
CDH6	112143	cadherin 6, type 2, K-cadherin (fetal kidney) [Source:HGNC Symbol;Acc:1765]
CDK1	101406	cyclin-dependent kinase 1 [Source:HGNC Symbol;Acc:1722]
CDK2	101416	cyclin-dependent kinase 2 [Source:HGNC Symbol;Acc:1771]
CDK4	101418	cyclin-dependent kinase 4 [Source:HGNC Symbol;Acc:1773]
CDK6	101427	cyclin-dependent kinase 6 [Source:HGNC Symbol;Acc:1777]

CDKN1A	102909	cyclin-dependent kinase inhibitor 1A (p21, Cip1) [Source:HGNC Symbol;Acc:1784]
CDKN2B	101439	cyclin-dependent kinase inhibitor 2B (p15, inhibits CDK4) [Source:HGNC Symbol;Acc:1788]
CEBPB	100269	CCAAT/enhancer binding protein (C/EBP), beta [Source:HGNC Symbol;Acc:1834]
CHN1	139743	chimerin (chimaerin) 1 [Source:HGNC Symbol;Acc:1943]
CHN2	125167	chimerin (chimaerin) 2 [Source:HGNC Symbol;Acc:1944]
COL1A1	100861	collagen, type I, alpha 1 [Source:HGNC Symbol;Acc:2197]
COL1A2	103048	collagen, type I, alpha 2 [Source:HGNC Symbol;Acc:2198]
COL2A1	138054	collagen, type II, alpha 1 [Source:HGNC Symbol;Acc:2200]
COL5A2	120754	collagen, type V, alpha 2 [Source:HGNC Symbol;Acc:2210]
CPM	109278	carboxypeptidase M [Source:HGNC Symbol;Acc:2311]
CSF1	112032	colony stimulating factor 1 (macrophage) [Source:HGNC Symbol;Acc:2432]
CSF1R	105951	colony stimulating factor 1 receptor [Source:HGNC Symbol;Acc:2433]
CSF2	110860	colony stimulating factor 2 (granulocyte-macrophage) [Source:HGNC Symbol;Acc:2434]
CSPG4	117237	chondroitin sulfate proteoglycan 4 [Source:HGNC Symbol;Acc:2466]
CTGF	100872	connective tissue growth factor [Source:HGNC Symbol;Acc:2500]
CX3CL1	102721	chemokine (C-X3-C motif) ligand 1 [Source:HGNC Symbol;Acc:10647]
CX3CR1	112338	chemokine (C-X3-C motif) receptor 1 [Source:HGNC Symbol;Acc:2558]
CXCL1	105522	chemokine (C-X-C motif) ligand 1 (melanoma growth stimulating activity, alpha) [Source:HGNC Symbol;Acc:4602]
CXCL1	137825	chemokine (C-X-C motif) ligand 1 (melanoma growth stimulating activity, alpha) [Source:HGNC Symbol;Acc:4602]

CXCL10	103807	chemokine (C-X-C motif) ligand 10 [Source:HGNC Symbol;Acc:10637]
CXCL11	110800	chemokine (C-X-C motif) ligand 11 [Source:HGNC Symbol;Acc:10638]
CXCL12	110618	chemokine (C-X-C motif) ligand 12 [Source:HGNC Symbol;Acc:10672]
CXCL13	110738	chemokine (C-X-C motif) ligand 13 [Source:HGNC Symbol;Acc:10639]
CXCL16	114685	chemokine (C-X-C motif) ligand 16 [Source:HGNC Symbol;Acc:16642]
CXCL2	103070	chemokine (C-X-C motif) ligand 2 [Source:HGNC Symbol;Acc:4603]
CXCL3	103888	chemokine (C-X-C motif) ligand 3 [Source:HGNC Symbol;Acc:4604]
CXCL5	110613	chemokine (C-X-C motif) ligand 5 [Source:HGNC Symbol;Acc:10642]
CXCL9	104231	chemokine (C-X-C motif) ligand 9 [Source:HGNC Symbol;Acc:7098]
CXCR1	110870	chemokine (C-X-C motif) receptor 1 [Source:HGNC Symbol;Acc:6026]
CXCR2	110641	chemokine (C-X-C motif) receptor 2 [Source:HGNC Symbol;Acc:6027]
CXCR3	113470	chemokine (C-X-C motif) receptor 3 [Source:HGNC Symbol;Acc:4540]
CXCR4	110817	chemokine (C-X-C motif) receptor 4 [Source:HGNC Symbol;Acc:2561]
CXCR6	113770	chemokine (C-X-C motif) receptor 6 [Source:HGNC Symbol;Acc:16647]
CXCR7	135913	chemokine (C-X-C motif) receptor 7 [Source:HGNC Symbol;Acc:23692]
CXCR7	135912	chemokine (C-X-C motif) receptor 7 [Source:HGNC Symbol;Acc:23692]
DDIT4	137543	DNA-damage-inducible transcript 4 [Source:HGNC Symbol;Acc:24944]
DDR1	110060	Epithelial discoidin domain-containing receptor 1 Precursor (Epithelial discoidin domain receptor 1)(EC 2.7.10.1)(Tyrosine kinase DDR)(Discoidin receptor tyrosine kinase)
DDR1	106545	Epithelial discoidin domain-containing receptor 1 Precursor (Epithelial discoidin domain receptor 1)(EC

		2.7.10.1)(Tyrosine kinase DDR)(Discoidin receptor tyrosine kinase)
DDR1	110125	Epithelial discoidin domain-containing receptor 1 Precursor (Epithelial discoidin domain receptor 1)(EC 2.7.10.1)(Tyrosine kinase DDR)(Discoidin receptor tyrosine kinase)
DLGAP1	138553	discs, large (Drosophila) homolog-associated protein 1 [Source:HGNC Symbol;Acc:2905]
DPP4	109445	dipeptidyl-peptidase 4 [Source:HGNC Symbol;Acc:3009]
ECE1	109591	endothelin converting enzyme 1 [Source:HGNC Symbol;Acc:3146]
EFNA3	138422	ephrin-A3, ephrin-A3 [Source:HGNC Symbol;Acc:3223]
EFNB2	137312	ephrin-B2 [Source:HGNC Symbol;Acc:3227]
EGF	136007	epidermal growth factor [Source:HGNC Symbol;Acc:3229]
EGFR	103085	epidermal growth factor receptor [Source:HGNC Symbol;Acc:3236]
ENG	104599	endoglin [Source:HGNC Symbol;Acc:3349]
ENTPD1	115339	ectonucleoside triphosphate diphosphohydrolase 1 [Source:HGNC Symbol;Acc:3363]
EPCAM	103663	epithelial cell adhesion molecule [Source:HGNC Symbol;Acc:11529]
EPHB2	105893	EPH receptor B2 [Source:HGNC Symbol;Acc:3393]
EPOR	140936	erythropoietin receptor [Source:HGNC Symbol;Acc:3416]
ERBB2	105654	v-erb-b2 erythroblastic leukemia viral oncogene homolog 2, neuro/glioblastoma derived oncogene homolog (avian) [Source:HGNC Symbol;Acc:3430]
ERBB3	106100	v-erb-b2 erythroblastic leukemia viral oncogene homolog 3 (avian) [Source:HGNC Symbol;Acc:3431]
ERBB4	105757	v-erb-a erythroblastic leukemia viral oncogene homolog 4 (avian) [Source:HGNC Symbol;Acc:3432]
ERCC4	115300	excision repair cross-complementing rodent repair deficiency, complementation group 4 [Source:HGNC Symbol;Acc:3436]

F3	113302	coagulation factor III (thromboplastin, tissue factor) [Source:HGNC Symbol;Acc:3541]
FABP4	115237	fatty acid binding protein 4, adipocyte [Source:HGNC Symbol;Acc:3559]
FADD	100417	Fas (TNFRSF6)-associated via death domain [Source:HGNC Symbol;Acc:3573]
FAP	108274	fibroblast activation protein, alpha [Source:HGNC Symbol;Acc:3590]
FAS	100426	Fas (TNF receptor superfamily, member 6) [Source:HGNC Symbol;Acc:11920]
FASLG	104048	Fas ligand (TNF superfamily, member 6) [Source:HGNC Symbol;Acc:11936]
FBLIM1	126341	filamin binding LIM protein 1 [Source:HGNC Symbol;Acc:24686]
FERMT1	115773	fermitin family member 1 [Source:HGNC Symbol;Acc:15889]
FGF1	110688	fibroblast growth factor 1 (acidic) [Source:HGNC Symbol;Acc:3665]
FGF2	100912	fibroblast growth factor 2 (basic) [Source:HGNC Symbol;Acc:3676]
FGF23	140778	fibroblast growth factor 23 [Source:HGNC Symbol;Acc:3680]
FGF4	140318	fibroblast growth factor 4 [Source:HGNC Symbol;Acc:3682]
FGF7	113109	fibroblast growth factor 7 [Source:HGNC Symbol;Acc:3685]
FGF9	111498	fibroblast growth factor 9 (glia-activating factor) [Source:HGNC Symbol;Acc:3687]
FGFR1	105972	fibroblast growth factor receptor 1 [Source:HGNC Symbol;Acc:3688]
FGFR2	105812	fibroblast growth factor receptor 2 [Source:HGNC Symbol;Acc:3689]
FGFR3	105621	fibroblast growth factor receptor 3 [Source:HGNC Symbol;Acc:3690]
FGFR4	137059	fibroblast growth factor receptor 4 [Source:HGNC Symbol;Acc:3691]
FLT1	105673	fms-related tyrosine kinase 1 (vascular endothelial growth factor/vascular permeability factor receptor) [Source:HGNC Symbol;Acc:3763]

FOS	100917	FBJ murine osteosarcoma viral oncogene homolog [Source:HGNC Symbol;Acc:3796]	
FST	112452	follistatin [Source:HGNC Symbol;Acc:3971]	
FUT4	118619	fucosyltransferase 4 (alpha (1,3) fucosyltransferase, myeloid-specific) [Source:HGNC Symbol;Acc:4015]	
FZD9	104380	frizzled homolog 9 (Drosophila) [Source:HGNC Symbol;Acc:4047]	
G6PD	102098	glucose-6-phosphate dehydrogenase [Source:HGNC Symbol;Acc:4057]	Reference Gene
GAPDH	101128	glyceraldehyde-3-phosphate dehydrogenase [Source:HGNC Symbol;Acc:4141]	Reference Gene
GATA4	112829	GATA binding protein 4 [Source:HGNC Symbol;Acc:4173]	
GDNF	100445	glial cell derived neurotrophic factor [Source:HGNC Symbol;Acc:4232]	
GLG1	115669	golgi glycoprotein 1 [Source:HGNC Symbol;Acc:4316]	
GMFB	118616	glia maturation factor, beta [Source:HGNC Symbol;Acc:4373]	
GRB2	110953	growth factor receptor-bound protein 2 [Source:HGNC Symbol;Acc:4566]	
HDGF	119183	hepatoma-derived growth factor [Source:HGNC Symbol;Acc:4856]	
HGF	108357	hepatocyte growth factor (hepapoietin A; scatter factor) [Source:HGNC Symbol;Acc:4893]	
HIF1A	110660	hypoxia inducible factor 1, alpha subunit (basic helix-loop-helix transcription factor) [Source:HGNC Symbol;Acc:4910]	
HLA-G	135876	HLA class I histocompatibility antigen, alpha chain G Precursor (HLA G antigen) [Source:UniProtKB/Swiss-Prot;Acc:P17693]	
HRAS	110892	v-Ha-ras Harvey rat sarcoma viral oncogene homolog [Source:HGNC Symbol;Acc:5173]	
ICAM1	100945	intercellular adhesion molecule 1 [Source:HGNC Symbol;Acc:5344]	
ICAM2	126792	intercellular adhesion molecule 2 [Source:HGNC Symbol;Acc:5345]	
ID1	104631	inhibitor of DNA binding 1, dominant negative helix-loop-helix protein [Source:HGNC Symbol;Acc:5360]	

IDO1	103804	indoleamine 2,3-dioxygenase 1 [Source:HGNC Symbol;Acc:6059]
IER3	141172	Radiation-inducible immediate-early gene IEX-1 (Immediate early protein GLY96)(Immediate early response 3 protein)(PACAP-responsive gene 1 protein)(Protein PRG1)(Differentiation-dependent gene 2 protein)(Protein DIF-2) [Source:UniProtKB/Swiss-Prot;Acc:P46695]
IFNG	110609	interferon, gamma [Source:HGNC Symbol;Acc:5438]
IFNGR1	111882	interferon gamma receptor 1 [Source:HGNC Symbol;Acc:5439]
IFNGR2	114055	interferon gamma receptor 2 (interferon gamma transducer 1) [Source:HGNC Symbol;Acc:5440]
IGF1	103127	insulin-like growth factor 1 (somatomedin C) [Source:HGNC Symbol;Acc:5464]
IGF1R	100524	insulin-like growth factor 1 receptor [Source:HGNC Symbol;Acc:5465]
IGF2	113548	insulin-like growth factor 2 (somatomedin A), insulin-like growth factor 2 (somatomedin A) [Source:HGNC Symbol;Acc:5466]
IGF2R	111759	insulin-like growth factor 2 receptor [Source:HGNC Symbol;Acc:5467]
IL10	137153	interleukin 10 [Source:HGNC Symbol;Acc:5962]
IL10RA	103952	interleukin 10 receptor, alpha [Source:HGNC Symbol;Acc:5964]
IL10RB	103569	interleukin 10 receptor, beta
IL12A	112242	interleukin 12A (natural killer cell stimulatory factor 1, cytotoxic lymphocyte maturation factor 1, p35) [Source:HGNC Symbol;Acc:5969]
IL13	112368	interleukin 13 [Source:HGNC Symbol;Acc:5973]
IL1B	100950	interleukin 1, beta [Source:HGNC Symbol;Acc:5992]
IL1R1	100951	interleukin 1 receptor, type I [Source:HGNC Symbol;Acc:5993]
IL1R2	102462	interleukin 1 receptor, type II [Source:HGNC Symbol;Acc:5994]
IL1RN	103133	interleukin 1 receptor antagonist [Source:HGNC Symbol;Acc:6000]

IL2	100958	interleukin 2 [Source:HGNC Symbol;Acc:6001]	
IL2RA	111304	interleukin 2 receptor, alpha [Source:HGNC Symbol;Acc:6008]	
IL2RB	113971	interleukin 2 receptor, beta [Source:HGNC Symbol;Acc:6009]	
IL3	137634	interleukin 3 (colony-stimulating factor, multiple) [Source:HGNC Symbol;Acc:6011]	
IL3RA	117429	interleukin 3 receptor, alpha (low affinity) [Source:HGNC Symbol;Acc:6012]	
IL4R	110880	interleukin 4 receptor [Source:HGNC Symbol;Acc:6015]	
IL5RA	112257	interleukin 5 receptor, alpha [Source:HGNC Symbol;Acc:6017]	
IL6	113614	interleukin 6 (interferon, beta 2) [Source:HGNC Symbol;Acc:6018]	
IL6R	112272	interleukin 6 receptor [Source:HGNC Symbol;Acc:6019]	
IL7R	114202	interleukin 7 receptor [Source:HGNC Symbol;Acc:6024]	
IL8	103136	interleukin 8 [Source:HGNC Symbol;Acc:6025]	
ILK	110108	integrin-linked kinase [Source:HGNC Symbol;Acc:6040]	
INHBA	103779	inhibin, beta A [Source:HGNC Symbol;Acc:6066]	
IPO8	102132	importin 8 [Source:HGNC Symbol;Acc:9853]	Reference Gene
ITGA1	110762	integrin, alpha 1 [Source:HGNC Symbol;Acc:6134]	
ITGA10	127809	integrin, alpha 10 [Source:HGNC Symbol;Acc:6135]	
ITGA11	140155	integrin, alpha 11 [Source:HGNC Symbol;Acc:6136]	
ITGA2	111263	integrin, alpha 2 (CD49B, alpha 2 subunit of VLA-2 receptor) [Source:HGNC Symbol;Acc:6137]	
ITGA2B	113049	integrin, alpha 2b (platelet glycoprotein IIb of IIb/IIIa complex, antigen CD41) [Source:HGNC Symbol;Acc:6138]	

ITGA3	111330	integrin, alpha 3 (antigen CD49C, alpha 3 subunit of VLA-3 receptor) [Source:HGNC Symbol;Acc:6139]
ITGA4	110765	integrin, alpha 4 (antigen CD49D, alpha 4 subunit of VLA-4 receptor) [Source:HGNC Symbol;Acc:6140]
ITGA5	113140	integrin, alpha 5 (fibronectin receptor, alpha polypeptide) [Source:HGNC Symbol;Acc:6141]
ITGA6	113076	integrin, alpha 6 [Source:HGNC Symbol;Acc:6142]
ITGA7	111900	integrin, alpha 7 [Source:HGNC Symbol;Acc:6143]
ITGA8	140643	integrin, alpha 8 [Source:HGNC Symbol;Acc:6144]
ITGA9	127494	integrin, alpha 9 [Source:HGNC Symbol;Acc:6145]
ITGAE	127153	integrin, alpha E (antigen CD103, human mucosal lymphocyte antigen 1; alpha polypeptide) [Source:HGNC Symbol;Acc:6147]
ITGAL	113362	integrin, alpha L (antigen CD11A (p180), lymphocyte function-associated antigen 1; alpha polypeptide) [Source:HGNC Symbol;Acc:6148]
ITGAM	140359	integrin, alpha M (complement component 3 receptor 3 subunit) [Source:HGNC Symbol;Acc:6149]
ITGAV	110698	integrin, alpha V (vitronectin receptor, alpha polypeptide, antigen CD51) [Source:HGNC Symbol;Acc:6150]
ITGAX	116588	integrin, alpha X (complement component 3 receptor 4 subunit) [Source:HGNC Symbol;Acc:6152]
ITGB1	110652	integrin, beta 1 (fibronectin receptor, beta polypeptide, antigen CD29 includes MDF2, MSK12) [Source:HGNC Symbol;Acc:6153]
ITGB2	103578	integrin, beta 2 (complement component 3 receptor 3 and 4 subunit) [Source:HGNC Symbol;Acc:6155]
ITGB3	110631	integrin, beta 3 (platelet glycoprotein IIIa, antigen CD61) [Source:HGNC Symbol;Acc:6156]
ITGB4	140120	integrin, beta 4 [Source:HGNC Symbol;Acc:6158]
ITGB5	110842	integrin, beta 5 [Source:HGNC Symbol;Acc:6160]
ITGB6	119126	integrin, beta 6 [Source:HGNC Symbol;Acc:6161]
ITGB7	111111	integrin, beta 7 [Source:HGNC Symbol;Acc:6162]

ITGB8	119759	integrin, beta 8 [Source:HGNC Symbol;Acc:6163]
JAG1	108043	jagged 1 [Source:HGNC Symbol;Acc:6188]
KDR	105649	kinase insert domain receptor (a type III receptor tyrosine kinase) [Source:HGNC Symbol;Acc:6307]
KIT	105674	v-kit Hardy-Zuckerman 4 feline sarcoma viral oncogene homolog [Source:HGNC Symbol;Acc:6342]
KITLG	112398	KIT ligand [Source:HGNC Symbol;Acc:6343]
KRAS	110975	v-Ki-ras2 Kirsten rat sarcoma viral oncogene homolog [Source:HGNC Symbol;Acc:6407]
KRT7	103587	keratin 7 [Source:HGNC Symbol;Acc:6445]
LGALS1	100568	lectin, galactoside-binding, soluble, 1 [Source:HGNC Symbol;Acc:6561]
LIF	113007	leukemia inhibitory factor (cholinergic differentiation factor) [Source:HGNC Symbol;Acc:6596]
LIG4	115063	ligase IV, DNA, ATP-dependent [Source:HGNC Symbol;Acc:6601]
LTBP1	104651	latent transforming growth factor beta binding protein 1 [Source:HGNC Symbol;Acc:6714]
LY6E	140662	lymphocyte antigen 6 complex, locus E [Source:HGNC Symbol;Acc:6727]
MAPK1	100597	mitogen-activated protein kinase 1 [Source:HGNC Symbol;Acc:6871]
MCAM	105530	melanoma cell adhesion molecule [Source:HGNC Symbol;Acc:6934]
MCM3	101501	minichromosome maintenance complex component 3 [Source:HGNC Symbol;Acc:6945]
MET	105981	met proto-oncogene (hepatocyte growth factor receptor) [Source:HGNC Symbol;Acc:7029]
MIF	138424	macrophage migration inhibitory factor (glycosylation-inhibiting factor)
MKI67	101512	antigen identified by monoclonal antibody Ki-67 [Source:HGNC Symbol;Acc:7107]
MME	109438	membrane metallo-endopeptidase [Source:HGNC Symbol;Acc:7154]

MMP1	103943	matrix metallopeptidase 1 (interstitial collagenase) [Source:HGNC Symbol;Acc:7155]
MMP12	103818	matrix metallopeptidase 12 (macrophage elastase) [Source:HGNC Symbol;Acc:7158]
MMP13	140652	matrix metallopeptidase 13 (collagenase 3) [Source:HGNC Symbol;Acc:7159]
MMP14	109081	matrix metallopeptidase 14 (membrane-inserted) [Source:HGNC Symbol;Acc:7160]
MMP15	108327	matrix metallopeptidase 15 (membrane-inserted) [Source:HGNC Symbol;Acc:7161]
MMP16	108882	matrix metallopeptidase 16 (membrane-inserted) [Source:HGNC Symbol;Acc:7162]
MMP17	109447	matrix metallopeptidase 17 (membrane-inserted) [Source:HGNC Symbol;Acc:7163]
MMP2	103899	matrix metallopeptidase 2 (gelatinase A, 72kDa gelatinase, 72kDa type IV collagenase) [Source:HGNC Symbol;Acc:7166]
MMP24	108460	matrix metallopeptidase 24 (membrane-inserted) [Source:HGNC Symbol;Acc:7172]
MMP25	109262	matrix metallopeptidase 25 [Source:HGNC Symbol;Acc:14246]
MMP3	103167	matrix metallopeptidase 3 (stromelysin 1, progelatinase) [Source:HGNC Symbol;Acc:7173]
MMP7	104396	matrix metallopeptidase 7 (matrilysin, uterine) [Source:HGNC Symbol;Acc:7174]
MMP9	136019	matrix metallopeptidase 9 (gelatinase B, 92kDa gelatinase, 92kDa type IV collagenase) [Source:HGNC Symbol;Acc:7176]
MST1R	105683	macrophage stimulating 1 receptor (c-met-related tyrosine kinase) [Source:HGNC Symbol;Acc:7381]
MYC	100977	v-myc myelocytomatosis viral oncogene homolog (avian) [Source:HGNC Symbol;Acc:7553]
MYH11	116429	myosin, heavy chain 11, smooth muscle [Source:HGNC Symbol;Acc:7569]
NANOG	114796	Nanog homeobox pseudogene 8 [Source:HGNC Symbol;Acc:23106]
NAV1	133030	neuron navigator 1 [Source:HGNC Symbol;Acc:15989]
NCAM1	111243	neural cell adhesion molecule 1 [Source:HGNC Symbol;Acc:7656]

NES	140436	nestin [Source:HGNC Symbol;Acc:7756]
NGF	113440	nerve growth factor (beta polypeptide) [Source:HGNC Symbol;Acc:7808]
NGFR	100652	nerve growth factor receptor [Source:HGNC Symbol;Acc:7809]
NGFRAP1	118787	nerve growth factor receptor (TNFRSF16) associated protein 1 [Source:HGNC Symbol;Acc:13388]
NLGN1	130877	neuroligin 1 [Source:HGNC Symbol;Acc:14291]
NLGN3	126309	neuroligin 3 [Source:HGNC Symbol;Acc:14289]
NMB	137724	neuromedin B [Source:HGNC Symbol;Acc:7842]
NOS1	113254	nitric oxide synthase 1 (neuronal) [Source:HGNC Symbol;Acc:7872]
NOS2	102470	nitric oxide synthase 2, inducible [Source:HGNC Symbol;Acc:7873]
NOS3	139599	nitric oxide synthase 3 (endothelial cell) [Source:HGNC Symbol;Acc:7876]
NOTCH3	112380	notch 3 [Source:HGNC Symbol;Acc:7883]
NRG1	113134	neuregulin 1 [Source:HGNC Symbol;Acc:7997]
NRG1	139822	neuregulin 1 [Source:HGNC Symbol;Acc:7997]
NRP1	111930	neuropilin 1 [Source:HGNC Symbol;Acc:8004]
NRP2	111705	neuropilin 2 [Source:HGNC Symbol;Acc:8005]
NT5E	105242	5'-nucleotidase, ecto (CD73) [Source:HGNC Symbol;Acc:8021]
NTF3	100692	neurotrophin 3 [Source:HGNC Symbol;Acc:8023]
NTRK1	136972	neurotrophic tyrosine kinase, receptor, type 1 [Source:HGNC Symbol;Acc:8031]
NTRK2	105907	neurotrophic tyrosine kinase, receptor, type 2 [Source:HGNC Symbol;Acc:8032]

NTRK3	105821	neurotrophic tyrosine kinase, receptor, type 3 [Source:HGNC Symbol;Acc:8033]
PAMR1	109653	peptidase domain containing associated with muscle regeneration 1 [Source:HGNC Symbol;Acc:24554]
PARVB	138591	parvin, beta [Source:HGNC Symbol;Acc:14653]
PARVG	116543	parvin, gamma [Source:HGNC Symbol;Acc:14654]
PDCD1LG2	117537	programmed cell death 1 ligand 2 [Source:HGNC Symbol;Acc:18731]
PDGFA	110648	platelet-derived growth factor alpha polypeptide [Source:HGNC Symbol;Acc:8799]
PDGFB	110713	platelet-derived growth factor beta polypeptide (simian sarcoma viral (v-sis) oncogene homolog) [Source:HGNC Symbol;Acc:8800]
PDGFRA	105613	platelet-derived growth factor receptor, alpha polypeptide [Source:HGNC Symbol;Acc:8803]
PDGFRB	105627	platelet-derived growth factor receptor, beta polypeptide [Source:HGNC Symbol;Acc:8804]
PECAM1	137855	platelet/endothelial cell adhesion molecule
PGF	111326	placental growth factor [Source:HGNC Symbol;Acc:8893]
PLEKHC1	103255	fermitin family member 2 [Source:HGNC Symbol;Acc:15767]
PODXL	116328	podocalyxin-like [Source:HGNC Symbol;Acc:9171]
POU5F1	113034	POU domain, class 5, transcription factor 1 (Octamer-binding transcription factor 3)(OTF-3)(Octamer-binding protein 3)(Oct-3)(Octamer-binding protein 4)(Oct-4) [Source:UniProtKB/Swiss-Prot;Acc:Q01860]
POU5F1P1	138243	POU class 5 homeobox 1B [Source:HGNC Symbol;Acc:9223]
PPARG	110607	peroxisome proliferator-activated receptor gamma [Source:HGNC Symbol;Acc:9236]
PPP2R5C	108132	protein phosphatase 2, regulatory subunit B', gamma [Source:HGNC Symbol;Acc:9311]
PTMA	138099	microRNA 1244-3 [Source:HGNC Symbol;Acc:38390]

PTN	137382	pleiotrophin [Source:HGNC Symbol;Acc:9630]	
PTPRC	104880	protein tyrosine phosphatase, receptor type, C [Source:HGNC Symbol;Acc:9666]	
PXN	112950	paxillin [Source:HGNC Symbol;Acc:9718]	
RB1	101538	retinoblastoma 1 [Source:HGNC Symbol;Acc:9884]	
RB1	101596	retinoblastoma 1 [Source:HGNC Symbol;Acc:9884]	
RGS4	114601	regulator of G-protein signaling 4 [Source:HGNC Symbol;Acc:10000]	
RHOA	104675	ras homolog gene family, member A [Source:HGNC Symbol;Acc:667]	
ROBO1	103193	roundabout, axon guidance receptor, homolog 1 (Drosophila) [Source:HGNC Symbol;Acc:10249]	
ROBO4	127380	roundabout homolog 4, magic roundabout (Drosophila) [Source:HGNC Symbol;Acc:17985]	
RP11-330H6.5	136102	cDNA FLJ56277, highly similar to Toll-like receptor 9 [Source:UniProtKB/TrEMBL;Acc:B4E0A1]	
RPL13A	102119	small nucleolar RNA, C/D box 32A [Source:HGNC Symbol;Acc:10159]	Reference Gene
RUNX2	113380	runt-related transcription factor 2 [Source:HGNC Symbol;Acc:10472]	
S100A4	110779	S100 calcium binding protein A4 [Source:HGNC Symbol;Acc:10494]	
S100A6	136966	S100 calcium binding protein A6 [Source:HGNC Symbol;Acc:10496]	
SDC1	113025	syndecan 1 [Source:HGNC Symbol;Acc:10658]	
SDC2	113656	syndecan 2 [Source:HGNC Symbol;Acc:10659]	
SDHA	102136	succinate dehydrogenase complex, subunit A, flavoprotein (Fp) [Source:HGNC Symbol;Acc:10680]	Reference Gene
SELE	135943	selectin E [Source:HGNC Symbol;Acc:10718]	
SELL	112968	selectin L [Source:HGNC Symbol;Acc:10720]	

SELP	113067	selectin P (granule membrane protein 140kDa, antigen CD62) [Source:HGNC Symbol;Acc:10721]
SELPLG	137888	selectin P ligand [Source:HGNC Symbol;Acc:10722]
SEMA3C	130242	sema domain, immunoglobulin domain (Ig), short basic domain, secreted, (semaphorin) 3C [Source:HGNC Symbol;Acc:10725]
SEMA3F	119222	sema domain, immunoglobulin domain (Ig), short basic domain, secreted, (semaphorin) 3F [Source:HGNC Symbol;Acc:10728]
SERPINE1	101014	serpin peptidase inhibitor, clade E (nexin, plasminogen activator inhibitor type 1), member 1 [Source:HGNC Symbol;Acc:8583]
SERPINE2	103642	serpin peptidase inhibitor, clade E (nexin, plasminogen activator inhibitor type 1), member 2 [Source:HGNC Symbol;Acc:8951]
SFRP2	104431	secreted frizzled-related protein 2 [Source:HGNC Symbol;Acc:10777]
SFRP2	116705	secreted frizzled-related protein 2 [Source:HGNC Symbol;Acc:10777]
SHC1	110943	SHC (Src homology 2 domain containing) transforming protein 1 [Source:HGNC Symbol;Acc:10840]
SHC4	133970	SHC (Src homology 2 domain containing) family, member 4 [Source:HGNC Symbol;Acc:16743]
SNAI1	112995	snail homolog 1 (Drosophila) [Source:HGNC Symbol;Acc:11128]
SNX2	138448	sorting nexin 2 [Source:HGNC Symbol;Acc:11173]
SNX6	125013	sorting nexin 6 [Source:HGNC Symbol;Acc:14970]
SOX2	111867	SRY (sex determining region Y)-box 2 [Source:HGNC Symbol;Acc:11195]
STAT1	101180	signal transducer and activator of transcription 1, 91kDa [Source:HGNC Symbol;Acc:11362]
STC1	116867	stanniocalcin 1 [Source:HGNC Symbol;Acc:11373]
STC2	118034	stanniocalcin 2 [Source:HGNC Symbol;Acc:11374]
TAPBP	138030	tapasin isoform 1 precursor [Source:RefSeq peptide;Acc:NP_003181]

TBP	101145	TATA box binding protein [Source:HGNC Symbol;Acc:11588]	Reference Gene
TEK	105772	TEK tyrosine kinase, endothelial [Source:HGNC Symbol;Acc:11724]	
TERT	110619	telomerase reverse transcriptase [Source:HGNC Symbol;Acc:11730]	
TFPI2	108032	tissue factor pathway inhibitor 2 [Source:HGNC Symbol;Acc:11761]	
TGFA	110787	transforming growth factor, alpha [Source:HGNC Symbol;Acc:11765]	
TGFB1	101210	transforming growth factor, beta 1 [Source:HGNC Symbol;Acc:11766]	
TGFBR1	104725	transforming growth factor, beta receptor 1 [Source:HGNC Symbol;Acc:11772]	
TGFBR2	104727	transforming growth factor, beta receptor II (70/80kDa) [Source:HGNC Symbol;Acc:11773]	
THBS1	104740	thrombospondin 1 [Source:HGNC Symbol;Acc:11785]	
THY1	116810	Thy-1 cell surface antigen [Source:HGNC Symbol;Acc:11801]	
TIMP1	103847	TIMP metallopeptidase inhibitor 1 [Source:HGNC Symbol;Acc:11820]	
TIMP2	110664	TIMP metallopeptidase inhibitor 2 [Source:HGNC Symbol;Acc:11821]	
TIMP3	101221	TIMP metallopeptidase inhibitor 3 [Source:HGNC Symbol;Acc:11822]	
TIMP4	112044	TIMP metallopeptidase inhibitor 4 [Source:HGNC Symbol;Acc:11823]	
TLN1	116516	talin 1 [Source:HGNC Symbol;Acc:11845]	
TLN2	130026	talin 2 [Source:HGNC Symbol;Acc:15447]	
TLR1	111000	toll-like receptor 1 [Source:HGNC Symbol;Acc:11847]	
TLR2	101225	toll-like receptor 2 [Source:HGNC Symbol;Acc:11848]	
TLR3	111008	toll-like receptor 3 [Source:HGNC Symbol;Acc:11849]	

TLR4	135752	toll-like receptor 4 [Source:HGNC Symbol;Acc:11850]
TLR5	103674	toll-like receptor 5 [Source:HGNC Symbol;Acc:11851]
TLR6	111018	toll-like receptor 6 [Source:HGNC Symbol;Acc:16711]
TLR7	111012	toll-like receptor 7 [Source:HGNC Symbol;Acc:15631]
TLR8	103816	toll-like receptor 8 [Source:HGNC Symbol;Acc:15632]
TNC	113344	tenascin C [Source:HGNC Symbol;Acc:5318]
TNF	103295	Tumor necrosis factor Precursor (TNF-alpha)(Tumor necrosis factor ligand superfamily member 2)(TNF-a)(Cachectin) [Contains Tumor necrosis factor, membrane form;Tumor necrosis factor, soluble form] [Source:UniProtKB/Swiss-Prot;Acc:P01375]
TNFAIP6	113809	tumor necrosis factor, alpha-induced protein 6 [Source:HGNC Symbol;Acc:11898]
TNFRSF10A	101232	tumor necrosis factor receptor superfamily, member 10a [Source:HGNC Symbol;Acc:11904]
TNFRSF10B	101236	tumor necrosis factor receptor superfamily, member 10b [Source:HGNC Symbol;Acc:11905]
TNFRSF1A	102679	tumor necrosis factor receptor superfamily, member 1A [Source:HGNC Symbol;Acc:11916]
TNFRSF1B	102682	tumor necrosis factor receptor superfamily, member 1B [Source:HGNC Symbol;Acc:11917]
TP53	101277	tumor protein p53 [Source:HGNC Symbol;Acc:11998]
TSC22D3	101316	TSC22 domain family, member 3 [Source:HGNC Symbol;Acc:3051]
TWIST1	110770	twist homolog 1 (Drosophila) [Source:HGNC Symbol;Acc:12428]
VCAM1	103286	vascular cell adhesion molecule 1 [Source:HGNC Symbol;Acc:12663]
VEGFA	101034	vascular endothelial growth factor A [Source:HGNC Symbol;Acc:12680]
WISP1	110191	WNT1 inducible signaling pathway protein 1 [Source:HGNC Symbol;Acc:12769]

XCR1	137009	chemokine (C motif) receptor 1 [Source:HGNC Symbol;Acc:1625]	
XPNPEP1	109516	X-prolyl aminopeptidase (aminopeptidase P) 1, soluble [Source:HGNC Symbol;Acc:12822]	
YWHAQ	115267	tyrosine 3-monooxygenase/tryptophan 5-monooxygenase activation protein, theta polypeptide [Source:HGNC Symbol;Acc:12854]	
YWHAZ	102125	tyrosine 3-monooxygenase/tryptophan 5-monooxygenase activation protein, zeta polypeptide [Source:HGNC Symbol;Acc:12855]	Reference Gene
ZEB1	114775	zinc finger E-box binding homeobox 1 [Source:HGNC Symbol;Acc:11642]	
ZEB2	114816	zinc finger E-box binding homeobox 2 [Source:HGNC Symbol;Acc:14881]	